ICEBERG SCOUR RISK ANALYSIS FOR PIPELINES ON THE LABRADOR SHELF

ANTHONY D. KING

ICEBERG SCOUR RISK ANALYSIS FOR PIPELINES ON THE LABRADOR SHELF

by

Anthony D. King, P.Eng.

A thesis submitted to the
School of Graduate Studies
in partial fulfillment of the
requirements for the degree of
Master of Engineering

Faculty of Engineering and Applied Science
Memorial University of Newfoundland
December, 2002

St. John's Newfoundland Canada

ABSTRACT

An iceberg risk analysis was performed for a network of 3 pipelines proposed by Petro-Canada (1983) to allow the transport of natural gas on the Makkovik Bank to a landfall at Cape Harrison on the Labrador Coast. The risk analysis originally performed indicated that scouring icebergs would make direct contact with these three pipelines an average of thirteen times per year (total for all three) if the pipelines were trenched to provide a cover depth of 2.5 m. The required burial depth to reduce failure rates to one every second year for the pipeline network was estimated to be approximately 5 m, which was not considered technically feasible.

Since the original Petro-Canada (1983) analysis, a significant amount of work has been done on iceberg scour and the associated risk to subsea facilities. Given increasing interest in the development of offshore natural gas reserves, it was considered worthwhile to perform a review of the original work and, if warranted, perform another risk analysis. Certain elements of the original risk analysis were identified as being extremely conservative: the mean scour depth, the iceberg draft distribution, and the method used to determine the proportion of icebergs scouring over the pipelines.

In order to perform a risk analysis for the pipeline network, a model was developed to estimate iceberg grounding rates on the seabed. The model was tested using data from the Grand Banks, where iceberg parameters are fairly-well established. The model was

verified using scour rates estimated at the Hibernia and White Rose sites from seabed surveys and was found to provide reasonable estimates of iceberg scour rates.

Data for the Makkovik Bank was reviewed for use in the grounding model, to allow calculation of pipeline scour crossing rates and to determine the scour depth distribution. The failure rates depend on the criterion used to define pipeline failure. If direct contact between a scouring iceberg keel and a trenched pipeline was defined as failure (which was the criterion used for the Petro-Canada (1983) analysis) then the mean time between failures for the three pipelines with 2.5 m cover varied from 18 to 23 years, with a resulting mean time between failures of 7.5 years for the entire network. While the direct-contact criterion was commonly used at the time of the original analysis, modern analyses require a clearance between a scouring iceberg keel and the top of the pipeline. If a conservative criterion of 1 scour depth clearance between the scouring pipeline keel and the crown of the pipeline (i.e. 2 m cover for 1 m scour) is used to define pipeline failure, the mean time between failures for the three pipelines (2.5 m cover) varies from 3.4 to 5.3 years, with a mean time between failure events for the pipeline network of 1.4 years. A detailed analysis of pipeline response would yield more favourable results.

Additional work is recommended to allow better definition of scour parameters and iceberg frequency. A high-quality seabed survey would likely indicate a shallower mean scour depth than was used in the analysis (0.75 m), potentially in the range currently used for pipeline risk analyses for the Grand Banks (< 0.5 m).

ACKNOWLEDGEMENTS

I would like to thank Dr. Richard McKenna, formerly of C-CORE, and Dr. Ian Jordaan of the Faculty to Engineering for their supervision and guidance during the completion of this work. I would particularly like to acknowledge Dr. McKenna for giving me the opportunity to work in the Ice Engineering field and acquire the skills and experience necessary to tackle this topic. I wish him the best of luck in future endeavors. I am very grateful for the financial support provided by Judith Whittick of C-CORE during the completion of this thesis. Her confidence in my ability to produce something worthwhile was very encouraging.

I would like to express gratitude to Shawn Hurley and Dr. Ahmed Ewida of Petro-Canada for giving me access to the Bjarni Development Study (Petro-Canada, 1983), which was a valuable source of information and contributed significantly to this thesis. I would also like to thank Gary Sonnichsen of the Geological Survey of Canada (Atlantic) for resurrecting the Regional Ice Scour Database and providing some of the scour data presented in this thesis, as well as Pat Campbell of Canadian Seabed Research for his assistance with the Grand Banks Scour Catalogue. I would like to thank workterm students Sabrina Stuckless and Michelle Rose for their work on the iceberg track data, and my mother, Doris King, for many hours of spent deciphering hand-written iceberg logs and manually entering iceberg track data into spreadsheets. I would like to acknowledge Dr. Alvin Simms of the Geography Department for providing some iceberg track data for comparison.

This thesis drew heavily on many years of work by others who have worked in the field of iceberg scour. A comprehensive list would not be feasible, however I would like to specifically acknowledge Dr. Christopher Woodworth-Lynas for his many fine publications in the field.

Last, but not least, I would like to thank my wife, Diane, for her patience and support throughout this ordeal.

CONTENTS

LIST OF FIGURES

LIST OF TABLES

LIST OF SYMBOLS

A	Representative area of seabed where a scour can form
B	Scour width
$\overline{B}$	Mean scour width
C	Pipeline cover depth (mudline to crown of pipe)
D	Scour depth
D_i	Iceberg draft
L_i	Iceberg waterline length
L_p	Length of pipeline
N	Total number of ice features scouring over a pipeline
N_a	Annual number of ice features scouring over a pipeline
N_D	Number of scours reaching a specified depth
N_m	Number of scour feature depths measured during surveys
N_{obs}	Number of scour features observed in mosaics
$P(I)$	Probability that a given scour will cross over a pipeline
S	Seabed slope
T	Lifetime of pipeline
$\overline{U}$	Mean iceberg drift speed
W	Width of representative section of seabed
a	Area around a pipeline in which a scour can form
f_g	Frequency at which icebergs contact the seabed
f_{sc}	Seabed scour formation rate (#/unit area/year)
$f(\alpha)$	Probability density function for the distribution of scour orientation
$\overline{g}$	Average number of scours per kilometer per year along pipeline route
k	Exponential decay constant for scour depth (-1/mean scour depth)
l_s	Scour length

$\bar{l}_s$	Mean scour length
n_0	Areal density of icebergs
r_d	Proportion of iceberg drafts in specified depth range (i.e. 1 m increment)
r_θ	Proportion of icebergs drifting in a specified direction
$u(0,0,0)$	Displacement of soil underneath scour keel
z	Depth below bottom of scour
α	Scour orientation
ϕ	Pipeline orientation
γ	Angle between the pipeline route and scours
λ_θ	Frequency of scours along a linear track
μ_a	Mean scour depth, adjusted for number of sub-resolution scours
μ_m	Mean of the measured scour depths
θ	Angle relative to seabed upslope direction
ρ	Density of scours on the seabed
ρ_g	Grounding rate per unit area of seabed
ρ_k	Areal density of iceberg keels capable of striking the seabed

1 INTRODUCTION

The development of Newfoundland and Labrador's offshore hydrocarbon reserves has been complicated by the presence of icebergs, which have the potential to damage drilling and production platforms, and subsea facilities such as wellheads and pipelines. Despite these risks, development of petroleum reserves on the Grand Banks has proceeded. At this point, natural gas reserves on the Grand Banks and the Labrador Shelf have not yet been developed.

Total offshore natural gas reserves for Newfoundland and Labrador are estimated to be 262×10^9 m^3 (CNOPB, 2001), of which 142.4×10^9 m^3 are located on the Grand Banks and 119.6×10^9 m^3 are located on the Labrador Shelf. Figure 1 shows the location of the various natural gas deposits, along with the volume associated with each site. For comparison, the total gas reserves for the Sable Island field have been estimated to be 171×10^9 m^3 (CNSOPB, 1997), while Deep Panuke has been estimated to contain 26.3×10^9 m^3 of recoverable natural gas (PanCanadian, 2002). Pipelines are used to transport Nova Scotia's natural gas to shore, however icebergs are not a consideration for this region. No major pipeline developments exist in waters subject to iceberg incursions.

Subsea pipelines are often trenched to provide insulation, stability and protection from fishing activities, anchors and dropped objects. On the Grand Banks and the Labrador Shelf, an additional consideration is icebergs that are driven into the seabed by environmental forces drift, plowing out linear features known as iceberg scours. A

number of studies have been conducted to assess iceberg scour risk to gas pipelines on the Grand Banks (C-CORE 1999, 2000, 2001a). These studies used iceberg scour rates derived either from numerical modeling of iceberg drift and grounding or an interpretation of scour density observed during seabed surveys. Scour width, depth and length parameters were based on comprehensive seabed surveys. The stress/strain response of pipeline to icebergs scouring over (but not contacting) the buried pipeline was analyzed using finite element modeling. These studies have shown pipelines to be a feasible method for transporting natural gas in this region.

The iceberg conditions on the Labrador Shelf are much more severe than those on the Grand Banks. Icebergs are more frequent than on the Grand Banks and the density of scours visible on the seabed is greater. An iceberg scour risk analysis was performed by Petro-Canada (1983) for pipelines linking the Bjarni and North Bjarni sites with a landfall at Cape Harrison on the Labrador Coast. Various pipeline configurations were analyzed, however the base case consisted of three pipelines (a pigging pipeline and redundant flowlines). The risk analysis indicated that with a 2.5 m cover depth (distance from pipe crown to surface) each pipeline would be struck by an iceberg keel three times annually. In order to reduce impact frequency to one collision every two years for all three pipelines (required in order to allow time for repair while maintaining operation) it was necessary to have cover depths in the 4 to 8 m range. It is worth noting that the criterion for failure for the Petro-Canada study was direct pipeline/iceberg contact, whereas an allowance for sub-scour soil deformations is typical in modern risk analyses.

1.1 Objectives

In order to determine the risk to pipelines on the Labrador Shelf, the following objectives were addressed:

- Initially, a thorough review of the original risk analysis was performed. This allowed any aspects of the analysis, assumptions or parameters that may have led to overly conservative results to be identified.

- A simple grounding model was developed that allowed iceberg scour rates to be calculated. The grounding model was calibrated using data from the Grand Banks, where the environmental parameters and scour rates have been determined with a certain degree of confidence.

- A risk analysis was performed for the base case pipeline scenario using the grounding model and the best available site-specific information. Where appropriate, differences between the input parameters and those used in the original Petro-Canada (1983) analysis were identified. Risk levels associated with a 2.5 m cover depth were determined. These values were determined considering direct contact (as with the original analysis) and with a sub-gouge deformation allowance.

Figure 2 is a flowchart that illustrates the general approach used for the pipeline risk analysis, along with references to the corresponding Sections.

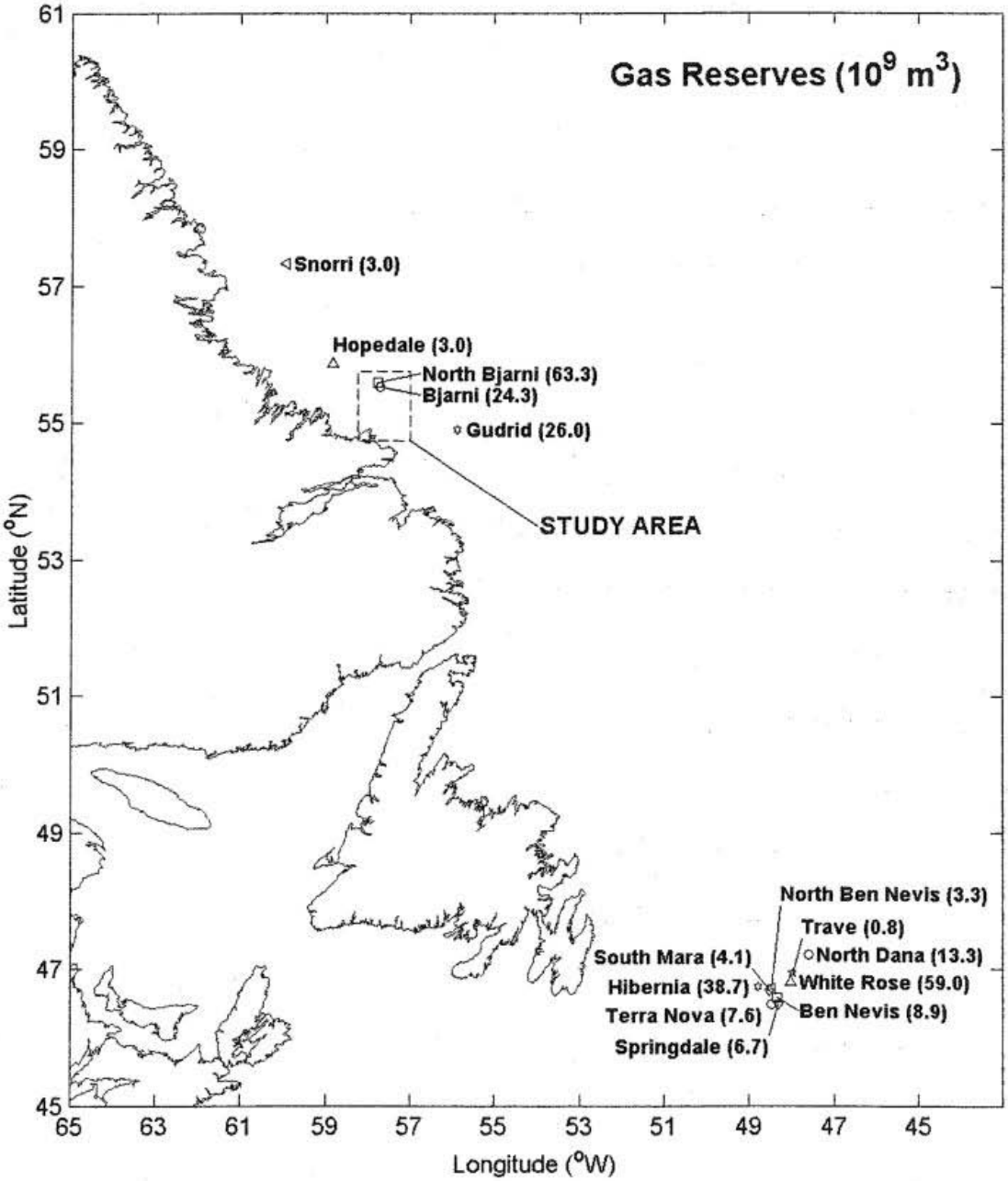

Figure 1 Offshore Newfoundland and Labrador gas reserves (CNOPB, 2001)

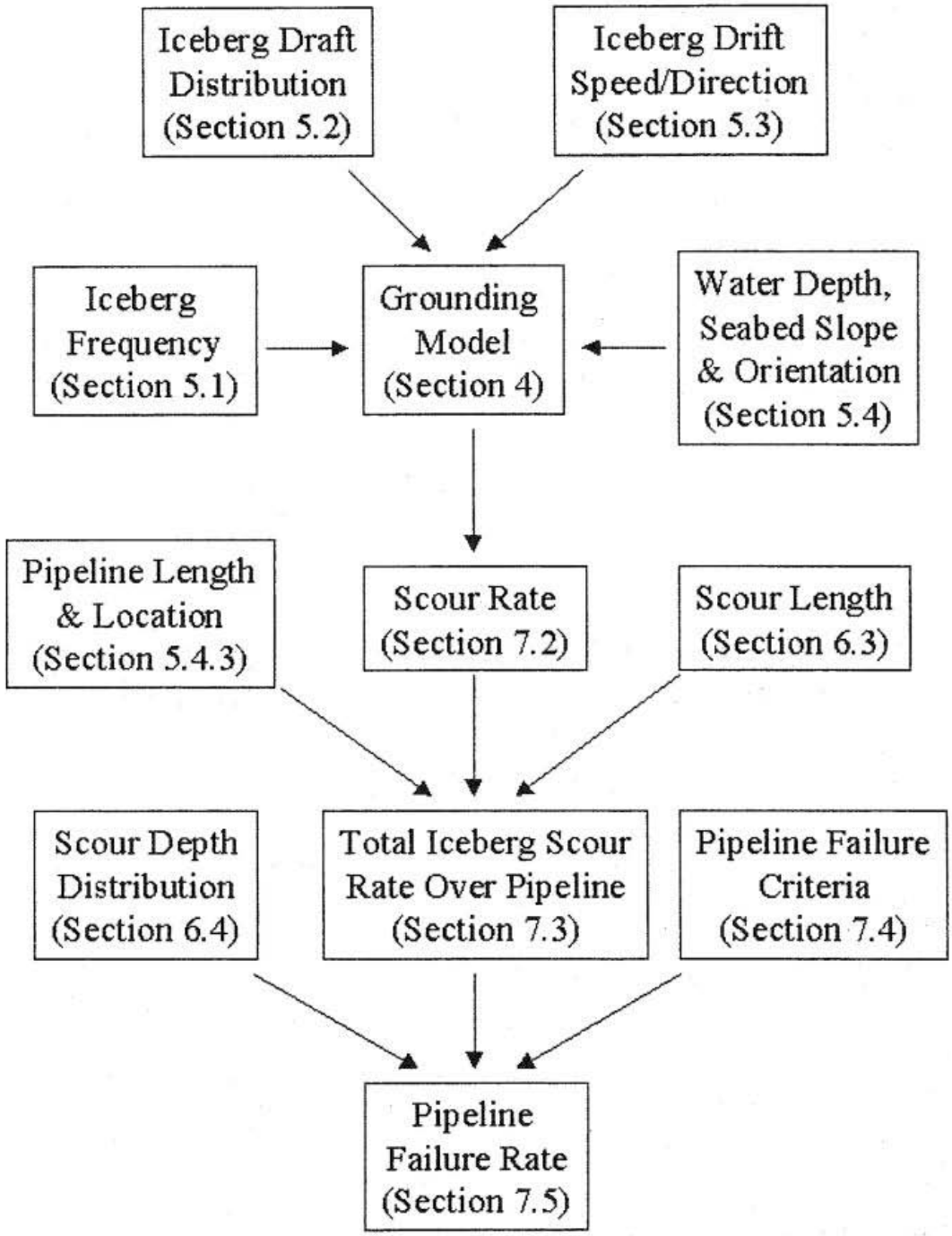

Figure 2 Flowchart showing general approach used for pipeline risk analysis

2 ICEBERG SCOUR AND RISK TO TRENCHED PIPELINES

2.1 Introduction

The purpose of this section is to provide a brief review of the iceberg scour phenomenon and the associated risk to trenched pipelines. Although there has been a substantial body of research published on iceberg scour, this is not intended to be an exhaustive review of the topic. Pipelines laid directly on the seabed are exposed to both free-floating and scouring icebergs, however the risk from free-floating icebergs is a separate issue and will not be addressed. Other approaches for protecting pipelines from ice scouring have been considered, such as protective berms, freezing the soil around a pipeline (Palmer et al., 1979), or strengthening the soil around the pipe using cement (Morgenstern and Sterne, 1980). However, the focus here will be on pipelines that have been trenched, a widely used method for pipeline protection, without the use of any additional protective measures.

No major pipelines have been constructed in areas prone to iceberg scouring, and a review of the available literature indicates no pipeline failures attributed to iceberg scouring. However, El-Tahan et al. (1985) documented 25 incidents of damage to submarine communications cables that were attributed to iceberg impact. Pipeline failures have been attributed to scouring by ice ridge keels, which are formed when sea or lake ice is rafted by environmental forces. Although the source of the ice differs, the mechanism involved in the scouring process is essentially the same, and much of the early work in ice scour risk analysis was conducted to assess the risk posed by ice ridge keel scouring to pipelines in the Beaufort Sea. The 1978/79 failure of a water supply

pipeline in Great Slave Lake was attributed to ice ridge keel scouring (Noble and Comfort, 1980). Damage to gas pipelines in Lake Erie from ice ridge keel scouring has also been reported (Grass, 1986).

The analysis of the risk posed to trenched pipelines by scouring icebergs can be broken down into three steps: (1) the assessment of the frequency of scour formation on the seabed in the vicinity of a pipeline, (2) the rate at which scours would be expected to cross a pipeline, and (3) the probability that the scour-crossing event results in damage to the pipeline.

2.2 Iceberg Scours

2.2.1 Origin of Iceberg Scours

Icebergs are formed when masses of ice calve from glaciers. The majority of icebergs in the North Atlantic originate from the west coast of Greenland, where iceberg production is concentrated in 21 glaciers (Murray, 1969). It is estimated that it takes approximately three years for an iceberg to drift from its source glacier to the Grand Banks (Kollmeyer, 1977). Figure 3 shows the general drift pattern of icebergs in the vicinity of Greenland and the east coast of Canada, along with a number of documented grounding sites (Lewis and Blasco, 1990). When an iceberg drifts into a water depth that is less than its draft, the keel can displace the sediment to form a scour or pit feature.

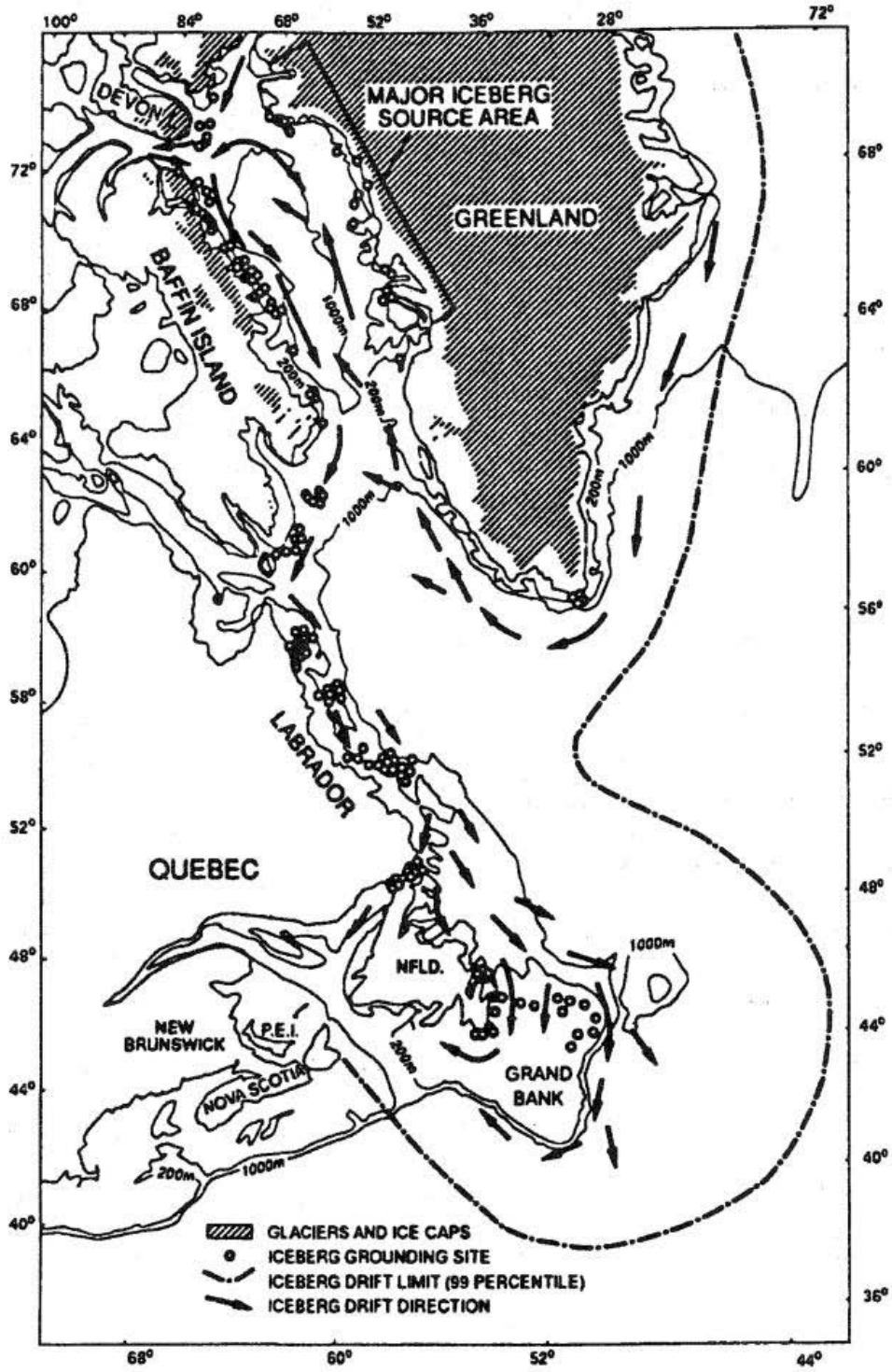

Figure 3 Iceberg source, drift pattern and known grounding sites off Greenland and Eastern Canada (Lewis and Blasco, 1990)

2.2.2 Scour Morphology

Figure 4 (from Woodworth-Lynas, 1992) shows scour features associated with an iceberg scouring through a fine-grained sediment. This figure is based on a 3-dimensional model of the iceberg "Bertha" that was observed during the DIGS (Dynamics of Iceberg Grounding and Scouring) project (Hodgson et al., 1988), conducted on the Makkovik Bank. This iceberg had a waterline length (maximum waterline dimension) of 160 m, a draft of 110 m and a mass of approximately 2 million tonnes.

As an iceberg scours through the sediment it pushes a mound of sediment (leading edge surcharge) in front of the keel that accumulates and spills to either side of the scouring keel to form berms. Woodworth-Lynas (1992) gives a detailed description of scour features observed during submersible surveys of the seabed during the DIGS project. These included blocks (1 to 2 m) of sediment on the top of the berms; smaller blocks of sediment (5 to 50 cm) on the outer flanks of the berms; a network of open fractures (<1 to 20 cm wide) on the inside of the berm; occasional dissolution voids in the scour trough (up to 2 m wide and 1 m deep), presumably formed by blocks of ice broken from the keel; and ridges and grooves on the inside the berm and the bottom of the scour, presumably caused by irregularities on the bottom of the scouring keel. When a scouring iceberg enters a slightly deeper part of the seabed (i.e. a depression or an older, deeper, scour) it will push sediment into the depression and occasionally shear off the top of any protrusions, forming flat-topped mounds. The bottoms of the scours appeared to be flat, suggesting that the iceberg keels were reshaped during the scouring process. Scours formed in non-cohesive sediments (sand) would not be expected to have the same range

of detail as those observed in cohesive sediments, however the same basic features would be observed (berms, trough, frontal mound).

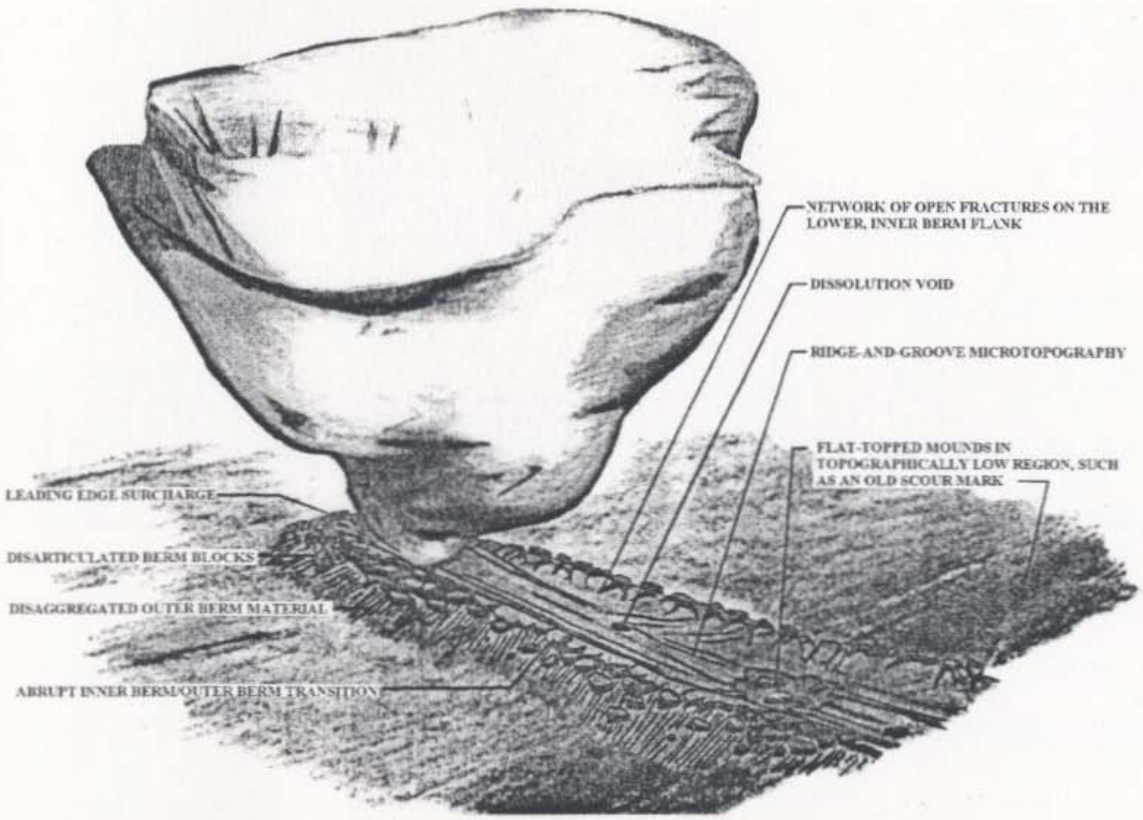

Figure 4 Iceberg scouring through fine-grained sediment, with some characteristic features indicated (Woodworth-Lynas et al., 1992, with modifications)

In addition to small-scale features, scours also display large-scale features with regards to their overall shape. Many scours are straight, but others display more complex shapes. The straight scours are classified as linear, scours with a single curve (usually the scour itself is a single large curve) are classified as arcuate, while a scour with 2 or more curves is classified as sinuous (Geonautics, 1989).

Figure 5 (Geonautics, 1989) shows the scour dimensions that would be typically be recorded. Berm height is not a consideration for pipeline risk. Detailed discussion of the parameters relevant to pipeline risk may be found in Chapter 6. It is worth noting that the scour width is defined as the distance between the top of the berms, rather than the width of the incision. Incision width can only be determined accurately using high quality sounder data, and cannot be measured at all using sidescan data, however berms are relatively easy to discern. The result is a systematic overestimation of scour width. The orientation of the vessel relative to the scour is required to apply the appropriate corrections to the data for measuring width. Scour depth is an important factor in pipeline risk, however interpreting scour depth is complicated by the presence of scours with depths less than the resolution of the measuring system (PERD, 2000). Measurements of scour length can be complicated by the fact that scours often extend outside the survey area. Average scour lengths on the Grand Banks are on the order of 0.6 km (PERD, 2000), but an extreme scour length of 24 km has been inferred on the Grand Banks from trajectory data (Banke, 1989a). Approximately 11 km of this scour has actually been verified from seabed surveys. Some very long scours have also been

inferred from iceberg trajectory data on the Labrador Shelf, (Woodworth-Lynas and Simms, 1985) but none of these have been verified from seabed records.

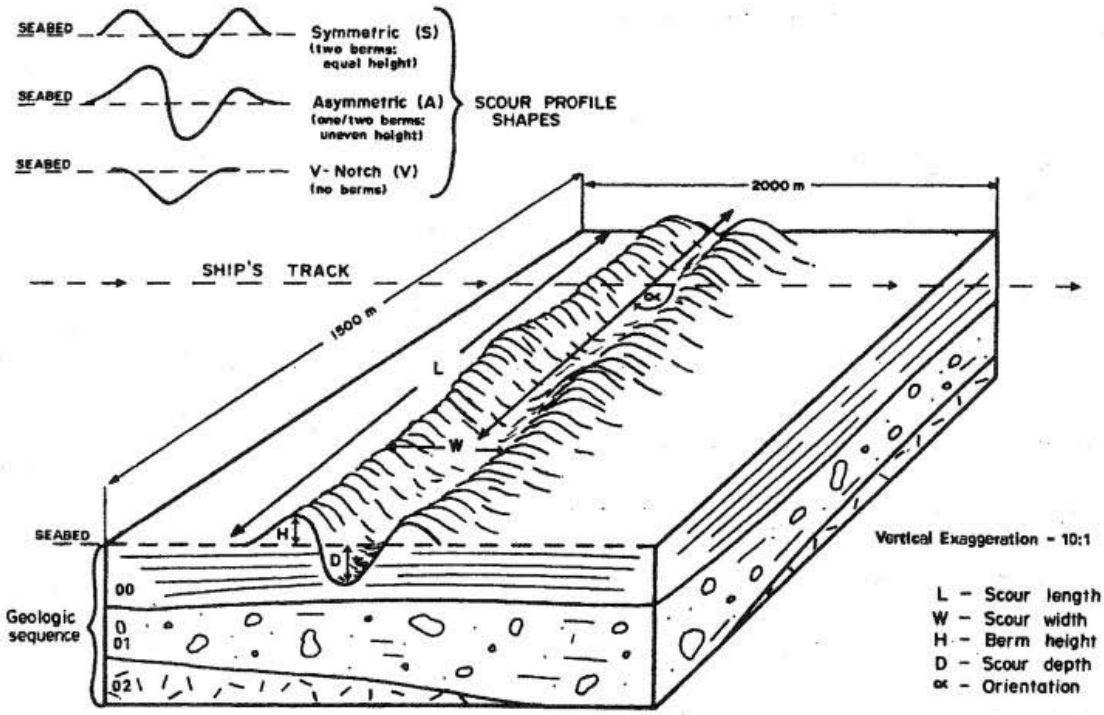

Figure 5 Iceberg scour showing relevant dimensions (Geonautics, 1989)

Figure 6 shows a sidescan mosaic from the Saglek Bank on the Labrador Shelf in 172 m water depth. This mosaic shows the extremely dense scouring that can be observed on the Labrador Shelf.

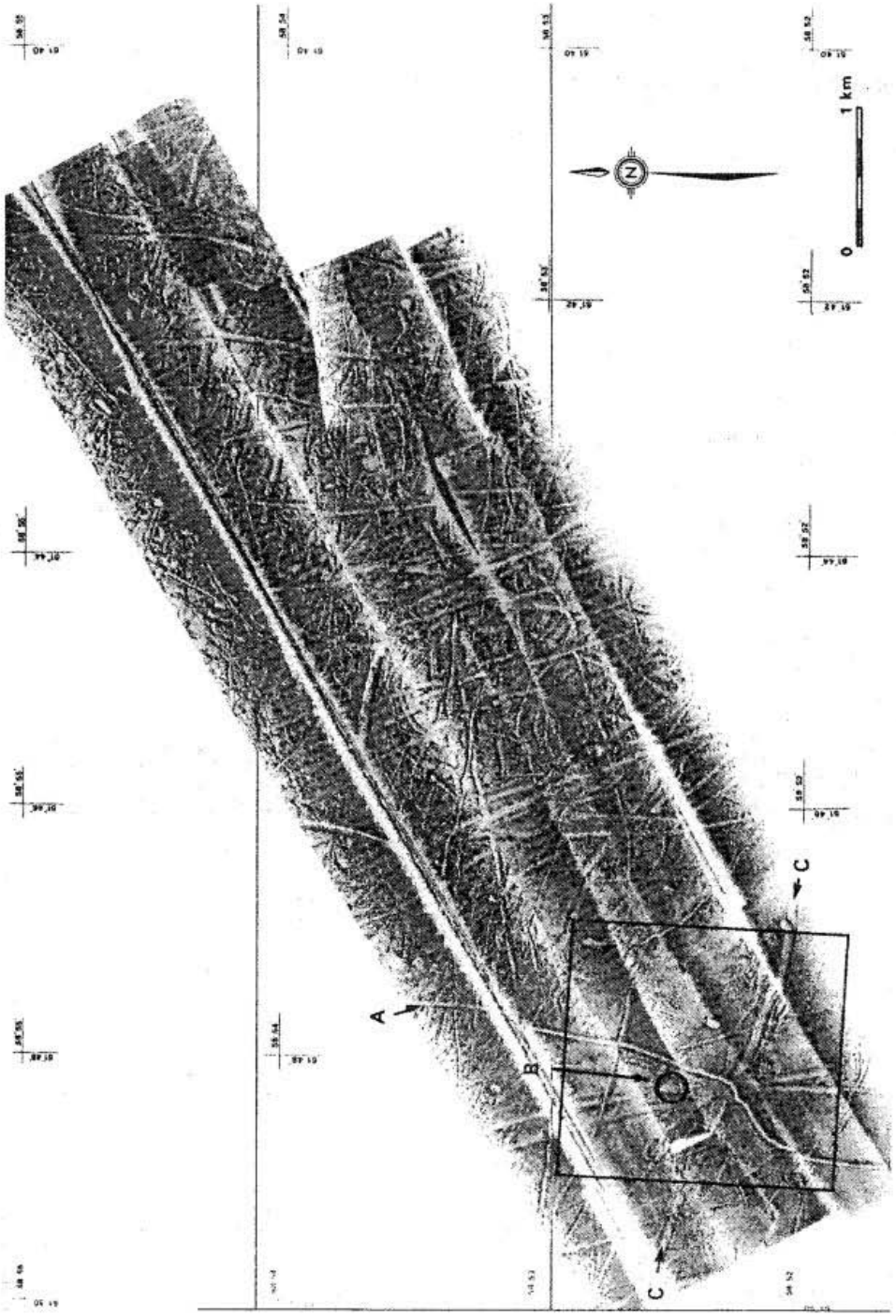

Figure 6 Sidescan sonar mosaic recorded on the Saglek Bank in 1979 in 172m of water showing location of submersible dive and two prominent furrows, "A" and "C", and a large pit, "B" (Hodgson et al., 1988)

2.2.3 Relict Scours

One of the factors that complicate the interpretation of scour parameters from seabed records is the presence of relict scours. A relict scour is a very old scour that may have been formed during a previous ice age and is not considered representative of the modern scouring regime. Relict ice scours have been excavated on the prairies (Woodworth-Lynas, 1993) and observed preserved in "fossil" form in rock. Relict scours have also been documented in the Laurentian Channel and on the St. Pierre Bank (King, 1976), which are areas not normally associated with modern-day ice scour. Although these scours were not dated, it has been estimated that there has not been any significant source of icebergs in the region within the last 12,000 years (King, 1976). An analysis of pollen in a sediment core from an iceberg pit off Notre Dame Bay at 260 m water depth indicated an age of 9500 years, while the analysis of a core from a scour in Conception Bay at a water depth of 183 m indicated an age of 6500 years (Mundie, 1986). These observations emphasize the extreme age of some of these features. Fillon and Harmes (1982) stated that the deglaciation of the Saglek Bank, on the northern Labrador Shelf, occurred between 8400 to 6000 years ago. This is within the age range noted for relict scours on the Grand Banks and suggests that relict scours should also be common in the vicinity of the Makkovik Bank.

Relict scour marks have also been observed in water depths greater than is generally considered to be possible for modern scouring. Lewis and Blasco (1990) report scours at water depths of 750m, well beyond the maximum observed iceberg draft of approximately 230m. These relict scours also tend to be wider and deeper than modern

scours. Observations on the Labrador Shelf indicate the distribution of relict scour orientation can differ significantly from that of modern scours, presumably due to differing iceberg drift patterns (Todd, 1988).

The presence of relict scours interferes with the derivation of scour parameters in various ways. Relict scours, which tend to be both wider and deeper than modern scours, influence the evaluation of these parameters for modern scours when it is not possible to make a distinction between the relict and modern scours. Although relict scours can be observed in very deep water, a mixture of relict and modern scours have been noted in water depths around 180 m (Barrie, 1980). It is not unlikely that some of the less distinct scours seen in Figure 6 are relict. Thus, estimations of scour rate based solely on the density of scours observed on the seabed can be influenced by the presence of relict scours.

2.2.4 Iceberg Pits

Iceberg pits are circular or near-circular seabed features formed by grounding icebergs. Several pit features are visible in Figure 6. Pits can form in a number of ways. A grounding iceberg may have insufficient driving forces to initiate scouring and become grounded, forming a depression on the seabed. Similarly, a scouring iceberg may stop due to insufficient driving forces and become grounded. A bearing capacity failure due to oscillatory wave loading, and potentially liquefaction of the seabed sediment, results in the formation of a pit (Davidson and Simms, 1997). Alternatively, as observed during DIGS (Hodgson et al., 1988), an iceberg rolling or splitting event may result in the

iceberg striking the seabed energetically, forming a pit. Bass and Woodworth-Lynas (1988) have also documented several cases of chains of craters observed during seabed surveys of the Labrador Shelf. Pits as deep as 10 m have been documented on the Grand Banks (Barrie et al., 1986), however the mean pit depth is on the order of 1.2 m (C-CORE, 2001b). The risk to trenched pipelines from pits, as opposed to scours, is less because the average pit covers a smaller area than the average scour and there are fewer pits than scours. For pipelines at White Rose, the risk from pitting icebergs was less than 10% of the risk from scouring icebergs (C-CORE, 2001a).

2.3 Scour Formation Rate

The scour rate is a significant factor in assessing risk to trenched pipelines. A number of methods have been employed to estimate the rate at which iceberg scours form on the seabed. These methods are described and their potential application to assessing scour rates on the Makkovik Bank are discussed.

2.3.1 Repetitive Mapping

Repetitive mapping allows the scour rate to be calculated directly from the surveyed area, using the number of new scour features observed and the time interval between surveys. The area surveyed, the scour rate, and the resolution of the instrumentation used to survey the seabed are all considerations when using this approach. The relatively low scour rate on the Grand Banks has resulted in few new scours being observed during repetitive mapping exercises. Lewis et al. (1986) could not positively identify any new scours while resurveying 130 km of line data on the Grand banks, however using a statistical

approach a scour rate of 1×10^{-3} scours/km^2/year was estimated. Meyers et al. (1996) identified 2 new scours from resurveyed lines between Hibernia and White Rose, allowing a scour rate of 6.7×10^{-4} scours/km^2/year to be estimated based on an elapsed period of 11 years and a total survey area of 273 km^2 (based on a total line length of 700 km and a swath width just under 400 m). The results of two other repetitive mapping efforts (i.e. Geonautics, 1991) yielded similar results. It was concluded by Geonautics (1991) that the use of mosaics providing 100% seabed coverage would be required to reliably assess scour rates.

Geonautics (1987) discussed the establishment of a repetitive mapping network using a site on the Makkovik Bank It was thought that substantially higher iceberg densities at this site would yield a significant number of new scours when the seabed was resurveyed, resulting in more reliable estimates of scour rates. The site recommended by Geonautics (1987) was later surveyed during the DIGS study (Hodgson et al., 1988), and was referred to as the "repetitive mapping mosaic". Three other sites were also surveyed during DIGS (see Figure 60). Also shown are two surveys by Geomarine (1976, 1980) and two other mosaics for which the source has yet to be determined. Therefore, the potential exists to use repetitive mapping to determine the scour rate on the Makkovik Bank based on existing survey data, however the cost of this exercise would be a consideration.

2.3.2 *Scour Rates Based on Observed Scour Density*

A number of approaches have been used to estimate scour rates from the observed density of scours on the seabed. Amos and Barrie (1982) estimated scour rates between 5×10^{-4} and 6×10^{-3} scours/km^2/year in the vicinity of Hibernia using the assumption that scours observed to cut through megaripple fields on the seabed were formed since the previous storm event capable of mobilizing the seabed, a period that they conservatively assumed to be 20 years. Gaskill et al. (1985) used scour density, scour depth distribution and sediment infill rates to obtain scour rates ranging from 9×10^{-6} (Hibernia) to 1×10^{-4} scours/km^2/year for various sites on the Grand Banks. Lewis and Parrott (1987) used sediment infill rates to estimate a scour rate of 3.3×10^{-3} scours/km^2/year for the Hibernia region. Woodworth-Lynas (1983) proposed an approach that required dating a limited number of scours using sediment cores and using scour cross-cutting relationships to determine scour rates. However, this approach has not yet been used to determine scour rate.

The method that is currently most often used to estimate scour rates on the Grand Banks is based on the inception of modern scouring. Lewis et al. (1987) suggested that modern scouring began on the Grand Banks about 2500 years ago with the strengthening of the inner branch of the Labrador Current, and used this as a basis for calculating a scour rate of 4×10^{-4} scours/km^2/year for the Hibernia site. This scouring period has also been used to calculate scour rates of 1×10^{-3} scours/km^2/year for the White Rose site (C-CORE, 2001b), based on observed scour densities at these sites. This technique is suited to shallower water depths on the Grand Banks since relict scours are not present.

The use of scour density to calculate scour rate is not suited to the Makkovik Bank due to insufficient data regarding sediment mobility, sedimentation rates, the age of specific scour marks, or the time since the inception of modern scouring (if applicable). The presence of relict scours is an additional complicating factor. However, scour rates for which there are a reasonable degree of confidence could be used to calibrate a numerical model that could then be applied to the Makkovik Bank.

2.3.3 Grounding Models

Scour rates can be estimated using iceberg frequency, draft distribution and bathymetry. The AGC grounding model (d'Apollonia and Lewis, 1986) divided the seabed floor into a grid with a cell size of 5 nautical miles, and calculated the number of iceberg groundings from the range of water depths for each cell, the annual number of icebergs drifting into each cell, and the iceberg draft distribution. Icebergs were introduced at a specified rate along an arbitrary line of latitude (i.e. 400 icebergs/year at 48°N for the Grand Banks), with an east/west distribution based on the distribution of iceberg sightings. A number of options were available with this model, including: a choice of four different draft distributions (Geomarine, 1987), the ability to simulate melting and degradation by constantly decreasing the number total number of icebergs as a function of southward drift, uniform southerly drift and non-uniform drift, and truncating the iceberg draft distribution according to the water depth.

The results obtained from the AGC grounding model depended on the particular set of input parameters used. Lewis and Parrott (1987) used the AGC grounding model to obtain a grounding rate of approximately 4×10^{-4} scours/km^2/year for the Hibernia site, however they noted that using an alternate draft distribution yielded a scour rate an order of magnitude higher. Lewis et al. (1987) showed results from the AGC grounding model that indicated grounding rates of 3.5×10^{-3} scours/km^2/year for the Hibernia site. Figure 7 shows grounding rates calculated for the Grand Banks and the Makkovik Bank (d'Apollonia and Lewis, 1986). Grounding rates of approximately 2×10^{-3} and 0.1 scours/km^2/year were predicted for the Hibernia and Bjarni sites, respectively. Geonautics (1987), who also calculated comparable grounding rates for the Makkovik Bank, made a comparison with grounding rates inferred from iceberg trajectory data collected during drilling operations and concluded that the AGC model predicted grounding rates that were several times higher. It appears that, due to the lack of sites with known grounding rates, that the AGC model was never properly calibrated. If this had been the case, the proper combination of input parameters could have been assessed.

More recently, PERD (2000) applied a simplified approach using the iceberg draft distribution and the annual iceberg flux and water depth range in the Hibernia degree square to estimate a scour rate of 4×10^{-4} scours/km^2/year.

It is possible to use a numerical model to predict scour rates for the Makkovik Bank. However, the model would have to be calibrated by using sites where scour rates have been determined with a reasonable degree of certainty using alternate methods (i.e.

inception of scouring) and comparing those values with scour/grounding rates calculated from the model.

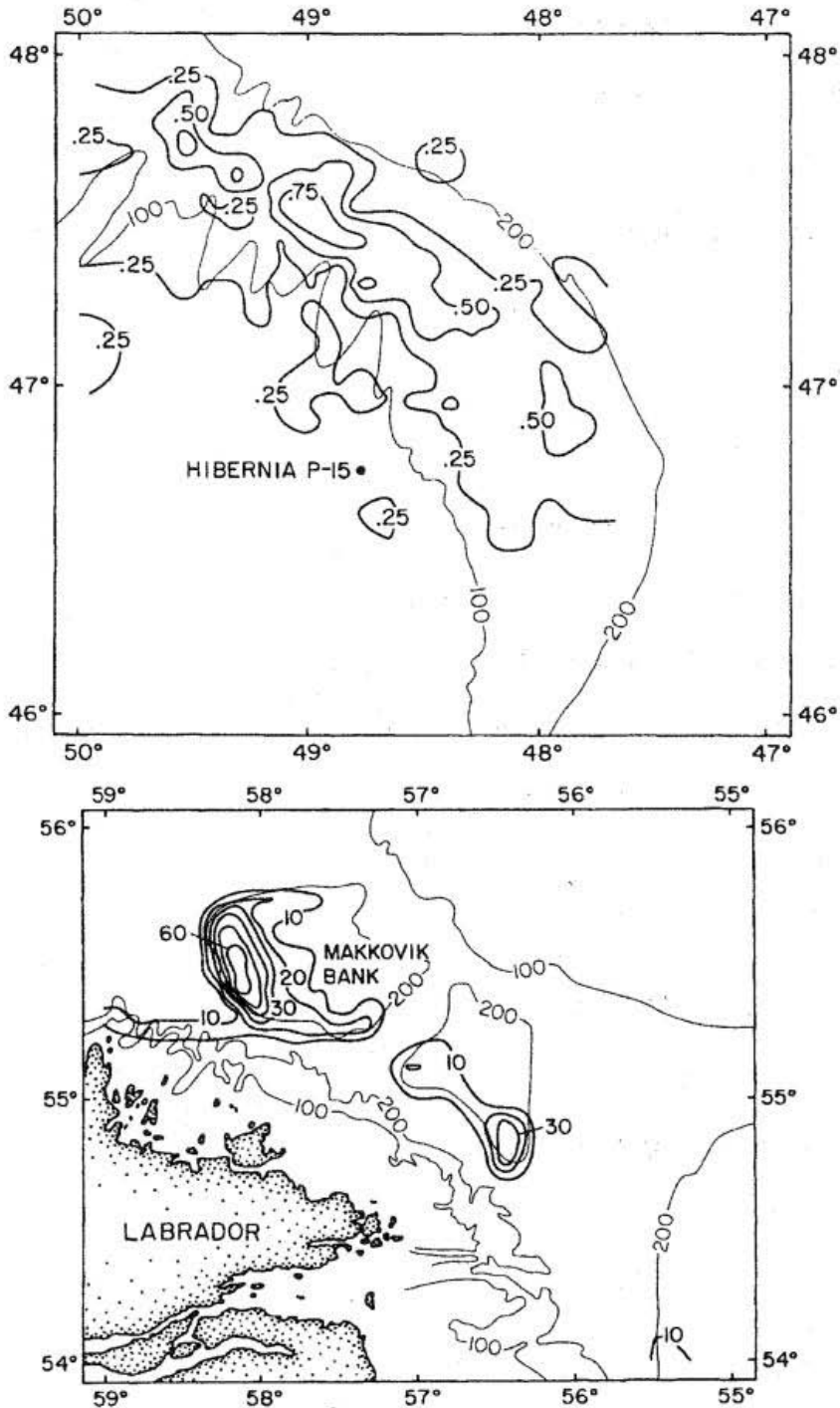

Figure 7 Grounding rates (#/100km^2/year) from AGC model (from d'Apollonia and Lewis, 1986) for Grand Banks (top) and Makkovik Bank (bottom)

2.3.4 Groundings Inferred from Iceberg Trajectory Data

Many icebergs that ground remain in contact with the seabed and are immobile for a considerable period of time. Grounding durations as long as a month have been reported on the Labrador Shelf (El-Tahan et al., 1985). Several studies have focused on analyzing iceberg trajectory data, to determine grounding frequencies (Barrie et al., 1981; Woodworth-Lynas et al., 1985; El-Tahan et al., 1985; Banke, 1989b), which, in turn, could be used to estimate iceberg scouring frequencies. Most of the iceberg trajectory data used during these studies was in the form of radar sightings from drill-rigs.

It was recognized that many iceberg groundings would not necessarily result in extended periods of immobility. Various criteria were defined to allow iceberg trajectory data to be used to determine grounding events based on relatively brief periods of immobility. Barrie et al. (1981) identified icebergs having a constant range and bearing for 4-6 hours or more, exhibiting erratic motion or extremely slow drift speeds as being grounded. Woodworth-Lynas et al. (1985) classified icebergs exhibiting no motion for more than 12 hours as being grounded, with shorter periods classified as possible groundings. El-Tahan et al. (1985) considered iceberg sighting from drill-rig and shore-based radar, satellite telemetry and from International Ice Patrol surveys, and developed different classification systems for each data source. For drill-rig sightings, icebergs immobile for less than 6 hours were not considered to be grounded, icebergs immobile for 24 hours or more were considered positive groundings, and icebergs immobile for periods of 6 to 24 hours were classified (no grounding, probable grounding or positive grounding) using the motion of other icebergs, reports from ice observers, environmental forces and

comparisons of measured iceberg drafts to water depth. Banke (1989b) considered icebergs immobile for 24 hours or more in water depths less than 200 m to be definite groundings.

Based on an analysis of iceberg track data collected on the northeast Grand Banks from 1983 to 1989, Banke (1989b) estimated the grounding frequency to be approximately 2×10^{-4} groundings/km^2/year, which is lower than scour rates based on seabed records, but comparable in magnitude. Including probable groundings increased this value 50%. C-CORE (2001d) identified 9 potential grounding events (Figure 8) on the Grand Banks during the 2000 iceberg season, based on an analysis of iceberg trajectories, ship reports and environmental driving conditions. All these groundings occurred in 130 m water depth and less. Using the area in Figure 8 less than this depth (≈14,500 km^2) gives an approximate grounding rate of 6×10^{-4} groundings/km^2/year, which compares fairly well with values from other sources. Other studies (Barrie et al., 1981; Woodworth-Lynas et al., 1985; El-Tahan et al., 1985) focused primarily on icebergs on the Labrador Shelf and reported their results in terms of the percentage of icebergs that grounded, rather than the frequency or density of grounding events. Barrie et al. (1981) reported an average of 9% of icebergs grounding once or more on the Makkovik Bank (two years of data), while Woodworth-Lynas et al. (1985) reported 3% and El-Tahan et al. (1985) reported 6% (seven years of data).

A comparison of the grounding rates for the Makkovik Bank indicates that the results depended on the grounding criteria used and the interpretation of the data. An analysis of

available iceberg track data for the Makkovik Bank could be performed to give an estimate of grounding rate (#/km^2/year) for verification purposes, however the reliability associated with this approach would not make it suitable as a sole means of assessing grounding rates.

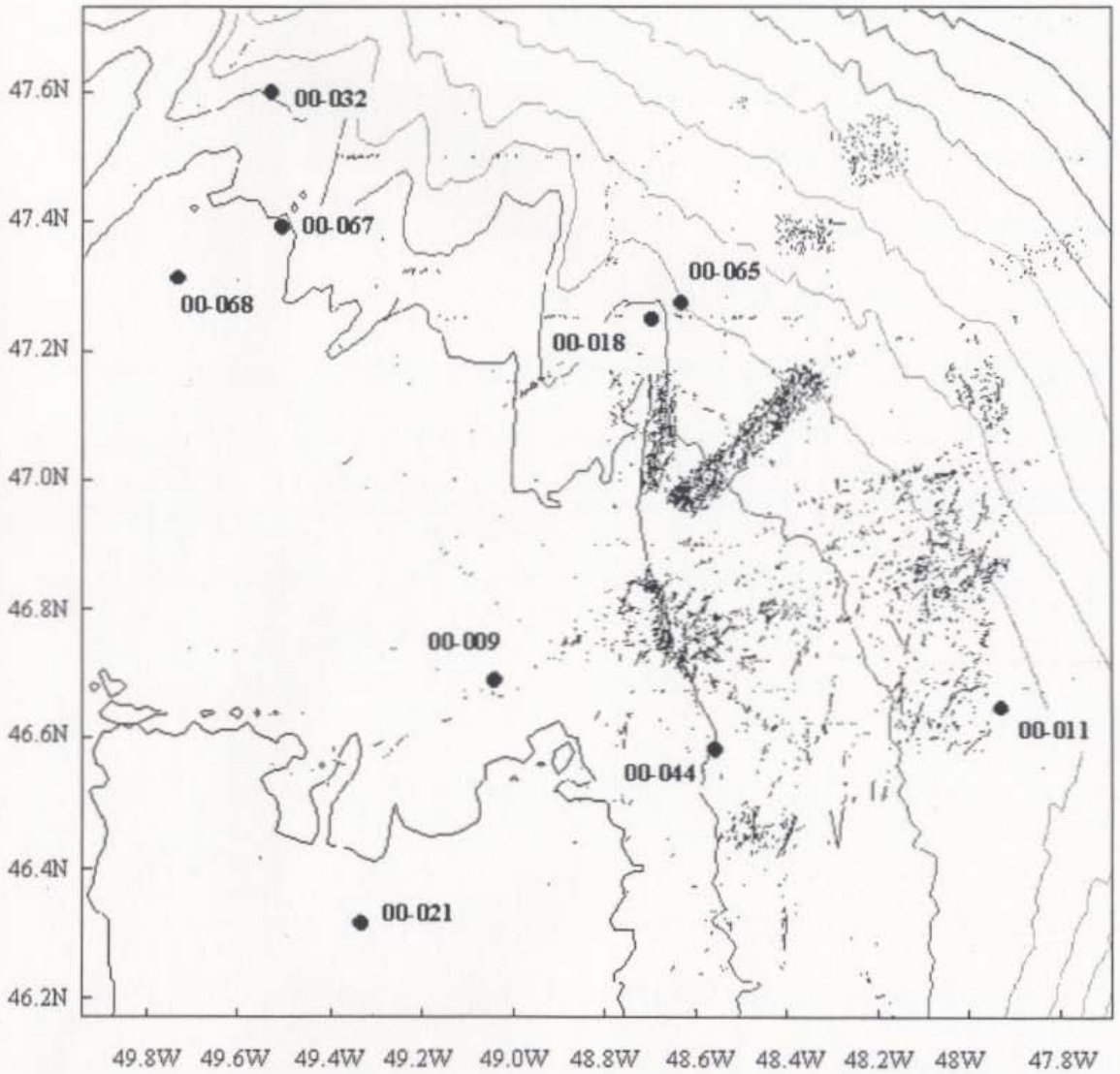

Figure 8 Iceberg groundings (with associated iceberg identification numbers) during 2000 iceberg season (C-CORE, 2001d), along with iceberg scour features from Grand Banks Scour Catalog

2.4 Frequency of Pipeline Scour Crossing Events

A number of approaches have been proposed to estimate the rate at which scours cross over a pipeline. Allan (1986) described a method that used iceberg frequency, drift pattern, draft distribution, scour riseup and water depth to calculate scour crossing frequency for pipelines. This was also the approach used by Petro-Canada (1983) for the Bjarni Development Study and is discussed in greater detail in Chapter 3. Pilkington and Marcellus (1983) proposed a similar method for estimating ice ridge keel crossing rates that involved the use of the keel draft distribution and drift speed. These approaches essentially incorporated a scouring model directly into the scour-crossing calculation. The emphasis here will be on methods that used grounding or scouring rates assessed independently (through modeling, seabed surveys or trajectory analysis) along with some scour parameters (i.e. length, width, orientation) to calculate pipeline scour crossing frequencies. These relationships were originally developed to assess ice ridge keel crossing rates, however they apply equally well to iceberg scours.

Weeks et al. (1983) proposed a relationship describing the total number, N, of ice features that would scour over a pipeline during its proposed lifetime:

$$N = \overline{g} T L_p \sin\gamma \tag{2.1}$$

where $\overline{g}$ is the average number of scours per kilometer per year occurring along the pipeline route, T is the proposed lifetime of the pipeline (years), L_p is length of the pipeline and γ is the angle between the pipeline route and the gouges. The gouge frequency, which was assessed from an analysis of the scour density on the seabed, was

expressed in terms of a linear, rather than areal, basis. This can be reconciled with current scour rate statistics, as will be discussed.

Nessim (1986) developed the following relationship to predict the number of scours, λ_θ, per unit length of a linear track (i.e. pipeline) with an orientation ϕ:

$$\lambda_\theta = \rho \bar{l}_s \int_0^\pi |\sin(\phi - \alpha)| f(\alpha) d\alpha \tag{2.2}$$

where ρ is the areal density of scours, $\bar{l}_s$ is the mean scour length, α is the scour orientation and $f(\alpha)$ is the associated probability density function.

Gaskill and Lewis (1988) derived the following relationship to calculate the probability, $P(I)$, that a given scour would cross over a pipeline:

$$P(I) = \frac{2 l_s L_p}{a\pi} \tag{2.3}$$

where l_s is the scour length, L_p is the pipeline length, and a is the area of the region around the pipeline in which the scour can form. A random distribution of scour direction and a constant scour length was assumed.

Astafyev et al. (1997) developed a method for calculating the number of scours crossing a pipeline based on Buffon's Needle, which is a classical problem that considers the probability of a needle dropped on a lined piece of paper crossing a line (the needle length was assumed to be less than the spacing between the lines). Assuming many needles (or scours) with a uniform distribution (density and orientation) on a surface, a solution was developed for the crossings of one line (or pipeline) of the form:

$$N = \frac{2}{\pi} L_p \rho \bar{l}_s \tag{2.4}$$

where N is the number of crossings, L_p is the pipeline length, ρ is the scour density and $\bar{l}_s$ is the mean scour length.

PERD (2000) gave a relationship describing the annual number of icebergs scouring to a specified depth over a pipeline. If the term describing keel penetration depth is set to a value of one, all scour crossings are calculated, giving an annual number of pipeline crossings, N_a, of:

$$N_a = f_{sc}(\overline{B} + \langle L_p |\sin(\alpha - \phi)| \rangle \bar{l}_s \tag{2.5}$$

where f_{sc} is the scour rate (#/unit area/year), $\overline{B}$ is the mean scour width, L_p is the pipeline length, α is the scour orientation, ϕ is the pipeline orientation and $\bar{l}_s$ is the mean scour length.

For all intents, the previous equations can be treated as equivalent. The $\overline{g}$ term from the Weeks et al. (1983) equation can be calculated directly from the scour rate and average scour length. The Gaskill and Lewis (1988) equation considers one scour, but this would be equivalent to scour rate if the average time interval between scour events was included and the event was averaged over the specified area, a, essentially reducing this equation to the same form as that developed by Astafyev et al. (1997). The PERD (2000) equation includes average scour width, however this is actually a very minor term if it is considered that the mean scour width for the Grand Banks is 25 m and pipelines typically are on the order of kilometers long. The PERD (2000) equation does not explicitly give

an integration term, as does Nessim (1986), but this seems to be implied. The Nessim (1986) equation seems to be the most complete of the equations, in that it includes the distribution of scour orientations. If the scour orientation is uniform, Nessim's equation is equivalent to that derived by Astafyev et al. (1997).

2.5 Probability of Scour Crossing Event Causing Pipeline Failure

Once the rate at which scours cross the trenched pipeline has been established, the proportion of these events that cause failure of the pipeline is required in order to calculate the overall failure rate. The following sections describe various approaches to this problem.

2.5.1 Direct Pipeline Contact

Initially, it was assumed that direct contact between the keel and the pipeline was required to cause damage to a pipeline. Therefore, the probability that a scour event would cause damage to a pipeline was based solely on the distribution of scour penetration depths (e.g. Pilkington and Marcellus, 1981; Petro-Canada, 1983; Weeks et al., 1983; Gaskill et al., 1985; Allan, 1986; Pilkington, 1986). For example, Pilkington (1986) gave the following relationship:

$$N_D = N_a T e^{-kC} \tag{2.6}$$

where N_D is the number of scours reaching a specified depth, N_a is the annual number of scour crossings for a pipeline, T is the lifetime of the project, k is a constant describing the exponential distribution of gouge depths and C is the pipeline cover depth. Equation 2.6 can be solved explicitly for burial depth if all other parameters (including the

acceptable number of keel contacts) can be determined. However, this approach is no longer acceptable, since it does not account for soil deformations below the scouring keel.

2.5.2 Subscour Soil Deformations and Pipeline Response

Soil deformations have been observed during excavations of exposed relict ice scour features (Woodworth-Lynas, 1993), although the soil motions observed are primarily in the vertical direction. Been et al. (1990) described the types of deformations expected to occur beneath a scour. Figure 9(from PERD, 2000) shows an ice feature creating a scour mark in sediment. Figure 9(a) shows the creation of a rupture surface in front of the advancing keel. Figure 9(b) shows several features: a frontal mound of sediment that accumulates in front of the keel, a "dead wedge" of sediment in front of the keel that remains relatively stable, and a rupture surface that defines the failure plane in the soil. Also shown are three zones: (1) soil is displaced by the keel (any pipeline would be contacted directly), (2) soil undergoes plastic deformation, decreasing in magnitude with depth (potentially causing significant loads in a pipeline), and (3) soil undergoes very little deformation. Figure 9(c) shows the vertical movement of soil directly in front of the advancing keel. While a number of analytical models have been developed to estimate scour reaction forces (e.g. Chari, 1975; Fenco, 1975; Been et al., 1990; Surkov, 1995; Walter and Phillips, 1998) these have not been useful for assessing soil deformations. This has largely been accomplished through physical modeling.

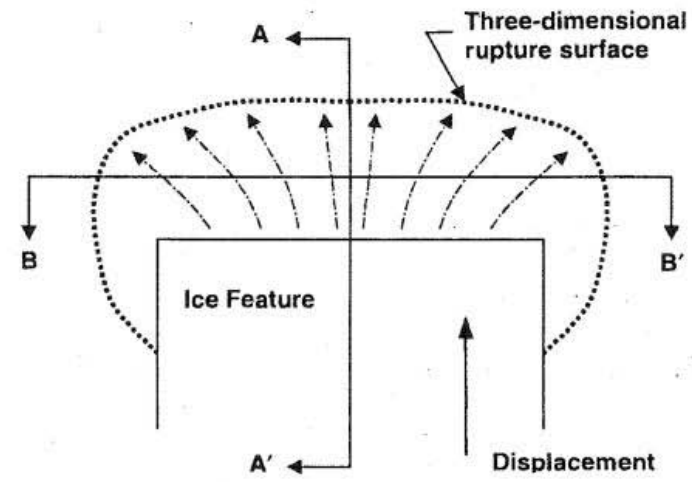

(a)

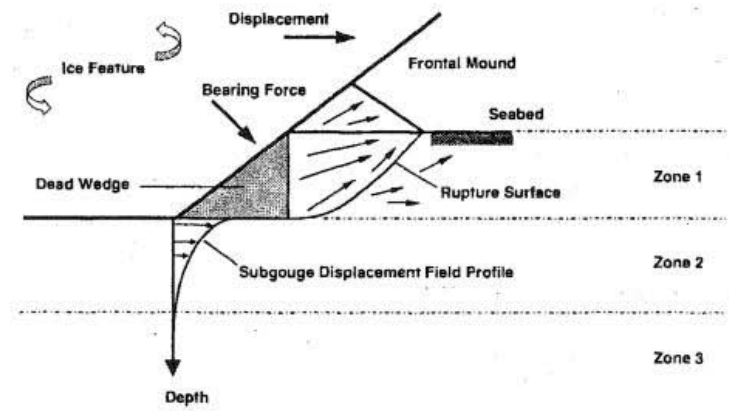

(b)

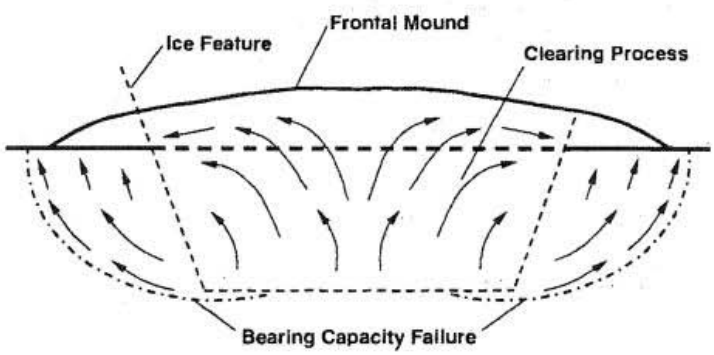

(c)

Figure 9 Ice gouge mechanisms (a) plan view, (b) section A-A′, (c) section B-B′ (PERD, 2000) see text for description.

Numerous laboratory studies have been conducted to model the scour process (e.g. Chari, 1975; Abdelnour et al., 1981; Dunwoody, 1984; Green, 1984; Weaver et al., 1988; Poorooshasb et al., 1989; Been et al., 1990; Paulin, 1992; PERD, 2002), however only a few of these have addressed subscour deformations. Weaver et al. (1988) used passive markers buried in the soil, however no results were reported. Poorooshasb et al. (1989) reported vertical deformations in the test bed, but did not address horizontal deformations. Been et al. (1990) and Paulin (1992) used passive markers buried in the test bed and determined soil displacements by excavating the markers and performing a post-test survey.

Some studies have been reported that measured the response of instrumented model pipelines to soil deformations during simulated ice scouring events. These tests were performed in order to calibrate numerical and analytical models. Green (1984) used a 0.5 m wide model keel and a 0.13 m diameter plexiglass model pipeline equipped with flush-mounted pressure transducers. Green used model keels with vertical and inclined faces and noted that soil resistance and pipeline response was higher with the inclined face. Green also noted that the zone of influence extended below the model keel. Weaver et al. (1988) described a ¼ scale test facility (ISPI, or Ice-Soil-Pipeline Interaction Facility) established by Esso Resources Canada Limited in Calgary. A 3 m wide model keel was pushed, using a 1 MN reaction frame, towards a 30 m long pipeline buried at depths up to 1 m. The pipeline was instrumented with strain gauges and additional instrumentation was used to measure keel displacements and loads, soil surface movements, soil pressures and soil deformations. No test results were shown and no further reports of this facility

could be located, therefore it is assumed that results of the program were proprietary. Kioka et al. (2001) described field tests that involved dragging a 2 m wide model keel over a 30 mm diameter, 6 m long pipeline. Two sites with different slopes were used and the weight of the keel was varied using ballast. The model keel was dragged over the pipeline in a direction parallel to the pipe orientation and pipeline strains and horizontal keel reaction forces were monitored.

Centrifuge modelling allows stresses or pressures in soil due to self-weight to be reproduced in models, reduced in size by a factor N, by the application of a centripetal acceleration field with a magnitude N times normal gravity (Schofield, 1980). Centrifuge modelling of iceberg scour has been conducted at Cambridge University (Lach, 1996) and at C-CORE in St. John's, Newfoundland (Hynes, 1996; Woodworth-Lynas et al., 1996). Lach (1996) used a 0.1 m wide keel and performed tests at 100 g's (100 times normal gravitational acceleration) using kaolin clay. Figure 10 (top) shows the test configuration used by Lach (1996). A similar configuration was used by Hynes (1996) for tests in sand at 100 g's and for the centrifuge tests conducted as a component of PRISE (Pressure Ridge Ice Scour Experiment), which modeled scouring in both sand and clay (Woodworth-Lynas et al., 1996) at 150 g's. Horizontal and vertical reaction forces were monitored during the scouring process and soil deformations were monitored using passive markers (coloured spaghetti strands, as well as lead solder or lead shot). Figure 10 (bottom) shows sub-scour deformations observed in a clay test bed, as indicated by the deformations of embedded spaghetti strands (Woodworth-Lynas et al., 1996).

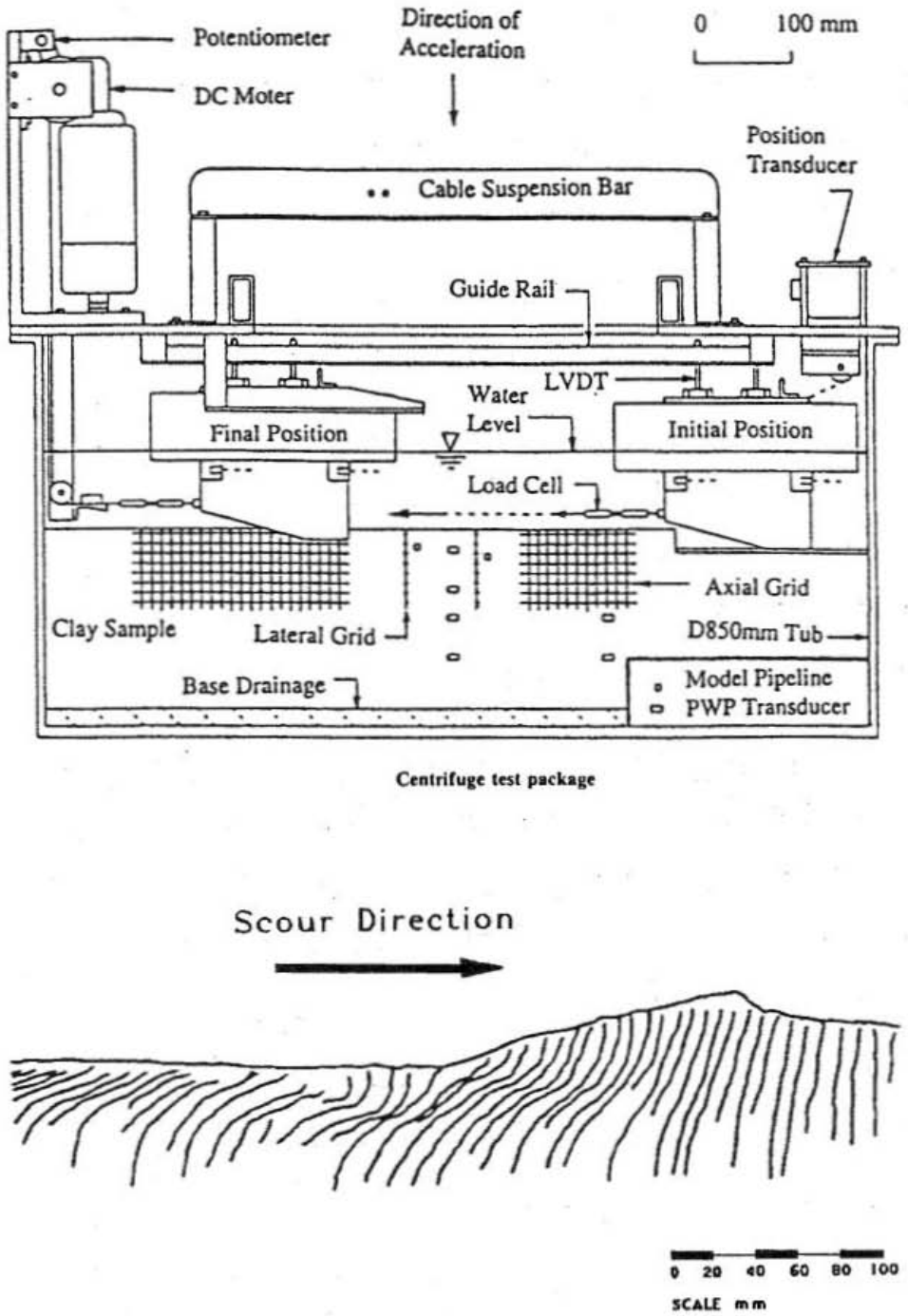

Figure 10 Centrifuge test package for modeling scour (top, Yang et al, 1996) and subscour deformations observed using passive markers in clay (Woodworth-Lynas et al., 1996)

Woodworth-Lynas et al. (1996) presented relationships, based on the results from the PRISE program, that give soil displacements as a function of gouge dimensions. The horizontal soil displacement directly under the center and in the direction of the iceberg scour, *u(0,0,0)*, is given by:

$$u(0,0,0) = 0.6\sqrt{BD} \tag{2.7}$$

where B is the scour width and D is the scour depth. The corresponding displacement, u(0,0,z), at various depths, z, below the bottom of a scour with depth, D, is given by:

$$\frac{u(0,0,z)}{u(0,0,0)} = e^{-\frac{2z}{3D}} \tag{2.8}$$

Relationships were also given for the horizontal displacement of the centerline of the scour, as well as the vertical displacement. Woodworth-Lynas et al. (1998) described a number of soil features observed during the PRISE centrifuge tests that correspond to those observed in large-scale naturally occurring scour marks.

Kenny et al. (2000), PERD (2000) and C-CORE (2001a) have presented results of finite element modeling of pipeline response due to sub-scour soil deformation, based on the sub-scour parameters developed from the PRISE program. Figure 11 shows a representation of the finite element model. To perform a finite element analysis of this type, many parameters must be specified (e.g. pipeline diameter, wall thickness and material properties, internal and external pressure, burial depth, scour depth, scour width, subscour deformation profile, and various soil parameters). The results of the finite element analysis can then be used, along with the gouge crossing frequency and gouge

geometry (the distribution of gouge widths and depths) to determine the overall pipeline risk. There has yet to be a publication that ties together these various elements in a comprehensive fashion. C-CORE (2000) used conservative subscour deformation allowance of one scour depth between the scouring iceberg keel and the top of the pipeline for pipeline risk analyses on the Grand Banks, however this simplified approach would not be used for a detailed pipeline design.

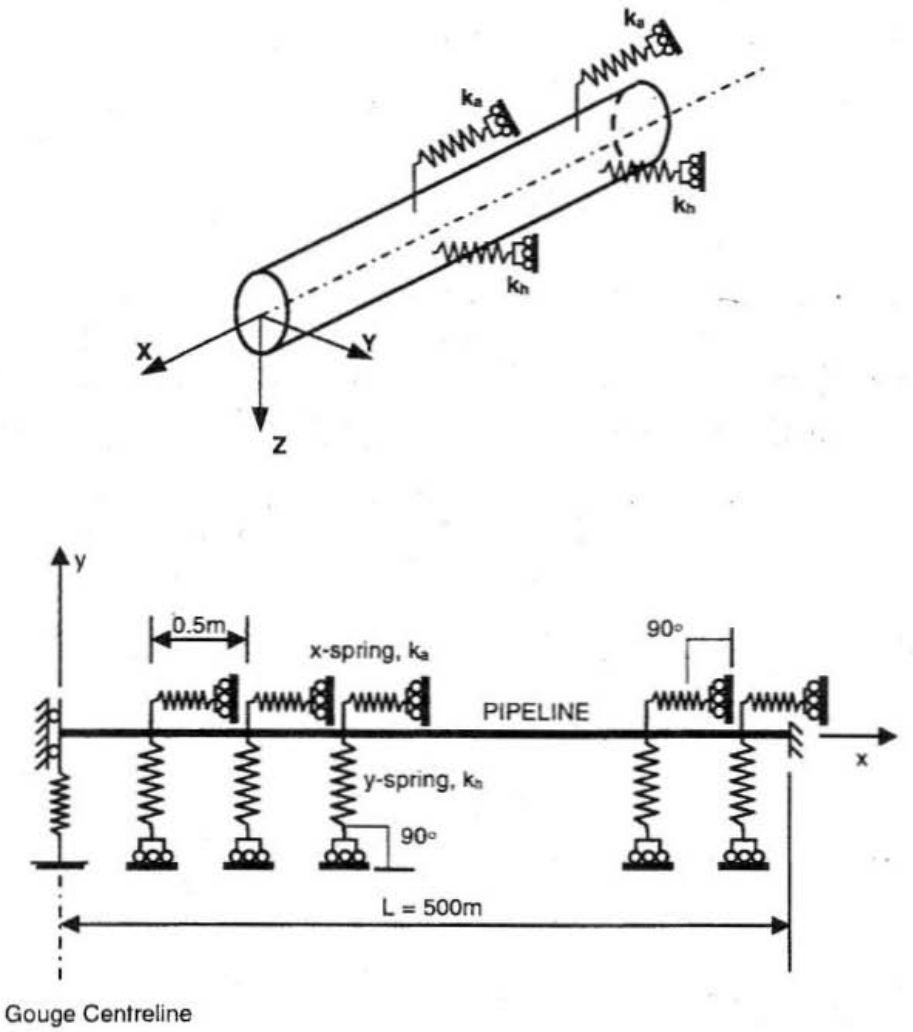

Figure 11 Idealized three-dimensional soil-pipeline interaction model (top) and two dimensional finite element representation (PERD, 2000)

3 BJARNI DEVELOPMENT STUDY (PETRO-CANADA, 1983)

3.1 Introduction

The feasibility of developing the gas reserves on the Makkovik Bank was the subject of a 10-volume study conducted during the early 1980's (Petro-Canada, 1983). Various development options were considered and it was concluded that the most promising alternatives utilized trenched pipelines to transport the natural gas from its source to a landfall at Cape Harrison, where it would be transported to market via pipeline or in tankers.

A variety of pipeline scenarios, as shown in Figure 12, were considered. Redundant pipelines were used to avoid interruptions in production due to iceberg damage. In water depths where scouring was considered likely, pipelines were routed such that they were separated by a difference in bathymetry of 15 m to minimize the probability that a single scour event would affect more than one pipeline. Pipeline scenarios A and B (Figure 12) consist of subsea templates in dredged glory holes and multiphase pipelines transporting natural gas and condensate fluids to shore. The multiphase pipelines require regular sphering to limit liquid hold up and clear liquids, therefore an additional pigging pipeline would be required to ferry spheres out to the site. Once on shore, the product would be processed in a gas plant and transported by pipeline to market or liquefied and transported using tankers. In pipeline scenarios C and D (Figure 12) gas and condensate liquids are separated at a gravity base platform on site and two pipeline bundles consisting of dry gas and condensate lines are used to transported the product to shore, where it is transported to market via pipeline. A variety of pipeline diameters, permitting

various flow rates, were considered as part of the economic analysis. Scenario "A" was selected as the base case for the iceberg risk analysis (Petro-Canada, 1983). This scenario will also be considered in this thesis, allowing a direct comparison of results.

The final recommendation of the original study was not to proceed with the development, however this was based on the economic analysis rather than the results of the iceberg risk analysis. Following a reassessment of reserves by the CNOPB in 1991, Sheps et al. (1992) presented a review of the original study. Citing low projected gas prices, the remoteness of the site and the technical challenges associated with the iceberg scour issue, it was concluded that development of these reserves was still not feasible. However, it was acknowledged that these factors could change.

There has recently been a renewed interest in exploration on the Labrador Shelf, which could result in the discovery of additional reserves. Gas prices are sufficiently high to justify the development of an extensive offshore and onshore pipeline to exploit Nova Scotia's offshore gas reserves, as well as to consider much more ambitious projects to access gas reserves in the Beaufort. The incremental cost of extending existing pipeline networks to access natural gas reserves on the Labrador Shelf may be justifiable if the iceberg risk issue for the offshore pipelines could be resolved.

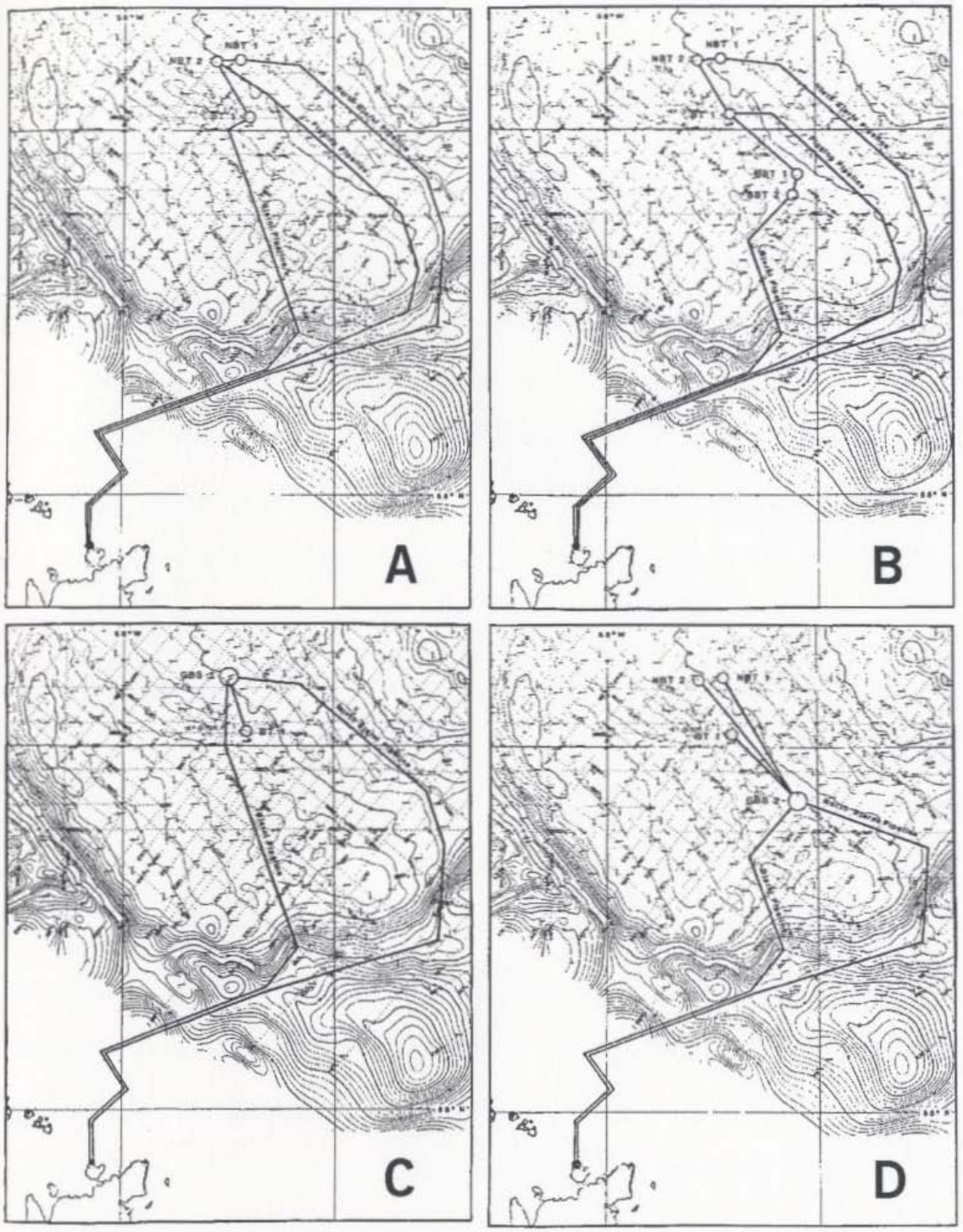

Figure 12 Production scenarios A & B using subsea templates and two-phase pipelines and C & D showing gravity base structure with separate gas and condensate pipelines (from Petro-Canada, 1983)

3.2 Model Inputs Used for Pipeline Risk Analysis

Iceberg flux was given relative to a reference line perpendicular to the Labrador coast. Iceberg flux was determined to be 5.8 icebergs/km/year on the Makkovik Bank and 33.2 for the marginal trough (Petro-Canada, 1983). The initial portion of each pipeline route where water depths were less than 250 m was considered to be on the Makkovik Bank, while the remaining portion of the route was assigned trough flux values.

Icebergs in the marginal trough were assumed to flow parallel to the coast, with no meandering, as opposed to the Makkovik Bank, where considerable meandering was observed during drilling operations. Unlike those on the Makkovik Bank, an iceberg in the marginal trough would only be expected to cross a pipeline segment once. For pipeline segments in the trough region, the iceberg flux per km of pipeline for segments not parallel to the reference line perpendicular to the coast was corrected based on the projected length of the pipeline segment on the reference line (typically, the correction fact was approximately 0.75). For pipeline segments on the bank, iceberg track simulations were conducted to assess the influence of a meandering trajectory on the number of times an iceberg would be expected to cross a given pipeline segment. An analysis of 25 iceberg trajectories (1100 observations) was used to develop a statistical description of iceberg drift speed and direction, allowing iceberg drift to be modeled as a Markov process. By overlaying the simulated tracks on lines at various orientations it was possible to establish a meander coefficient (the number of times a given iceberg would cross a pipeline segment) of 2.3 for icebergs on the Makkovik Bank.

The iceberg draft distribution was based on 41 measured iceberg drafts obtained between 45°N and 54°N. A gamma distribution provided the best fit to the measured drafts, which had a mean of 90.8 m and a standard deviation of 43 m. The gamma distribution was used to calculate the probability of an iceberg exceeding a given draft.

The scour depth distribution was based on observations from the Bjarni wellsite survey (Geomarine, 1976). The mean scour depth recorded during the survey was 1.45 m. The scour depth was best represented by an exponential distribution. An exponential distribution with a mean of 1.45 m was used to calculate the probability of an iceberg scour exceeding a specified depth.

3.3 Risk Analysis Procedure

The procedure used for the analysis of the iceberg risk for the Bjarni pipeline routes was very similar to that outlined by Allan (1986) for a hypothetical pipeline route on the Grand Banks.

The pipeline was modeled as a series of line segments with a specific length and orientation. The water depth for each pipeline segment, which was considered to be constant, was determined from the mean value along each segment. The number of icebergs crossing each segment was determined from the iceberg flux, the length of the pipeline segment, and its projected length or the meander coefficient, depending whether the pipeline section was in the trough or on the bank.

The number of icebergs scouring over the pipeline was calculated from the number of icebergs drifting over the pipeline and the proportion of icebergs with sufficient draft to scour. The proportion of icebergs scouring over a pipeline segment was determined from the iceberg draft distribution. Based on the observation that few iceberg scours had been observed to traverse water depth ranges in excess of 10 m (riseup), the proportion of icebergs that could scour in a particular water depth was considered to be equal to the proportion of icebergs with drafts equal to or greater than the water depth and less or equal to the water depth plus 10 m. This was calculated directly from the gamma distribution describing the measured keel depths.

Once the number of icebergs drifting over a pipeline segment and the proportion resulting in scours had been determined, the proportion of scours that damaged the pipeline was determined using the scour depth distribution and the proportion of scour depths greater than the cover depth (depth of soil above pipeline crown).

3.4 Risk Analysis Results

As a result of the iceberg risk analysis, the following was concluded:

"The analysis showed that an average of 259 iceberg/pipeline collisions can be expected over the 20 year life of the pipeline, if it is buried with a cover depth of 2.5 m. This would translate into an average of 13 iceberg/pipeline hits per year. For an average of 10 iceberg/pipeline hits over the design life of the pipeline system, the pipeline would have to be buried with an average cover of 6 m over the entire length of the pipeline."

Table 1 and Figure 13 to Figure 15 show the results for each pipeline. The results shown do not include those for pipeline segments connecting North Bjarni Template 1 and 2 (NBT 1 & NBT 2) or Bjarni Template 1 (BT 1) or NMB 2. A subsea canyon situated near shore and a 2.3 km tunnel used for the final shore approach shields the final 18 km of the pipelines from iceberg scouring and impacts. It can be seen in Figure 13 to Figure 15 that a substantial portion of (42-53%) of the pipeline impacts are sustained in the 15 km section before the sheltered section where the pipelines are coming out of the trough and entering the shallower bathymetry of the inner shelf.

Deeper water gives the pigging pipeline a lower impact rate per kilometer than the Bjarni pipeline on the Makkovik Bank. However, the total impact rate for the pigging pipeline is greater due to the longer pipeline length. A slightly longer route allows the North Bjarni pipeline to pass through even deeper water, which is reflected in a lower impact rate per kilometer and a lower total impact rate.

Table 1 Risk Analysis Results for Pipelines in Base Case Scenario for a 20-Year Period (Petro-Canada, 1983)

Pipeline	Bjarni	Pigging	North Bjarni
Length (km)	91.5	122.1	132.2
Icebergs drifting over pipeline	38,452.9	46,339.0	49,853.0
Icebergs scouring over pipeline	515.6	524.9	410.8
Icebergs impacting pipeline (2.5m cover)	91.9	93.6	73.2

The results shown in Table 1 have been compared with the results obtained from the analysis presented in this thesis and found to be extremely conservative. The various input parameters used for the Petro-Canada (1983) analysis have also been discussed as the data was analyzed for use in this thesis.

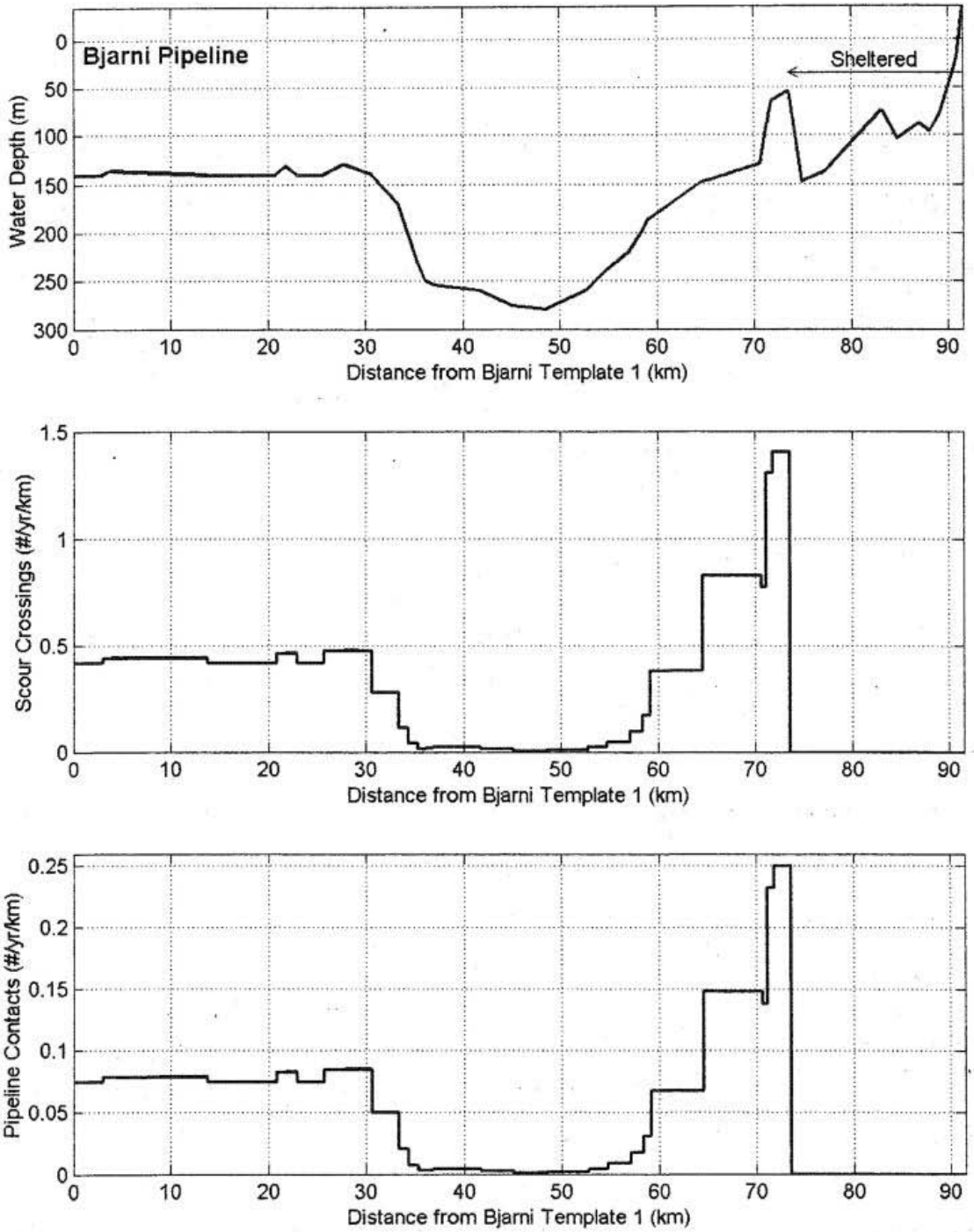

Figure 13 Risk analysis results for Bjarni pipeline, showing bathymetry along route, annual scour rate per km over pipeline and annual iceberg/pipeline contact rate for 2.5 m cover depth (Petro-Canada, 1983)

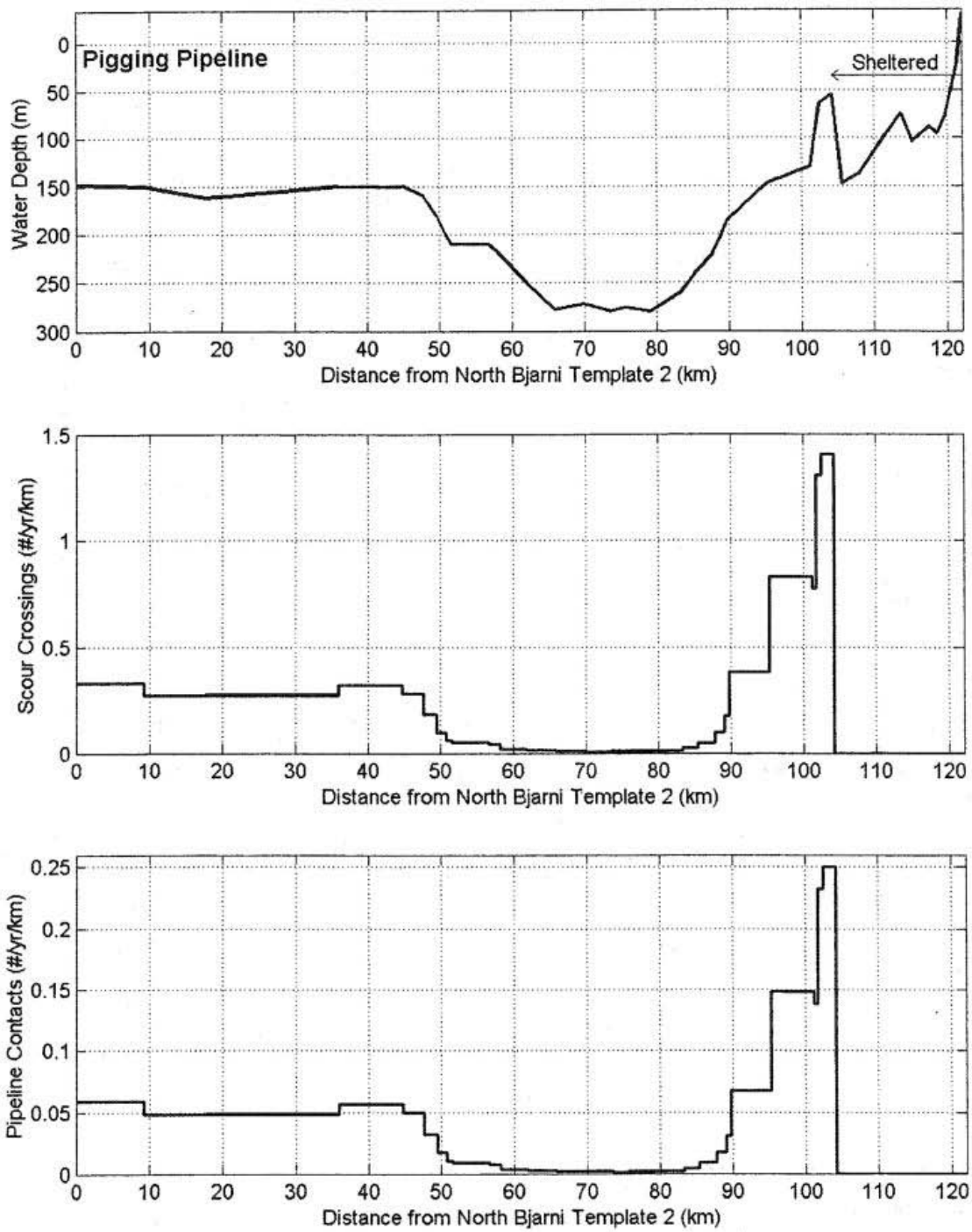

Figure 14 Risk analysis results for pigging pipeline, showing bathymetry along route, annual scour rate per km over pipeline and annual iceberg /pipeline contact rate for 2.5 m cover depth (Petro-Canada, 1983)

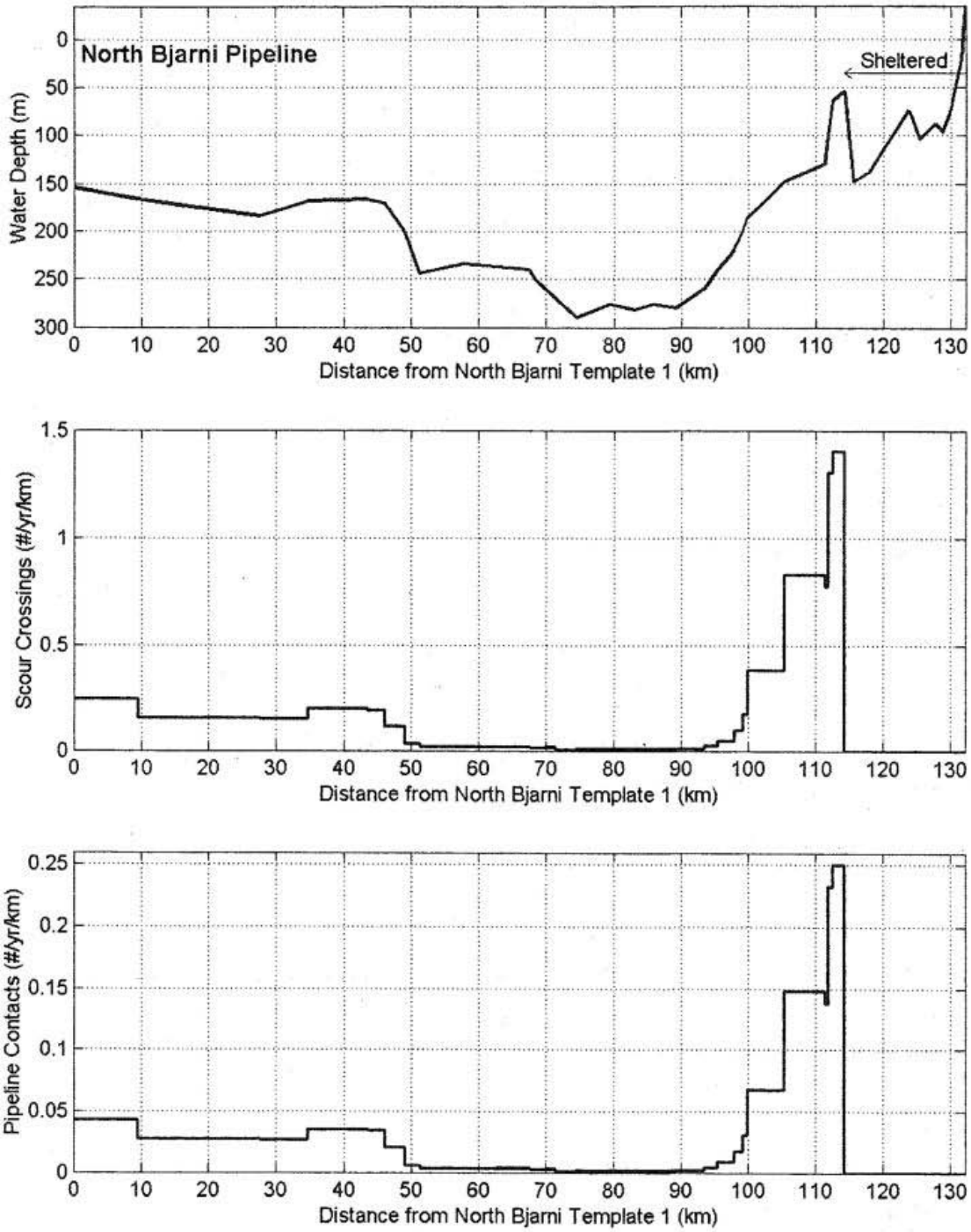

Figure 15 Risk analysis results for North Bjarni pipeline, showing bathymetry along route, annual scour rate per km over pipeline and annual iceberg /pipeline contact rate for 2.5 m cover depth (Petro-Canada, 1983)

4 GROUNDING MODEL

4.1 Grounding Model Formulation

A grounding model was developed that is similar to the geometric approaches used to predict iceberg or pack ice impact frequencies with floating structures (Jordaan, 1983; Dunwoody, 1983; Sanderson.1988 and Fuglem et al., 1996). Scour risk to trenched pipelines can be determined using a relationship between grounding and scouring frequencies, and scour geometry data.

4.2 Grounding Frequency for a Sloped Seabed

Figure 16 (top) depicts iceberg keels with an areal density ρ_k drifting with a mean drift speed $\overline{U}$ in a uniform direction directly towards a section of seabed of width W. For this case, the frequency, f_g, at which iceberg keels impact, or ground on the seabed is:

$$f_g = \rho_k \overline{U} W \tag{4.1}$$

Iceberg keels grounding in adjacent sections of seabed are not considered, even if some small portion of the keel extends over the boundary. This distinction is made to avoid double counting of grounding events and to make the solution independent of the width of the specified section of seabed. Figure 16 (bottom) shows the influence of the relative orientation between the seabed slope and the iceberg keel drift direction. If the orientation is changed by some angle θ, then the size of target presented to the keels is reduced and the iceberg keel grounding frequency is:

$$f_g = \rho_k \overline{U} W \cos(\theta) \tag{4.2}$$

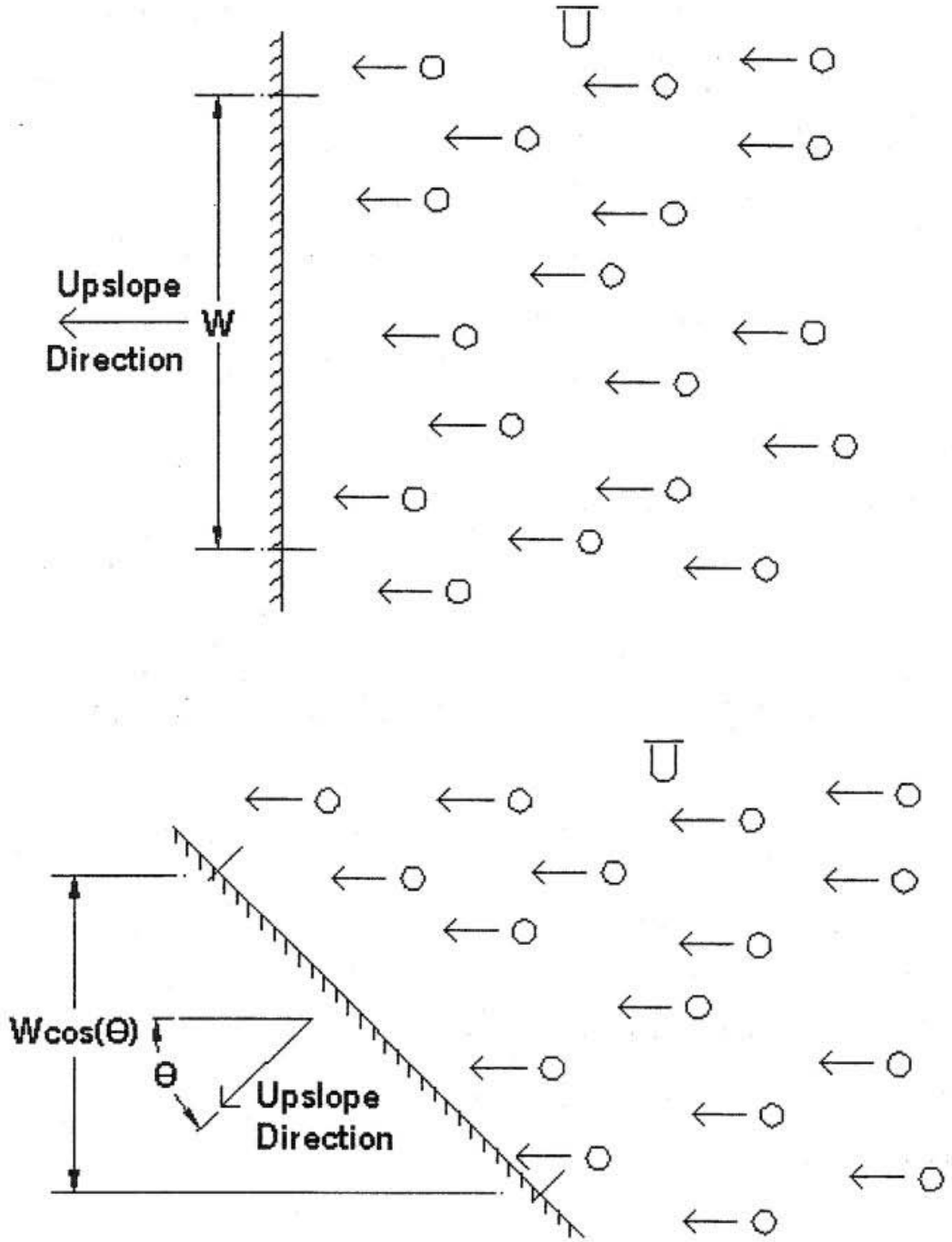

Figure 16 Iceberg grounding frequency on seabed slope and effect of drift orientation

Thus far, consideration has been given only to the density of iceberg keels capable of striking the seabed. However, the available data only gives the density of icebergs that can be observed on the surface, n_o (with icebergs with waterline lengths < 16 m excluded). Only icebergs that have sufficiently deep draft can impact the seabed. The number of icebergs that can strike a sample section of seabed covering a specific water depth range is limited to those with drafts in this depth range. Iceberg with lower drafts will ground in shallower water (if at all) and icebergs with greater drafts will ground in deeper water depths. A reduction factor (r_d), equal to the proportion of icebergs with drafts in the appropriate depth range (units: m^{-1}) was applied to the iceberg density to account for this effect, giving:

$$f_g = n_o r_d \overline{U} W \cos(\theta) \tag{4.3}$$

where θ is the orientation of iceberg drift direction relative to the upslope direction. The range of drift direction that needs to be considered is ± 90° relative to the upslope direction. If the drift direction relative to the upslope direction exceeds ± 90° then the iceberg is drifting down-slope and will not ground, unless it undergoes some draft change due to rolling or calving. This latter effect was ignored in this formulation. To calculate the total grounding frequency it was recognized that the mean drift speed usually varies with drift direction and that the distribution of drift direction is not uniform. An additional term, r_θ, was introduced to specify the proportion of time that icebergs drift in a specified direction. This allowed the total grounding rate to be expressed as

$$f_g = r_d n_o W \int_{-\pi/2}^{\pi/2} r_\theta(\theta) \overline{U}(\theta) \cos(\theta) d\theta \tag{4.4}$$

4.3 Grounding Density for a Sloped Seabed

Thus far, no consideration has been given to the seabed slope or the proportion of iceberg keel to be considered for grounding. Figure 17 shows a square sample section of seabed with a dimension W parallel and perpendicular to the seabed isobath and with a slope of S. The sample seabed section was defined on the basis of a 1m rise, so $S=1/W$ and, except for extreme slopes, the area of the seabed section was considered to be W^2 or $1/S^2$ (the error is less than 5% for a slope of 30%). The frequency of groundings, f_g, was expressed in terms of grounding rate per unit area, ρ_g, as follows:

$$\rho_g = r_d n_o \frac{W}{A} \int_{-\pi/2}^{\pi/2} r_\theta(\theta) \overline{U}(\theta) \cos(\theta) d\theta \tag{4.5}$$

where r_d is now more specifically defined as the proportion of iceberg keels in a 1 m increment above the seabed. Expressing W and A in terms of slope gives:

$$\rho_g = r_d n_o S \int_{-\pi/2}^{\pi/2} r_\theta(\theta) \overline{U}(\theta) \cos(\theta) d\theta \tag{4.6}$$

If directional drift data are available, Equation 4.6 can be evaluated using numerical integration. Alternatively, when directional drift data are not available, a non-directional form of Equation 4.6 can be used. By assuming a mean drift speed that is independent of direction and a uniform distribution of drift direction ($r_\theta = 1/2\pi$), Equation 4.6 can be integrated over the prescribed limits to yield

$$\rho_g = \frac{1}{\pi} r_d n_o S \overline{U} \tag{4.7}$$

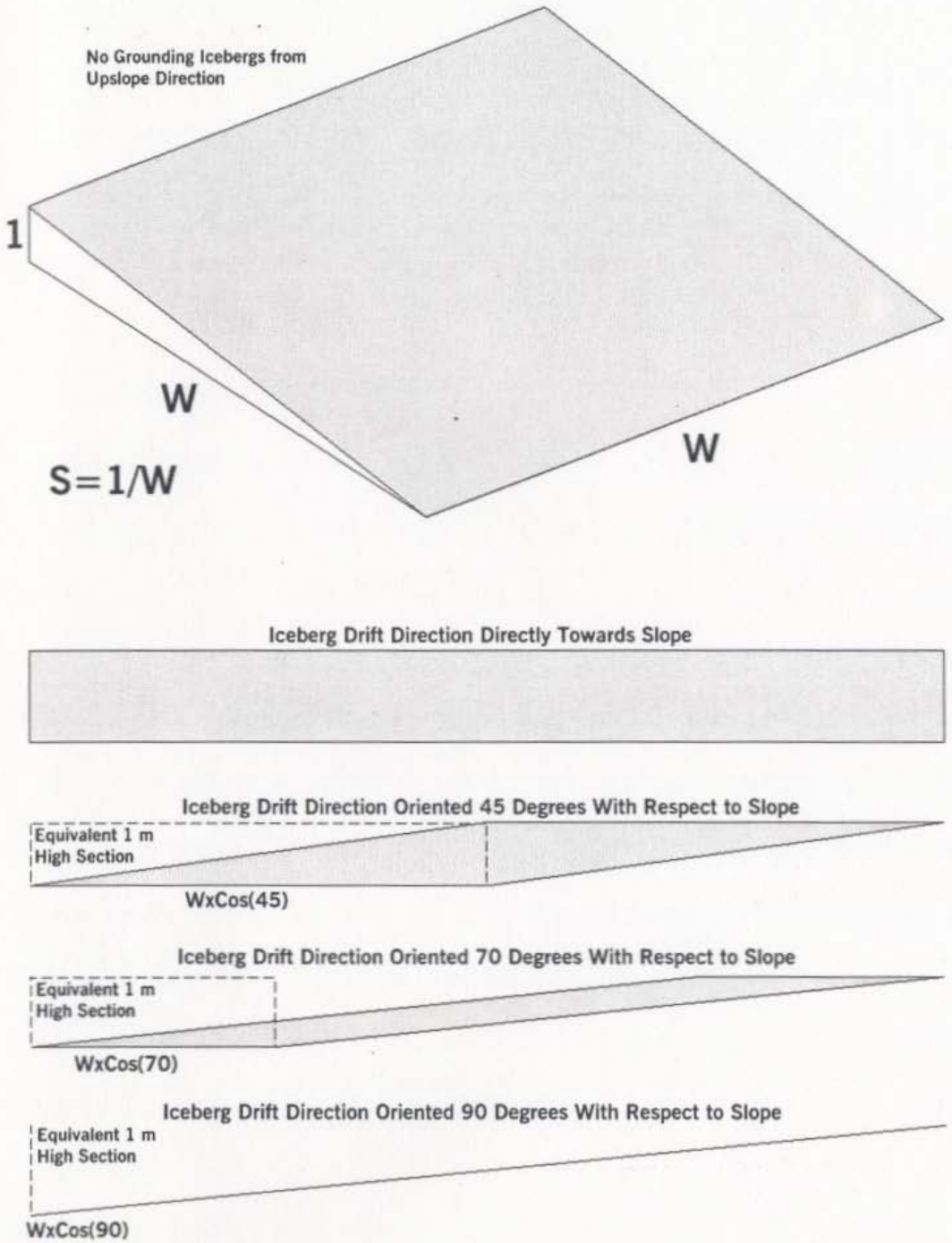

Figure 17 Seabed slope definition for grounding density and effect of drift orientation on target size

4.4 Grounding Model Verification

An initial verification of the grounding model was made using data for the White Rose and Hibernia areas, where scour frequency and the associated iceberg parameters are fairly well documented. The required parameters for the grounding model are iceberg frequency, draft distribution, drift speed and direction and seabed depth, slope and orientation.

4.4.1 Scour Rates from Seabed Surveys

The estimated scour rate in the vicinity of White Rose is 1×10^{-3} scours/km^2/year (C-CORE, 2001b) and at Hibernia, 4×10^{-4} scours/km^2/year (PERD, 2000). For both of these cases scour rates were determined using the observed scour density on the seabed and, following the approach developed by Lewis et al. (1987), assuming that these scours accumulated over the last 2500 years. However, it should be noted that there is some degree of uncertainty associated with this approach. It has been acknowledged that 2500 years may be a conservative value (Gary Sonnichsen, GSC, personal communication), and that the actual period may be longer. Also, short term climatic fluctuations may have resulted in higher iceberg incursion rates, and resulting scour rates, over the time of formation. While the assumption of a 2500 year constant scour rate is an approximation, it does represent the best approach currently available.

4.4.2 Seabed Slope and Orientation

Figure 18 shows the bathymetric contours in the immediate vicinity of the White Rose development (C-CORE, 2001a). The water depth at the site is approximately 121m. The

seabed has a mean slope of about 1/1000 and the up-slope direction is oriented 240° from north. As determined from regional bathymetry (see Figure 19), the water depth at Hibernia is approximately 80m, the mean slope is 0.6/1000 and the up-slope direction is oriented 232° from north. Using the same regional bathymetry gives a slope of 1/1000 and an up-slope orientation of 247° for White Rose, which agrees fairly well with values determined from the detailed bathymetry.

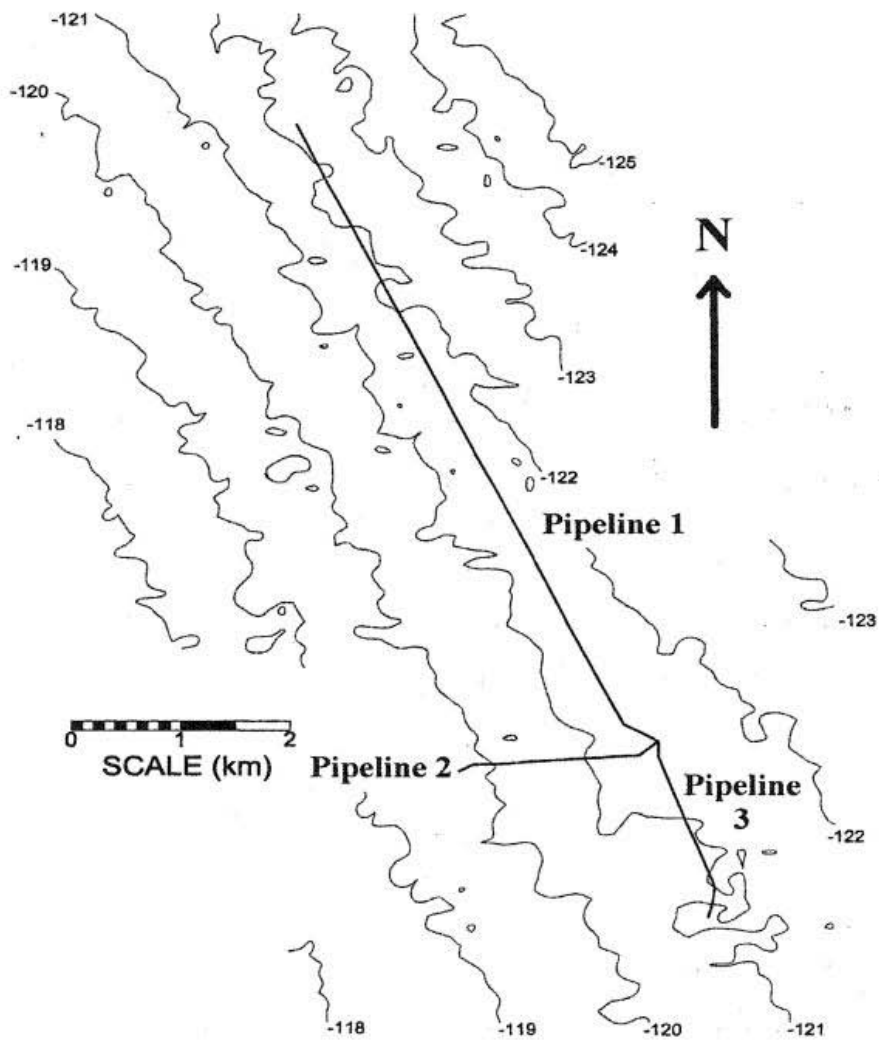

Figure 18 Bathymetry in the White Rose area, along with proposed pipeline routes (from C-CORE, 2001a – water depths in meters)

4.4.3 Iceberg Frequency

Iceberg frequency is usually expressed in terms of areal density, which is the average number of icebergs that expected to be seen in a given area (typically a degree square) at any given instant in time. The most reliable source of iceberg sightings on the Grand Banks in terms of frequency and coverage of surveys is the International Ice Patrol (IIP). The IIP regularly issues bulletins throughout the iceberg season showing the number of icebergs sighted per degree square. Jordaan et al. (1999) analyzed the IIP data to produce areal density values for icebergs with waterline lengths ≥ 16m on the Grand Banks and the immediate region. Figure 19, which includes data up to 2000, shows the annual average density of icebergs per degree square on the Grand Banks. A difference has been noted in the areal densities calculated from the last 20 years of data (1981-2000) and the entire 1960-2000 period. This could be attributed to either improved detection techniques or long-term iceberg frequency fluctuations. Therefore, values for both time periods have been presented. Areal density expressed on a degree square basis can be converted to density per square kilometer as follows:

$$n_o\,(km^{-2}) = n_o\,(degree^{-2}) / (cos(\phi) \times 1.237 \times 10^{4}) \qquad (4.8)$$

where ϕ is the latitude of the site. Table 2 gives the interpolated areal density values for the White Rose and Hibernia sites.

Table 2 Annual Average Areal Density Values for Icebergs at White Rose and Hibernia

	1960-2000		1981-2000	
	$Degree^{-2}$	Km^{-2}	$Degree^{-2}$	Km^{-2}
White Rose	0.90	1.06×10^{-4}	1.09	1.29×10^{-4}
Hibernia	0.67	7.94×10^{-5}	0.80	9.44×10^{-5}

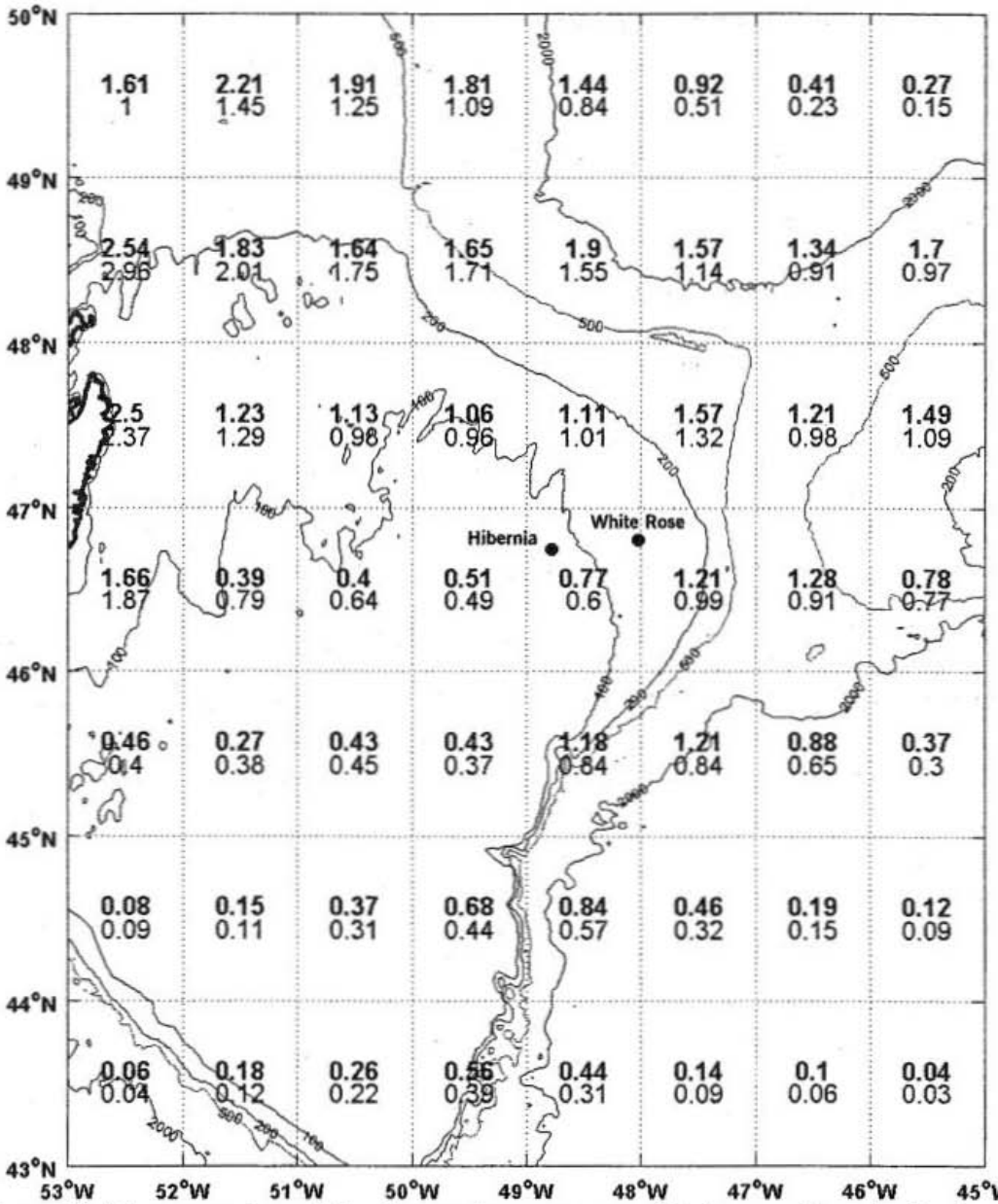

Figure 19 Mean annual areal density per degree square of icebergs with waterline lengths ≥16m, bottom values based on data from 1960-2000, top values based on data from 1981-2000 (Jordaan et al., 1999), water depths in meters

4.4.4 Iceberg Draft Distribution

Measurements of iceberg draft have typically been conducted on larger icebergs, thus the distribution of measured iceberg drafts is biased towards larger icebergs. However, the iceberg waterline length distribution is fairly well documented and by utilizing the appropriate iceberg length/draft relationship it is possible to generate the iceberg draft distribution.

The iceberg waterline length distribution on the Grand Banks follows an exponential distribution with a mean of 59 m (Jordaan et al., 1995). Figure 20 shows 211 known iceberg drafts obtained off the coast of Newfoundland (C-CORE, 2000), along with the best-fit line and the 95% confidence intervals. The mean iceberg waterline length for this data set is 115 m and the mean draft is 80 m. The relationship between the iceberg waterline length and draft is:

$$D_i = 3.23\, L_i^{0.68} \tag{4.9}$$

The standard deviation of the residuals is 0.25. Thus, to generate a sample of iceberg drafts, a population of iceberg waterline lengths with a mean of 59 m and an exponential distribution is generated, and the following relationship was applied:

$$D_i = exp(ln(3.23) + 0.68\, ln(L_i) + N(0,0.25)) \tag{4.10}$$

where $N(0,0.25)$ is a random variable with a mean of 0 and a standard deviation of 0.25. Only icebergs with waterline lengths $\geq$ 16 m were considered because the areal density value does not include icebergs smaller than this value.

Once a population of iceberg keels has been generated, there are two approaches that can be used to determine the proportion of icebergs within a specific range. The first is a simple ratio of the number of keels within a 1 m depth range (recall that the grounding model assumes a 1 m depth increment) to the total number of iceberg keels. The second approach considered that icebergs with drafts greater than the water depth will ground and be filtered out of the keel population. The remaining keel population has been truncated and should be normalized accordingly. The normalized value was calculated from the number of keels in the 1 m depth range and the number of icebergs with keels equal to or less than the water depth (icebergs with keels exceeding the water depth were excluded). Figure 21 shows the proportion of iceberg keels within 1m depth increments, using an exponential waterline length distribution and Equation 4.10. The influence of bathymetric filtering was not noticeable at water depths beyond 150 m, but at a 50 m water depth was substantial (a factor of 2 difference). The water depth at the White Rose site is approximately 121m. The water depth range that considered for grounding was 120 m to 121 m. The water depth at Hibernia is 80m so only the proportion of keels with drafts between 79 m and 80 m needed to be considered. Table 3 lists the proportion of iceberg keels to be considered for a grounding analysis for the Hibernia and White Rose sites.

Table 3 Proportion of Iceberg Keels Considered for Iceberg Grounding Model

Site	Water Depth Range	Proportion of iceberg keels (m^{-1})	Normalized proportion of iceberg keels (m^{-1})
Hibernia	79m – 80m	0.0064	0.0082
White Rose	120m – 121m	0.0019	0.0020

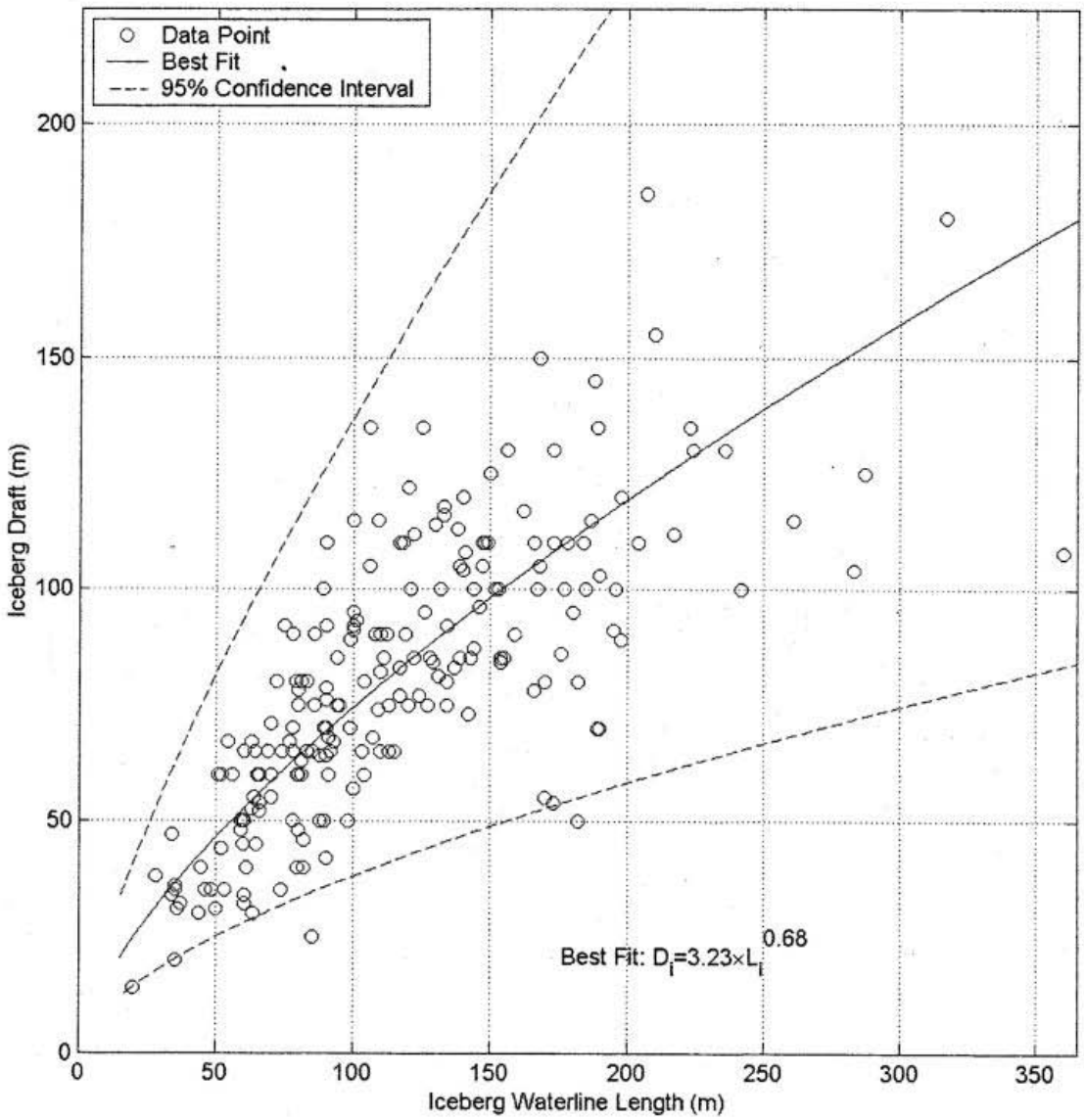

Figure 20 Iceberg draft measurements off the Newfoundland coast

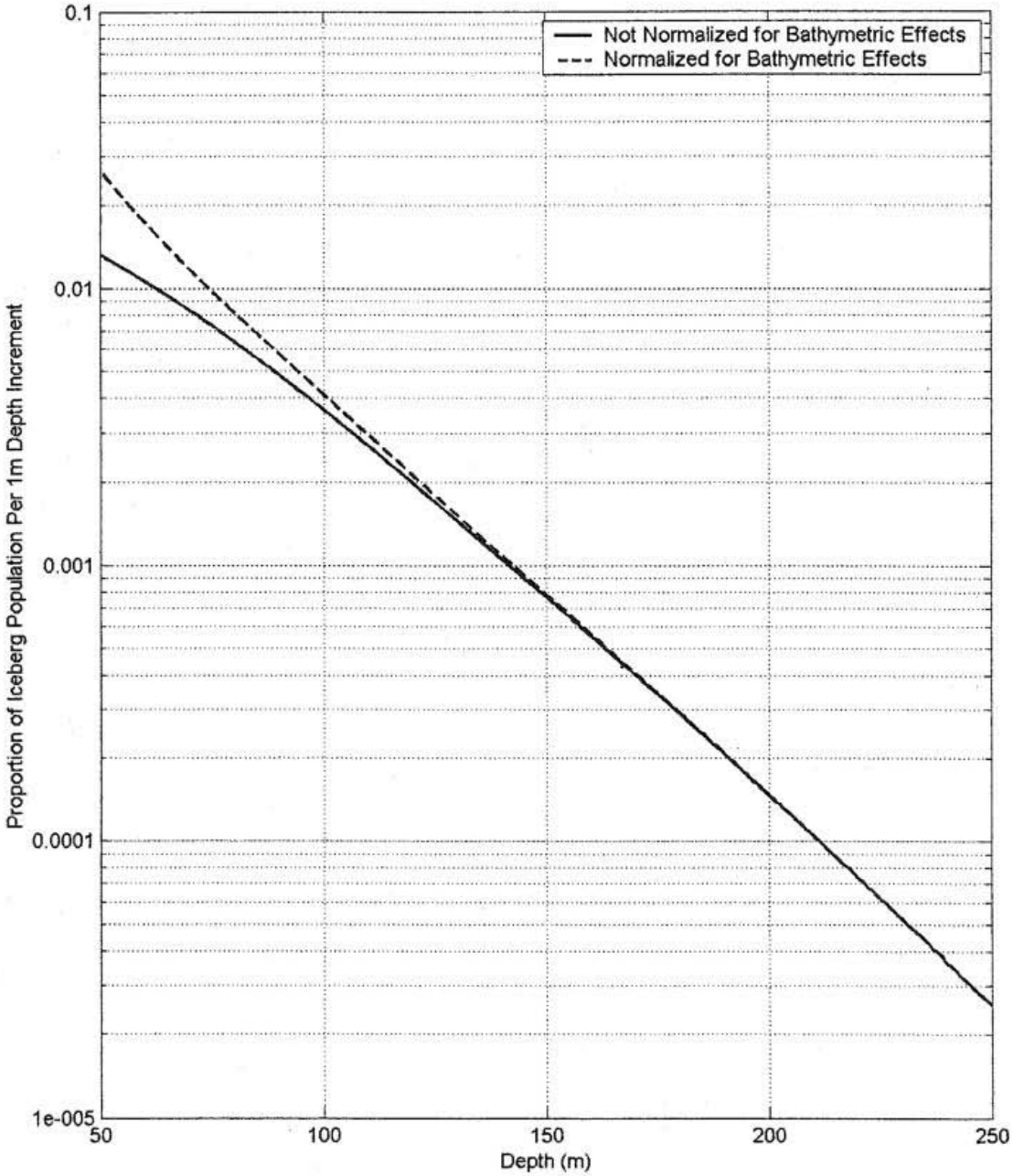

Figure 21 Proportion of iceberg drafts per 1 m depth increment used for Grand Banks model calibration (normalized and unnormalized for water depth)

4.4.5 Iceberg Drift Speed

Iceberg drift velocities can be determined from radar sightings obtained during drilling operations. Figure 22 shows drift vectors obtained from radar sightings on the northeast Grand Banks. These were obtained from the Marine Environmental Data Service Canadian Offshore Oil and Gas Data (MEDS, 1997) database, as well as industry sightings from 2000 (PAL, 2000). Dashed lines indicate the areas around the Hibernia and White Rose sites where representative drift vectors have been selected. The mean drift speed for both of the areas shown is approximately 0.34 m/s. The majority of drift velocities in this data set are based on radar sightings at 1-hour intervals. Grounded and towed icebergs have been eliminated. Table 4 gives a breakdown of iceberg velocities in 30° bearing increments, showing the proportion of velocity measurements in each bearing increment and the associated mean drift speed. There were a total of 555 drift vectors in the White Rose zone and 329 in the Hibernia zone.

Table 4 Breakdown of Iceberg Drift Vectors for Hibernia and White Rose

Bearing Range (drifting "to")	White Rose		Hibernia	
	(%)	Mean Speed (m/s)	(%)	Mean Speed (m/s)
0°-30°	7.7	0.26	14.3	0.31
30°-60°	6.8	0.35	14.0	0.38
60°-90°	7.4	0.36	10.6	0.41
90°-120°	11.2	0.42	13.3	0.39
120°-150°	11.4	0.42	5.5	0.33
150°-180°	12.3	0.42	10.3	0.37
180°-210°	12.6	0.37	6.4	0.32
210°-240°	6.3	0.30	6.1	0.34
240°-270°	5.6	0.25	4.6	0.21
270°-300°	8.1	0.23	3.6	0.27
300°-330°	4.3	0.23	4.0	0.24
330°-360°	6.3	0.31	7.3	0.34

It can be seen in Figure 23 that there is a distinct difference between the distribution of drift vectors at Hibernia and White Rose. Since currents are the dominant driving force influencing iceberg drift, current data were consulted. Figure 24 shows gridded current values based on the drift trajectories of drifter buoys equipped with drogues (Murphy et al., 1996). The depth of the drogue was typically about 40m. The vectors were generated by averaging the easterly and westerly components of the drifters' velocity, thus these vectors are not useful for evaluating mean drift speeds, however they are indicative of mean drift direction. Interpolating between the available data indicated a mean drift bearing of 126° at Hibernia (slightly down-slope) and the mean at White Rose is 150° (essentially across-slope). The mean easterly and northerly components of the iceberg drift velocities for the two drift datasets were calculated and mean drift bearing of 77° and 140° was calculated for Hibernia and White Rose, respectively. Table 5 tabulates the interpolated mean drift components from the IIP drifter dataset and the iceberg drift datasets. Although the direction of the mean drift agrees well for White Rose, there is a discrepancy for the Hibernia site. The differences between the IIP drifter and the iceberg tracks may be due to limited track and drifter data near the Hibernia site. Also, currents at depths of 40 m may not be representative of the currents that are most influential for iceberg drift. Additional iceberg drift track data would be useful and are anticipated in the near future from offshore ice management operations.

Table 5 Comparison of Mean Drift Components from Icebergs and IIP Drifter Data

Site	Mean Easterly Drift (m/s)	Mean Northerly Speed (m/s)
Hibernia (icebergs)	+0.118	+0.027
Hibernia (IIP drifter)	+0.043	-0.032
White Rose (icebergs)	+0.074	-0.089
White Rose (IIP drifter)	+0.031	-0.055

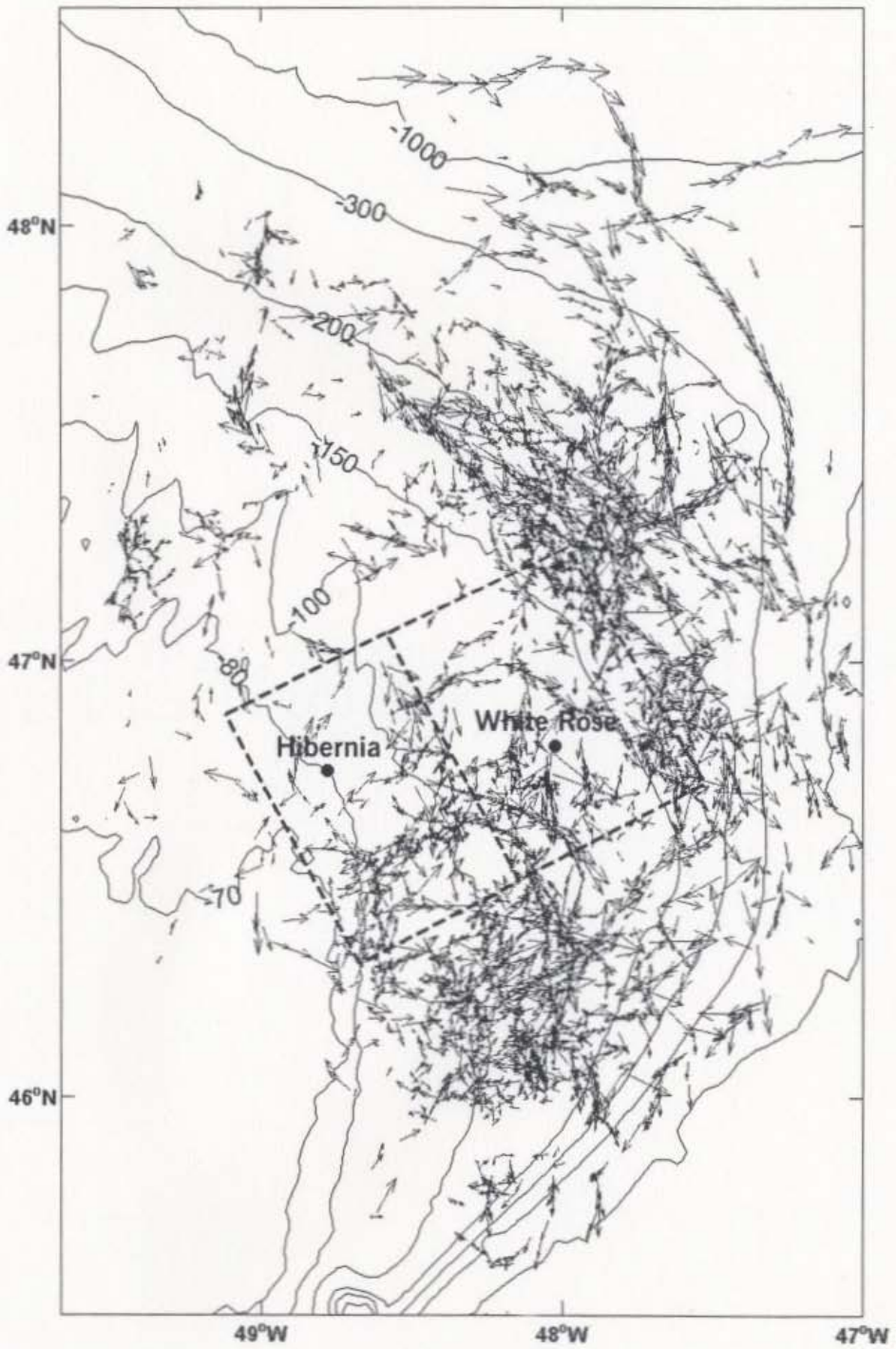

Figure 22 Iceberg drift vectors on northeast Grand Banks

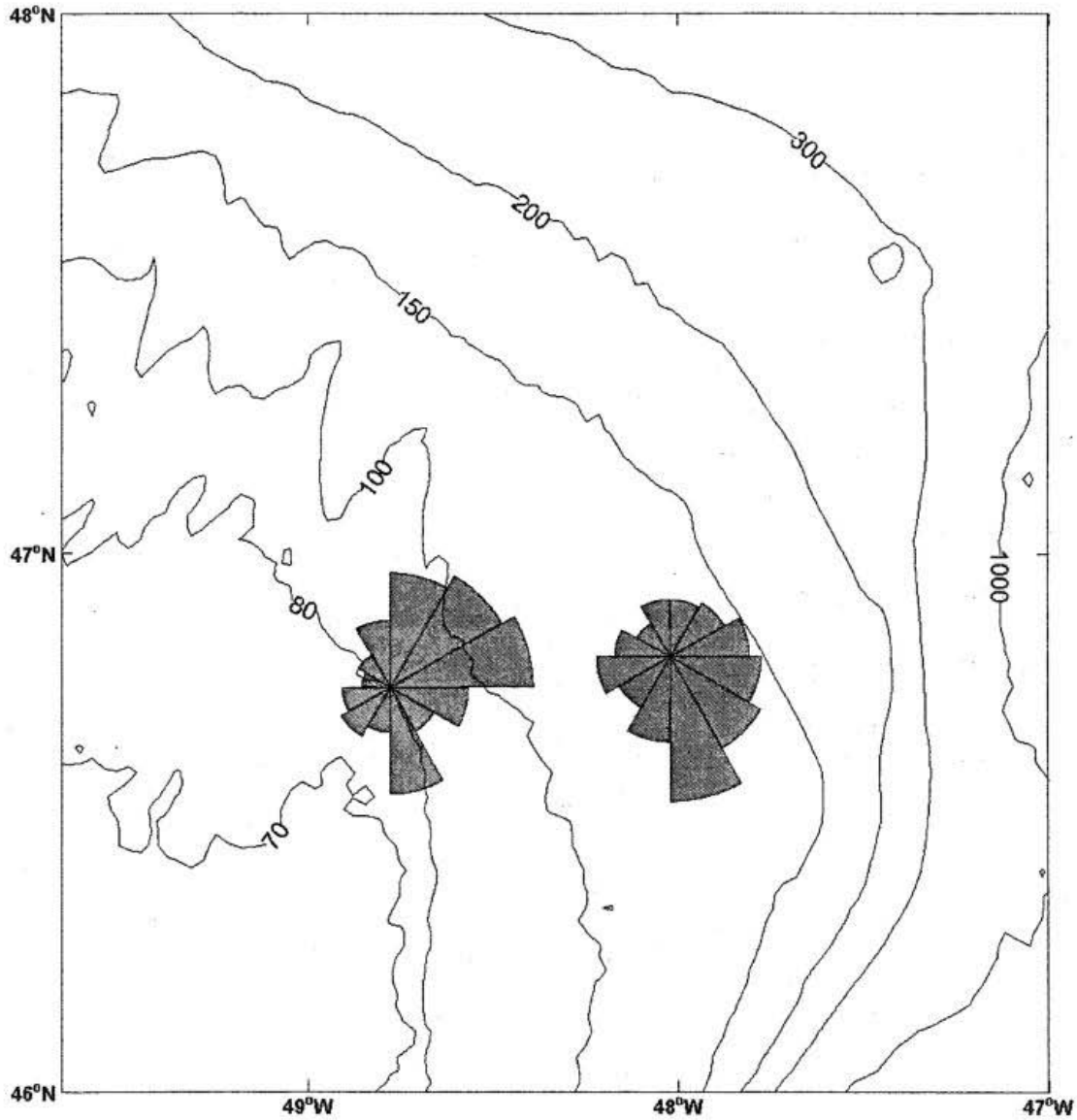

Figure 23 Roses showing distribution of drift direction (drifting "from" target) for Hibernia and White Rose

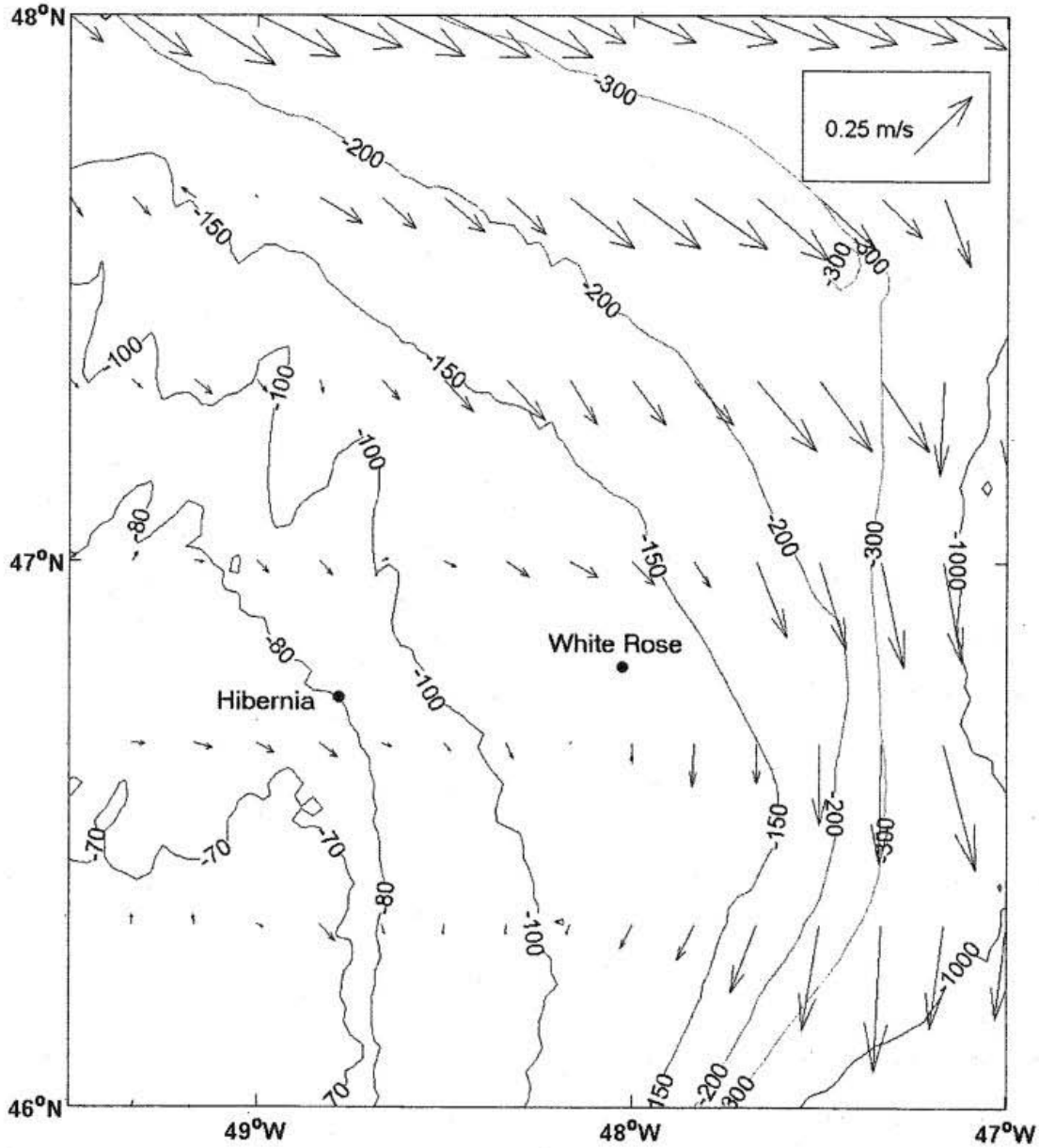

Figure 24 Mean drift vectors on derived from IIP drifter Buoys (Murphy et al., 1996)

4.4.6 Grounding Calculation

Initially, the simplified grounding model (Equation 4.7) was used for the White Rose and Hibernia sites. Then, for comparison, directional drift statistics were used to calculate grounding rates using Equation 4.6.

Table 6 summarizes the various input parameters for calculating the grounding rate using Equation 4.7. The calculated grounding rate at Hibernia is 2.5 to 4 times higher than the scour rate estimated from the seabed record – depending on the combination of parameters used to calculate grounding rate, and for White Rose is 12% to 31% lower. A sample calculation for Hibernia with inputs A and C (see table) follows.

$$\rho_g = \frac{1}{\pi} r_d n_o S \overline{U}$$

$$\rho_g = \frac{1}{\pi} \times 0.0064 m^{-1} \times 7.94 \times 10^{-5} km^{-2} \times 0.0006 \times 0.34 m/s \times 31556900 s/year$$

$$\rho_g = 1.03 \times 10^{-3} km^{-2} year^{-1}$$

Table 6 Calculated Grounding Rates Using Equation 4.7 (non-directional drift)

Parameter	Hibernia		White Rose	
Iceberg Areal Density - n_o (#/km^2)	7.94×10^{-5} (1960-2000) 9.44×10^{-5} (1981-2000)	A B	1.06×10^{-4} (1960-2000) 1.29×10^{-4} (1981-2000)	A B
Water Depth (m)	80 m		121 m	
Iceberg Keels in 1m increment, r_d (m^{-1})	0.0064 0.0082 (normalized)	C D	0.0019 0.0020 (normalized)	C D
Seabed Slope, S	0.0006		0.001	
Mean Drift Speed (m/s)	0.34		0.34	
Calculated Grounding Rate (#/km^2/year)	1.0×10^{-3} (A & C) 1.3×10^{-3} (A & D) 1.2×10^{-3} (B & C) 1.6×10^{-3} (B & D)		6.9×10^{-4} (A & C) 7.2×10^{-4} (A & D) 8.4×10^{-4} (B & C) 8.8×10^{-4} (B & D)	
Scour Rate from Seabed Records (#/km^2/year)	$\approx 4\times10^{-4}$		$\approx 1\times10^{-3}$	

The orientation of the seabed restricts the range of directions from which grounding icebergs can drift. The seabed upslope direction at White Rose (240°) restricts grounding icebergs to those that have drift bearings between 150° and 330°, and at Hibernia (232°) restricts grounding iceberg to those with drift bearings between 142° and 322°. Table 7 and Table 8 show sample calculations for White Rose and Hibernia using directional drift statistics and Equation 4.6.

Table 7 Grounding Rate for White Rose using Equation 4.6 (Directional Drift)

Iceberg Areal Density - n_o (#/km^2)					1.06×10^{-4} (1960-2000) 1.29×10^{-4} (1981-2000)	A B
Water Depth					121 m	
Iceberg Keels in 1m Increment, r_d					0.0019 0.0020 (normalized)	C D
Seabed Slope, S					0.001	
Orientation of Upslope Direction					240°	
Drift Bearing Range	Mean Bearing	θ	$r_\theta(\theta)$	$\overline{U}(\theta)$ (m/s)	$Sr_\theta(\theta)\overline{U}(\theta)\cos(\theta)$	
0°-30°	15°	-225°	0.077	0.26	< -90° - not included	
30°-60°	45°	-195°	0.068	0.35	< -90° - not included	
60°-90°	75°	-165°	0.074	0.36	< -90° - not included	
90°-120°	105°	-135°	0.112	0.42	< -90° - not included	
120°-150°	135°	-105°	0.114	0.42	< -90° - not included	
150°-180°	165°	-75°	0.123	0.42	1.34×10^{-5}	
180°-210°	195°	-45°	0.126	0.37	3.30×10^{-5}	
210°-240°	225°	-15°	0.063	0.30	1.83×10^{-5}	
240°-270°	255°	+15°	0.056	0.25	1.35×10^{-5}	
270°-300°	285°	+45°	0.081	0.23	1.32×10^{-5}	
300°-330°	315°	+75°	0.043	0.23	2.56×10^{-6}	
330°-360°	345°	+105°	0.063	0.31	> 90° - not included	
				Total	9.38×10^{-5} s^{-1}	
$\times r_d \times n_o \times$ 31,556,925 s/yr Grounding Rate (#/km^2/yr)				(A & C) (A & D) (B & C) (B & D)	6.0×10^{-4} 6.3×10^{-4} 7.3×10^{-4} 7.6×10^{-4}	
Scour Rate from Seabed Records					$\approx 1\times10^{-3}$	

Table 8 Grounding Rate for Hibernia using Equation 4.6 (Directional Drift)

Iceberg Areal Density - n_o (#/km^2)					7.94×10^{-5} (1960-2000) A 9.44×10^{-5} (1981-2000) B
Water Depth					80 m
Iceberg Keels in 1m Increment, r_d					0.0064 C 0.0082 (normalized) D
Seabed Slope, S					0.0006
Orientation of Upslope Direction					232°
Drift Bearing Range	Mean Bearing	θ	$r_d(\theta)$	$\overline{U}(\theta)$ (m/s)	$Sr_\theta(\theta)\overline{U}(\theta)\cos(\theta)$
0°-30°	15°	-217°	0.143	0.31	< -90° - not included
30°-60°	45°	-187°	0.140	0.38	< -90° - not included
60°-90°	75°	-157°	0.106	0.41	< -90° - not included
90°-120°	105°	-127°	0.133	0.39	< -90° - not included
120°-150°	135°	-97°	0.055	0.33	2.03×10^{-7} (8° of 30°)
150°-180°	165°	-67°	0.103	0.37	8.93×10^{-6}
180°-210°	195°	-37°	0.064	0.32	9.81×10^{-6}
210°-240°	225°	-7°	0.061	0.34	1.24×10^{-5}
240°-270°	255°	+23°	0.046	0.21	5.34×10^{-6}
270°-300°	285°	+53°	0.036	0.27	3.51×10^{-6}
300°-330°	315°	+83°	0.040	0.24	8.05×10^{-7} (22° of 30°)
330°-360°	345°	+113°	0.073	0.34	> 90° - not included
				Total	4.10×10^{-5} s^{-1}
$\times r_d \times n_o \times$ 31,556,925 s/yr Grounding Rate (#/km^2/yr)				(A & C) (A & D) (B & C) (B & D)	6.6×10^{-4} 8.4×10^{-4} 7.8×10^{-4} 1.0×10^{-3}
Scour Rate from Seabed Records					$\approx 4\times10^{-4}$

A comparison of the grounding rates predicted by Equations 4.6 and 4.7 with scour rates derived from seabed surveys indicate that the directional approach (Equation 4.6) provides calculated grounding rates that are more consistent with scour rates than the non-directional approach (Equation 4.7). Thus, given sufficient data, the directional approach would be preferred.

Grounding rates were calculated using a keel draft distribution that was corrected (normalized) for bathymetric filtering effects and another that was not corrected. A comparison of the results obtained using these two draft distributions did not lead to any definite conclusions regarding which was more appropriate. The effect of bathymetric filtering on the keel draft distribution for the water depths at Hibernia and White Rose was not significant. Better agreement with scour rates inferred from the seabed records was achieved using the uncorrected draft distribution. With respect to the appropriate iceberg areal density values to use (1960-2000 or 1981-2000 based) for grounding rate calculations, there is a preference for values derived from 1981-2000 data. The reliability of the survey data from this period is considered to be higher, although this is not an issue that has been considered in a comprehensive manner in this thesis. If this particular combination of input parameters (inputs B & C in Table 7 and Table 8) is considered the "base case", the predicted grounding rates using directional data for Hibernia and White Rose are 7.8×10^{-4} and 7.3×10^{-4} groundings/km^2/year, respectively, compared to scour rates of 4×10^{-4} and 1×10^{-3} scours/ km^2/year. Thus, if all groundings are assumed to result in scours, the grounding model over-predicts scour by 100% at Hibernia and under-predicts scours at White Rose by 25%. Given the degree of uncertainty associated with scour frequency estimates, even from high-quality seabed survey, the conservative approach was taken and a 1:1 ratio between groundings and scours was assumed for the risk analysis for the Labrador pipelines.

5 ICEBERG AND BATHYMETRY PARAMETERS FOR STUDY AREA

Various data sources dealing with icebergs and bathymetry in the Bjarni development area was reviewed and appropriate input parameters for the grounding model were determined. Data from the original Petro-Canada (1983) study were considered, as well as data from more recent studies. The required parameters are: iceberg frequency, draft distribution, drift speed and direction, water depth, seabed slope and orientation.

5.1 Iceberg Frequency

Iceberg frequency is the number of icebergs that would be expected to occur in a given region. Iceberg frequency has been described both in terms of flux and areal density. Iceberg flux refers to the total number of icebergs that cross a particular boundary (a specified degree square or line of latitude) during a specified time interval (typically a year). Iceberg areal density is the average number of icebergs that would be sighted in a particular area (i.e. a degree square) at any given instant. Iceberg densities can be broken down into monthly or seasonal average values or can be expressed in terms of annual average areal iceberg density.

The average residence time of icebergs is the distinguishing characteristic between iceberg flux and areal density. The residence time, which is simply the length of time an iceberg spends in an area, is a function of the drift speed, the variability of drift direction (i.e. relatively straight versus meandering trajectories) and the proportion of time the iceberg is grounded. Areal density is directly proportional to both flux and residence time.

Although the iceberg grounding model, as well as the method described by Sanderson (1988) for calculating impact frequency relies on areal density, much of the early work on iceberg frequency dealt with flux. Since areal density and flux are closely related and insight into areal density can be attained by considering flux values, both will be considered in order to determine areal density values for the study area.

5.1.1 Iceberg Flux

Anderson (1971) analyzed International Ice Patrol (IIP) surveys conducted on the Labrador Shelf from 1963-1969. Iceberg sightings were combined with deterioration and drift models to produce monthly flux values across lines of latitude ranging from 48°N to 62°N. Results covering 48°N to 56°N are shown in Table 9. It can be seen that the flux across 56°N (966 per year), immediately north of the Makkovik Bank, is approximately six times higher than that at 48°N (157 per year), which is considered representative of the Grand Banks.

Ebbesmeyer et al. (1980) analyzed iceberg flux values across 48°N from 1900 to 1977 and found that the annual flux values followed an exponential distribution. An analysis of Anderson's flux values from 67°N to 48°N revealed that flux values decreased linearly, with a slope corresponding to a loss rate of approximately 2 icebergs/km.

Miller (1981) analyzed IIP data from 1880 to 1969 and found an annual average flux of 362 icebergs across 48°N, which is substantially higher than the value Anderson (1971)

determined for 48°N. Using the assumption that the relative flux values Anderson produced were correct, Miller used the ratio of the long-term 48°N flux to Anderson's 48°N values to produce a revised flux rate for 56°N. These values, taken from Petro-Canada (1983) are given in Table 10.

Annual iceberg flux values from the IIP (IIP, 2001) are shown in Figure 25 (top) for 1900-2000. The average flux for the whole record is 480 icebergs/year. The average flux from 1900-1969 is 365 icebergs/year, which is very close to the value calculated by Miller (1981). The average flux from 1963-1969 is 171 icebergs/year, which compares well with Anderson's (1971) value for the same time period. Examination of the time series indicates that the data that Anderson used for his analysis were collected during a period when there were relatively low iceberg frequencies. However, the average flux from 1981-2000 is 917 icebergs/year, which is considerably higher than the average for the entire record. The increase in flux after 1980 may be a result of improved detection methods, a natural increase in iceberg numbers, or simply a random fluctuation (or some combination of all three). A comparison between monthly 48°N flux values is shown in Figure 25 (bottom). If iceberg flux is adjusted using the same approach as Miller (1981), but by using the mean flux across 48°N from 1981-2000, a revised annual iceberg flux of 5640 (966×917/157) icebergs per year would be expected to cross 56°N.

Table 9 Iceberg Flux Across Various Degrees of Latitude (Anderson, 1971)

	56°N	55°N	54°N	53°N	52°N	51°N	50°N	49°N	48°N
Jan.	49	31	17	12	9	4	3	2	0
Feb.	77	59	39	30	23	14	8	5	5
Mar.	112	99	82	73	62	40	35	25	18
Apr.	112	105	98	93	89	76	66	53	46
May	133	126	116	111	106	86	75	67	57
June	134	130	118	107	102	67	32	29	23
July	122	120	91	64	42	37	22	15	8
Aug.	106	118	81	54	34	11	5	1	0
Sept.	68	75	49	33	22	2	1	0	0
Oct.	28	35	32	23	14	5	2	0	0
Nov.	10	11	15	11	9	5	3	0	0
Dec.	19	10	6	2	0	0	0	0	0
Total	966	909	744	613	512	347	263	197	157

Table 10 Iceberg Flux Across 56°N (Miller, 1981)

Month	Icebergs	% of Total
Jan.	90	4
Feb.	157	7
Mar.	269	12
Apr.	292	13
May	292	13
June	426	19
July	314	14
Aug.	225	10
Sept.	90	4
Oct.	45	2
Nov.	22	1
Dec.	22	1
Total	2244	100

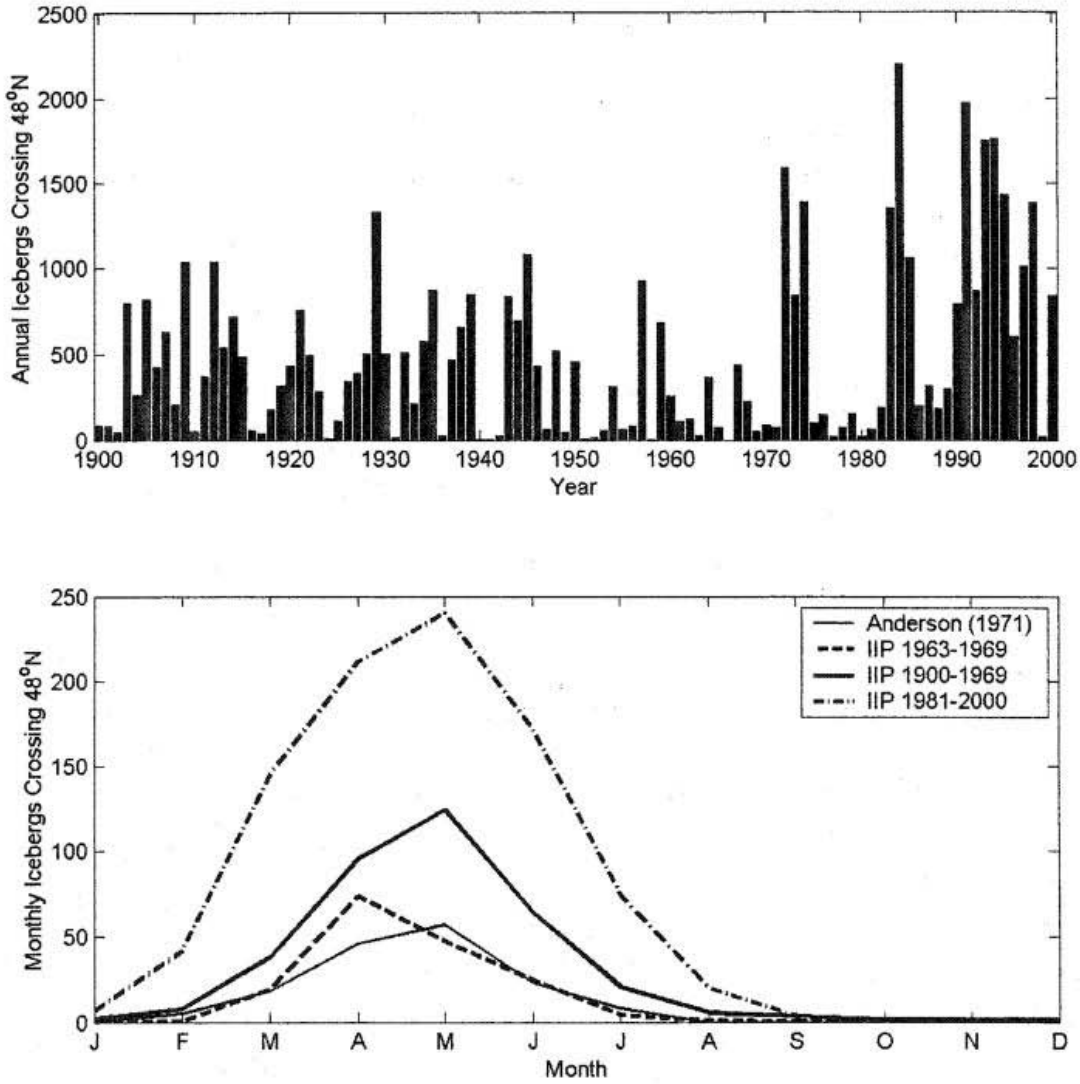

Figure 25 Iceberg flux across 48°N

5.1.2 Areal Density Inferred from Iceberg Flux and Distribution

It is possible to estimate iceberg density in the Makkovik Bank region based on a comparison of iceberg flux values, the distribution of iceberg sightings and iceberg density values on the Grand Banks.

Figure 26 shows the IIP iceberg sightings obtained during aerial surveys (PERD, 2001). The density of iceberg sightings clearly shows the lack of sightings on the Labrador coast compared to the Grand Banks. This reflects the difference in survey coverage, rather than the actual density of icebergs. It can also be seen that the east/west distribution of icebergs changes considerably with latitude. Icebergs along the Labrador coast (north of 55°N) tend to be concentrated along a relatively narrow band close to shore, 2 to 3 degrees longitude wide. Further south on the northern Grand Banks the distribution of icebergs widens to a band that covers approximately 10 degrees of longitude. If it were assumed that the number of icebergs were constant across a degree of latitude, iceberg flux per degree of latitude would be expected to decrease by a factor of 4 solely due to this dispersion between 56°N and 48°N. Given that a degree of longitude is 20% wider at 48°N than at 56°N this suggests a decrease of a factor of 5 on a per kilometer basis.

According to Anderson (1971), the annual iceberg flux across 56°N is approximately 6 times higher than the annual flux across 48°N. Combined with the longitudinal dispersion of icebergs, the resulting iceberg flux (on a per kilometer basis) across 56°N would be expected to be approximately 30 times higher than at 48°N. If it is assumed that the residence time of the icebergs in the degree latitude south of 56°N and 48°N are the same, then the average iceberg density would also be 30 times higher. An analysis of the IIP gridded current data (Murphy et al., 1996) indicates that the mean southerly drift rate in these two areas is approximately the same.

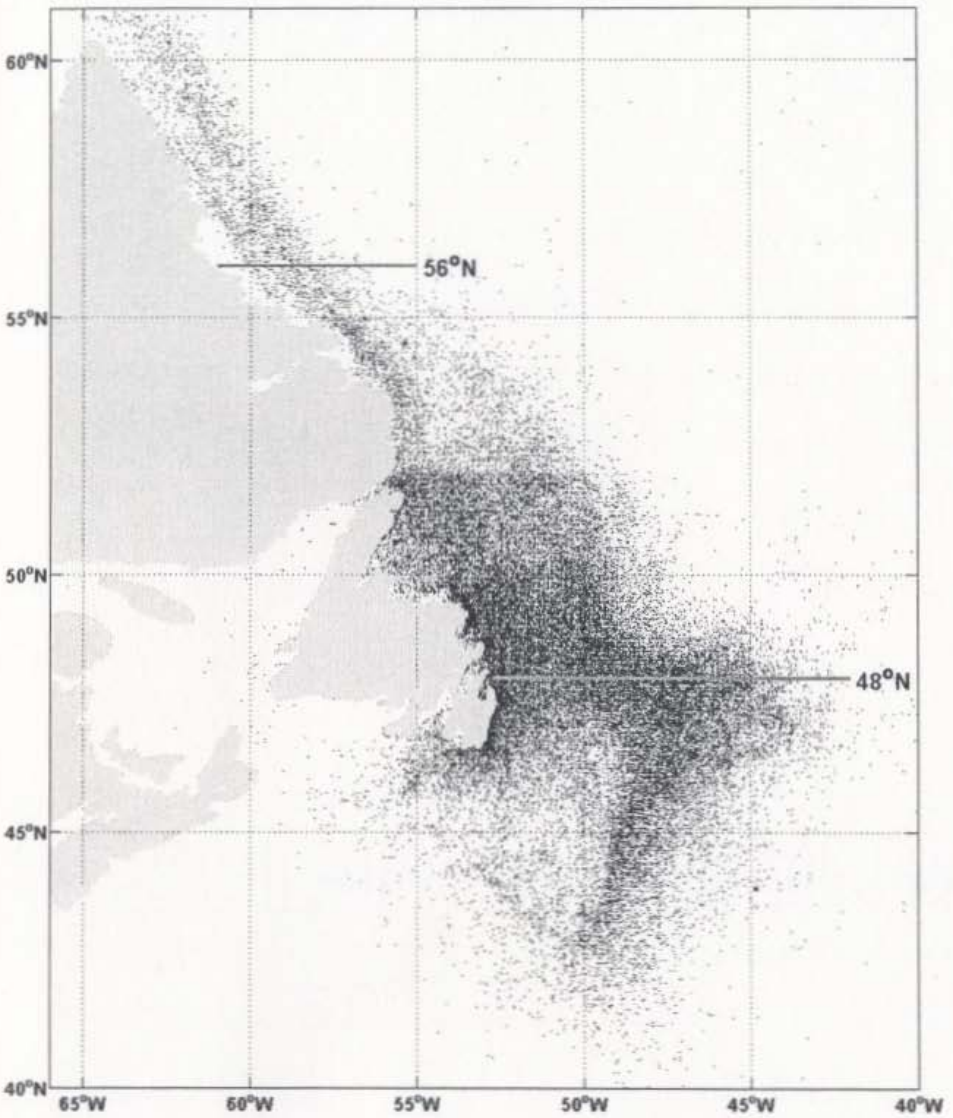

Figure 26 Distribution of IIP iceberg sightings obtained during aerial surveys (PERD, 2001)

The mean annual iceberg areal density based on IIP surveys from 1981-2000 (Jordaan et al., 1999) between 47°N and 48°N and 43°W and 53°W is 1.5×10^{-4} icebergs/km^2. Therefore, the average annual iceberg density between 55°N and 56°N, in the zone where icebergs are concentrated, would be expected to be approximately 4.5×10^{-3} icebergs/km^2.

5.1.3 Areal Density Based on IIP Iceberg Sightings

Gustajtis (1979) analyzed IIP iceberg sightings from 1963-1976 to generate iceberg distribution maps for offshore Labrador. Survey flights where coverage of the Labrador Shelf was not complete due to termination of the flight or poor visibility were not included in the analysis. Iceberg sightings were grouped into cells measuring 0.25 degrees latitude by 0.25 degrees longitude. Contouring routines were used to produce maps showing the concentrations of icebergs on the Labrador Shelf. Seasonal maps were produced covering winter (November-January), spring (February-April), summer (May to August) and fall (September and October). Due to the choice of presentation format, these charts do not readily lend themselves to use for risk analyses.

Petro-Canada (1983) also analyzed IIP data from 1963-1976 to produce iceberg density maps. Sightings were grouped into cells measuring one degree of longitude by a half-degree latitude. The total number of sightings for each cell was normalized by the number of flights over each cell, as determined by the number of instances when icebergs were reported. It is worth noting that there was no method to determine when a survey resulted in zero sightings, thus in this respect the results are conservative. The sightings were broken down into three "seasons": summer (July to October), winter (November to February) and spring (March to June). Note that these do not correspond with those defined by Gustajtis (1979). Results of the analysis are shown in Figure 27 to Figure 29. Also shown is the nominal number of flights over each cell.

A combined average annual iceberg density was determined for the study area, as indicated in Figure 30. A correction was also applied to account for the difference between the mean iceberg flux across 48°N based on recent data and iceberg flux during the period for which the original data were derived. The mean flux across 48°N was 387 icebergs/year for the 1963-1976 period and 917 icebergs/year for the 1981-2000 period. It was assumed that a similar increase would have been observed on the Makkovik Bank, so a factor of 2.4 (917/387) was applied to iceberg density values derived from data obtained in the 1963-1976 time period.

5.1.4 Areal Density Based on 1995 IIP Sightings

The PERD (2001) iceberg database contains limited iceberg sightings in the Makkovik Bank region after 1980. Iceberg sightings from aerial surveys are more suitable for density calculations than ship-based observations since aerial surveys tend to sample a large region over a fairly short time frame. In 1995 the International Ice Patrol conducted two aerial surveys that covered the Makkovik Bank region. The first was conducted on July 31, and the second on August 2. The locations of the icebergs sighted during these surveys are shown in Figure 31, along with the corresponding average iceberg areal density. These values are consistent with areal density values calculated by Petro-Canada (1983), however, they are only representative of mid-summer densities for one year and are of limited value for assessing long-term average values.

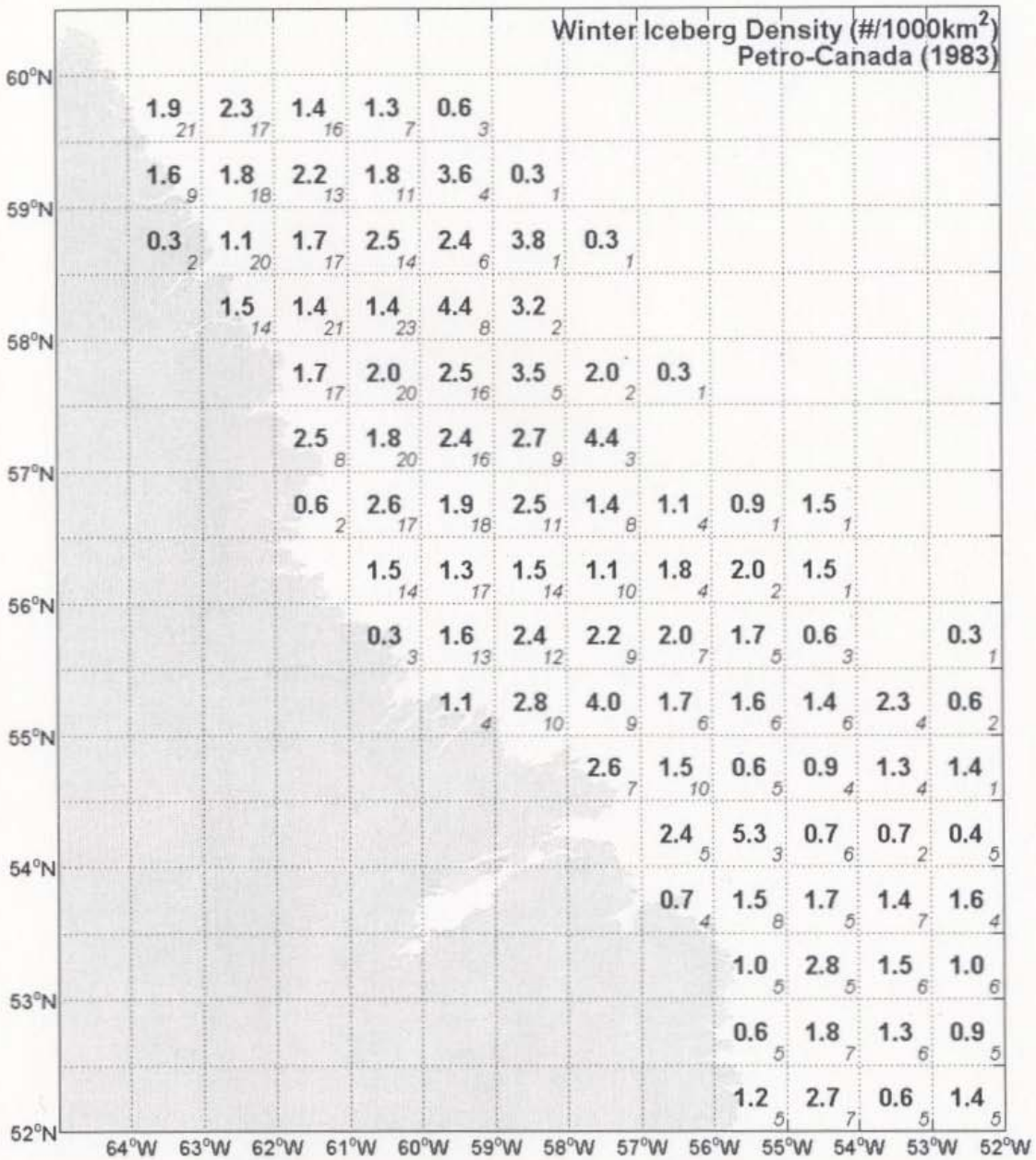

Figure 27 Average winter (November-February) iceberg areal density (#/1000 km^2) along Labrador coast and number of survey flights (Petro-Canada, 1983)

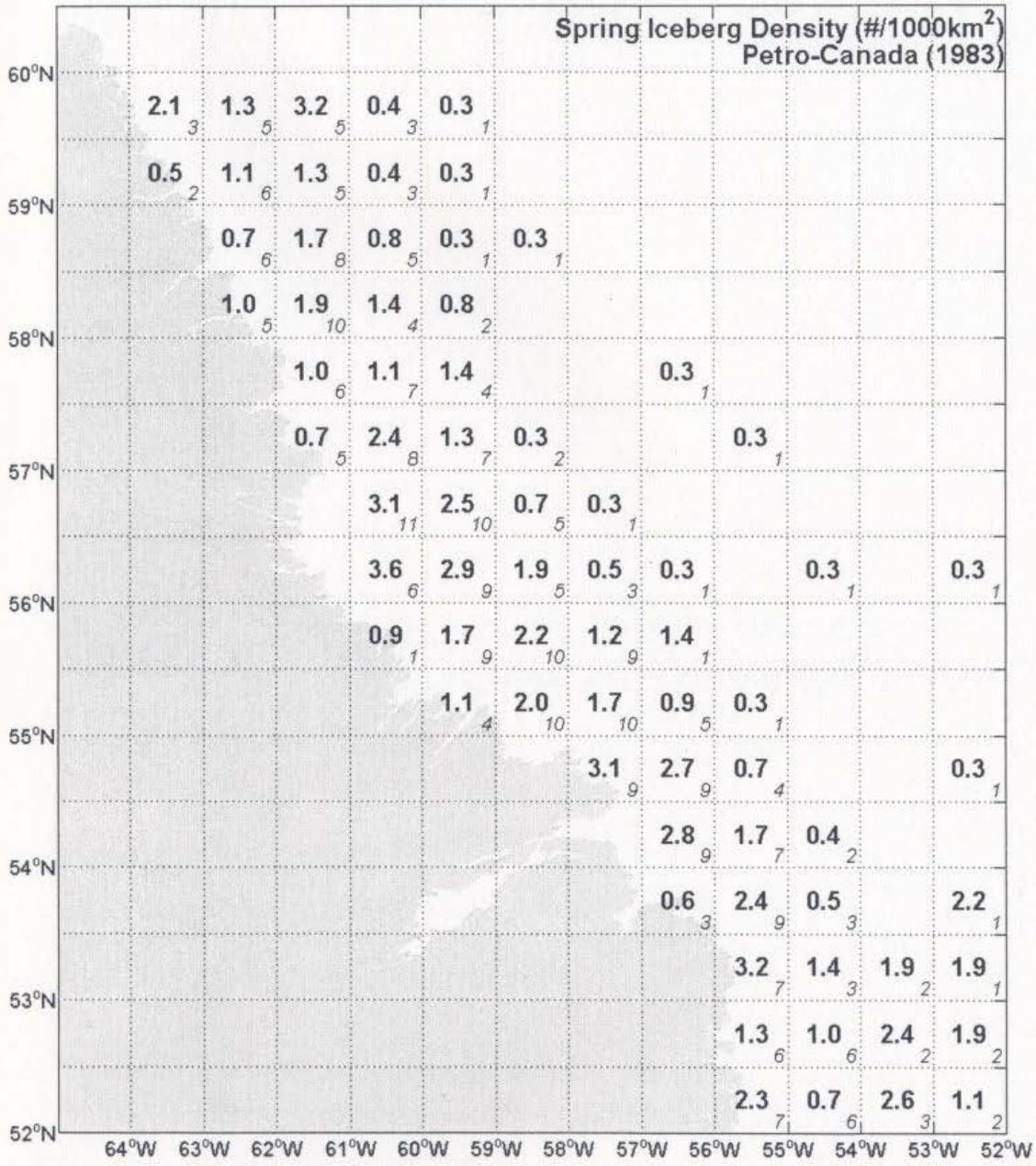

Figure 28 Average spring (March-June) iceberg areal density (#/1000 km^2) along Labrador coast and number of survey flights (Petro-Canada, 1983)

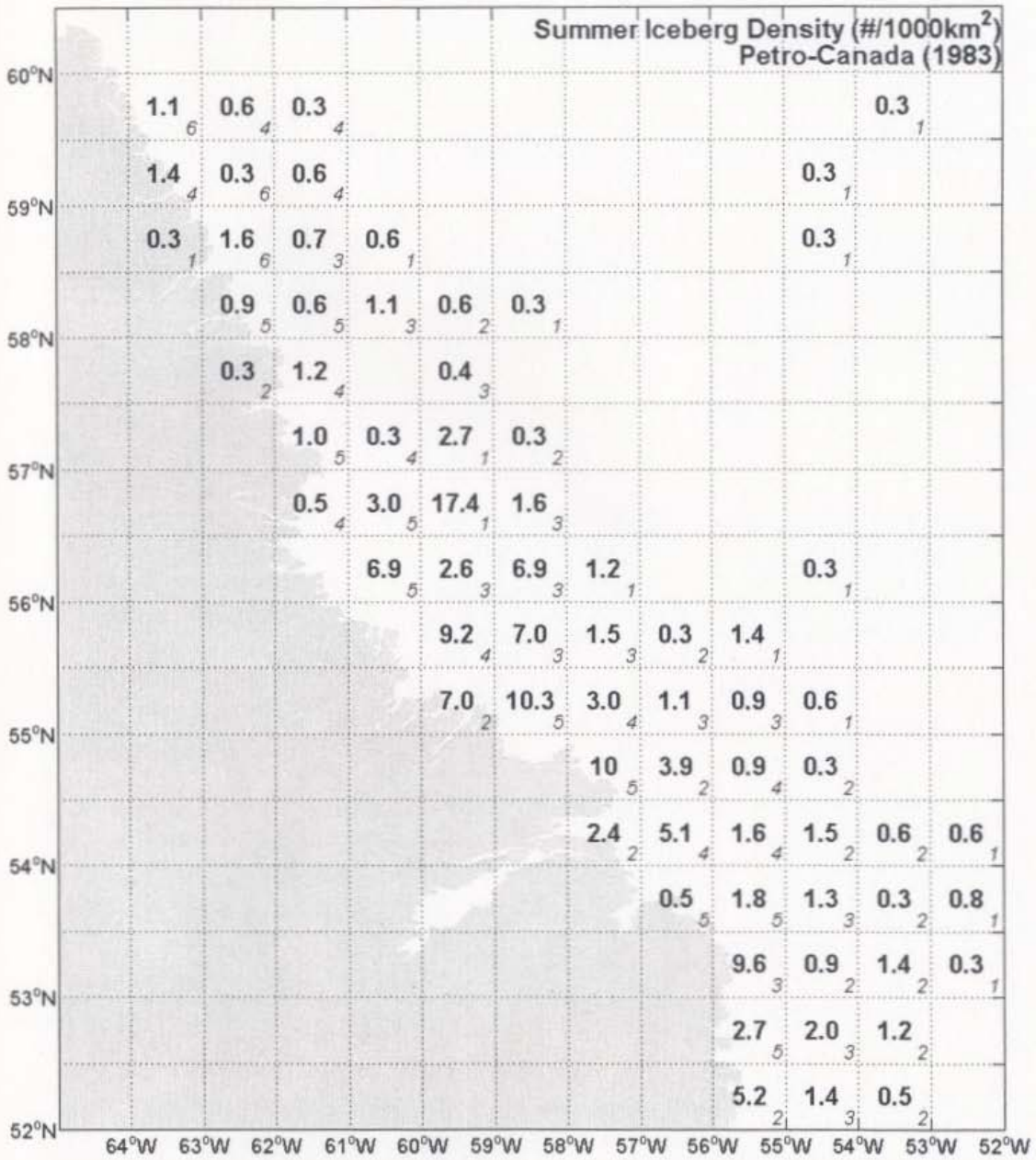

Figure 29 Average summer (July-October) iceberg areal density (#/1000 km^2) along Labrador coast and number of survey flights (Petro-Canada, 1983)

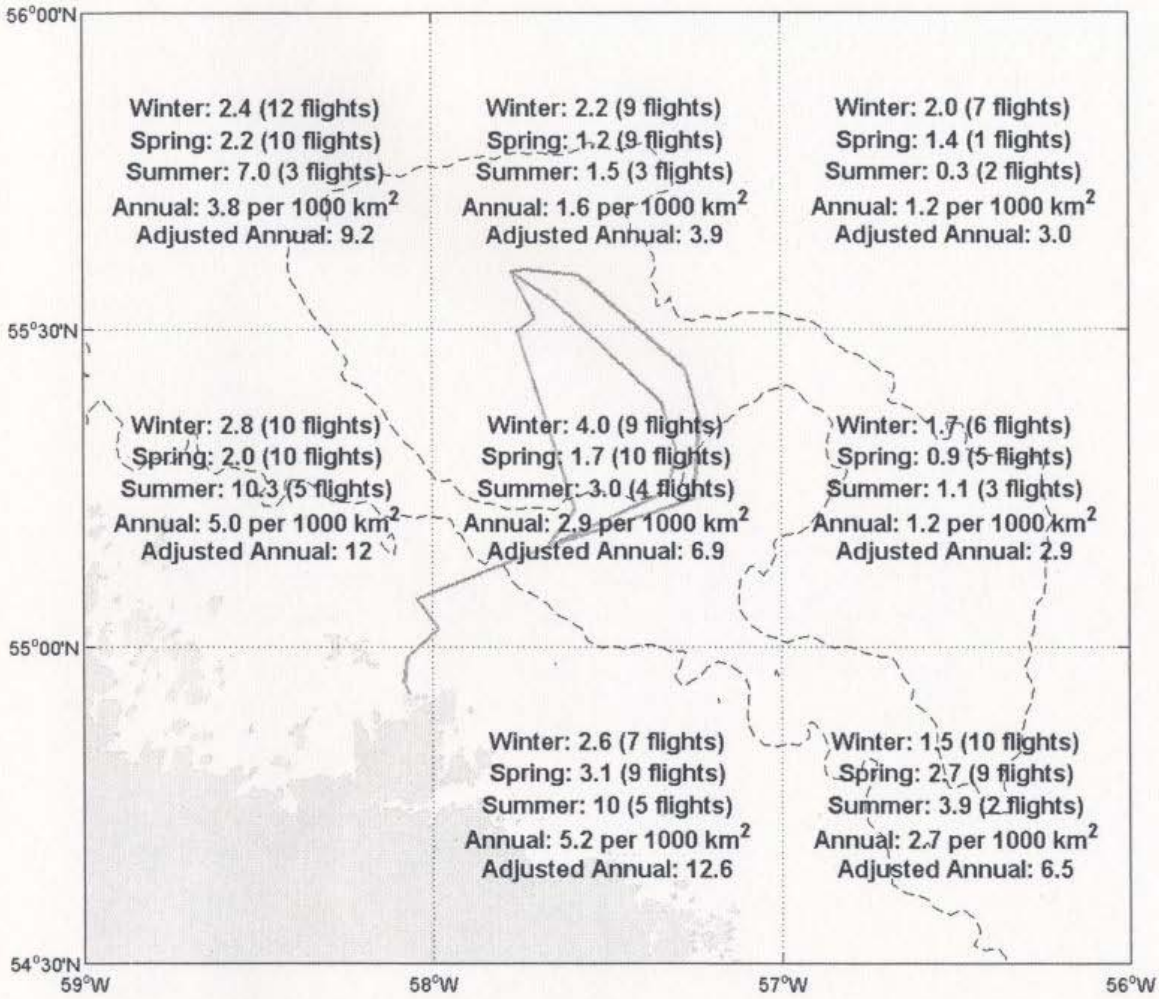

Figure 30 Annual iceberg density in study area, based on Petro-Canada (1983) analysis and an adjustment for 1981-2000 48°N flux values

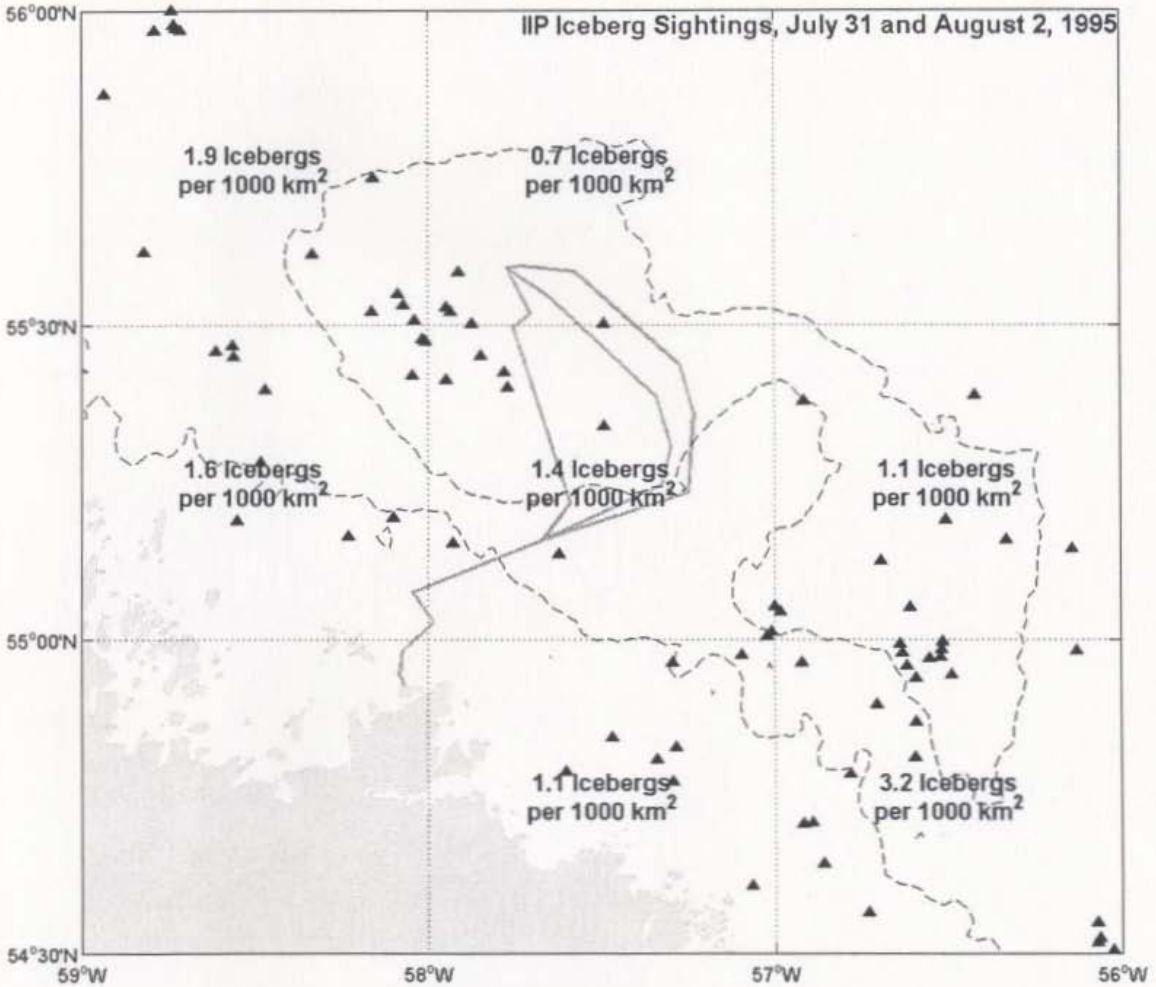

Figure 31 Iceberg densities based on IIP surveys, summer 1995

5.1.5 Iceberg Sightings During Survey Off Voisey's Bay (C-CORE, 1998)

C-CORE (1998) conducted iceberg surveys using a helicopter on March 31 and April 2, 1997, in the vicinity of Voiseys Bay (approximately 56°30′ N, 60° W). The locations of the icebergs sighted during the survey are shown in Figure 32, and are close enough to the study area to warrant consideration. The density of icebergs in the survey area was estimated to be approximately 0.13 icebergs per square nautical mile (0.04 per km^2). This is approximately 25 times higher than densities observed during the 1995 IIP surveys, however this can be attributed to seasonal variations.

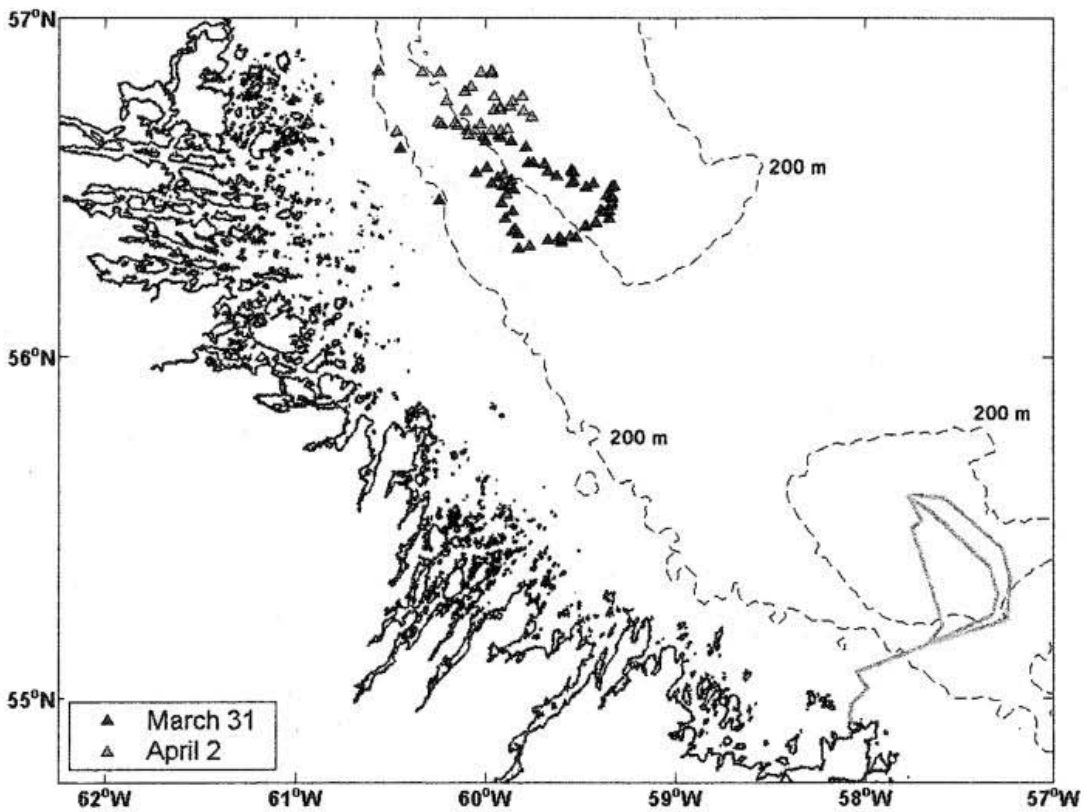

Figure 32 Locations of icebergs sighted off Voisey's Bay (C-CORE, 1998)

5.1.6 Areal Density Based on CIS Survey Data

Iceberg charts issued by the Canadian Ice Service (CIS) give iceberg frequencies off the coasts of Newfoundland and Labrador on a degree square basis. These charts are issued regularly during the ice season and are produced using a combination of aerial reconnaissance, ship reports and shore based observations. The data obtained via aerial reconnaissance are derived both from the CIS and the IIP. A sample iceberg chart is shown in Figure 33. The likely extent of icebergs is indicated with a thick continuous line, while the known data limit is indicated with a dashed line. While some iceberg counts are given beyond this line, a low confidence would be associated with these values. The area covered by these charts varies, and the Makkovik Bank region is not routinely covered. During late summer (August or September) ice charts are occasionally produced which show iceberg counts as far north as 61°N. Unfortunately, these are not produced during the peak of the iceberg season (June and July).

Iceberg charts dating back to 1988 were reviewed to obtain iceberg counts for the area ranging from 54°N to 56°N and 56°W to 59°W. Iceberg counts reported when the area was outside the known data limit were not included. When the known data limit included this area but there was no iceberg count indicated, a zero was assumed. Including zero counts had little effect on the results, except for the degree square centered on 54°30″N, 58°30″W, where excluding zeros increased iceberg density by 30%. The results of this analysis are given in Table 11 and shown in Figure 34.

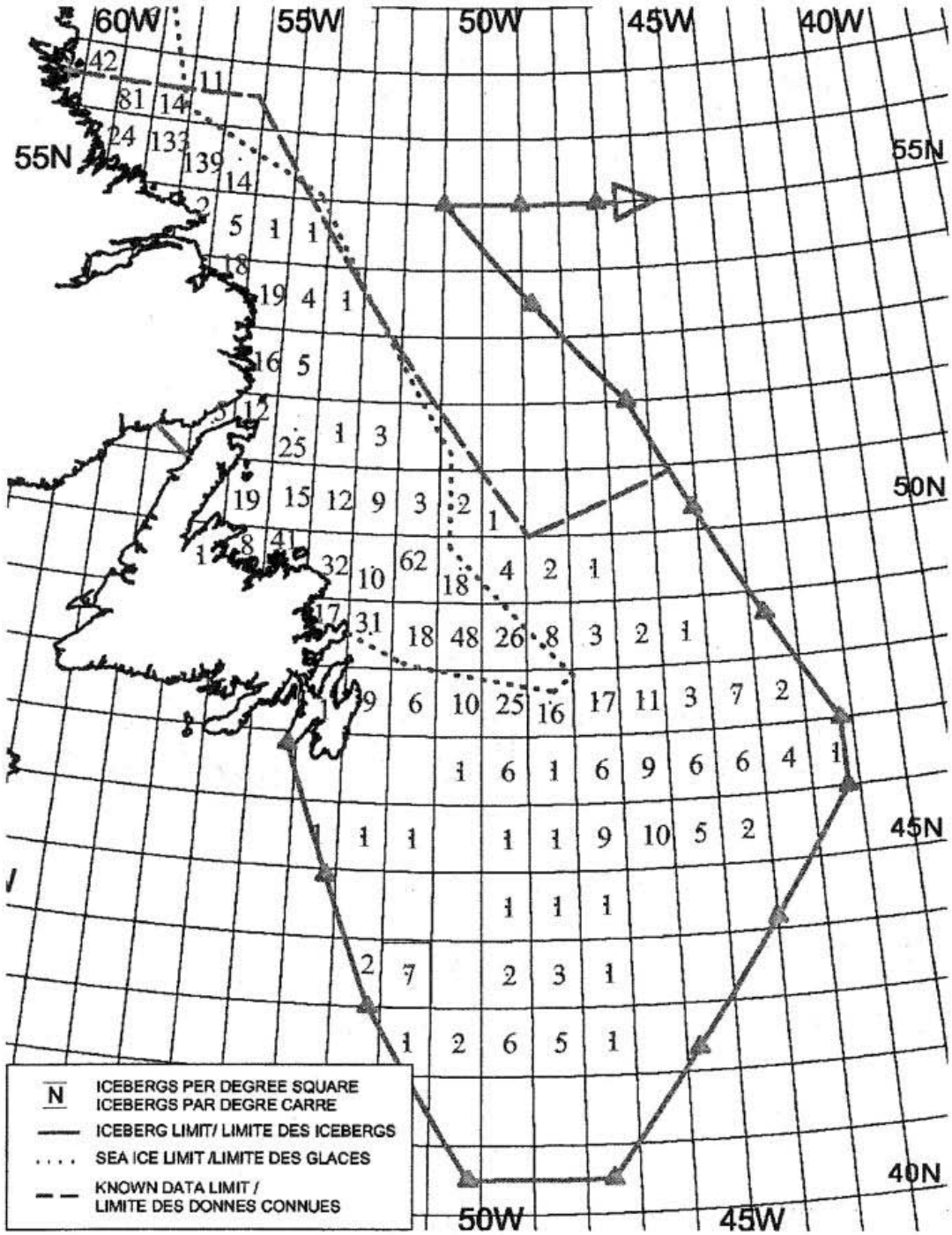

Figure 33 Canadian Ice Service iceberg chart for April 24, 2002

Table 11 Iceberg Densities from CIS Iceberg Charts (Years of Data Shown in Brackets)

Degree Square Center		55°30′N 58°30′W	55°30′N 57°30′W	55°30′N 56°30′W	54°30′N 58°30′W	54°30′N 57°30′W	54°30′N 56°30′W
Land		2%	0%	0%	75%	35%	0%
Average Icebergs per Degree Sqaure	Feb.	1.9 (2)	3.5 (2)	13.8 (2)	4.0 (2)	11.3 (2)	1.3 (2)
	Mar.	6.9 (2)	5.5 (2)	7.8 (2)	1.6 (4)	2.9 (4)	3.2 (4)
	Apr.	52.6 (2)	62.8 (2)	11.5 (2)	2.5 (3)	19.5 (4)	33.6 (5)
	May	28.2 (3)	23.7 (3)	29.1 (3)	7.1 (6)	23.5 (7)	32.0 (8)
	June	61.3 (4)	60.9 (5)	27.5 (5)	9.1 (5)	20.2 (6)	73.7 (7)
	July	172.3 (4)	99.0 (4)	61.2 (4)	108.8 (4)	103.3 (6)	83.8 (6)
	Aug.	31.9 (7)	17.5 (7)	33.4 (7)	9.0 (8)	19.3 (8)	22.5 (9)
	Sept.	5.3 (9)	5.2 (8)	3.6 (9)	4.5 (9)	3.3 (9)	4.6 (9)
Mean (km^{-2})		6.6×10^{-3}	5.0×10^{-3}	3.4×10^{-3}	10.2×10^{-3}	5.7×10^{-3}	4.6×10^{-3}

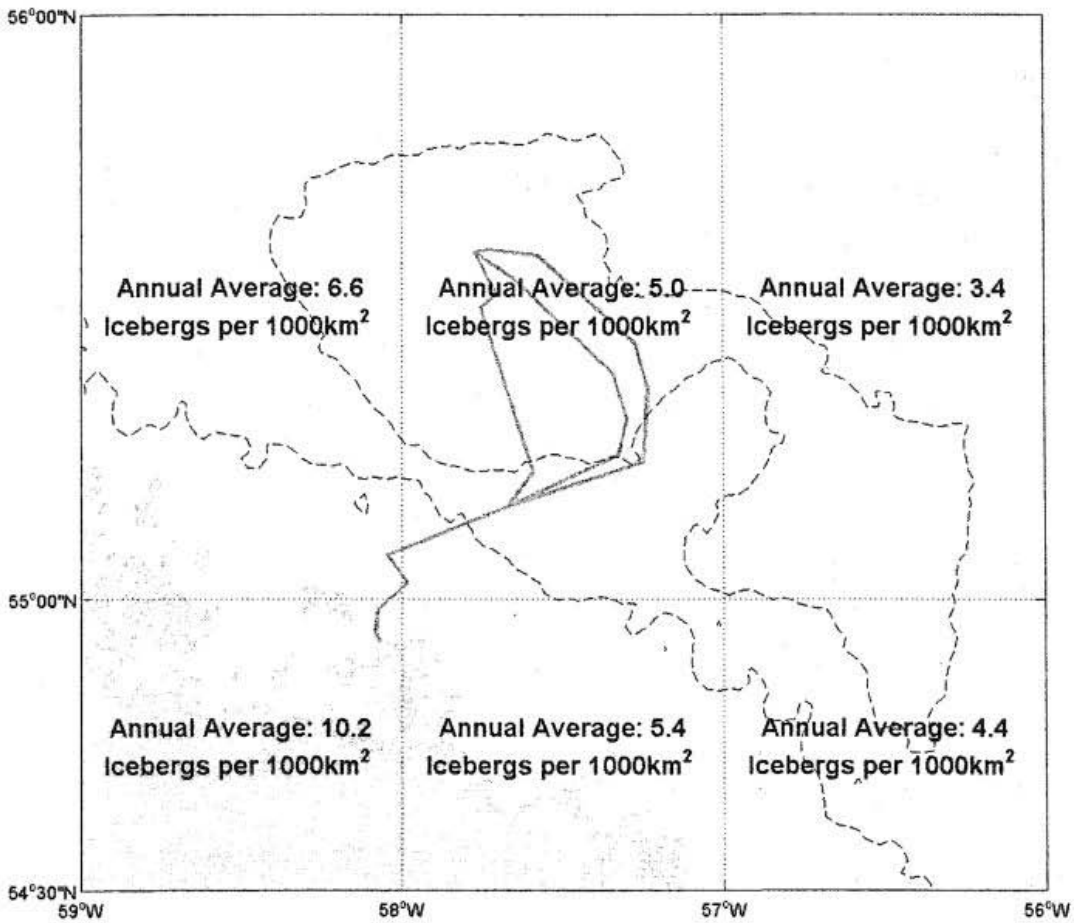

Figure 34 Annual iceberg densities based on analysis of CIS iceberg charts

The proportion of each degree square covered by land was determined and the iceberg densities were adjusted accordingly. To calculate an annual average density some assumptions were made for iceberg densities from October to January. Anderson's (1971) average flux values across 56°N from October to January are 25% of the average flux values from February to September, while Petro-Canada's (1983) average winter iceberg density values for the Makkovik Bank area are approximately half of the average of the spring and summer values. In order to produce a reasonably conservative annual value, it was assumed that the average iceberg density from October to January was the same as the average density from February to September. Using assumed October to January areal densities based on areal density data from Petro-Canada (1983) or Anderson (1971) decreased the annual average areal densities by 16% and 25%, respectively.

5.1.7 Conclusions

Iceberg densities for the Makkovik Bank region were estimated from a variety of sources. Densities based on single surveys varied considerably (i.e. Voisey's Bay survey and 1995 IIP sightings) but densities based on repeated surveys were reasonably consistent. Given the limited data and the likelihood of undercounting of icebergs, a conservative areal density value was adopted. For simplicity, a single areal density value of 1×10^{-2} icebergs/km^2 was used for the risk analysis, which corresponds to approximately 70 icebergs per degree square.

5.2 Iceberg Size

To determine the number of iceberg keels that can impact the seabed at a particular water depth, it is necessary to obtain the distribution of iceberg drafts. Several studies are available that document iceberg draft measurements. However, the icebergs that are selected for draft measurements are usually not representative of the overall iceberg population. For example, PERD (1999) presents a comprehensive collection of iceberg shape and size measurements from the Grand Banks and the Labrador Shelf. While the mean iceberg waterline length on the Grand Banks is generally considered to be 59 m (Jordaan et al., 1995), the PERD (1999) iceberg shape and geometry database shows that the mean waterline length of icebergs south of 48°N with measured drafts is 98 m (67 measurements). Clearly, an iceberg draft distribution based solely on measured iceberg drafts would not be representative of the overall population. The approach that is generally used is to develop an iceberg length/draft relationship based on icebergs with measured waterline lengths and drafts and combine this relationship with an iceberg waterline length distribution considered representative of the overall population to generate an iceberg draft distribution. This is the approach that will be used in this analysis.

5.2.1 Iceberg Physical Dimensions Study (Petro-Canada, 1983)

Above-water dimensions for over 600 icebergs were obtained from aerial surveys over the Labrador Sea during the spring of 1979 (Petro-Canada, 1983). Thirty-five flight lines were flown perpendicular to the coast between March 2 and June 11 at an altitude of

approximately 900 m. Nine flight lines, of which four passed over the Bjarni site, were selected for analysis. The areas covered by the flight lines are shown in Figure 35.

Icebergs were visually distinguished from the surrounding pack ice using cues such as height, the presence of open water tracks (due to differential movement), texture (icebergs are smoother), tone (icebergs are usually more reflective), waves breaking at their base, or the presence of underwater rams. The black and white stereo aerial photographs were processed using a Zeiss G-2 Sterocord that allowed the measurement of iceberg height. Iceberg length and width were measured using a measuring magnifier and waterline area was measured using a gridded overlay.

The mean iceberg waterline length observed for all icebergs was 35.4 m and the distribution is shown in Figure 36. Less than 10% of the data are in the bergy bit or growler classes. As shown in Figure 37, if only icebergs in the Bjarni area are considered (line 2 in Figure 35), the mean iceberg waterline length is 44.9 m. Less than 2% of these data are in the bergy bit or growler classes. Excluding icebergs with waterline lengths less than 16 m results in a mean overall waterline length of 37.5 m, and a mean waterline length of 45.1 m for the Bjarni area. The presence of so many small icebergs is counterintuitive, and may be an anomaly restricted to that particular year and season.

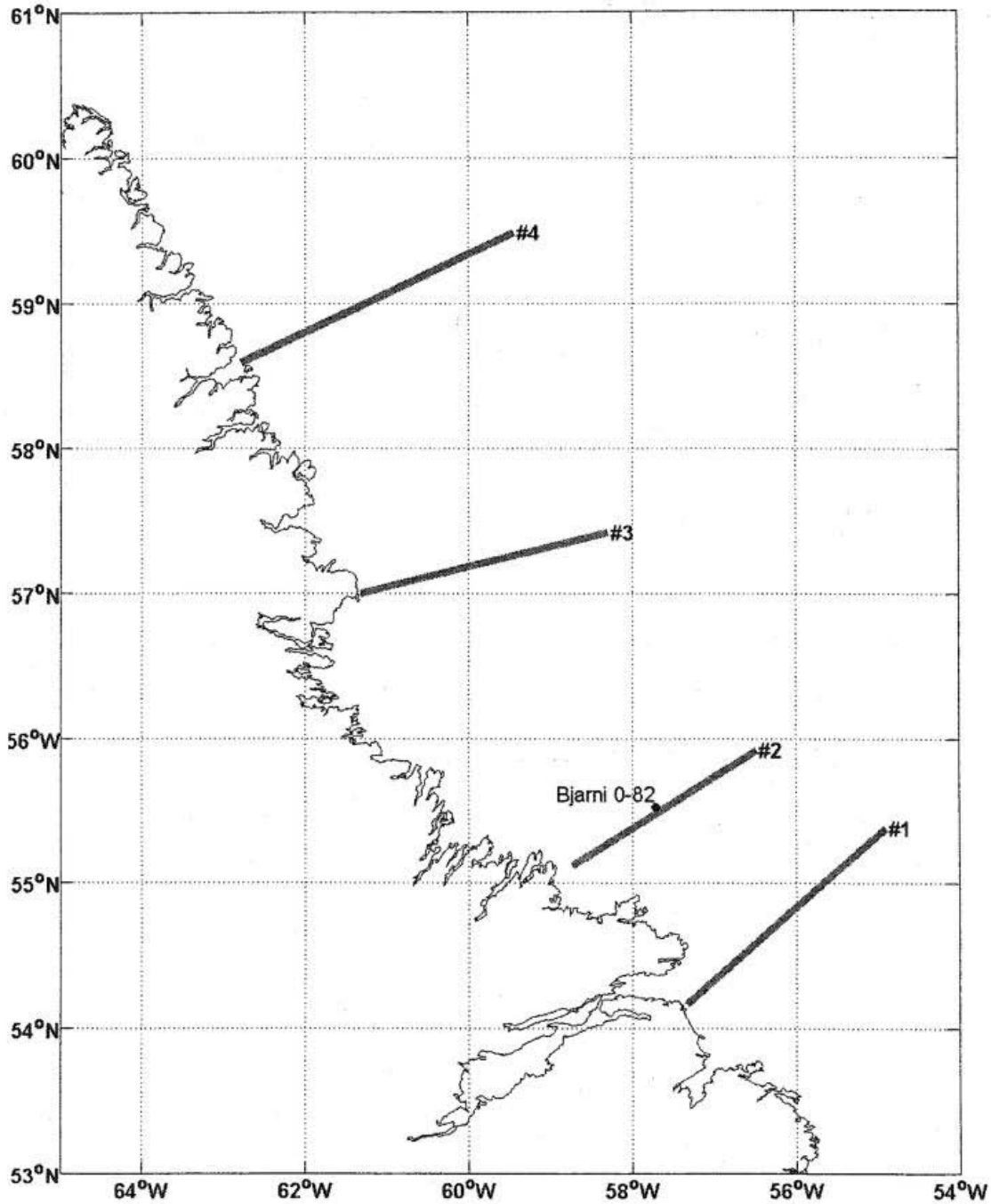

Figure 35 Location of flight lines for aerial surveys (from Petro-Canada, 1983)

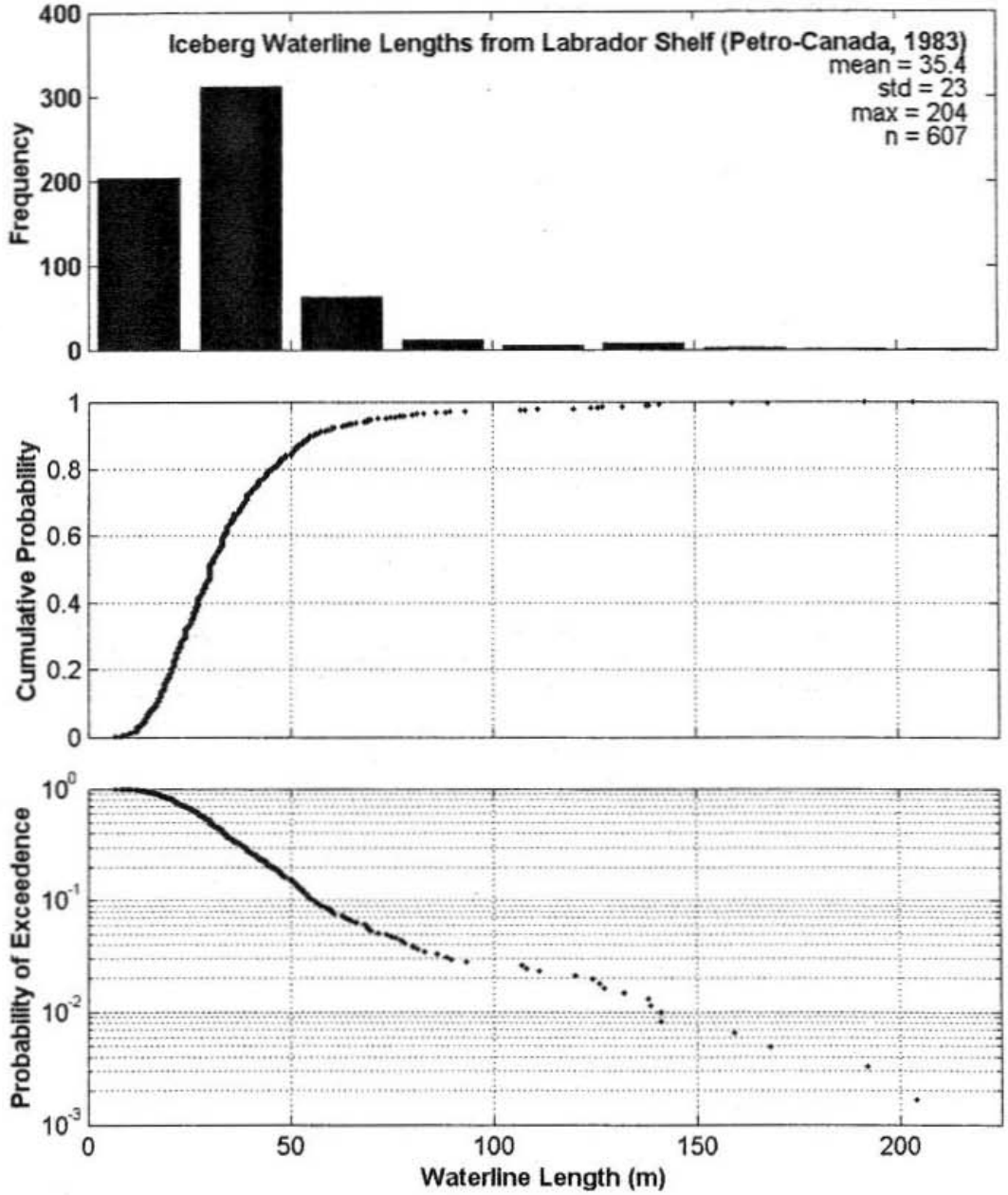

Figure 36 All iceberg waterline lengths from Petro-Canada (1983) study

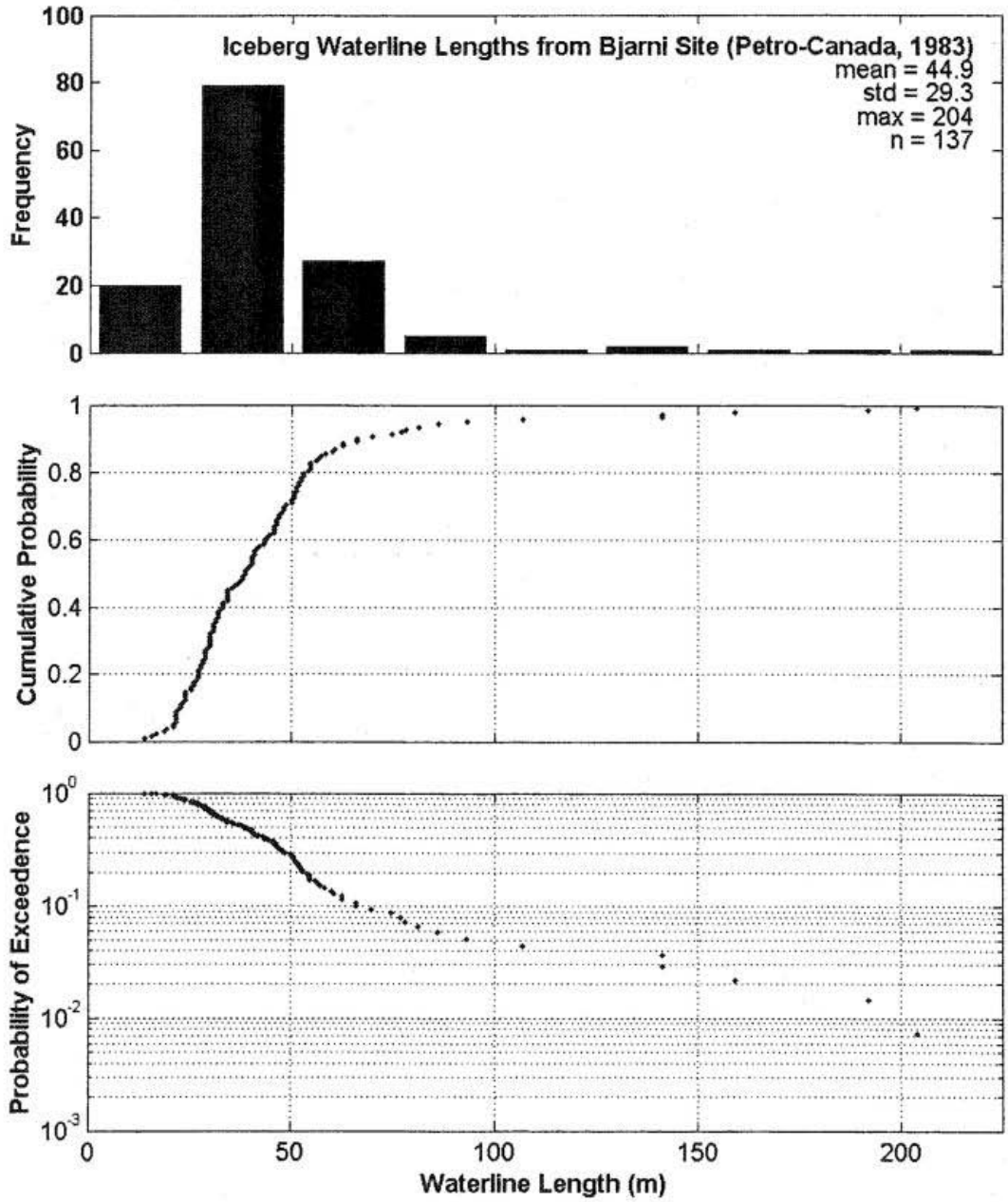

Figure 37 Iceberg waterline lengths from Bjarni site (Petro-Canada, 1983)

5.2.2 Iceberg Size Distribution Observed off Voisey's Bay (C-CORE, 1998)

C-CORE (1998) conducted iceberg surveys on in the vicinity of Voisey's Bay (see Figure 32). Two helicopter flights were used to locate icebergs that were recorded using a video camera. It can be seen that the survey area is approximately 100 km north of the study area, so it would be expected that the observed iceberg size distribution should be representative of the Makkovik Bank.

Iceberg dimensions were determined from an analysis of the videotape. The height of some of the larger icebergs was determined by hovering next to the icebergs and recording the values shown on the altimeter. Figure 38 shows the observed iceberg waterline length, which had a mean of 61 m. Excluding icebergs with waterline lengths less than 16 m has a minor effect, raising the mean waterline length to 63 m. Due to the roughness of the surrounding pack ice, it is thought that some growlers may have escaped detection.

5.2.3 Iceberg Size Distribution Observed During Drilling Operations

Iceberg waterline length data for collected during drilling operations on the Makkovik Bank were as obtained from wellsite reports (Marine Environmental Services, 1977; MacLaren Marex, 1980; MacLaren Plansearch, 1981, 1982). Iceberg waterline length measurements were given in towing logs as well as the iceberg track records.

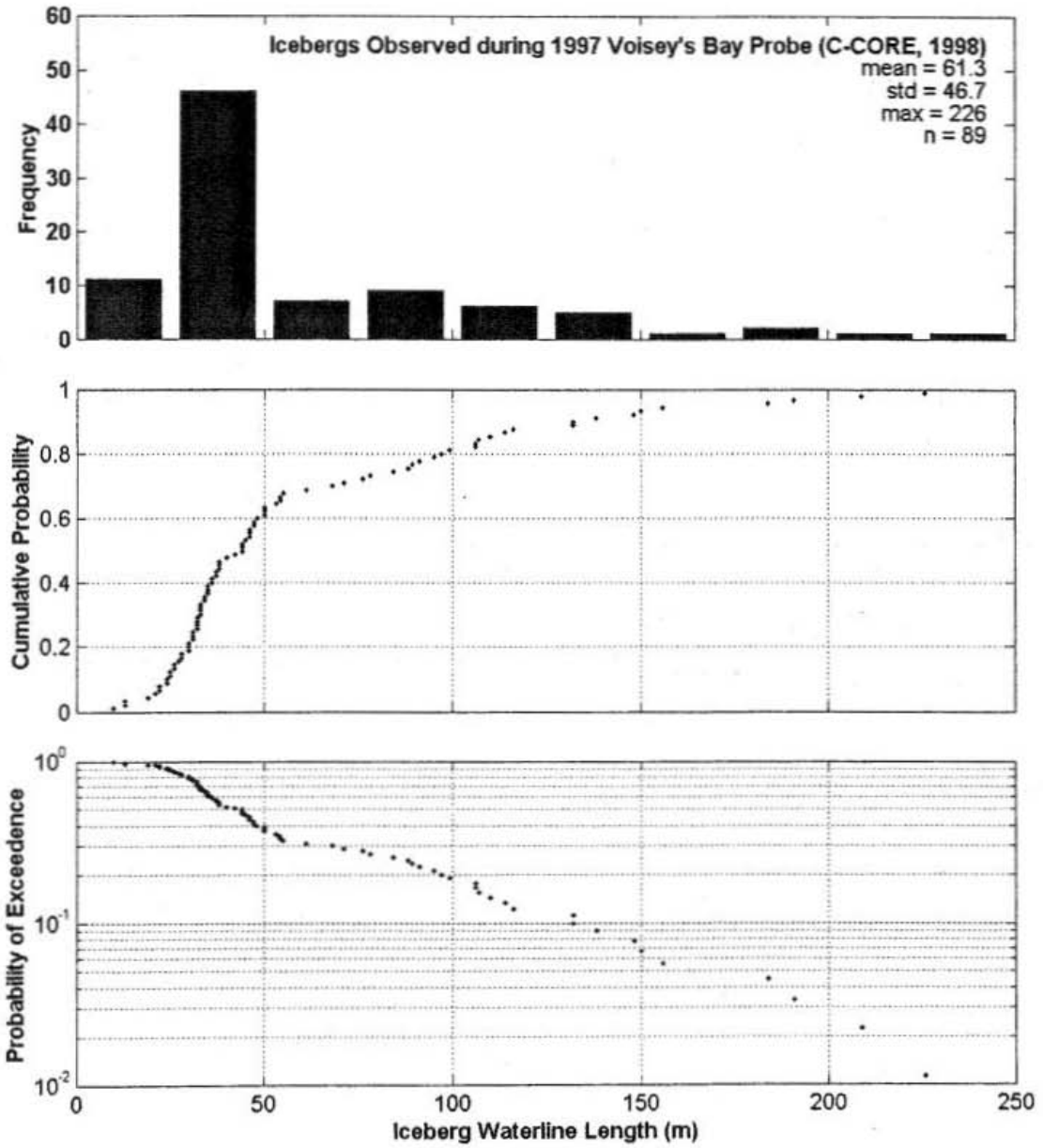

Figure 38 Waterline length distribution of icebergs observed during Voisey's Bay probe (C-CORE, 1998)

Approximately 20% of the icebergs recorded in the wellsite reports had waterline lengths reported. A small number were recorded as bergy bits or growlers and were not assigned waterline lengths. Approximately 10% (61) of the iceberg records consisted of one radar sighting, and 50% of the remaining records were of a total duration of less than a day, which did not allow much time for a support vessel to locate the icebergs and perform measurements.

Table 12 summarizes the iceberg waterline length data for each well and for the combined data set, for which the distribution is shown in Figure 39. Before combining the waterline measurements from the various wells to produce a composite waterline distribution, a check was performed to ensure different wellsite records from the same year did not contain duplicate values. One was found for 1979 (Bjarni 0-82 and Tyrk P-100) and one was found for 1981 (Bjarni 0-82 and North Bjarni F-06). The duplicate values were purged from the composite distribution.

It is interesting to note that the Tyrk P-100 (1979) and Bjarni (1979) data were located in the same year and location as the data for the Petro-Canada (1983) Iceberg Physical Dimension Study, yet there is more than a factor of two difference between the mean waterline length from the two data sets. The wellsite data were collected between mid-July and mid-October, while the aerial surveys were performed in May and early June, which may account for some of the difference. However, it is far more likely that the difference was due to a bias in wellsite iceberg measurements. Many smaller icebergs

were likely never detected by radar. Also, iceberg measurements were usually performed on icebergs that are candidates for towing, and towing efforts would have been focused on the icebergs that posed the largest threat, which, all other factor being equal, would have been the larger icebergs. For these reasons, it is thought that a iceberg waterline length distribution based solely on wellsite observations would be extremely conservative.

Table 12 Iceberg Waterline Lengths from Wellsite Observations on Makkovik Bank

Wellsite	Year	No. of Iceberg Records	Waterline Lengths Recorded	Mean (m)	Standard Deviation (m)
Herjolf M-92	1976	27	16	103.9	66.8
Tyrk P-100	1979	168	34	104.7	44.9
Bjarni O-82	1979	101	49	103.6	59.0
	1980	15	9	91.8	86.7
	1981	383	33	86.3	54.8
North Bjarni F-06	1981	57	19	114.2	57.6
Combined	N/A	749	158	100.3	57.6

5.2.4 Iceberg Size Observations from IIP Aerial Surveys

The PERD iceberg database (PERD, 2001) contains in excess of 180,000 iceberg sightings covering a very large geographic area with sightings from a variety of sources. There is a substantial quantity of iceberg size data, but there are no measured iceberg waterline lengths further north than 51°N. However, there are numerous sightings on the Labrador Shelf in the PERD iceberg database where the iceberg has been assigned to a size class.

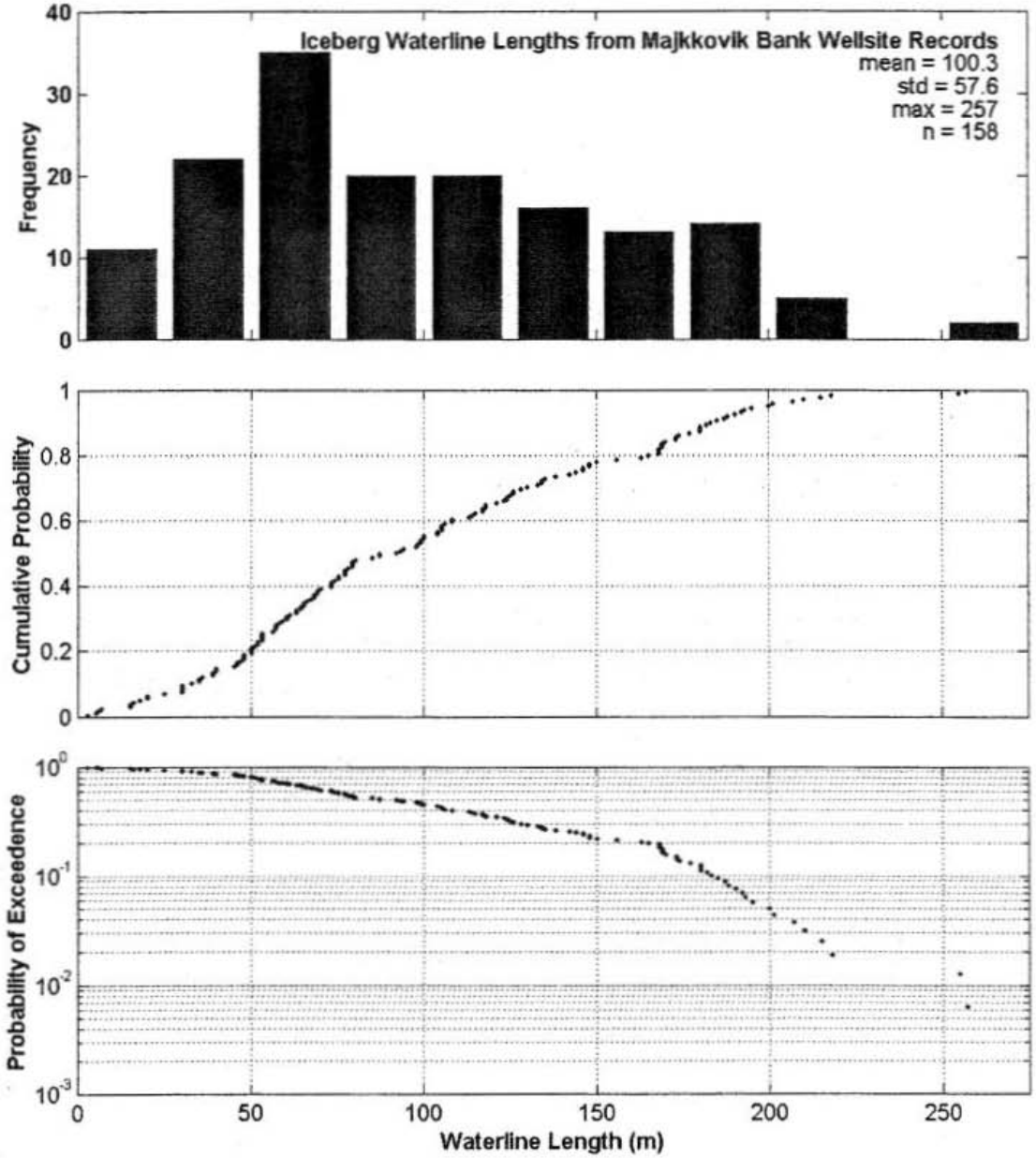

Figure 39 Iceberg waterline lengths recorded during drilling operations on Makkovik Bank (1976-1981)

Iceberg size classifications from some sources (i.e. ship's reports) are not reliable. For example, one of the towing logs reviewed for the iceberg drift analysis gave descriptions of two towed icebergs as bergy bits (usually a term reserved for icebergs with waterline lengths below 5m) and then reported waterline lengths of 30 and 50 m (MacLaren Marex, 1980). Iceberg size data were restricted to those obtained from aerial surveys performed by the International Ice Patrol (IIP). These observations, made by professional ice observers, would be expected to have a reasonable degree of consistency. Table 13 gives the waterline length ranges for the various size classes used by the IIP.

Table 13 International Ice Patrol Iceberg Size Classes

Size Classification	Waterline Length (m)
Growlers	0-15
Small	16-60
Medium	61-122
Large	123-213
Very Large	>213

The "Very Large" size class is a relatively recent invention. No icebergs are reported in this size class prior to 1993, which excludes most of the data collected on the Labrador Shelf. For this reason, any further discussion and analysis using iceberg size class data will lump together the "Large" and "Very Large" size classes. The number of icebergs reported in the "Growler" size class (which actually includes both growlers and bergy bits) seems to be much less than would be expected. Approximately 10% of icebergs assigned to a size class are in this group, however indications are that the actual number of icebergs in this size class is approximately equal to the total number of icebergs in all

other size classes combined (Crocker et al., 2000). Further analysis of IIP iceberg size class data will not consider this size class.

Table 14 shows a breakdown of the iceberg size class data from the Grand Banks, the Labrador Shelf and the Makkovik Bank. The Grand Banks data were taken from an area bounded by 46°N to 48°N and 47°W to 50°W, which was the approximate area from which measured iceberg lengths were used to derive the 59m mean value commonly used on the Grand Banks. The Labrador Shelf data were taken from an area bounded by 52°N to 62°N and the Makkovik Bank data were taken from an area bounded by 55°N to 56°N. A comparison of the relative proportions in each size class for each of the three areas indicates that there is very little difference.

Table 14 Size Class Data from IIP Aerial Surveys

Size Class	Grand Banks		Labrador Shelf		Makkovik Bank	
	Number	Proportion	Number	Proportion	Number	Proportion
Small	2020	49.4%	3937	52.7%	423	45.7%
Medium	1507	36.9%	2584	34.6%	349	37.7%
Large and Very Large	561	13.7%	951	12.7%	154	16.6%

Given that the iceberg survey off Voisey's Bay (C-CORE, 1998) and the Iceberg Physical Dimensions Study (Petro-Canada, 1983) were both conducted in the spring and early summer (March to early June) and the wellsite iceberg observations were obtained in mid-summer and fall (late June to October), there exists the possibility that the difference in iceberg size is a seasonal effect. For example, in the spring the water is colder and the melt rate of smaller icebergs could be slower, resulting in a higher proportion of small

icebergs. Table 15 shows an analysis of the iceberg size data for the Labrador Shelf broken down into two time periods corresponding to the times periods when the different data sets were obtained. June was excluded to ensure a clear demarcation between the two subsets. There were insufficient data to make a meaningful comparison for the Makkovik Bank. There does not appear any significant difference between the two time periods. An analysis of Labrador Shelf size data on a monthly basis did not indicate any meaningful trends. It was concluded that the difference in the mean observed iceberg lengths was not due to seasonal effects.

Table 15 Seasonal Size Class Data from IIP Aerial Surveys

Size Class	Labrador Shelf	
	March -May	July - October
Small	47.2%	41.9%
Medium	40.6%	42.2%
Large and Very Large	12.1%	15.9%

5.2.5 Iceberg Length Distribution for the Makkovik Bank

The iceberg waterline length distribution on the Grand Banks is represented by an exponential distribution with a mean of 59 m (Jordaan et al., 1995). When using this distribution to generate iceberg masses (i.e. for impact force simulations) or drafts (i.e. for impact probability with subsea structures) a sample population of icebergs is generated and icebergs with waterline lengths less than 15.5 m are discarded. The justification for discarding icebergs with waterline lengths less than 15.5 m is that the occurrence of these icebergs are not documented in iceberg surveys so that the frequency estimates do not include this size class. Note that the size classes in Table 13 are given as

integer values, so the distinction between growlers and small icebergs was set at 15.5 m when dealing with continuous variables.

Figure 40 compares the exceedance values for the various iceberg waterline datasets previous discussed. Also shown is the exceedance plot for the Grand Banks waterline length distribution, as well as exceedance plots for exponential distributions with means of 80 m and 100 m. All of these datasets and distributions have been normalized with respect to 16 m waterline length. The Grand Banks waterline length distribution predicts higher frequencies for medium and large icebergs than would be indicated by either the data from the Iceberg Physical Dimensions Study or the iceberg survey off Voisey's Bay. However, it does agree very well with the exceedance level for the large iceberg size class determined from the IIP sightings. Compared with the wellsite data, the Grand Banks distribution predicts lower frequencies for medium and large icebergs, but over-predicts the frequency of very large icebergs (> 213m). This is significant since this is the iceberg size range that poses the most risk in the water depth range of interest (140 m and greater). Exponential distributions with means of 80 and 100 m have been included for comparison, but there is no compelling reason to use them.

5.2.6 Iceberg Draft Distribution

Several sources have documented relationships between iceberg waterline length and measured draft that can be used to develop iceberg draft distributions for use in the grounding model.

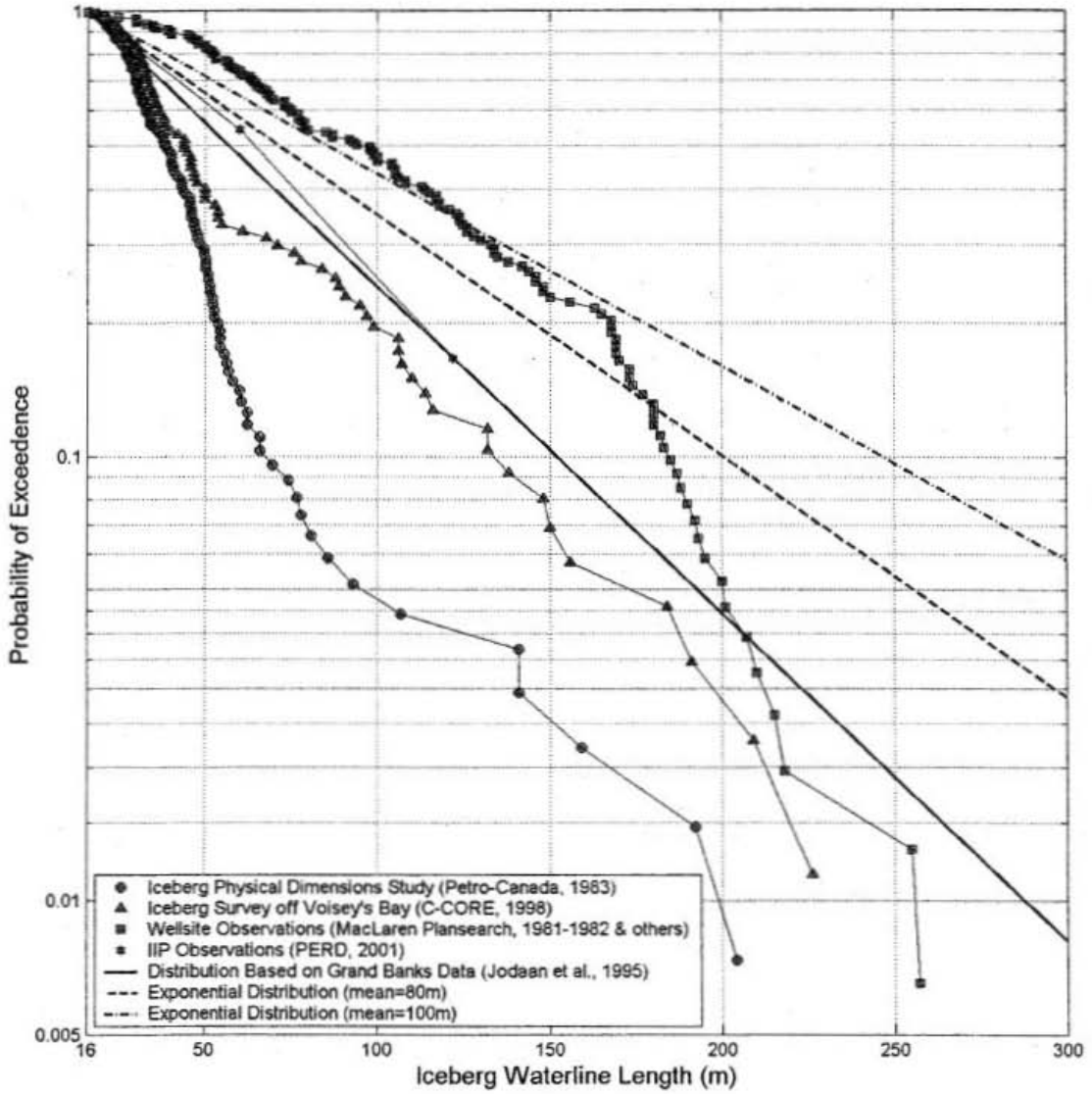

Figure 40 A comparison of waterline length distributions

Hotzel and Miller (1983) presented an analysis of iceberg dimension data collected between 1973 and 1978 off the coast of Labrador during drilling operations. Using 75 data points, the following equation was developed for waterline length (L_i) and draft (D_i):

$$D_i = 3.781\, L_i^{0.63} \tag{5.1}$$

The original data were not available, which precludes the construction of a draft exceedance curve since the distribution of the residuals could not be determined.

Brooks (1982) analyzed measured iceberg waterline lengths and drafts to determine whether an iceberg's waterline length could be considered its maximum possible draft. This was found to be true for over 90% of the available data. A relationship between draft and length was not derived. However, the original Brooks dataset, consisting of 214 draft and length measurements, was available and was analyzed to obtain:

$$D_i = 5.85\, L_i^{0.55} \tag{5.2}$$

The location of the original iceberg measurements is not known, however given the publication date it is likely they were obtained off the Labrador coast. However, it is possible that some of these data may have been obtained further north or off the coast of Newfoundland. The dataset contained a maximum waterline length of 599 m and a maximum draft of 219 m. Given the uncertainty of the origin of these data, this dataset was not considered a reliable basis for an iceberg draft exceedance curve.

PERD (1999) presented iceberg dimensional data from a variety of sources. A distinction was made between Grand Banks data and Labrador data based on whether the iceberg

was observed north or south of 50°N. Based on 108 data points, the following length to draft relationship was determined for the Labrador data:

$$D_i = 3.9\, L_i^{0.63} \tag{5.3}$$

There does not appear to be significant overlap with the Hotzel and Miller (1983) dataset, but the relationships are very similar. Based on 101 data points, the following length to draft relationship was determined for the Grand Banks data:

$$D_i = 1.95\, L_i^{0.79} \tag{5.4}$$

The data for the Grand Banks relationship is actually a subset of the 211 point dataset used by C-CORE (2000) to develop the following:

$$D_i = 3.23\, L_i^{0.68} \tag{5.5}$$

The various relationships are shown in Figure 41. It can be seen that the curves for the Labrador data (Hotzel and Miller, 1983; Brooks, 1982; PERD, 1999) are all reasonably consistent. The two curves for the Grand Banks (PERD, 1999; C-CORE, 2000) both predict deeper keels than the Labrador curves. This is likely due to the fact there are few data for very large icebergs in these datasets.

The procedure previously described was used to generate draft distributions for the data from Brooks (1982) and the Labrador data from PERD (1999). A comparison with the draft distribution developed using the C-CORE (2000) data showed that the Grand Banks draft distribution (based on an exponential waterline length distribution with a mean of 59m) had a slightly more conservative (higher) proportion of keels in deeper water, which would give slightly more conservative results for the grounding model in the water

depths of interest. For this reason, the draft distribution used for the risk analysis was based on the C-CORE (2000) Grand Banks length/draft relationship.

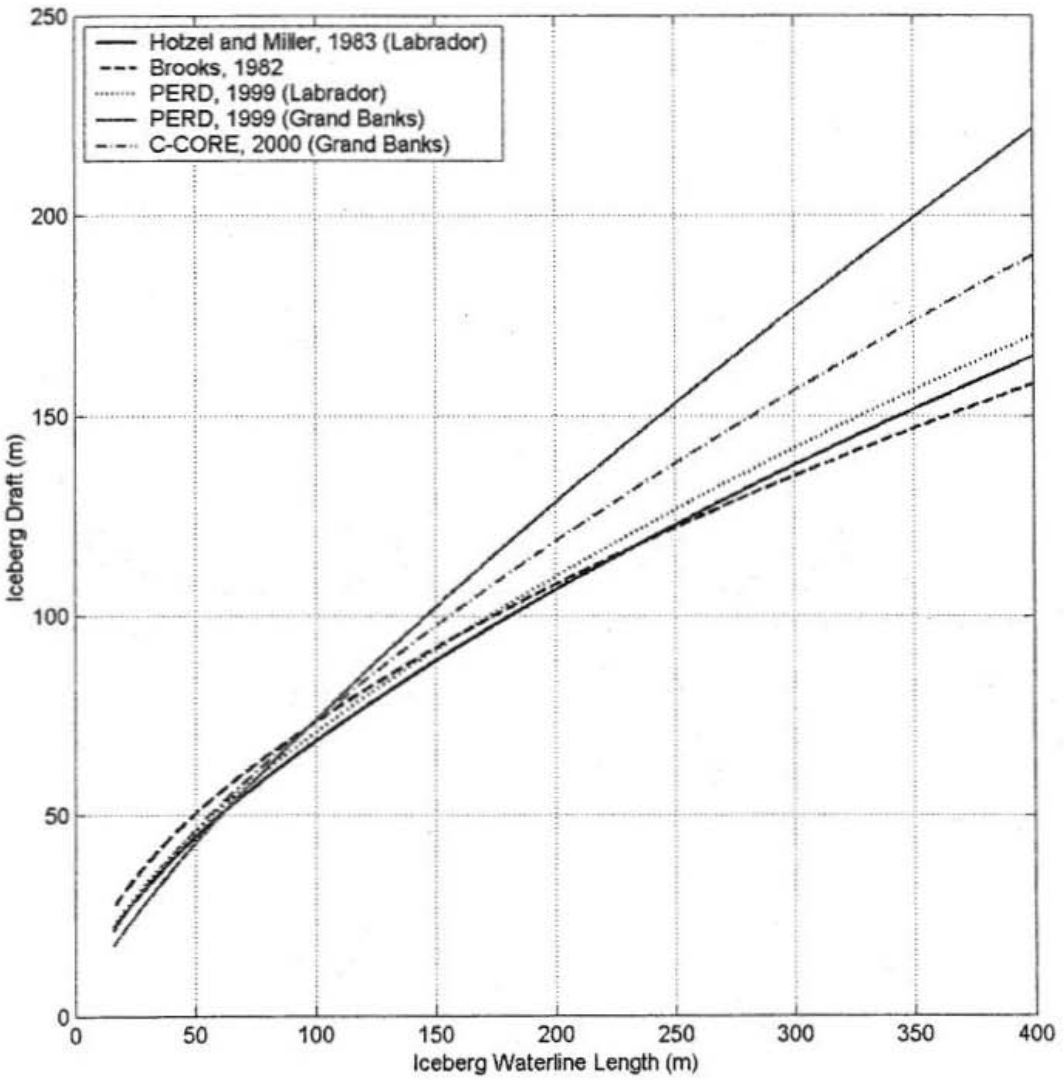

Figure 41 A comparison of length/draft relationships derived from various sources

5.3 Iceberg Drift

The frequency at which iceberg keels contact the seabed is a function of the mean iceberg drift speed and the distribution of drift direction. These factors are typically determined by the analysis of site-specific iceberg drift data. Iceberg drift could be modeled using environmental driving forces, however given the uncertainty associated with some of the parameters (particularly currents) this is not usually a viable alternative. Data collected during research and drilling operations on the Makkovik Bank are sufficient to determine drift parameters with a reasonable degree of confidence.

5.3.1 IIP Data Buoy Program (1977-1989)

From 1977 to 1989 the International Ice Patrol (IIP) monitored the drift of 21 icebergs off the coasts of Greenland, Labrador and Newfoundland using instrumented buoys placed on icebergs which allowed their positions to be monitored using satellites. Details are given by Murphy and Wright (1989), and the drift track data are publicly available.

The tracks of two of the icebergs that drifted in the vicinity of the Makkovik Bank are shown in Figure 42. A large tabular iceberg tagged with buoy 00160 passed by the Makkovik Bank between May 29 and June 5, 1977, during which time it had a mean drift speed of 0.61 m/s. A 600m waterline length iceberg tagged with buoy 01344 passed by the Makkovik Bank between April 27 and May 10, 1978, during which time it had a mean drift speed of 0.32 m/s. Despite the difference in the mean drift speed, the two icebergs display a similar trajectory, which is also observed when the trajectories for the two icebergs are plotted over their full range (approximately 50°N to 70°N). These

tracks are not useful in terms of providing velocity statistics for the pipeline risk analysis, but they are useful in terms of giving some indication of regional iceberg drift patterns.

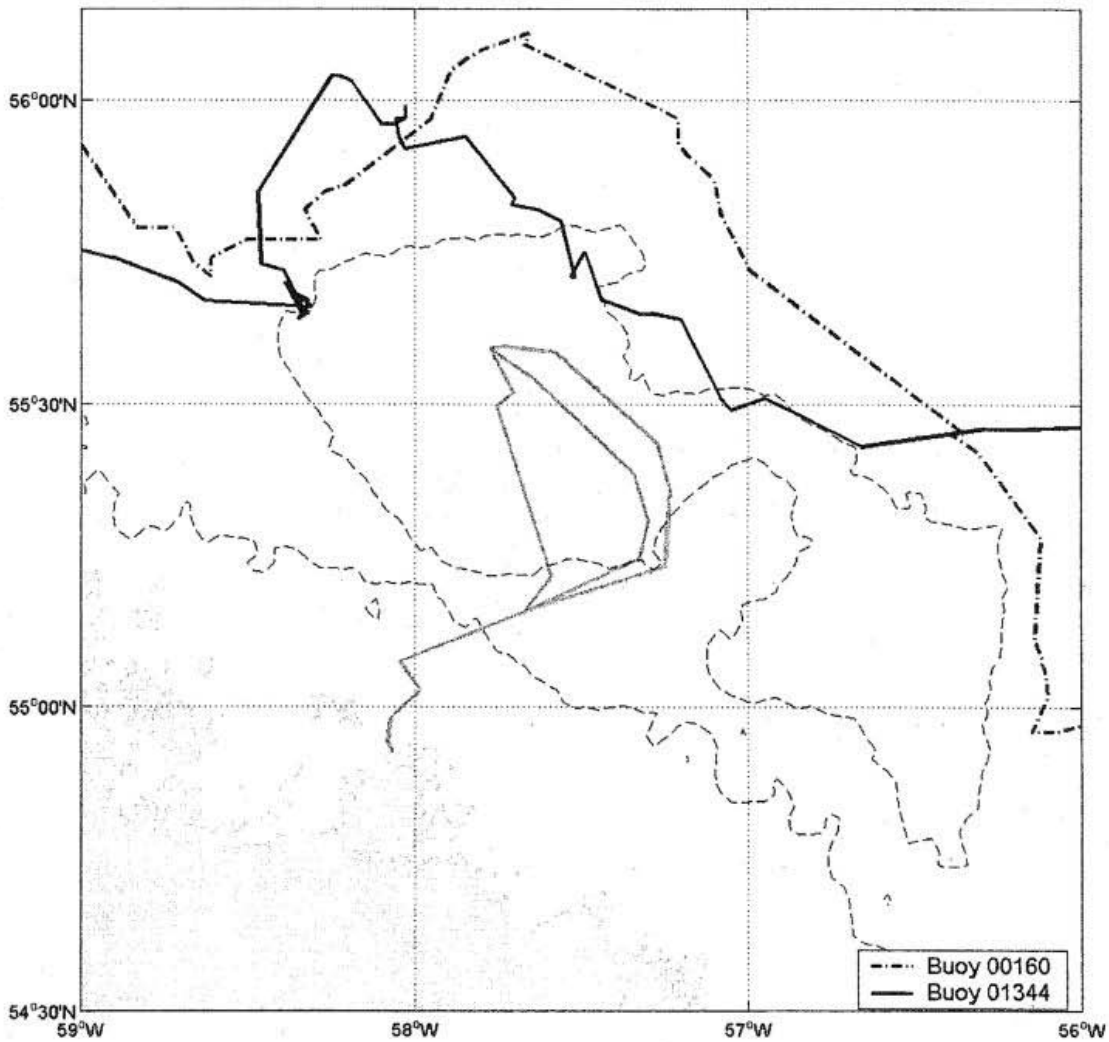

Figure 42 Iceberg tracks near Makkovik Bank from IIP Data Buoy Program

5.3.2 Analysis of Wellsite Observations (Simms, 1986)

Simms (1986) analyzed iceberg trajectories collected during drilling operations on the Labrador shelf. The data were obtained in digital form from Canada Oil and Gas Lands Administration (COGLA). The locations of the wellsites in the vicinity of the Makkovik Bank analyzed by Simms are shown in Figure 43. With the exception of Roberval C-02 (1980), no results for wellsite data obtained later than 1979 were presented.

The speed calculations were based on daily average iceberg positions. Since icebergs tend to meander, drift speeds based on average daily iceberg positions would not be instantaneous drift speeds, but would be somewhat slower. Since many iceberg tracks are less than two days duration, the use of daily average position limited the number of data points for some of the wellsites. For example, statistics for Bjarni H-81 (1974) are based on only 3 data points. Mean drift speeds and directions are given in Table 16.

The results presented here are only a fraction of the total presented by Simms (1986), who has, to date, presented the most comprehensive regional analysis of iceberg drift data.

Table 16 Iceberg Drift Characteristics in Makkovik Bank Region (Simms, 1986)

Wellsite	Year	Mean Drift Speed (m/s)	Mean Drift Bearing (°)	Number of Observations
Hopedale E-33	1978	0.293	160.6	83
Tyrk P-100	1979	0.184	186.7	65
Herjolf M-92	1976	0.323	130.6	23
Bjarni 0-82	1979	0.204	177.0	170
Bjarni H-81	1973	0.142	192.0	21
	1974	0.428	223.3	3

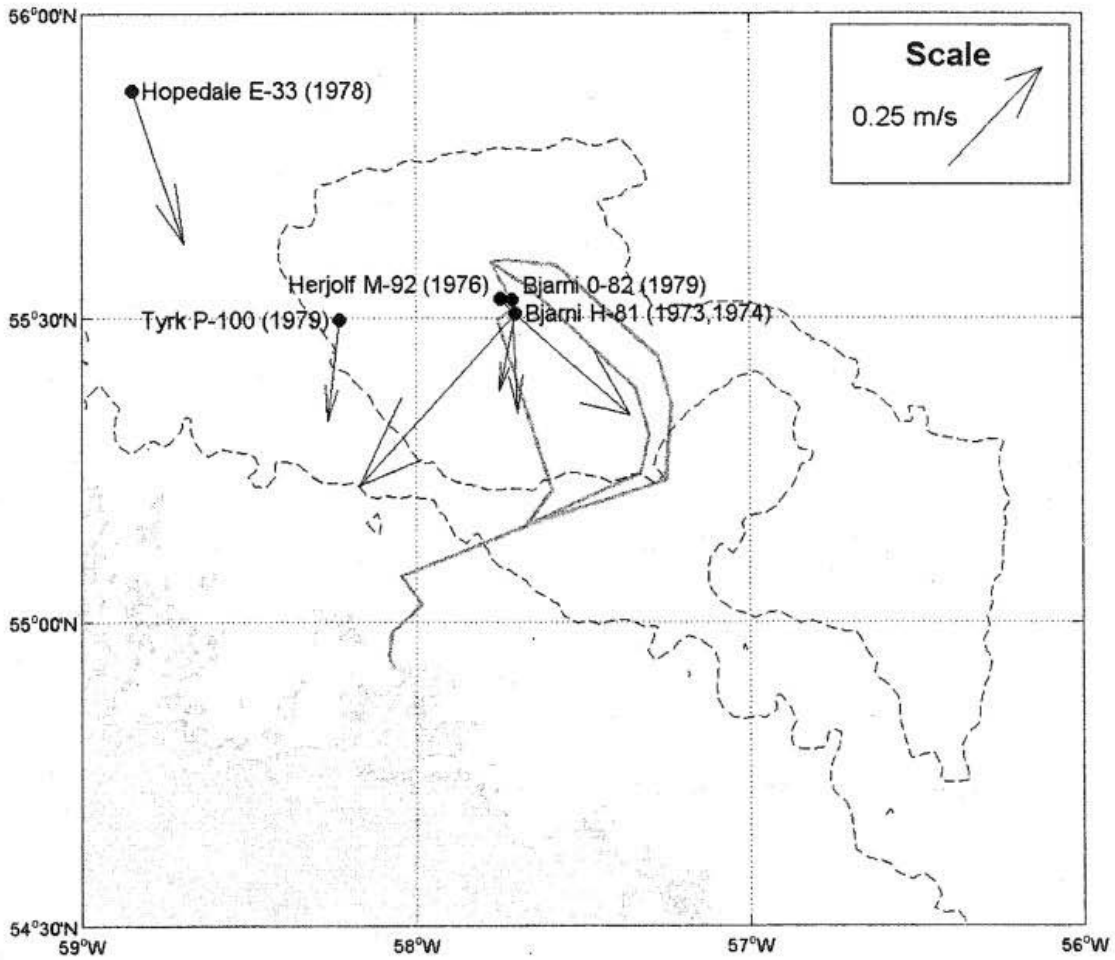

Figure 43 Mean iceberg drift speeds and bearings in study area (Simms, 1986)

5.3.3 IIP Drifter Buoy Data (Murphy et al., 1996)

The International Ice Patrol (IIP) uses a surface current database for the prediction of iceberg movement. This database is based on the trajectories of drifter buoys, the majority of which had drogues in the 30 to 50 m water depth range. The drift data were processed to determine the daily average eastward and northward drift components. Figure 44 shows the results of this analysis in the vicinity of the Makkovik Bank. It should be noted that there were relatively few drifter buoys in this region compared to areas further south. Although these current vectors cannot be directly utilized for the risk analysis, they are a useful indication of the iceberg drift behavior closer to shore where there is no actual iceberg trajectory data.

5.3.4 Analysis of Data from Two Labrador Wellsits (Ball et al., 1981)

Ball et al. (1981) analyzed iceberg trajectories collected at the Gudrid H-55 (1974) and the Bjarni 0-82 (1979) wellsites on the Labrador Shelf. Hourly iceberg drift statistics were derived, characteristics of the iceberg motion were described, and aspects of iceberg drift modeling and forecasting were discussed. The mean hourly drift speeds at the Gudrid H-55 and Bjarni 0-82 wellsites were found to be 0.202 m/s and 0.181 m/s, respectively. Simms (1986) mean daily drift speeds for the two sites were 0.217 m/s and 0.204 m/s, which is a discrepancy since a drift velocity based on hourly values would be expected to be greater than one based on daily values. The reason for the discrepancy is unknown, and as shown in the following section, hourly drift speeds are greater than daily drift speeds.

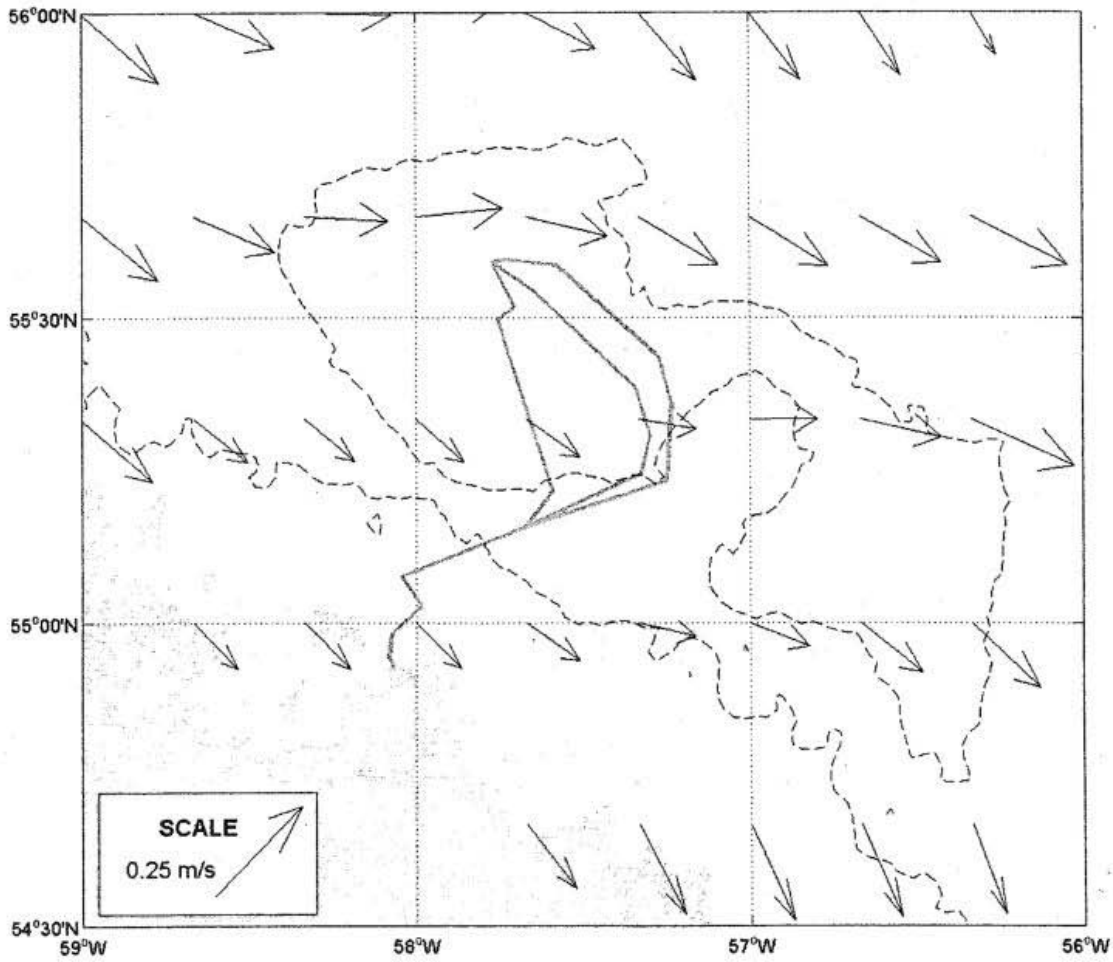

Figure 44 Gridded current vectors from IIP Drifter Buoys (Murphy et al., 1996)

5.3.5 Analysis of Wellsite Reports

Attempts to obtain the original wellsite iceberg data in digital format were unsuccessful. It appears that the data have been lost, mislaid or forgotten, and thus are no longer in the public domain.

Copies of wellsite reports (Marine Environmental Services, 1977; MacLaren Marex, 1980; MacLaren Plansearch, 1981, 1982) were obtained from the Canada-Newfoundland Offshore Petroleum Board (CNOPB) library. The iceberg track data were converted to digital format by either scanning the iceberg sighting data and using character recognition software or manually keying data into spreadsheets. Records were checked thoroughly to ensure that copying errors were minimized. The wellsites for which reports were copied and converted to digital format are shown in Figure 45.

Iceberg ranges and bearings were used to calculate iceberg positions in Cartesian coordinates (kilometers north and east) relative to the various wellsites. The iceberg tracks from the various wellsites are shown in Figure 46. It can seen that there are few tracks on the southern portion of the Makkovik Bank where the pipelines pass into water depths in excess of 200m, and none where the pipeline route approaches shore. Each iceberg sighting also has an associated date and time, allowing the elapsed time between sightings to be determined. When combined with easterly and northerly displacements calculated from the ranges and bearings, the drift speed and direction could easily be determined. Over 17,000 drift vectors were generated in this manner. The distribution of drift direction is shown in Figure 47 for each of the wellsites. The wellsites on the

western side of the Makkovik Bank show a preferential drift direction to the southwest, while for Tyrk P-100, on the eastern side of the Makkovik Bank, there is no clear trend.

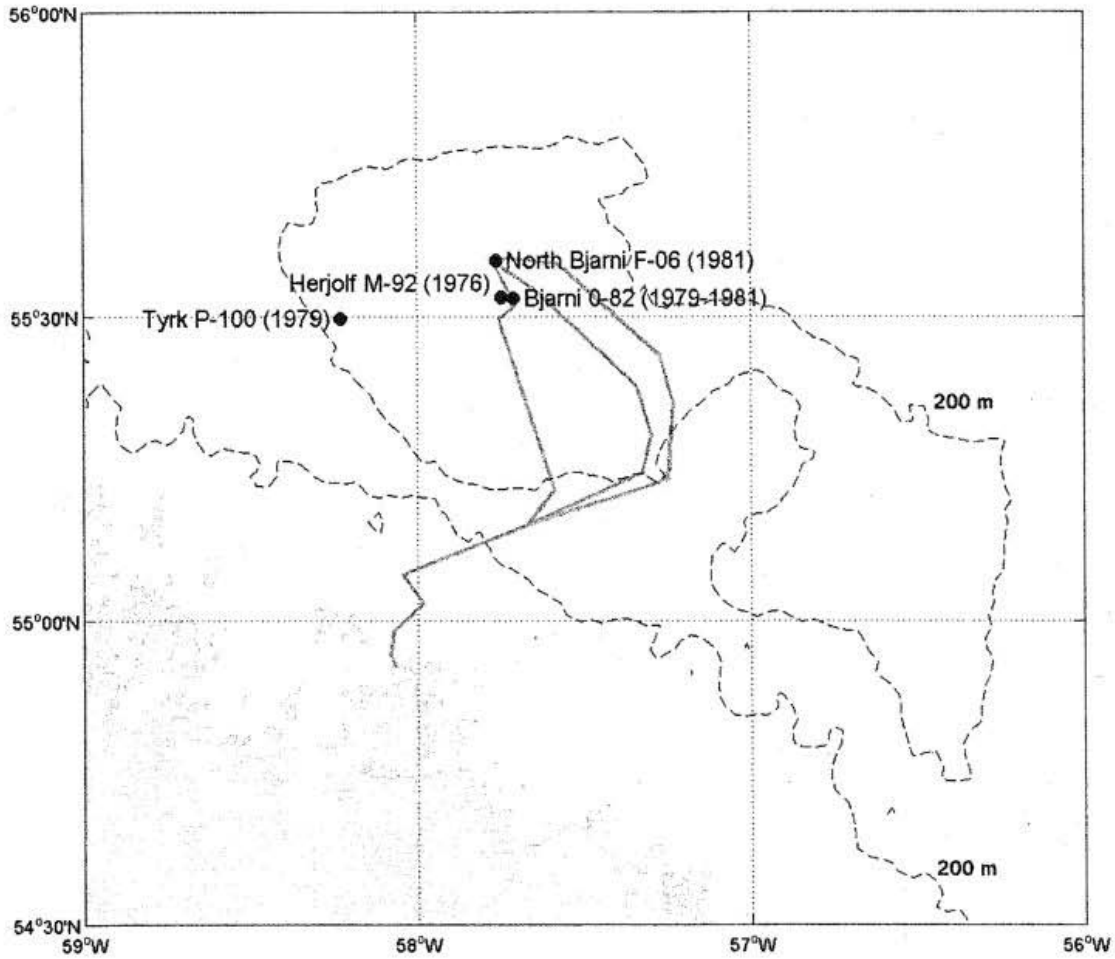

Figure 45 Locations of wellsites for which iceberg trajectories were processed

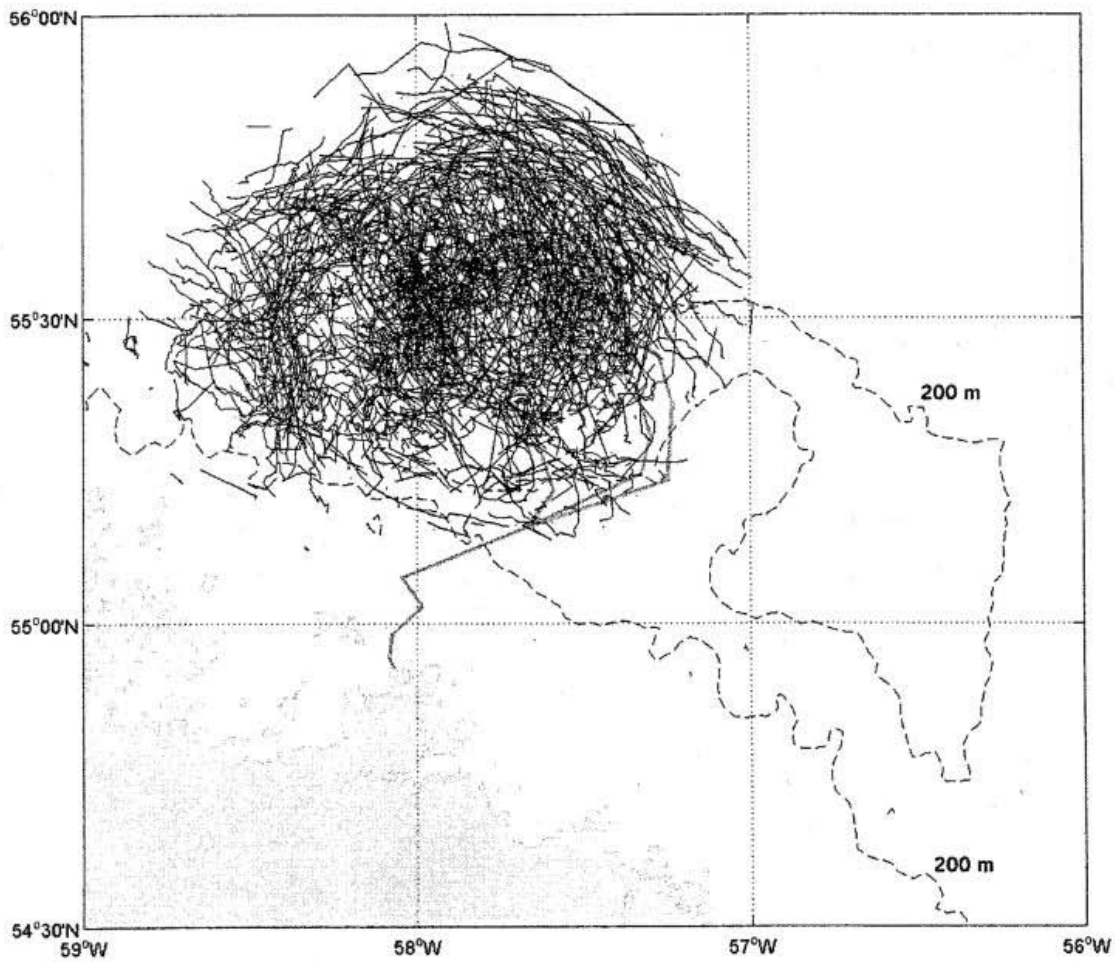

Figure 46 Combined iceberg tracks for all wellsites

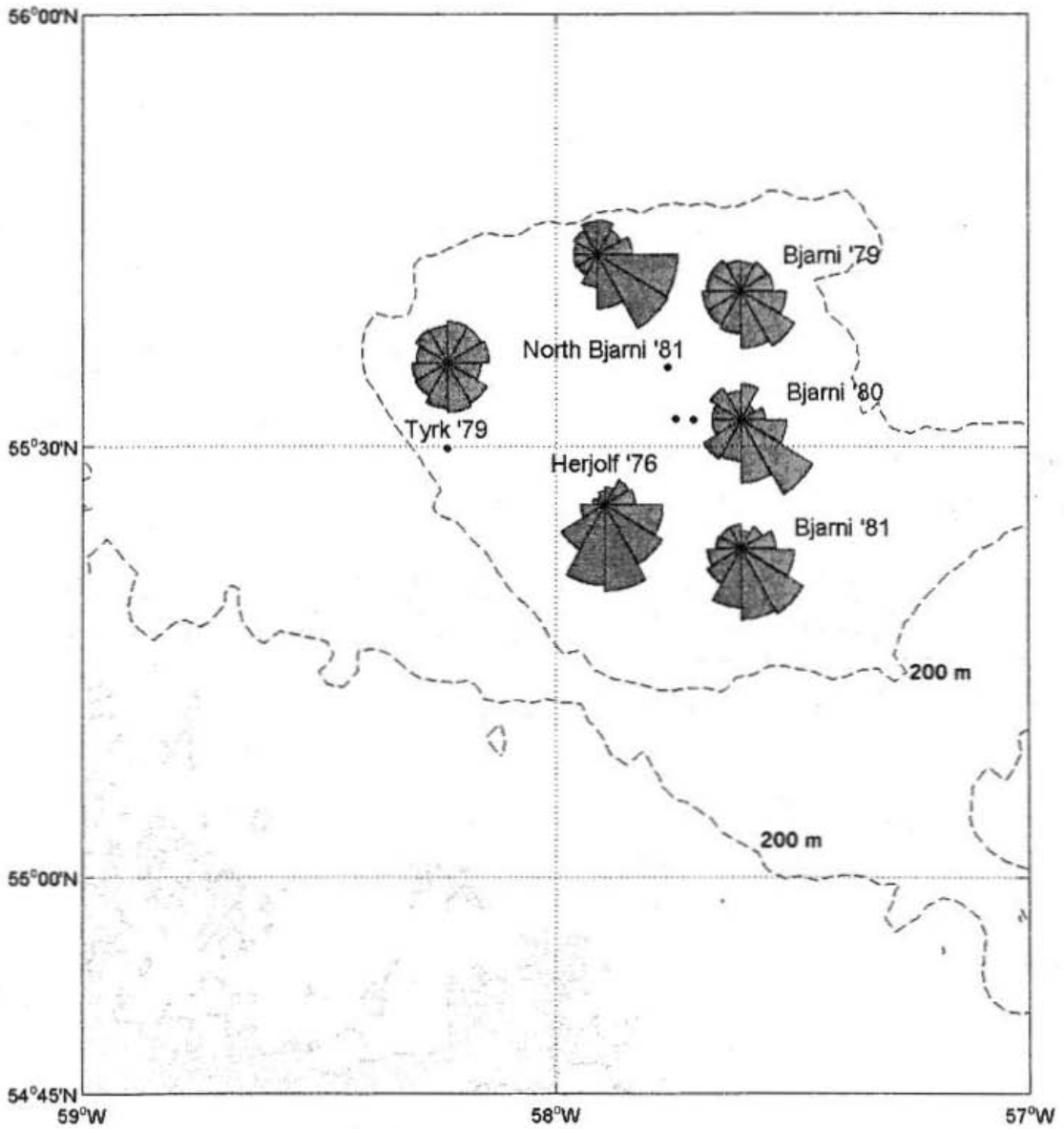

Figure 47 Distribution of iceberg drift direction for each data set

Periods during which icebergs were being towed were identified from the towing logs. Icebergs that were towed were identified and the towed and free-floating drift speeds for these icebergs were compared. The mean iceberg drift speed when under tow was approximately 25% higher than for the free-floating condition. Drift data for icebergs while towed were excluded from any further analysis (1,969 data points).

Approximately 7% of the remaining data points (1,134) were those where no change in iceberg location was recorded, resulting in zero drift speed. Some portion of these were considered due to the iceberg being grounded, while others were likely due to limitations in sensor resolution (i.e. very low drift speeds). This raised the issue of whether the iceberg drift speeds used for the risk analysis should be based only on free-floating drift velocities or if the time icebergs spent grounded should be considered. If the issue at hand concerned impact velocities (and the associated impact forces) with a structure, then zero drift speeds would definitely be excluded. However, for frequency of impacts with a structure or the seabed it could be argued that grounded icebergs cannot impact anything, so the correct drift speed would include the time spent grounded. However, the standard procedure for this type of analysis is to exclude the zero drift speeds with the understanding that this yields a conservative result. Therefore, zero drift speeds were excluded, however the impact on the overall mean drift speed was less than 10%.

The time interval between sightings was also considered. The majority of sightings (10,725) were collected at 1-hour time intervals. However, recorded sighting intervals were as short as 1 minute. Iceberg ranges were usually recorded in increments of 0.05 to

0.1 nautical miles (depending on the distance of the iceberg from the wellsite) and bearings were usually recorded in increments of 1°. It would be expected that speeds based on very short time intervals would be significantly greater than those based on longer time periods due to the finite nature of the displacements. Figure 48 (top) shows the relationship between the elapsed time between sightings and the resulting drift speed, along with the number of data points and the standard deviation of the drift speeds for each interval. For time intervals less than 15 minutes the drift speed is approximately 0.5 m/s, however this decreases considerably in the 15-45 minute range. Based on this, drift speeds based on time intervals of less than 15 minutes were excluded from further analysis. Beyond the 2-hour range the mean drift speed continues to slowly decrease. Figure 48 (bottom) shows a 215 m waterline length iceberg observed in the vicinity of the Bjarni 0-81 wellsite from August 23 to September 8, 1979. This type of meandering track is typical of the iceberg trajectories observed in the region. Obviously, this track consists of sightings observed on regular time intervals, however it can be appreciated that if drift speeds were based on positions at longer time intervals (i.e. a day) the mean drift speed would be decreased appreciably. An upper time interval was set (admittedly somewhat arbitrarily) at 4 hours, excluding a further 600 data points from the analysis.

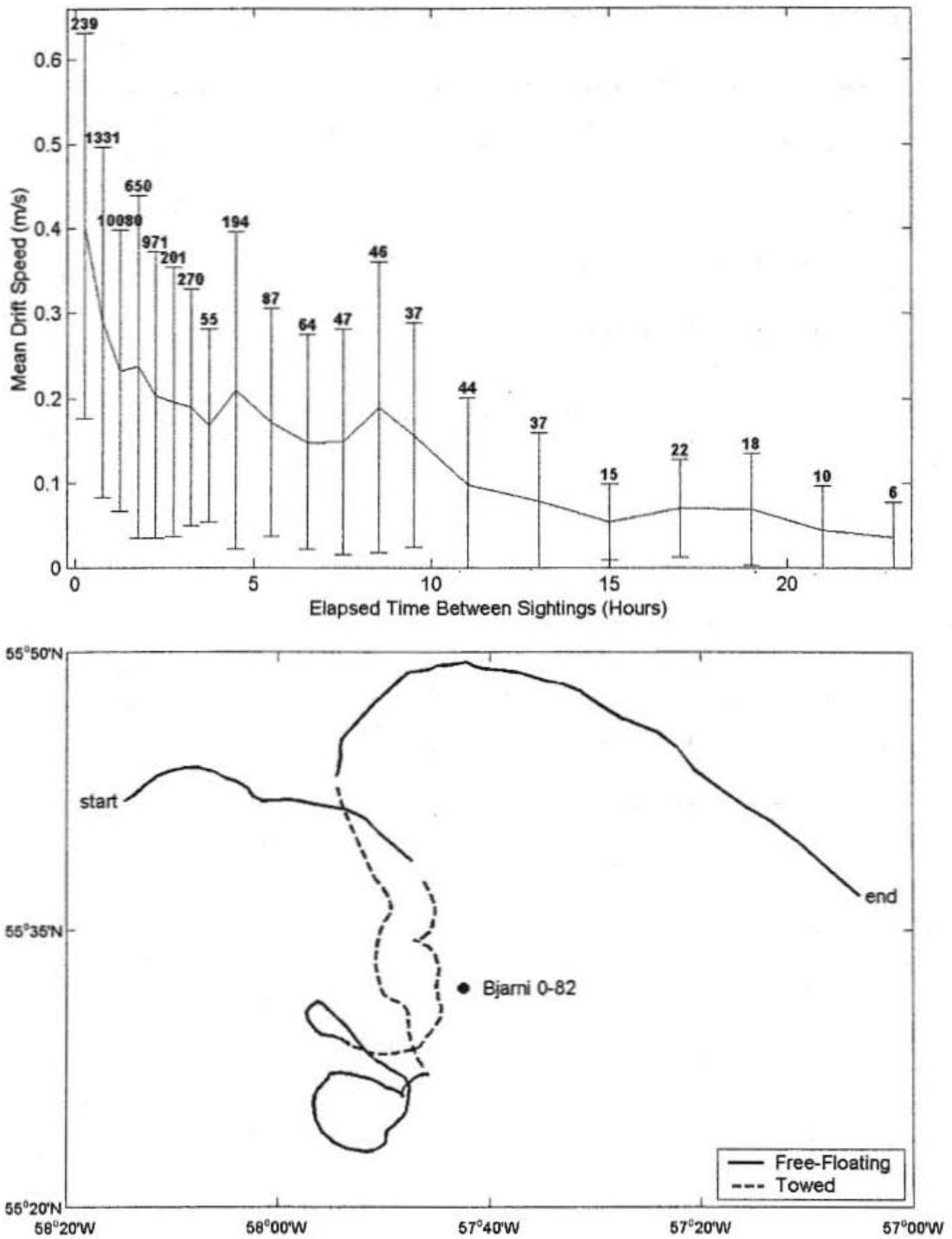

Figure 48 Relationship between elapsed sighting time and mean drift speed (top) and a meandering iceberg track demonstrating origin of phenomenon (bottom)

Table 17 gives the mean drift speed and the mean drift direction for each of the wellsites. The mean drift direction was calculated by summing the easterly and northerly components of all of the drift vectors and calculating the orientation of the resultant vector. The mean drift speeds and directions are reasonably consistent from site to site and, where direct comparisons can be made, the mean drift speeds are close to those calculated by Simms (1986).

Table 17 Wellsite Iceberg Data Analyzed

Wellsite	Location	Year	No. of Icebergs	Mean Speed (m/s)	Mean Direction (°)
Herjolf M-92	55° 31′ 53.53″ N 57° 44′ 48.82″ W	1976	27	0.31	147
Tyrk P-100	55° 29′ 49.87″ N 58° 13′ 47.05″ W	1979	168	0.23	127
Bjarni O-82	55° 31′ 48.45″ N 57° 42′ 30.99″ W	1979 1980 1981	101 15 383	0.23 0.31 0.26	158 143 154
North Bjarni F-06	55° 35′ 29.57″ N 57° 45′ 45.68″ W	1981	57	0.31	121

In order to gain some understanding of the variation in mean drift speed and drift direction the drift vectors from the various wellsites were combined and sorted into bins measuring 6′ latitude by 12′ longitude. The mean drift speed and drift orientation are shown for each bin in Figure 49. The mean drift direction was calculated using the same approach as was utilized for the individual wells. The lengths of the vectors are the vector sum of the easterly and northerly mean drift components ($\sum V_e$ & $\sum V_n$). Since the east/west and north/south components cancel each other out, comparing the length of the resulting vector with the mean drift speed gives some indication of the variability of

iceberg drift direction. It can be seen that iceberg drift is more directional in the northern portion of the Makkovik Bank and in deeper water to the north and east.

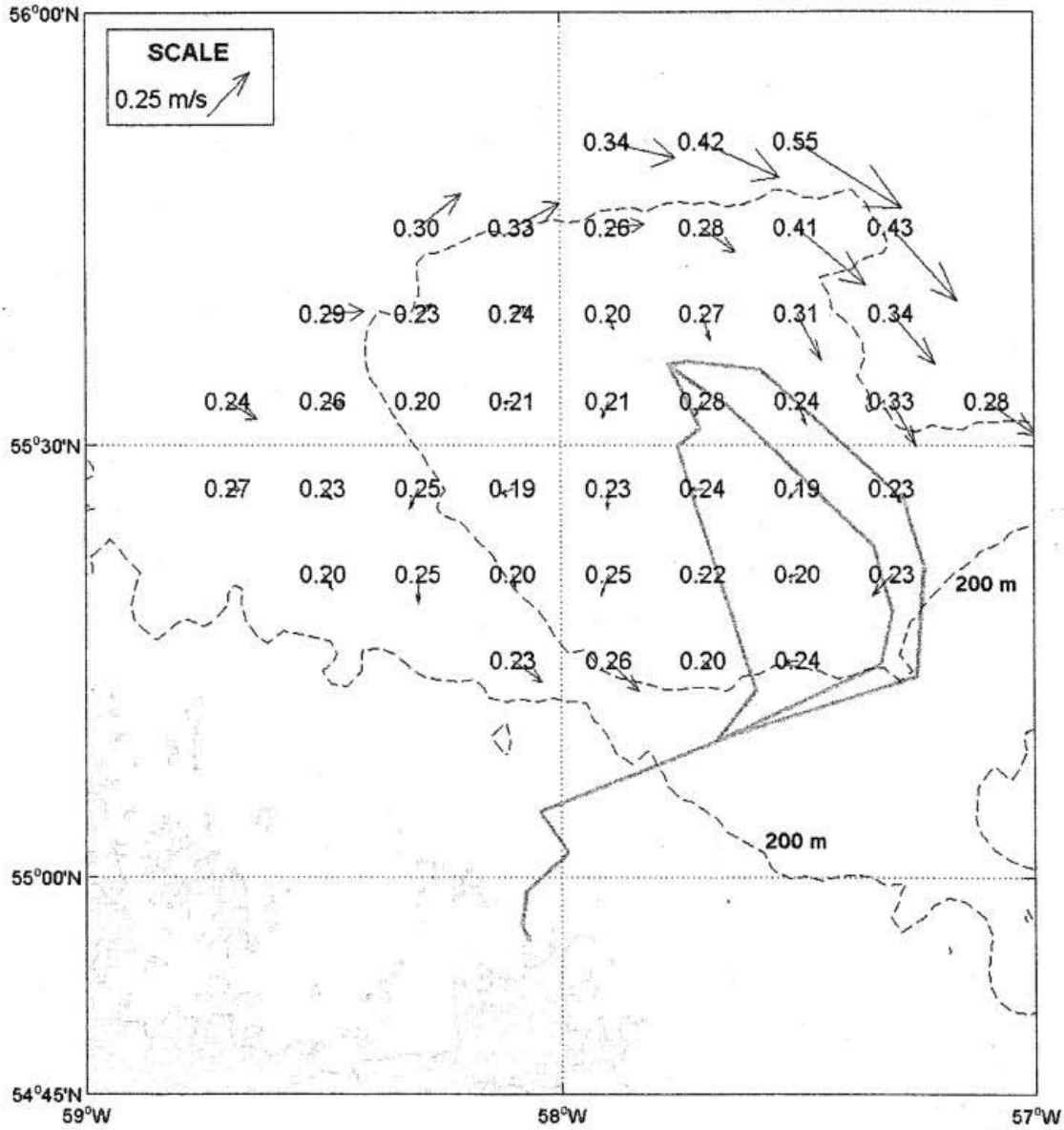

Figure 49 Gridded drift speeds for the Makkovik Bank, with mean drift speeds and vectors generated from the sum of the easterly and northerly velocity components

To obtain distributions of drift direction and speed for input into the grounding model, the drift vectors were distributed into three zones, as shown in Figure 50. Zone 1, with 2691 drift vectors, is intended to be representative of the central portion of the Makkovik Bank. Zone 2 is, with 1550, is intended to be representative of the western portion of the Makkovik Bank, where the water is deeper and drift appears to be more uniformly directed to the southwest. Zone 3, with 408 vectors, is intended to be representative of the southern portion of the Makkovik Bank, where the drift appears to be more random. Table 18 gives a breakdown of direction and mean drift speeds.

Table 18 Breakdown of Drift Speed and Direction by Zone Generated from Wellsite Observations

Bearing Range	Zone 1		Zone 2		Zone 3	
	Proportion (%)	Mean Speed (m/s)	Proportion (%)	Mean Speed (m/s)	Proportion (%)	Mean Speed (m/s)
0°-30°	6.5	0.21	4.5	0.22	4.4	0.20
30°-60°	5.8	0.21	4.7	0.20	4.4	0.16
60°-90°	6.5	0.17	5.3	0.19	10.3	0.21
90°-120°	7.5	0.21	11.7	0.24	14.5	0.22
120°-150°	11.5	0.24	17.9	0.34	9.3	0.20
150°-180°	11.6	0.31	16.0	0.33	10.5	0.15
180°-210°	11.1	0.30	11.3	0.26	4.2	0.24
210°-240°	8.3	0.24	7.8	0.23	7.1	0.30
240°-270°	8.6	0.23	7.0	0.19	9.8	0.21
270°-300°	7.6	0.24	4.9	0.17	11.0	0.27
300°-330°	8.6	0.23	4.8	0.16	5.4	0.24
330°-360°	6.4	0.25	4.1	0.22	9.1	0.17
All	N/A	0.24	N/A	0.26	N/A	0.21

The remaining issue is to assign a drift direction and speed distribution for the near-shore portion of the pipeline route. The IIP gridded currents (Figure 44) suggest that the mean drift direction would be parallel to the shore, and the few binned velocity vectors closer

to shore (Figure 49) would seem to support this assumption. A conservative assumption would be to assign a uniform distribution in drift direction, since this would drive more icebergs upslope and cause more groundings. A mean drift speed of 0.24 m/s (a mean of the mean drift speeds for the other zones) would also be a reasonable assumption.

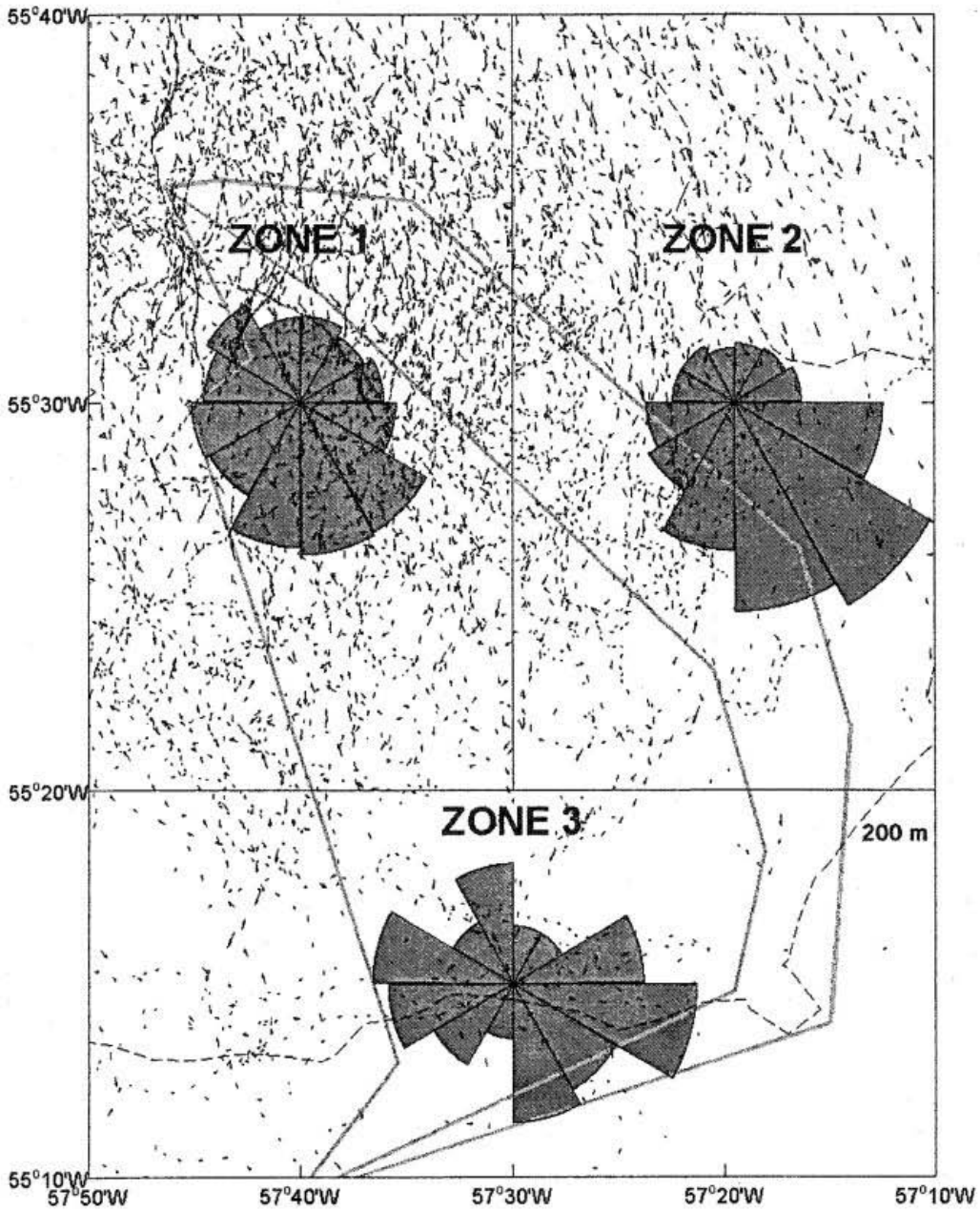

Figure 50 Drift direction distribution according to zone

5.4 Bathymetry

The Labrador Shelf, shown in Figure 51, can be considered to be broken down into three zones: (i) an outer shelf comprised of a series of banks including the Makkovik, Harrison, Nain, Hamilton and Saglek Banks; (ii) a marginal trough which runs parallel to the coastline; and (iii) an inner shelf adjacent to the shore.

The grounding model requires water depth, seabed slope and orientation. The following sections describe the sources of the bathymetric data used to determine the water depth along the pipeline route as well as the slope and orientation of the seabed. A comparison with the pipeline water depth profiles given by Petro-Canada (1983) is provided.

5.4.1 Makkovik Bank Bathymetry

Figure 52 shows bathymetric data from Natural Resource Map #18656 (Canadian Hydrographic Service). A Natural Resource Map (NRM) is generally derived from industry data and gives bathymetric data in the form of contour lines, however the source of the data used to generate this particular map is unknown. Contours are in 10 m intervals for water depths less than 400 m, with the exception of the 150 m and 200 m contour lines, which are absent. This map was obtained in digital format and consisted of three vectors giving the latitude, longitude and water depth. No individual soundings were included. The bathymetric contours were cropped to the area around the pipeline routes for illustrative purposes.

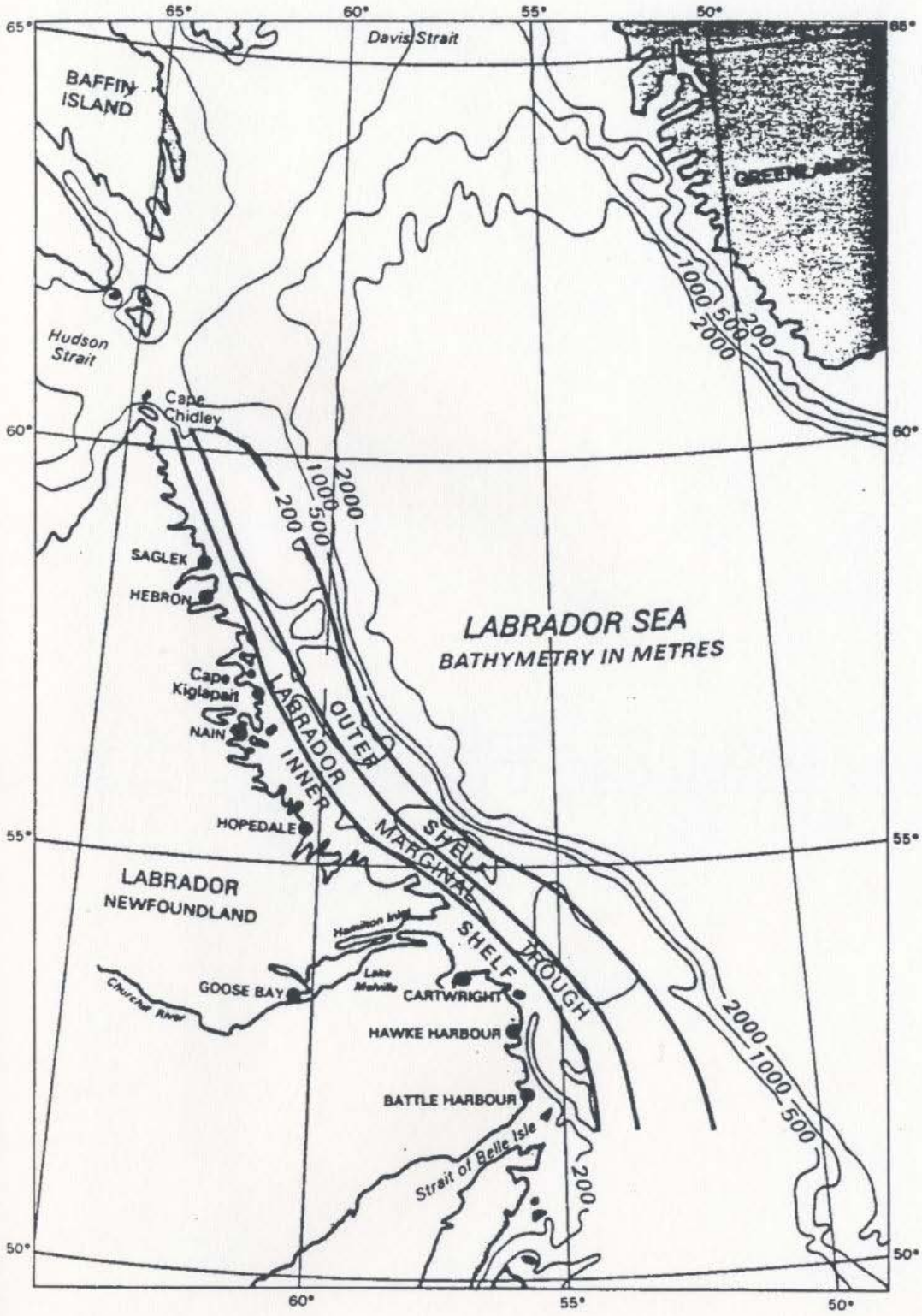

Figure 51 Bathymetry of Labrador Shelf (from Petro-Canada, 1983)

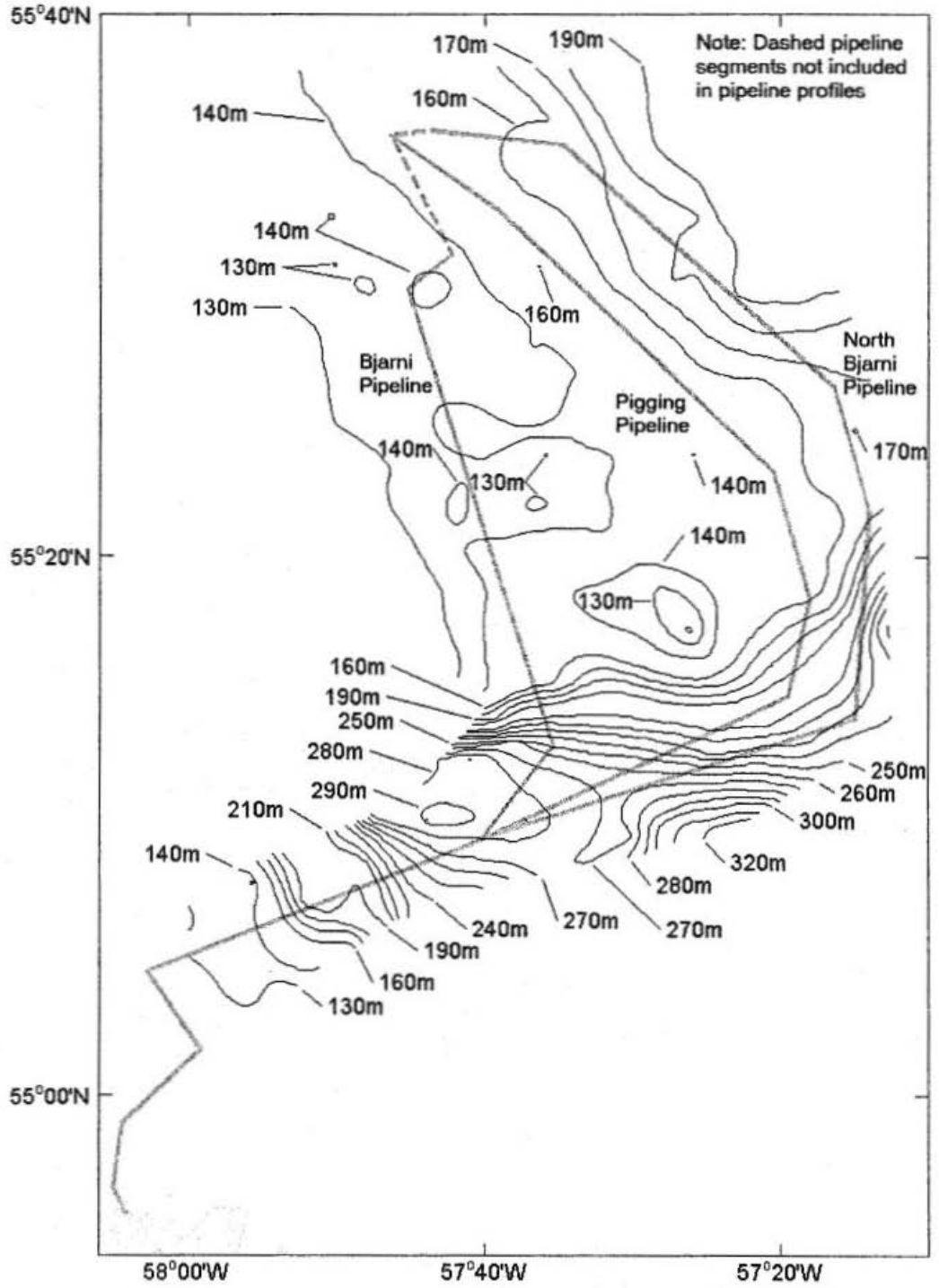

Figure 52 Bathymetric contours from Natural Resource Map #18656 on Makkovik Bank and marginal trough portions of pipeline route

Figure 53 shows a portion of a composite map derived from Canadian Hydrographic Chart 5150 and industry surveys on the Makkovik Bank (Petro-Canada, 1983). This map showed bathymetric contours at 10 m intervals, as well as numerous individual soundings. The region around the pipeline routes was scanned and the contour lines and sounding were digitized. This data will be referred to subsequently as digitized bathymetry.

5.4.2 Landfall Bathymetry

Figure 54 shows a portion of bathymetric chart (Canadian Hydrographic Chart 5150: White Bear Islands to Ragged Islands) upon which the landfall portion of the pipeline has been superimposed (Petro-Canada, 1983). This chart is no longer listed in the catalogue of nautical charts published by the Canadian Hydrographic Service. Water depths are in fathoms. The chart was scanned and soundings in the region shown in Figure 54 were digitized.

The presence of a submarine canyon was inferred from the sounding data (Petro-Canada, 1983), as shown in Figure 55. The landfall portion of the pipeline follows the canyon in order to exploit the natural shielding effect this feature provides against iceberg keels. It was assumed that there was zero risk from scouring icebergs inside this canyon, which protects approximately 15.7 km of the pipeline. The final 2.3 km of pipeline runs through a tunnel that protects it from iceberg damage.

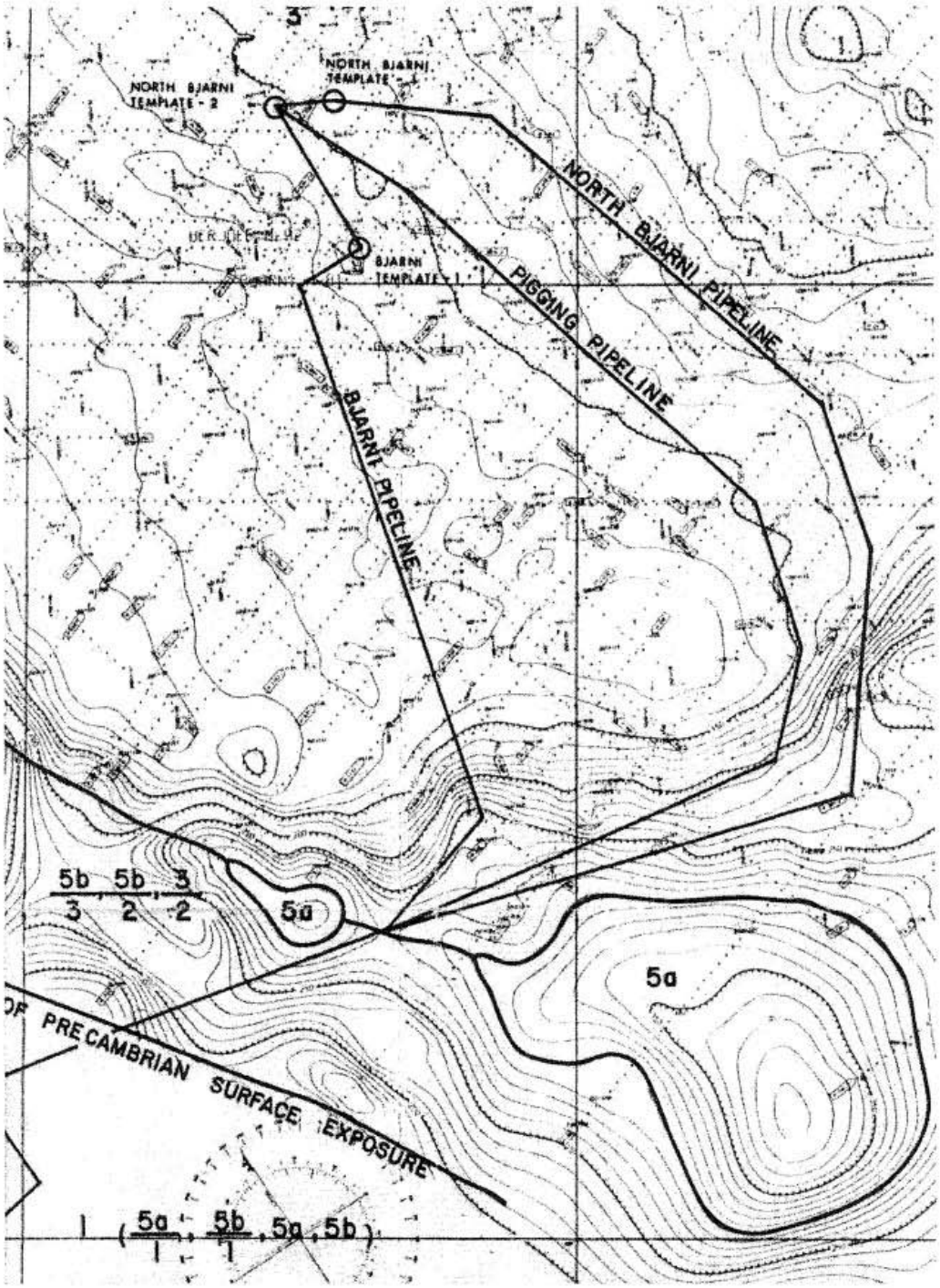

Figure 53 Bathymetry data in Makkovik Bank region (from Petro-Canada, 1983)

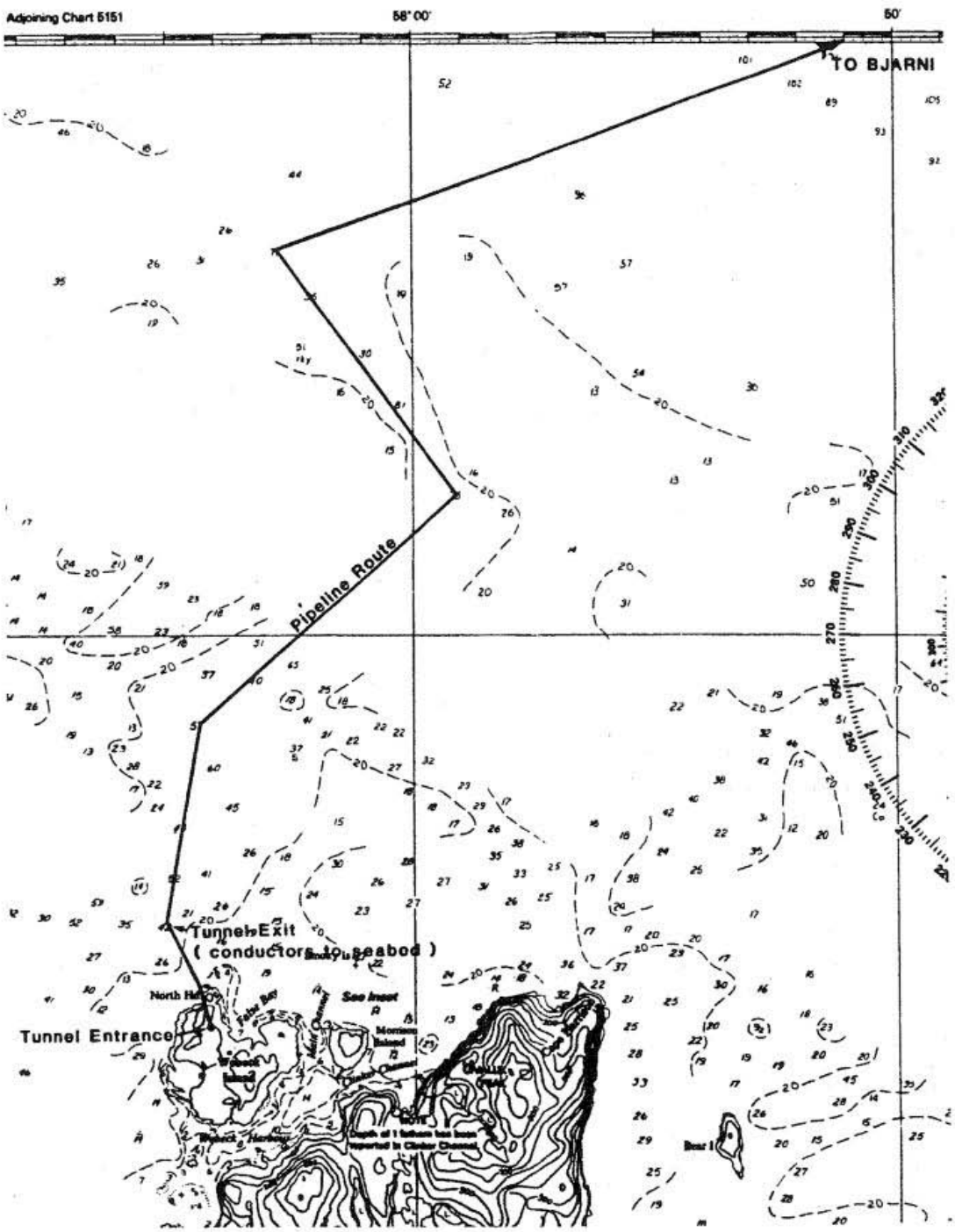

Figure 54 Bathymetric chart showing pipeline landfall (from Petro-Canada, 1983)

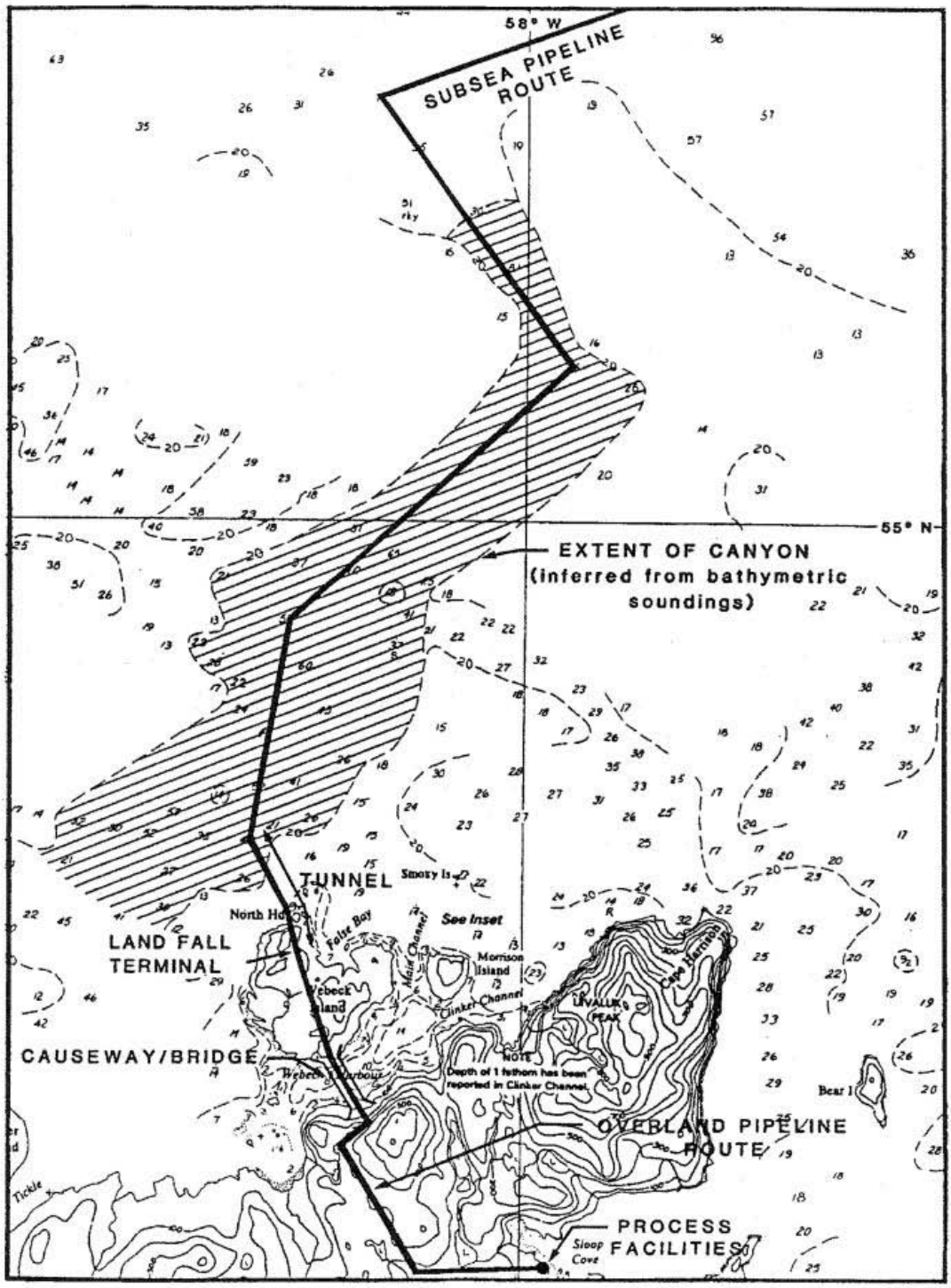

Figure 55 Canyon along landfall portion of pipeline as interpreted from soundings (from Petro-Canada, 1983)

5.4.3 Pipeline Profiles

The bathymetry data were used to generate water depth profiles along the various pipeline routes. Figure 56 and Figure 57 show comparisons between tabulated pipeline profile values (Petro-Canada, 1983) and the NRM and digitized bathymetry. In both cases digitized data were used for the landfall portion of the pipeline routes. The digitized bathymetry for the Makkovk Bank and the marginal trough gives much better agreement with the tabulated values than the NRM bathymetry, which is to be expected since the tabulated and digitized profiles are derived from the same source. The profiles for the landfall portion of the pipelines show some obvious differences with the tabulated data, however it should be noted that the bathymetric data in the landfall region are relatively sparse, leaving more leeway for interpretation in the original study.

5.4.4 Seabed Slope and Orientation

The seabed slope and orientation were determined at 2 km intervals along each of the pipelines on the Makkovik Bank and the marginal trough. Slopes and orientations for various points were determined by superimposing a 3 × 3 grid (1 km spacing) and interpolating water depths for each point. The mean easterly and northerly slopes were then used to determine overall slope and orientation for each point of interest. Figure 58 shows the magnitude and orientation of the seabed slope along the pipelines routes for the digitized bathymetry dataset.

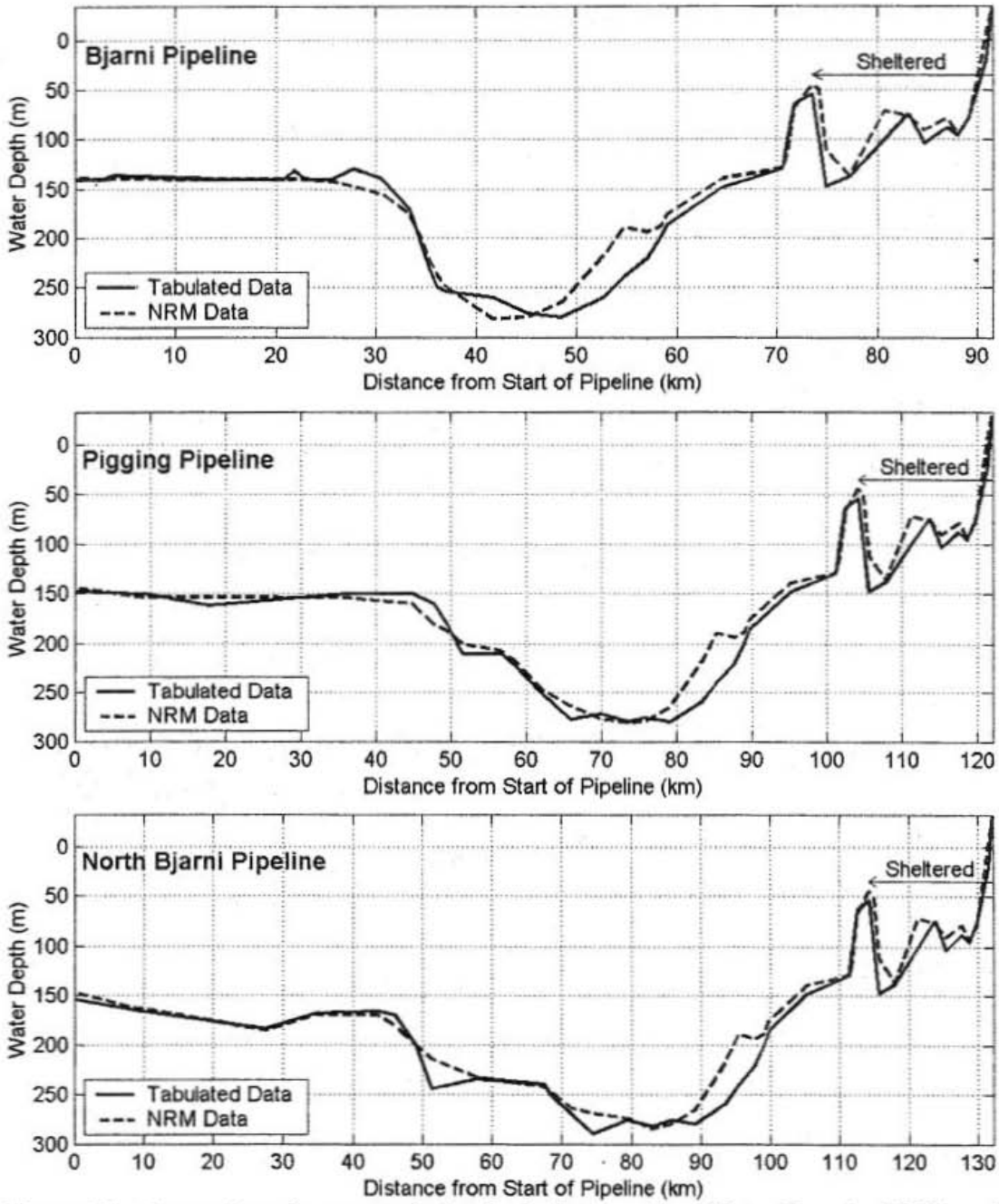

Figure 56 Comparison between tabulated pipeline profiles (Petro-Canada, 1983) and generated from NRM bathymetric data

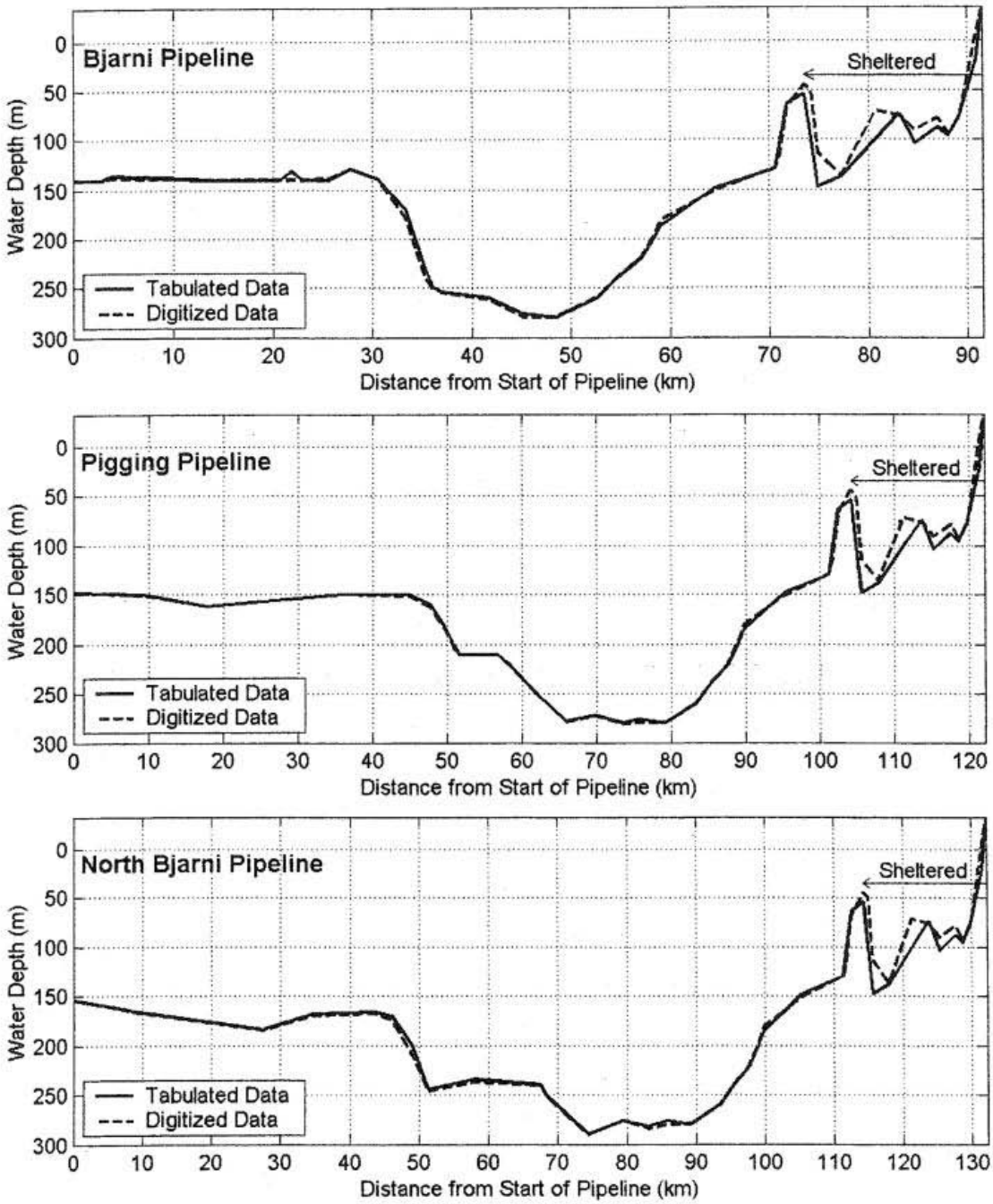

Figure 57 Comparison between tabulated pipeline profiles (Petro-Canada, 1983) and generated from digitized bathymetric data

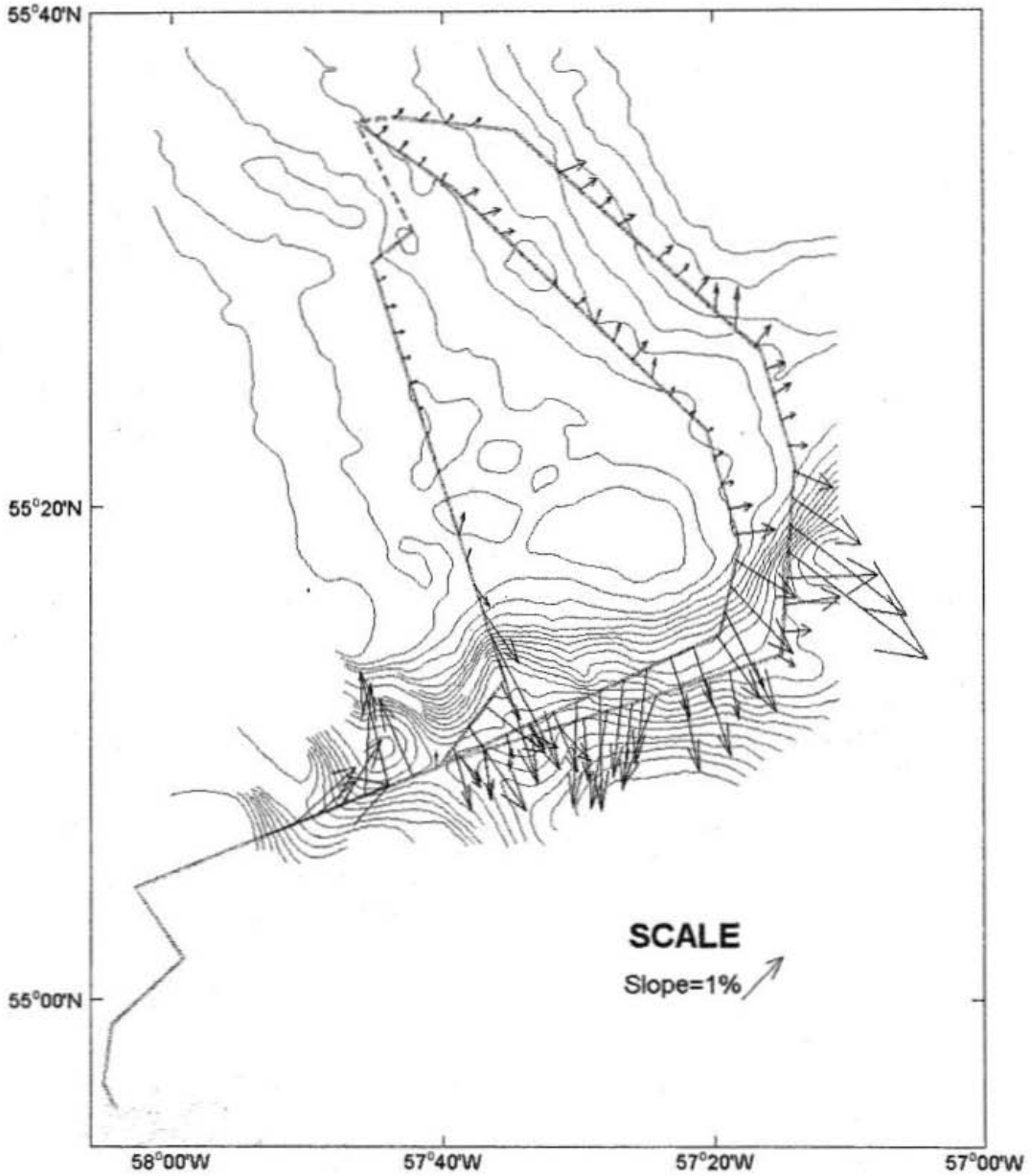

Figure 58 Seabed slopes and orientations generated from digitized bathymetry

Significant variations in seabed slope were seen along the routes. In water depths less than 150 m on the Makkovik Bank the mean seabed slope is approximately 0.002, while the mean seabed slopes for the pigging and North Bjarni pipelines are double this value.

Mean seabed slopes in the marginal trough along the pipeline routes are approximately 0.015. Slope orientations on the Makkovik Bank are predominantly to the northeast (down-slope directions). Slopes derived from the NRM and digitized bathymetry datasets were reasonably consistent, however some differences were noted for the initial portion of the Bjarni route where the NRM data indicated lower seabed slopes.

The bathymetry data for the shore approach are sparse and not useful for determining slope orientation. However, since there are no iceberg drift data for this area, seabed slope orientation was not required. Seabed slope magnitude was estimated from the tabulated pipeline profiles.

5.4.5 Conclusions

The digitized bathymetry appeared to be more detailed and complete than the NRM bathymetry and allowed for a more direct comparison with the input to the original iceberg risk analysis. Therefore, this source was used to generate water depths, seabed slopes and orientations for the risk analysis. Water depths and seabed slopes for the shore approach was taken from the pipeline profile data in the Bjarni Development Study (Petro-Canada, 1983)

5.5 Comparison With Petro-Canada (1983) Parameters

Petro-Canada (1983) used iceberg frequency data combined with iceberg drift characteristics to generate iceberg flux values for use in the risk analysis. The grounding model used in the risk analysis procedure presented in this thesis uses iceberg frequency as a direct input. The mean iceberg areal density value adopted for use in the risk analysis was approximately three times higher than the areal densities used by Petro-Canada (1983) to generate iceberg flux values.

Petro-Canada (1983) used a draft distribution based on 41 measured iceberg drafts to determine the proportion of icebergs capable of scouring the seabed. The drafts followed a gamma distribution and had a mean of 90.8 m and a standard deviation of 43 m. The draft distribution that was adopted for use in this risk analysis, based on observed iceberg waterline lengths and a waterline length/draft relationship, had a mean of 58.8 m and a standard deviation of 34.3 m. A comparison of the two distributions is given in Table 19 and shown in Figure 59.

Table 19 Iceberg Draft Distributions used for Bjarni Pipeline Risk Studies, Bergy Bits and Growlers Excluded

Draft Distribution	Mean (m)	Standard Deviation (m)	Percentage Exceeding 150m
Petro-Canada (1983)	90.8	43.0	10%
This Study	58.8	34.3	2%

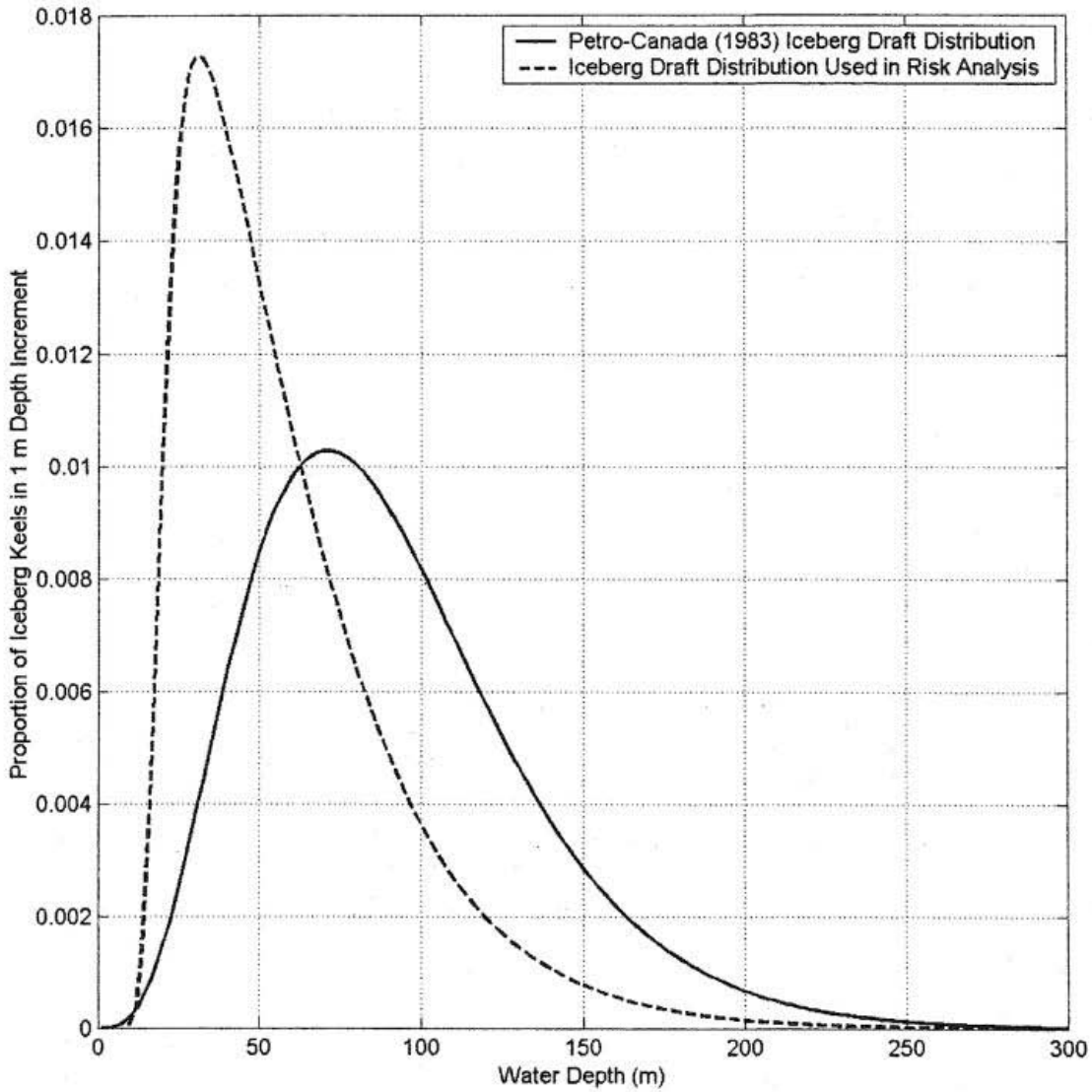

Figure 59 A comparison between iceberg draft distributions used in this pipeline risk analysis and the original Petro-Canada (1983) analysis

6 SCOUR PARAMETERS FOR STUDY AREA

The parameters of primary interest relate to scour geometry (width, length, and depth). The plan shape (width and length) of a scour is usually determined using sidescan sonar, while depths are determined using a depth sounder (i.e. echo sounder or multi-beam) or shallow geophysical instruments (i.e. sub-bottom profiler). The scour depth distribution used in the original Petro-Canada (1983) risk analysis was based on a single seabed survey at the Bjarni site, without any consideration for the resolution of the data. Additional data, obtained during subsequent surveys, has been analyzed for the relevant scour parameters and the effect of instrument resolution on scour depth measurements has been considered.

6.1 Data Sources

6.1.1 DIGS Mosaics

In 1985 a number of seabed surveys were conducted as part of the DIGS (Dynamics of Iceberg Grounding and Scouring) experiment (Hodgson et al, 1980). The locations of these mosaics are shown in Figure 60. A Klein Hydroscan 100-kHz sidescan sonar system, towed 20 to 25 m above the seabed, was used to provide high-resolution documentation of the seabed surface. A Huntec dual Deeptow Seismic (DTS) system was used to provide shallow stratigraphic data. DIGS provided the most extensive scour data set for the Makkovik Bank.

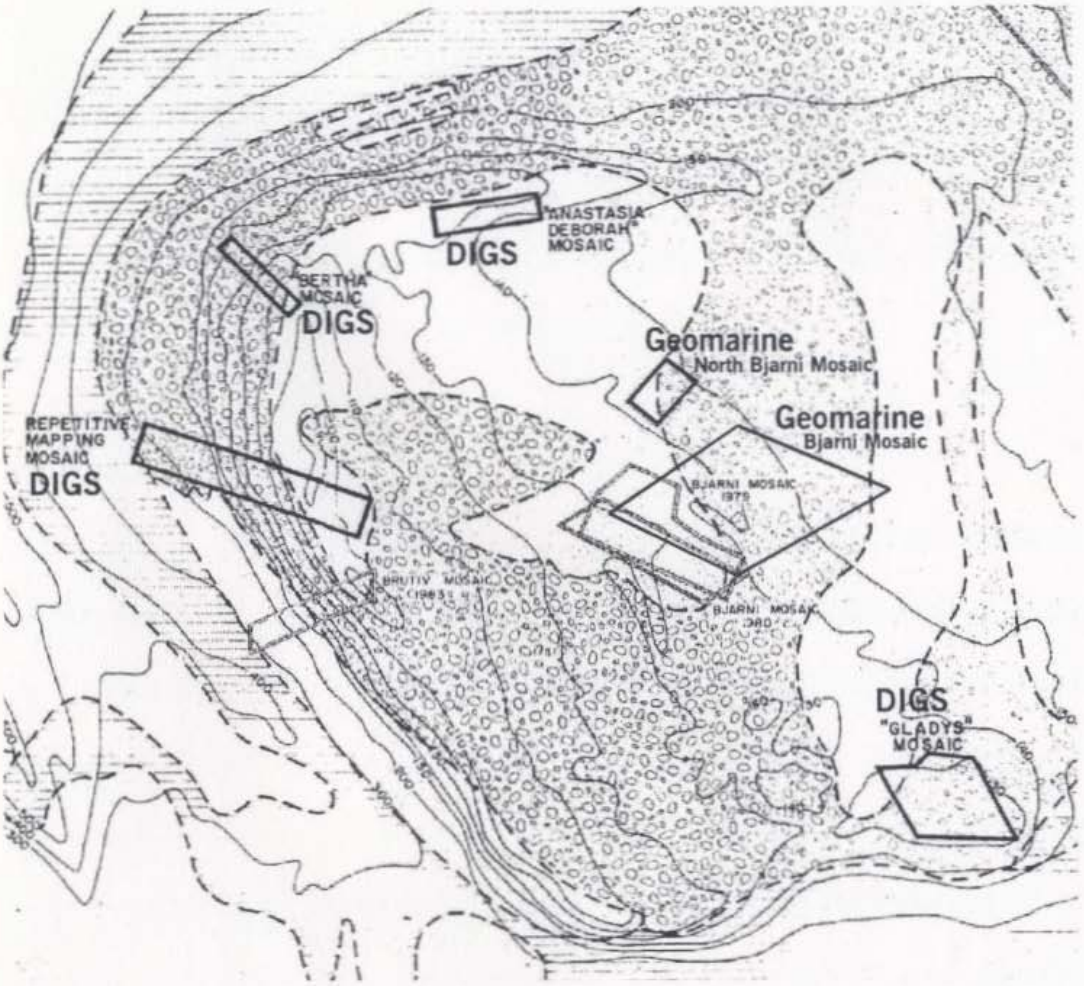

Figure 60 Mosaics on the Makkovik Bank

6.1.2 Bjarni Survey

Geomarine (1976) conducted an iceberg scour and bathymetric survey at the Bjarni site in 1975, as shown in Figure 60. At approximately 135 km^2, this mosaic covers the largest area of any of the mosaics on the Makkovik Bank. An ORE 100-kHz sidescan sonar and a Raytheon 719 high-resolution echo sounder were used to collect the scour data. Prominent scours were mapped and parameters were tabulated for scours with minimum depths of 1 m.

6.1.3 North Bjarni Survey

Geomarine (1980) also conducted a seabed survey at the North Bjarni site at the location indicated in Figure 60 using the same instrumentation as the 1975 survey (Geomarine, 1976). At approximately 12 km^2, this was a relatively small mosaic. All visible scours were mapped, although no scour data were tabulated.

6.1.4 Grand Banks Scour Catalog

Data from the Grand Banks Scour Catalog (Canadian Seabed Research, 2000) used for the White Rose scour analysis (C-CORE, 2001b) have been included for comparison with the Labrador data. The iceberg scour data, derived from a number of sources, are among the most recent and accurate available. The scour data were restricted to a region on the northeast Grand Banks considered representative of the White Rose site and bounded by the 110m and 140m isobaths (see Figure 61). This data set comprises in excess of 1000 ice scour records. Additional data from the PERD (2000) study were also considered.

6.1.5 Regional Ice Scour Database

This database (Geonautics, 1989) was the most comprehensive collection of iceberg scour data until it was supplanted by the Grand Banks Scour Catalog in the 1990's. The scour data originated from a variety of sources and, as shown in Figure 62, covered a vast region. This database, which represented the "state of the art" in terms of scour data available during its time period, has been included here for comparison with the Grand Banks Scour Catalog (GBSC) and the DIGS data, which were not incorporated.

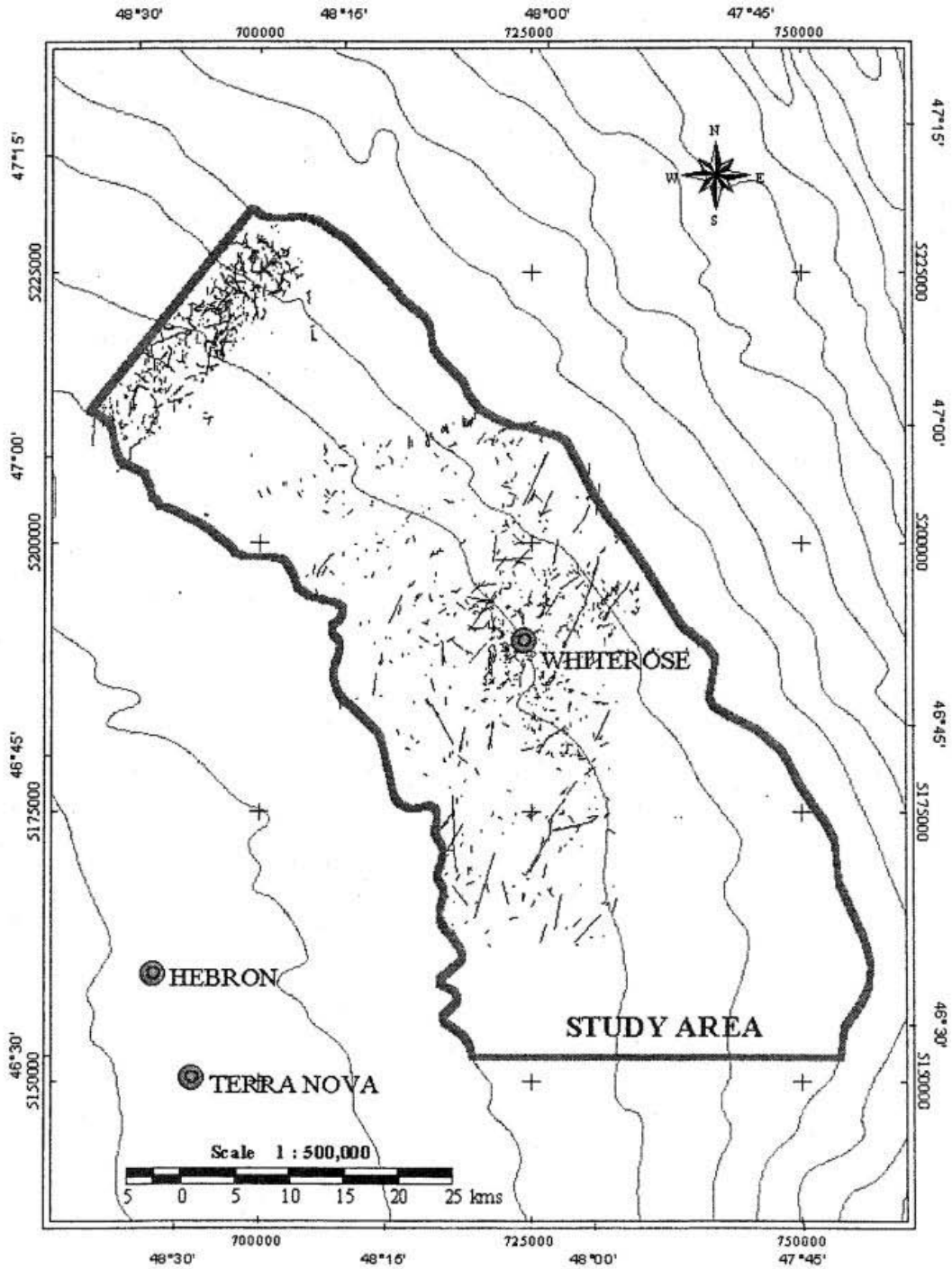

Figure 61 Study area covered for White Rose study (C-CORE, 2001b)

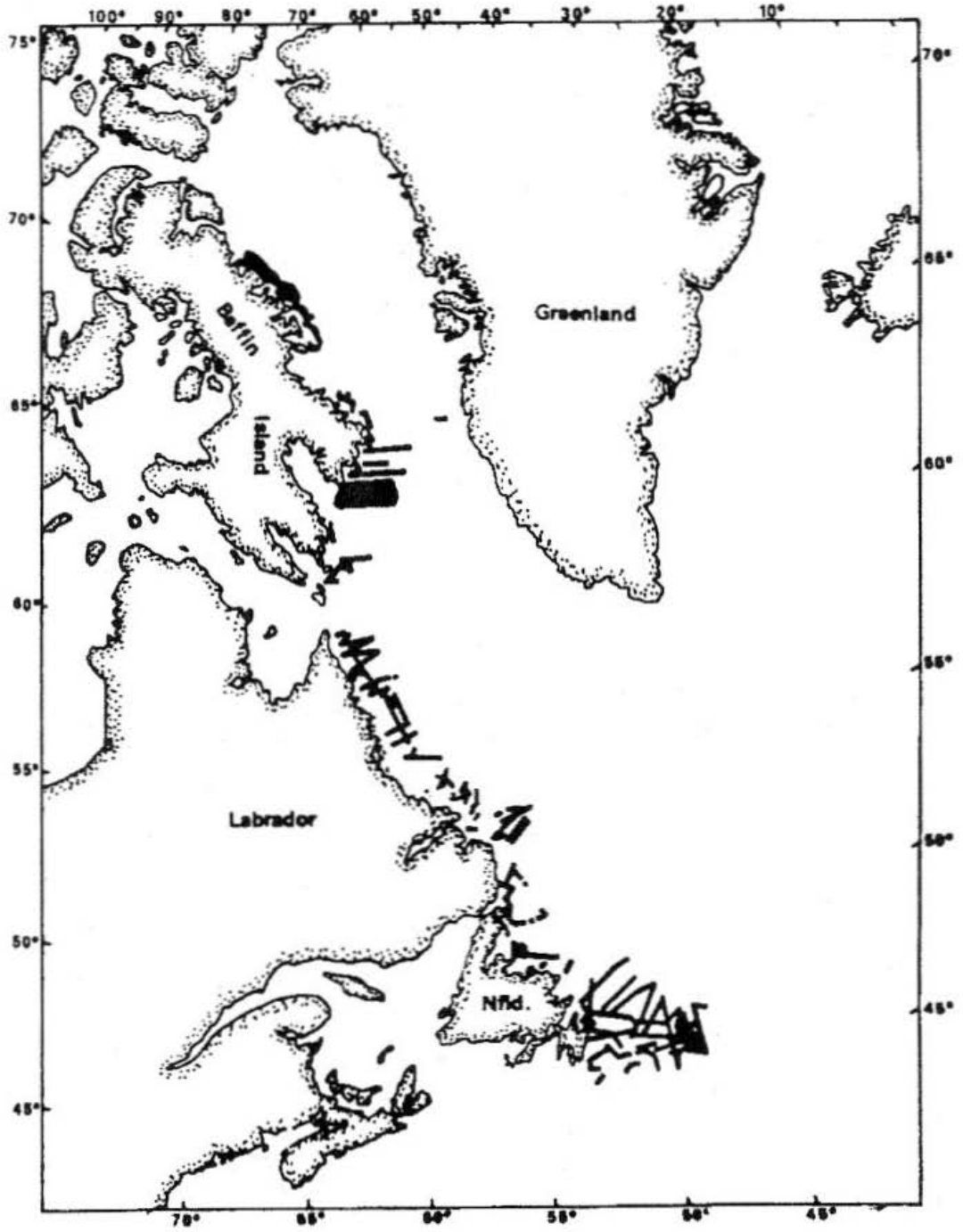

Figure 62 Area covered by Regional Ice Scour Database (from Geonautics, 1989)

6.2 Scour Width

Scour width is required for the calculation of scour crossing frequency over subsea structures. It also has an effect on soil deformations beneath the scour. Scour width is not a significant factor the scour crossing frequency for a structure such as a pipeline, which is dominated by the pipeline length. However, scour width can be used as a diagnostic tool when comparing scour data from various sources.

6.2.1 DIGS Mosaics

Figure 63 shows the combined scour width data from the DIGS mosaics. This includes scour width data from the Anastasia, Bertha and Repetitive mapping mosaics. The scour width data from the Gladys mosaic were not given in the DIGS report. As shown in Figure 63, the mean scour width observed during the DIGS study was 20 m from scours with multiple segments combined and 20.2 m if segments were not combined (572 widths). The mean scour widths for the Anastasia, Bertha and Repetitive Mapping mosaics were 17.5 m, 18.5 m and 22.1 m, respectively.

Table 20 gives scour width distributions for each soil type and water depth range. It can be seen that the difference between each of the sediment types is minimal, however there does appear to be a significant increase in width for water depths greater than 170m. This may be due to larger icebergs producing larger scours in deeper water, or these features may be relict scours. The mean scour width in the 170-210m water depth range is 25.5m. A similar increase in scour width is seen on the Grand Banks, with a mean scour width of 31.5 m in the 170 – 210 m water depth range (PERD, 2000).

In the DIGS study scour features with length/width ratios less than 2 were designated as pits. The pit width values documented in the DIGS report are the measurement along the longest axis. The mean pit width is 39.1m (204 values). The mean pit widths for the Anastasia, Bertha and Repetitive Mapping mosaics are 42.1, 30.0 and 42.8 m, respectively. Pit widths, broken down in terms of soil type and water depth range, are given in Table 20. The mean pit widths in Labrador Shelf Drift is less than the other 2 sediment types, however this material is mostly found in the shallower water depths. Pit width appears to increase with water depth.

6.2.2 Bjarni Survey Scour Width Data

The analysis of the Bjarni wellsite survey (Geomarine, 1976) was restricted to scour features with depths equal to or greater than 1 m. Reported scour feature widths were broken down into those with discernable orientations, for which the width was corrected for orientation, and those without discernable orientations (lengths were not listed for tabulated data). The mean corrected width (N=207) was 56.2 m and the mean uncorrected width (N=102) was 60.8 m. No distinction was made between pit and scour features in the data. The difference between the scour widths observed in this survey, compared to the DIGS data, is most likely due to the exclusion of scours with depths less than 1 m.

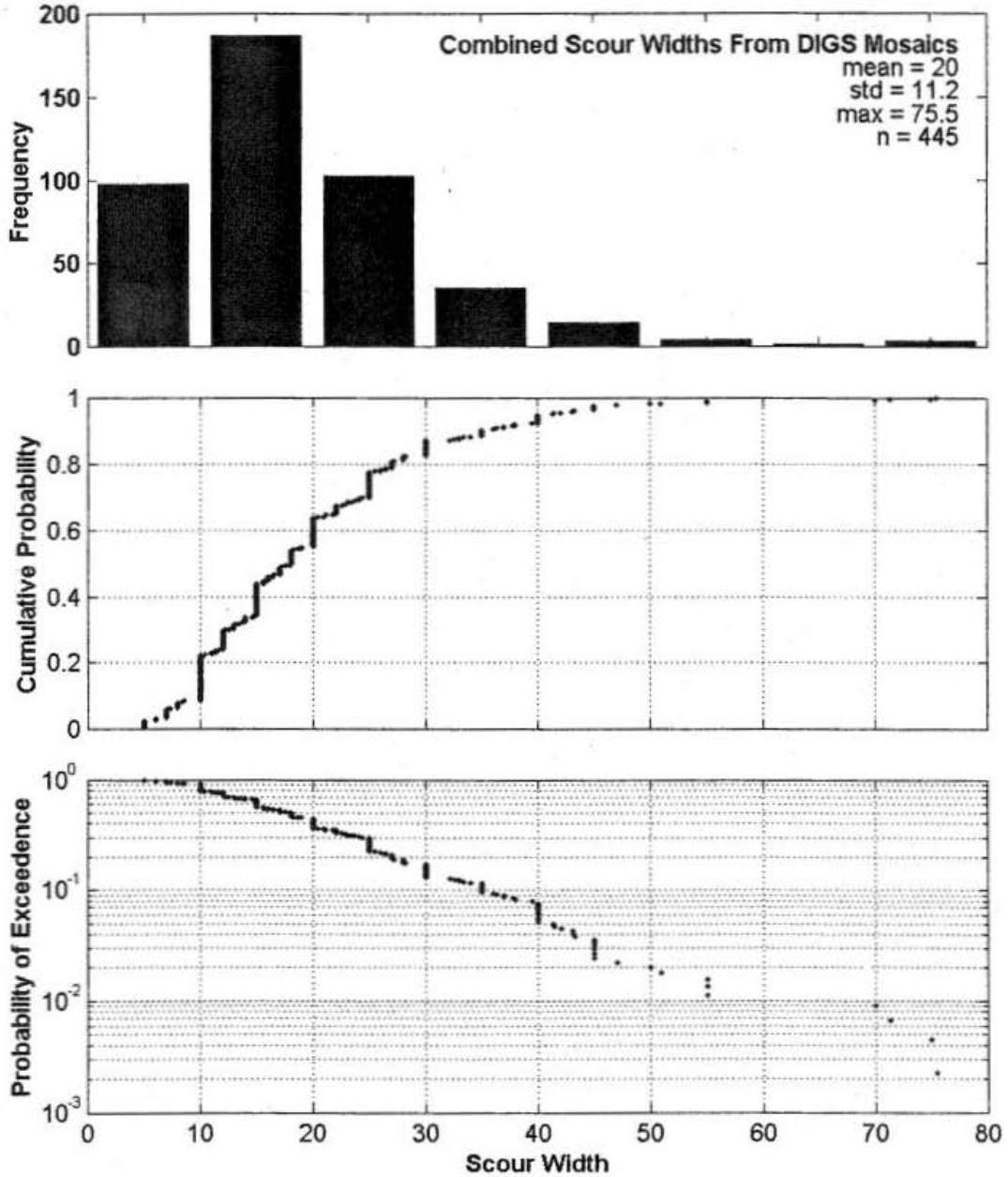

Figure 63 Distribution of scour width from DIGS mosaics

Table 20 Distribution of Scour and Pit Widths from DIGS Mosaics

	Water Depth Range	Scours			Pits		
		No.	Mean (m)	S.D. (m)	No.	Mean (m)	S.D. (m)
Soiraq Sand	90m-100m	2	22.5	10.6	3	40.0	17.3
	100m-110m	2	44.0	50.9	0	N/A	N/A
	110m-120m	21	29.2	22.0	9	39.4	16.3
	120m-130m	3	20.3	9.0	9	36.1	21.5
	130m-140m	42	17.4	6.5	35	47.5	24.5
	140m-150m	39	19.4	9.5	17	42.9	25.8
	All Depths	109	21.0	13.9	73	43.7	23.2
Qeovik Silt	110m-120m	7	16.7	8.8	0	N/A	N/A
	120m-130m	81	17.0	11.4	21	32.5	14.3
	130m-140m	44	22.0	10.7	11	32.5	10.7
	140m-150m	39	24.1	11.6	2	75	35.4
	150m-160m	44	20.9	13.3	3	43.3	7.6
	160m-170m	40	19.7	9.3	4	76.3	36.4
	170m-180m	26	26.5	14.9	10	36.4	21.0
	180m-190m	15	27.8	11.4	3	91.7	35.1
	190m-200m	8	32.5	13.3	0	N/A	N/A
	200m-210m	3	38.3	6.1	0	N/A	N/A
	All Depths	307	21.5	12.3	54	41.9	25.5
Labrador Shelf Drift	80m-90m	9	16.9	8.4	0	N/A	N/A
	90m-100m	17	18.4	9.9	2	22.5	10.6
	100m-110m	34	18.1	8.0	13	33.6	20.7
	110m-120m	43	17.7	8.9	33	28.2	18.5
	120m-130m	44	17.6	9.8	21	34.5	13.0
	130m-140m	16	17.9	8.2	8	47.4	21.0
	140m-150m	3	20.3	4.0	1	28.0	N/A
	All Depths	166	17.9	8.8	78	32.6	18.2
All Soil Types	80m-90m	9	16.9	8.4	0	N/A	N/A
	90m-100m	19	18.8	9.8	5	33.0	16.4
	100m-110m	36	19.5	13.1	13	33.6	20.7
	110m-120m	69	20.7	15.0	42	30.6	18.5
	120m-130m	124	16.7	9.8	50	34.4	14.9
	130m-140m	99	19.3	9.0	54	44.4	22.4
	140m-150m	80	21.6	10.7	20	45.4	27.2
	150m-160m	44	20.9	13.3	3	43.3	7.6
	160m-170m	40	19.7	9.3	4	76.3	36.4
	170m-180m	26	26.5	14.9	10	36.4	21.0
	180m-190m	15	27.8	11.4	3	91.7	35.1
	190m-200m	8	32.5	13.3	0	N/A	N/A
	200m-210m	3	38.3	6.1	0	N/A	N/A

6.2.3 Regional Ice Scour Database

The Regional Ice Scour Database (Geonautics, 1989) gives a mean scour width of 34 m for the Labrador Shelf, while the mean scour width for the Makkovik and Harrison Banks is 28.8 m. For comparison, the Regional Ice Scour Database gives a scour width of 29.6 m for the Grand Banks in water depths less than 90 m. A more recent assessment of scour width on the Grand Banks in water depths less than 90 m indicates a mean scour width of 22.1 m (PERD, 2000).

6.2.4 Grand Banks Scour Widths

The distribution of scour width in the White Rose scour study (C-CORE, 2001b) is shown in Figure 64. The mean scour width in the White Rose study area is 24.9 m (492 values). The mean pit size, defined in the White Rose study as the mean of the pit width and length, is 57m (178 values). The mean pit width is 43.8 m. If the greatest dimension is used, as in the DIGS project, a mean value of 71.1 m is obtained. The designation of pits in the Grand Banks Scour Catalog is not strictly according to the length/width ratio (Pat Campbell, Canadian Seabed Research, personal communication), as with the DIGS study, but also is based on feature morphology (i.e. appearance of berms, etc.). If the pit features with length/width ratio of 2 or greater are eliminated (21%) then the mean of the maximum pit dimension is 55.5 m. Regardless, both scour and pit widths on the Grand Banks appear to be greater than those on the Makkovik Bank.

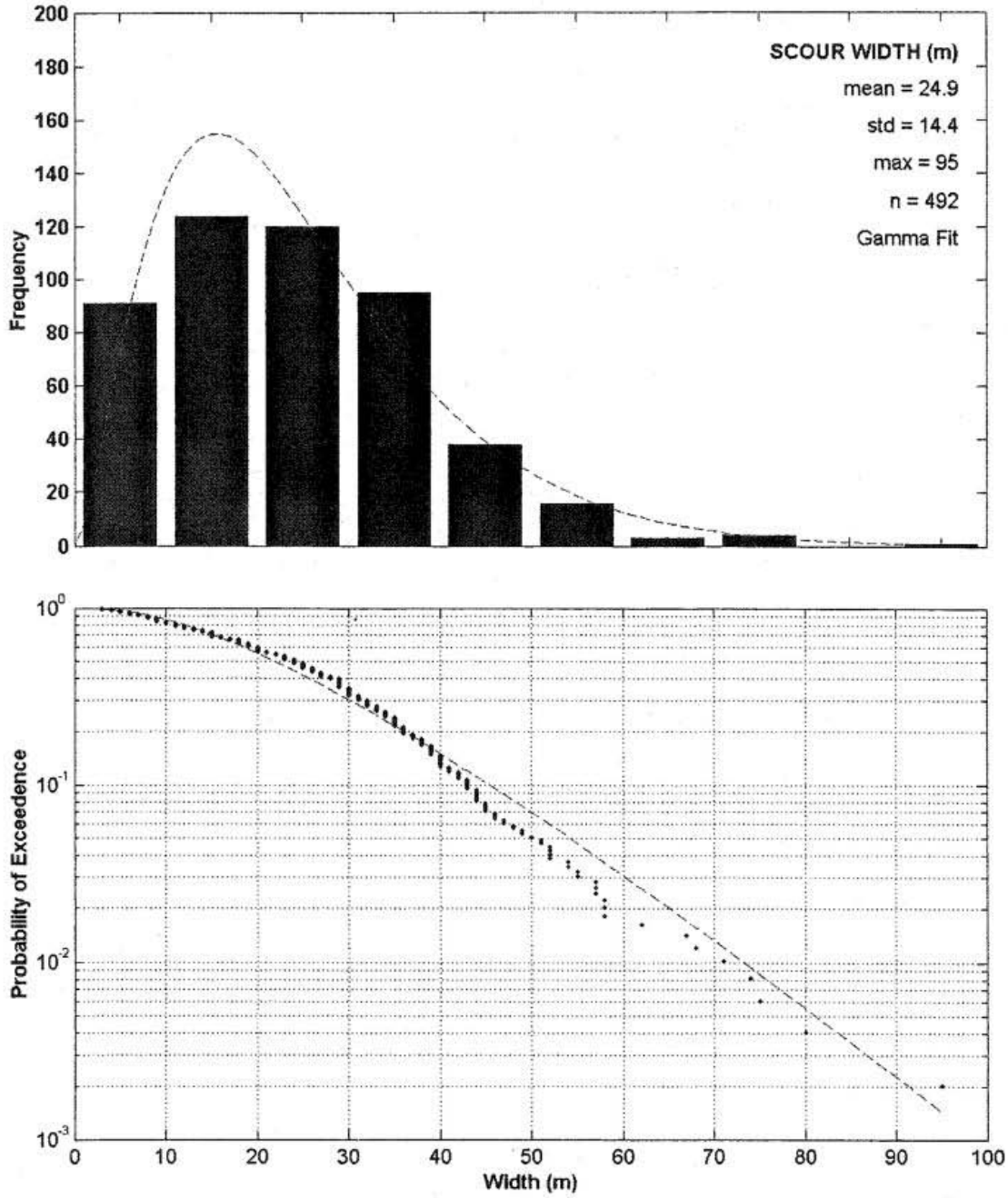

Figure 64 Distribution of scour widths in White Rose study area (from C-CORE, 2001b)

6.3 Scour Length

The mean scour length is required to calculate the frequency at which scours cross over subsea structures or pipelines. The interpretation of scour length is complicated by the truncation of scours by the edge of the mosaics, which lower the average scour length. However, for larger mosaics this has less influence on the mean scour length.

6.3.1 DIGS Mosaics

Scour lengths were tabulated for three of the four DIGS mosaics. The mean scour lengths for the Anastasia, Bertha and Repetitive Mapping mosaics are 290m, 185m and 317 m, respectively. Examination of the mosaics indicated that a significant number of scours were truncated by the edge of the mosaics. This is not surprising, given that these mosaics were relatively narrow (generally less than 2 km) compared to their lengths. It was concluded that the scour length data from the DIGS mosaics would underestimate the mean scour length.

An analysis of scanned images of the DIGS mosaics was attempted in order to perform an independent assessment of scour length. While it was possible to identify where a scour crossed near the center of individual side-scan swaths, where the quality of the image was the highest, following individual scours from swath to swath was not possible except for the largest and most prominent scours. This clearly would have resulted in an biased representation of scour length, therefore this endeavor was abandoned.

6.3.2 Bjarni Mosaic

The Bjarni mosaic covered the largest area of all the mosaics from the Makkovik Bank. The mosaic for the Bjarni site is a line-drawing traced from the side-scan swaths. The mosaic was scanned and digitized to obtain the scour length distribution. The average scour length determined in this manner was 469m. Of the 177 scours shown on this mosaic at least 27 were truncated by the edge of the mosaic, however this was difficult to determine assess since the edge of the mosaic was not well-defined. In order to assess the effect of scour truncation, a zone was defined within the mosaic where there was a high degree of confidence that no scours were truncated (Figure 65) and scours with both endpoints outside this zone were excluded. Scour features with length/width ratios of 2 or less (defined as pits in the DIGS study) were excluded. The mean scour length for the remaining scours was 542 m. The distribution of these scour lengths are shown in Figure 66. If scours with length/width ratios less than 5 (which tends to be a lower bound value for scours on the Grand Banks) are discarded, then the mean scour length is 610 m.

6.3.3 North Bjarni Mosaic

The North Bjarni mosaic, also a line-drawing traced from the side-scan swaths, was scanned and digitized using the same procedure employed for the Bjarni mosaic. The North Bjarni mosaic covers less area the Bjarni mosaic, but no depth cutoff was used so more scours were included on the mosaic. The mean scour length for this mosaic is 281m. Of the 212 scours, at least 37 are truncated by the edge of the mosaic. Given the relatively low mean scour length and the likely influence of scour truncation, these data were disregarded.

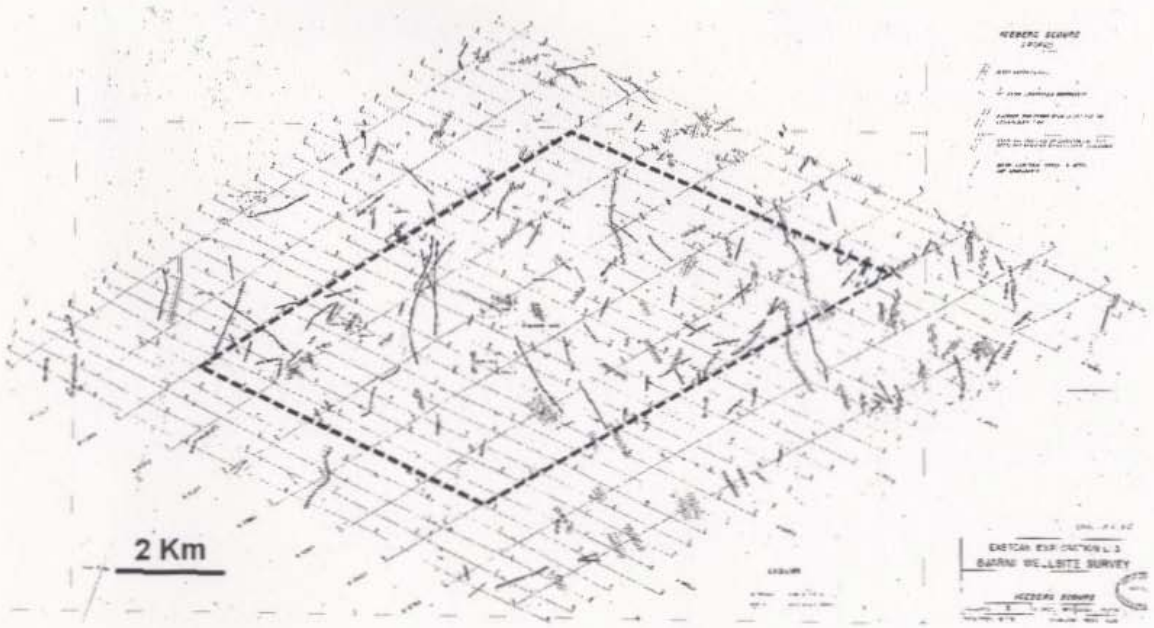

Figure 65 Bjarni mosaic showing digitized scour marks and area sampled for scour length

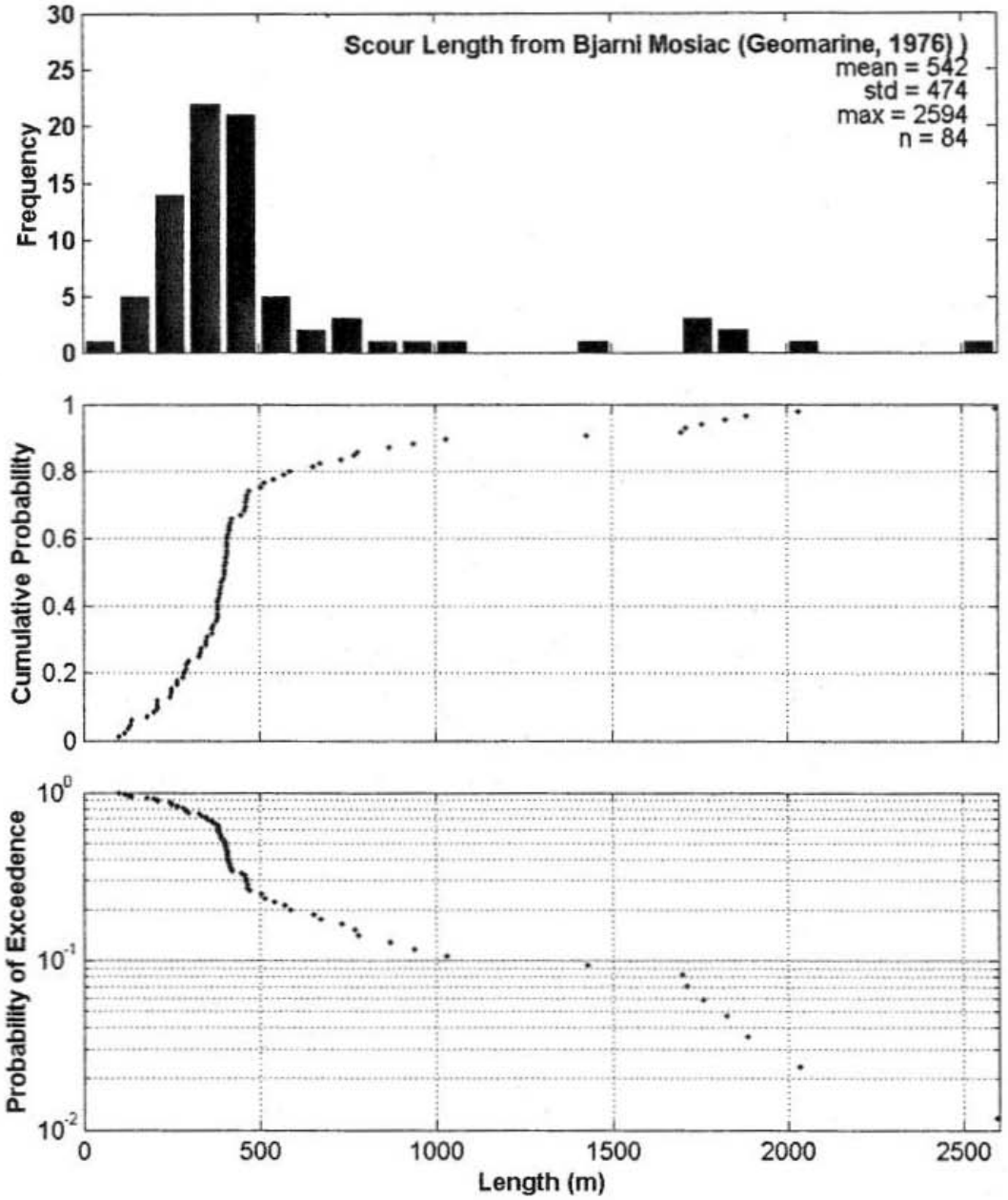

Figure 66 Scour length distribution from sampled area within Bjarni mosaic

6.3.4 Grand Banks Data

The distribution of scour lengths measured in the White Rose study area (C-CORE, 2001b) is shown in Figure 67. The mean scour length is 588m. An analysis of the effect of scour length truncation suggested that a mean scour length of 650 m was more representative for the study area (C-CORE, 2001a). For the entire Grand Banks region, the mean scour length is 622m, based on 2910 records (PERD, 2000). No significant relationship was noted between scour length and water depth.

The agreement between the Grand Banks mean scour length and the mean scour length in the Bjarni mosaic is reasonably good. There are two reasons why scour length would be expected to be longer on the Grand Bank than on the Makkovik Bank. First, observed iceberg drift speeds on the Grand Banks (≈0.34m/s) are higher than those on the Makkovik Bank (≈0.24m/s) and would be expected to produce longer scour lengths. Also, seabed slopes on the Grand Banks in the vicinity of the White Rose (0.1%) and Hibernia (0.06%) developments are less than those generally seen on the Makkovik Bank (generally 0.15% and greater). These factors considered, a mean scour length of 600 m on the Makkovk Bank is a reasonable estimate and was used for the risk analysis.

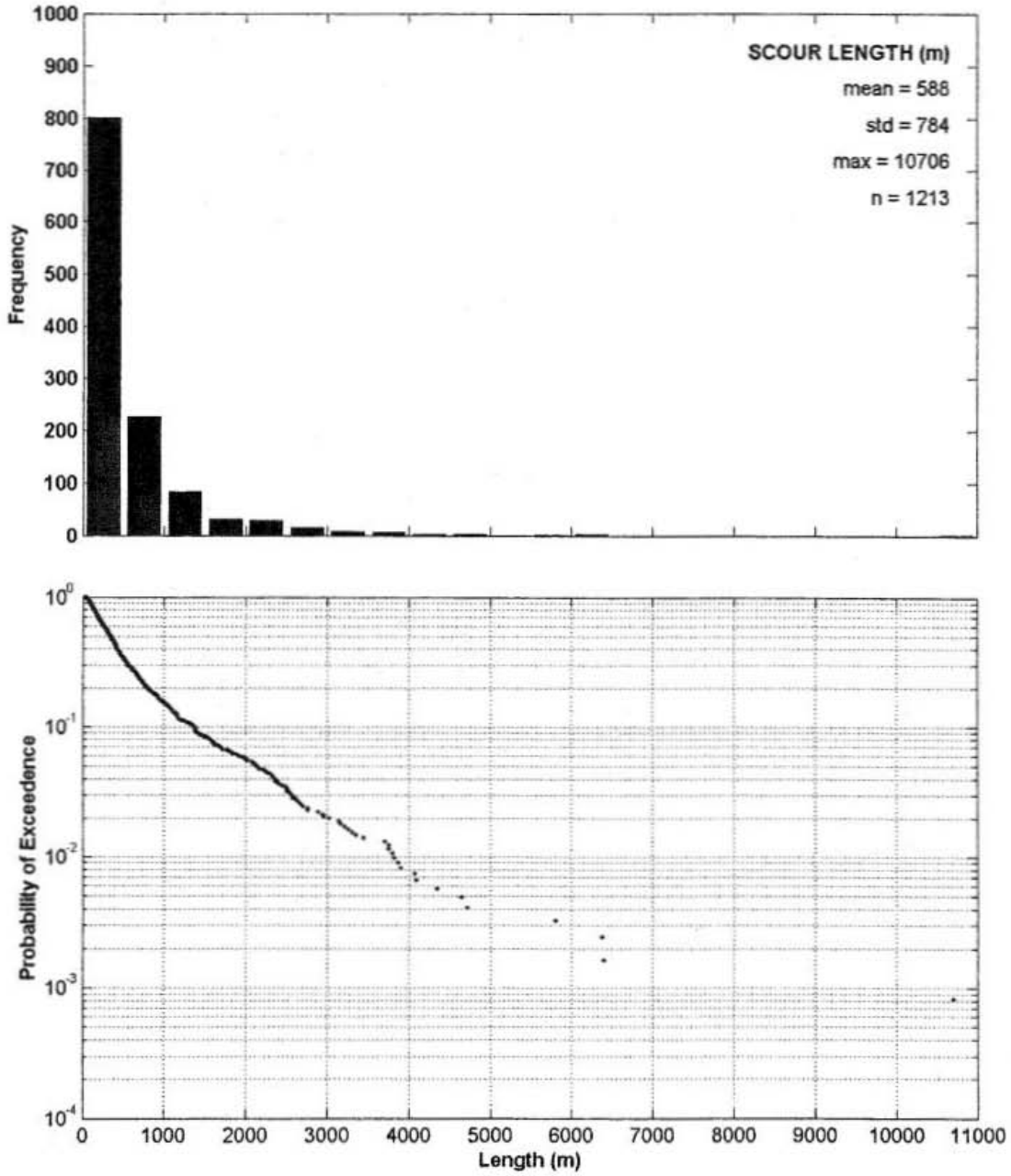

Figure 67 Scour length distribution in White Rose study area (from C-CORE, 2001b)

6.4 Scour Depth

The scour depth distribution is required to determine the proportion of scours that penetrate deep enough into the seabed to damage a pipeline or installation placed below the mudline. Scour depth is easily the most contentious aspect of iceberg scour risk. In interpreting scour depth data, the aspect that is most often overlooked is the number of scours below the resolution of the measuring system and the resulting influence of the overall depth distribution. This effect was considered in establishing a scour depth distribution for the risk analysis.

6.4.1 Bjarni Survey

The scour depths reported in the Bjarni survey (Geomarine, 1976) are a sub-sample of the overall population. Scour statistics derived by Geomarine from this survey were based only on scours with depths equal to or greater than 1 m. Therefore, in order to determine the actual distribution of scour depths it was necessary to account for the proportion of scours below 1m in depth.

The mosaic produced from the survey was a line drawing traced from the sidescan records. There is insufficient information in this drawing to reliably make the distinction between pits and scours. An initial attempt to discern between pit and scour features based on length to width ratio, as was used in the DIGS study, revealed no significant difference in the depth or width distribution. Therefore, no distinction between pit and scour features will be made in the depth analysis. The extreme scour depths (i.e. over 4

m) were associated with very short features or with the terminus of longer scour features, suggesting that these are all pit features.

Of the 310 scour/pit depths recorded by the Raytheon 719 echo sounder employed during the survey, only 10 had depths less than 1 m, with a minimum value of 0.5 m. An analysis of the mosaic revealed a total of 231 scour features, with many of the longer scours having more than one associated scour depth measurement. It is worth mentioning that the longer scours often had depths that were below resolution during some (if not the majority) of the occasions when the ship's track crossed the scour. Obviously, if depth measurements were available on these occasions and combined with the other depth measurements for those scours, the result would be an overall lower mean scour depth. The mean recorded scour depth (excluding those less than 1 m) is 1.48 m. The distribution of these is shown in Figure 68.

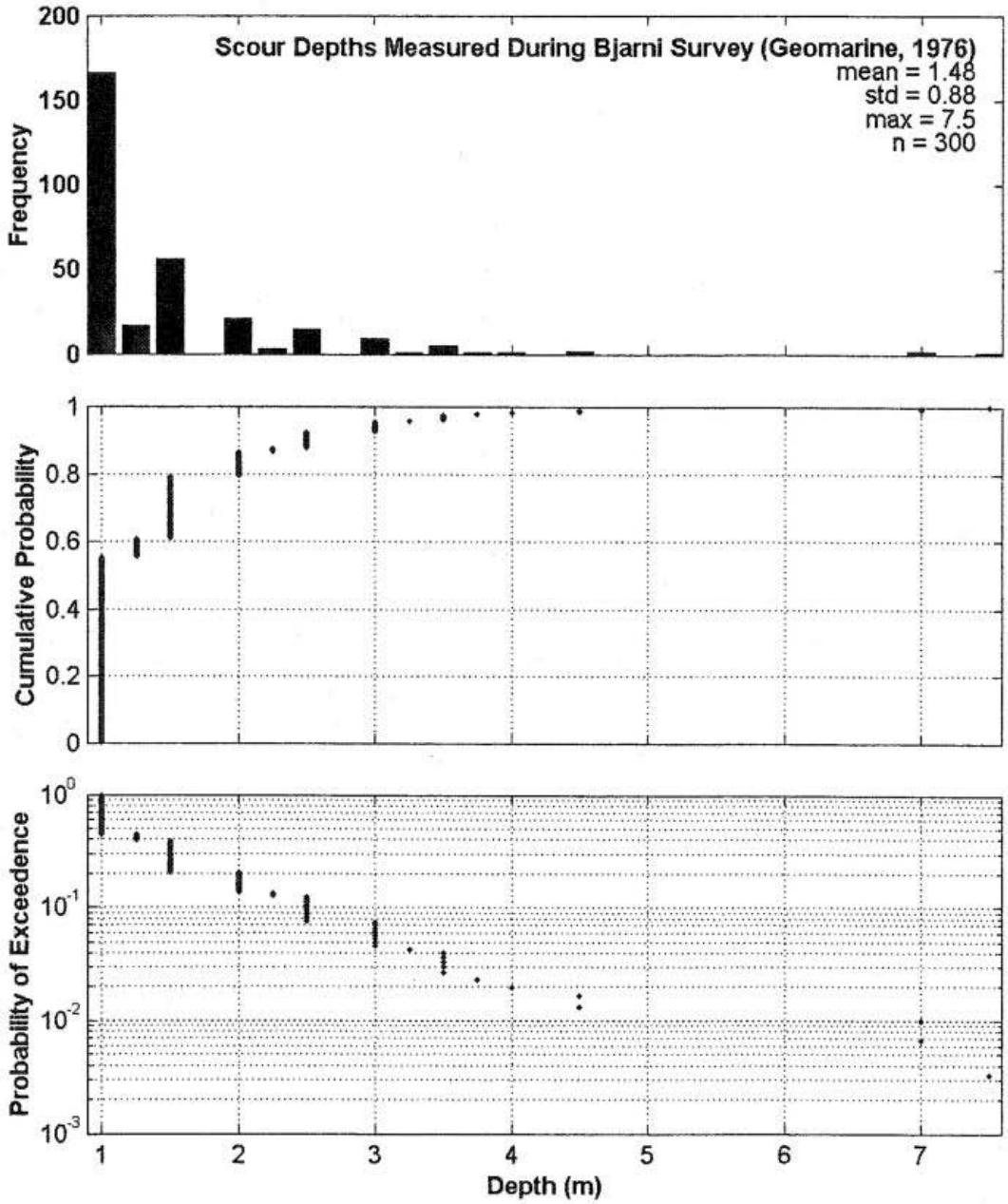

Figure 68 Distribution of scour and pit depths measured during Bjarni survey (Geomarine, 1976)

To determine the actual distribution of scour depth, it was assumed that the overall depth distribution was exponential. This is generally considered to be the case for iceberg scours (PERD, 2000) and has been noted for scours caused by ice pressure ridges in the Beaufort Sea (Lewis, 1977; Pilkington and Marcellus, 1981). In order to assess the effect of the 1 m scour cutoff, a series of exponentially-distributed scour depth populations (mean depths of 0.1 to 0.9 m) were generated and, for each population, the mean of the scour depths ≥1 m was calculated. The result of this analysis is shown in Figure 69 (top). A mean scour depth of 0.6 m produces the observed mean scour (1.48 m) when gouges less than 1 m are dropped. This result was produced using scour depths that were rounded to the nearest 0.25 m, as was the original data. If the sour depths are not rounded, the mean scour depth required to produce a truncated mean of 1.48 m is 0.48 m. Figure 69 (middle) also shows the proportion of sub-resolution scours in the overall scour population. According to this method, approximately 75% of the scours were not documented. Figure 69 (bottom) shows a comparison of the documented scour depth population and a scour depth population with a mean of 0.6 m, rounded to 0.25 m, with values less than 1 m truncated. It can be seen that the distribution agrees fairly well with the observed distribution.

Several samples of side-scan and profiler data were included in the Geomarine (1980) report, of which two have been included. Figure 70 shows seven well-defined features, of which six cross the ship's track. Close examination of the side-scan suggests there are other, less well-defined features, which have not been included. Of the six well-defined

features crossing the ship's track, depths were recorded for three (b, c, and g). Features b and c are clearly pit features. Lines drawn on the profile show the interpreted depths. Close examination of the profile for feature g suggests that both the width and depth may have been overestimated. Figure 71 shows another sample with seven well-defined features, of which six cross the ship's track. Of the six features, only one (c) was considered of sufficient clarity and depth to be included as a documented scour. Thus, for this limited sample of twelve scours, 67% were sub-resolution (less than 1m).

An alternate estimation of the proportion of sub-resolution scours may be obtained using scour records from the North Bjarni survey (Geomarine, 1980). Scour depth data from this survey were not recorded, however a mosaic was produced in which the better-defined scours were traced. The North Bjarni survey was close to the Bjarni survey and in a similar water depth range (150-158 m for North Bjarni, 130-165 m for Bjarni). The area covered by the North Bjarni survey was approximately 12.2 km^2. A total of 212 scours were shown in the mosaic. Since the Bjarni survey covered 134.7 km^2, it can be reasonably assumed that there should have been 2340 scours visible, assuming the same scour density. Since 231 scour features with depths $\geq$1 m were recorded, it could be argued that the recorded scours represent only 10% of the total scour population. When it is considered that only the better-defined scours were shown in the North Bjarni mosaic, this suggests that the approach used for analyzing the Bjarni scour depths is conservative and the mean scour depth may, if fact, be less.

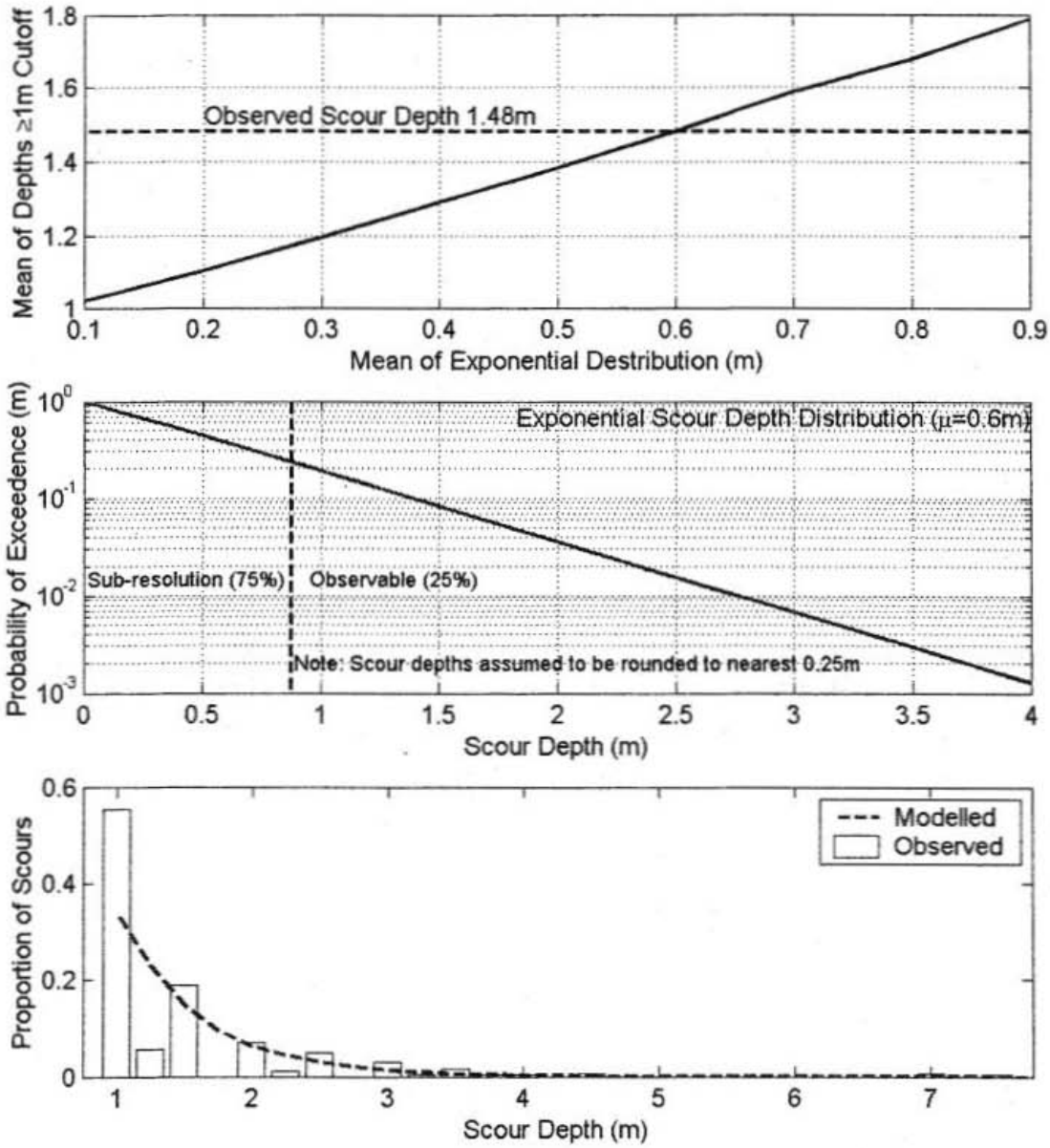

Figure 69 Methodology for correcting for sub-resolution scours: (top) calculating mean scour depth, (middle) determining proportion of sub-resolution scours, and (bottom) a comparison of measured and modeled scour depths

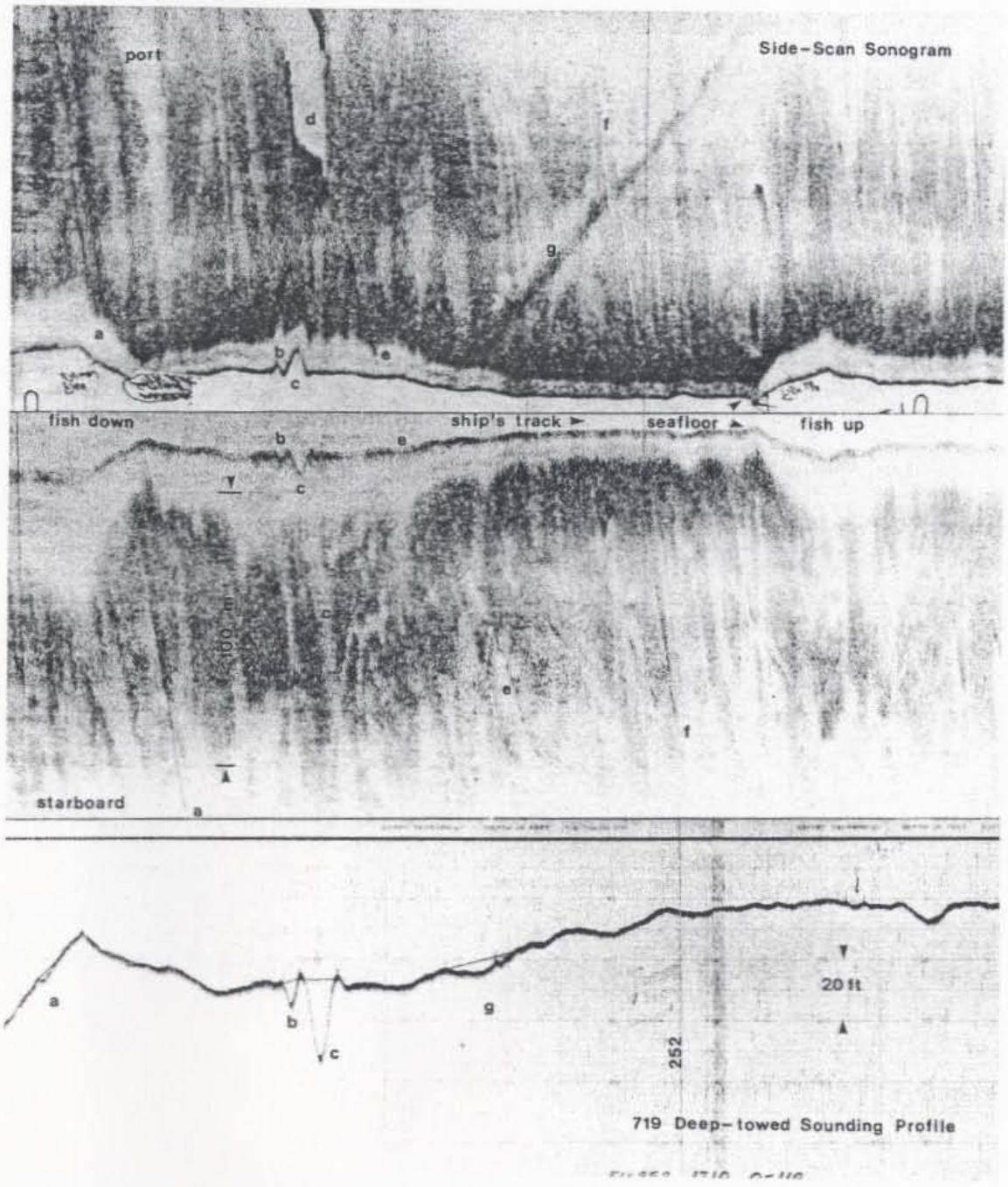

Figure 70 Side-scan and sounder data from Bjarni survey (Geomarine, 1976) in which three (b, c and g) of six features crossed by the ship's track was documented

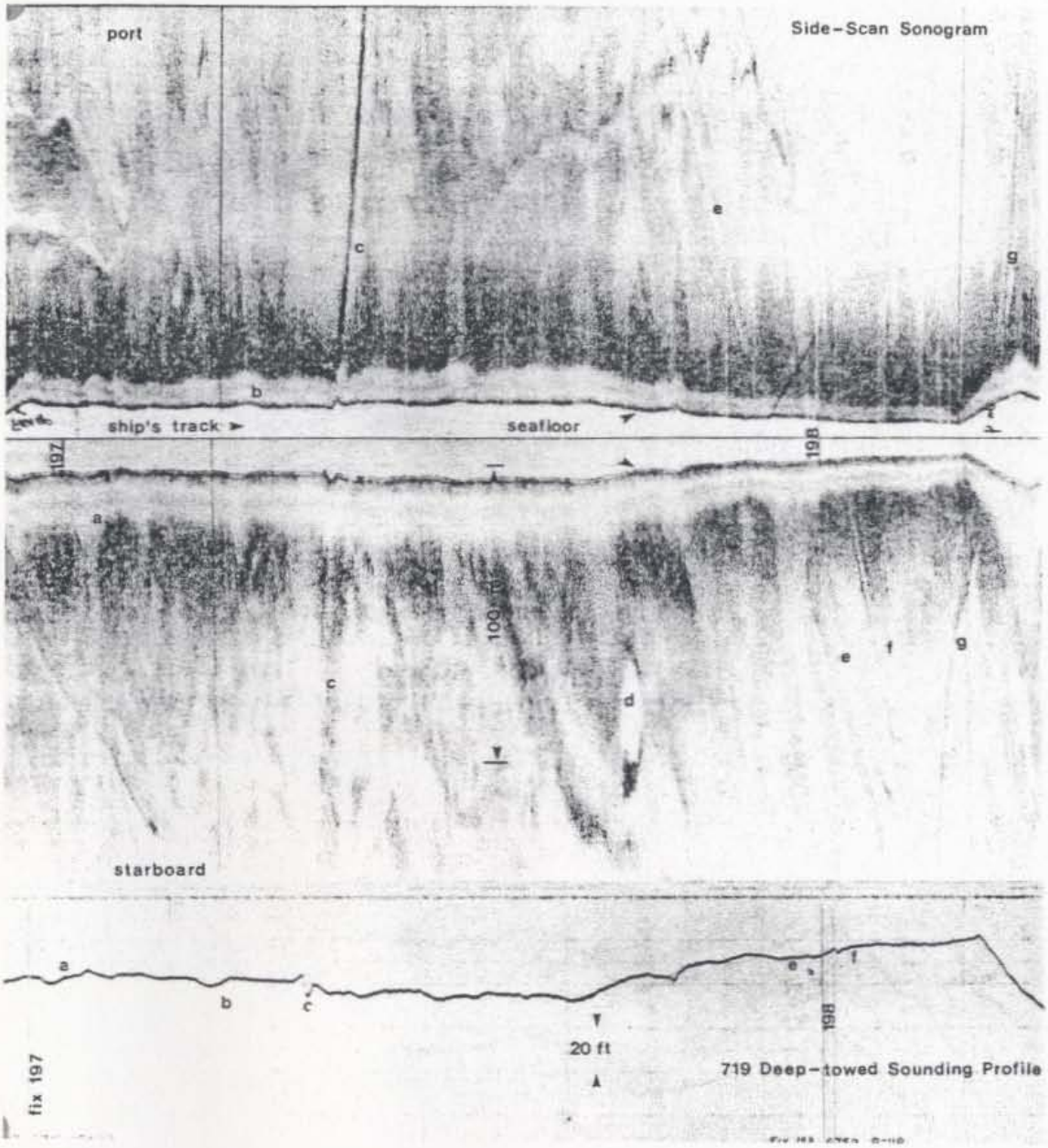

Figure 71 Side-scan and sounder data from Bjarni survey (Geomarine, 1976) in which only one (c) of six scours crossing the ship's track was documented

6.4.2 DIGS Mosiacs

The scour depth measurements from the DIGS project are the best available data for the Makkovik Bank. The scour data discussed here are given in Appendix 10 of the DIGS report. Scour depth data were presented in two ways: (1) analyses of the mosaics were used to tabulate individual scour features which were classified with respect to scour feature type, orientation (if applicable), length and depth and (2) measured depths of scour features crossed by the ship's track were tabulated on an event-by-event basis without any classification regarding feature type (scour or pit). Table 21 summarizes the scour depth data from the mosaics. There are far fewer depth data values given for the mosaics than for the lines. There was no detailed analysis for the Gladys mosaic, which covered the largest area. Table 22 summarizes the depth data from the tracks. Due to the limited number of scour depths associated with the first data set, the analysis of scour depths from the DIGS project was based on the track data, with the understanding that these data include both scour and pit depths.

Table 21 Scour Depth Data from Mosaics

Mosaic	Total Scours	Depths Reported	Mean (m)	S.D. (m)
Repetitive Mapping	241	19	0.94	0.55
Bertha	92	5	0.66	0.34
Anastasia	111	7	1.19	0.55
Gladys	No mosaic data for Gladys Mosaic			
All	444	31	0.95	0.54

It is worth noting that some of the scours in the mosaic data were broken down into segments for which depths were recorded. If this is taken into account and the segment depth values for each scour are averaged, the number of scour depths drops to 25, with a mean of 0.93 m.

Table 22 Scour Feature Depth Data from Tracks

Mosaic	Scour/Pit Depths	Mean (m)	S.D. (m)
Repetitive Mapping	102	1.16	0.76
Bertha	52	0.83	0.52
Anastasia	38	1.11	0.61
Gladys	209	1.01	0.75
All	401	1.04	0.72

Based on the ratio of length to width ($W/L \leq 2$), an additional 204 features in the Repetitive Mapping, Bertha and Anastasia mosaics were classified as pits. However, in the mosaic data, only one pit depth (1.5m, in the Anastasia mosaic) was reported.

Initially, the analysis of scour depth data from the DIGS project will consider the data set as a whole. Figure 72 shows the distribution of the scour feature depths measured from the track data. It can be seen that the distribution of depths scour depths does not follow an exponential distribution. However, the decrease in the number of measured scour depths less than 0.4 m is very likely due to the resolution of the profiling system used in the survey. According to Woodworth-Lynas (1992), the resolution of the Huntec system used to measure the scour feature depths was approximately 0.25 to 0.30 m. Thus, an analysis of the scour depth distribution should consider scour depths greater than the resolution of the profiling system since interpreted scour depths less than this would be considered unreliable. The depth distribution of scour features ≥0.4 m deep is shown in Figure 73. The mean scour depth is 1.12 m (364 measurements), with a standard deviation of 0.7 m and a maximum of 4.2 m.

Initially, the same approach used to determine the number of sub-resolution scours for the Bjarni survey was employed. Exponential scour depth populations were generated with the mean varying from 0.1 to 0.9 m. Scour depths were rounded to the nearest 0.1 m (as was the majority of the DIGS data) and the mean of the scour depths ≥0.4 m was calculated. As shown in Figure 74 (top), the mean scour depth that would produce a truncated mean of 1.12 m is 0.77 m. As shown in Figure 74 (middle), approximately 40% of the scour population would be expected to be below the 0.4 m cutoff. Figure 74 (bottom) shows a comparison of the measured scour feature depths with a scour depth population of 0.77 m, rounded to the nearest 0.1 m, which indicates a fairly good agreement. Repeating the process with a cutoff of 0.5 m, rather than 0.4 m, yielded a mean scour depth of 0.75 m, which was consistent with results using a cutoff of 0.4 m.

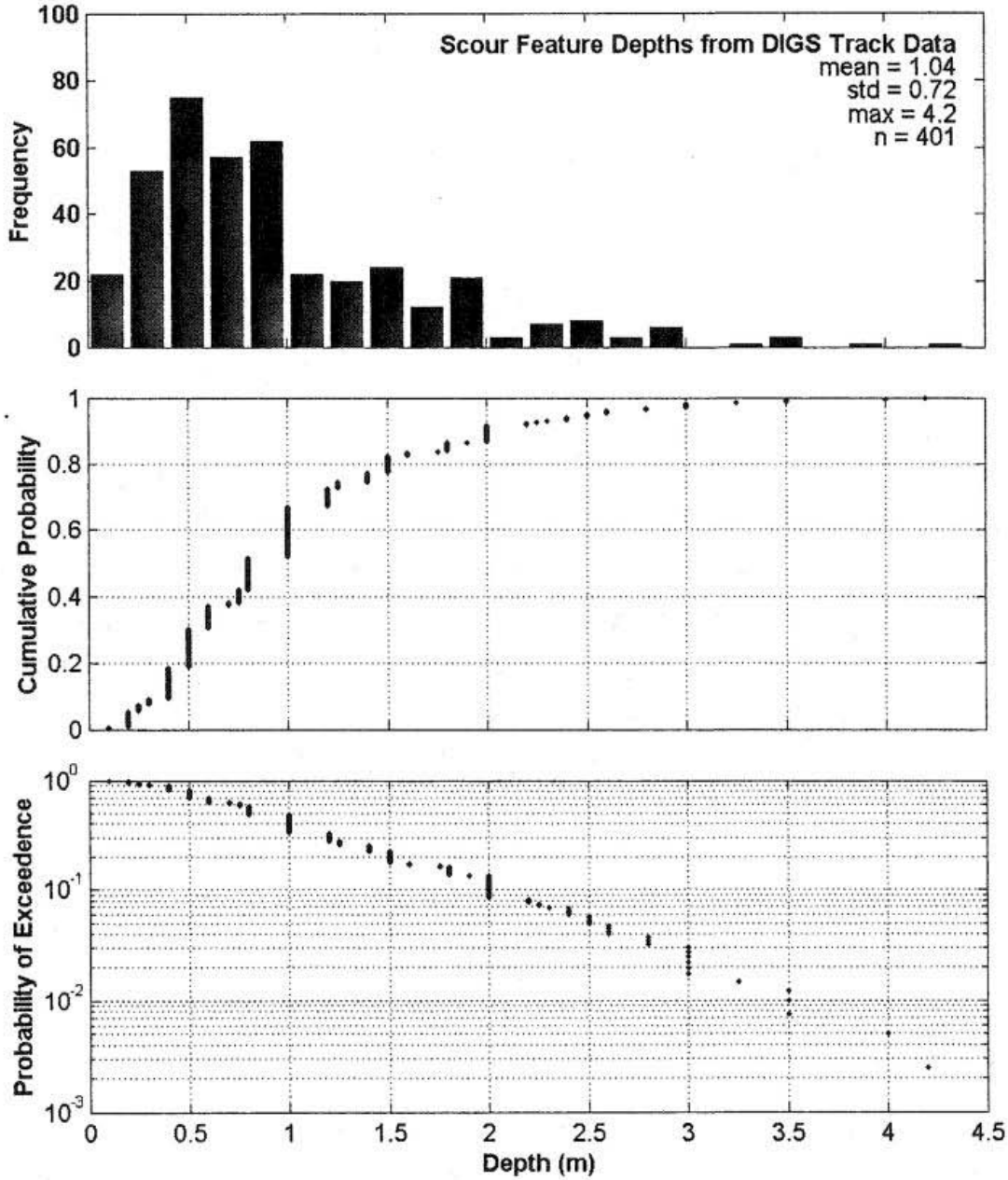

Figure 72 Distribution of all scour feature depths measured during DIGS project

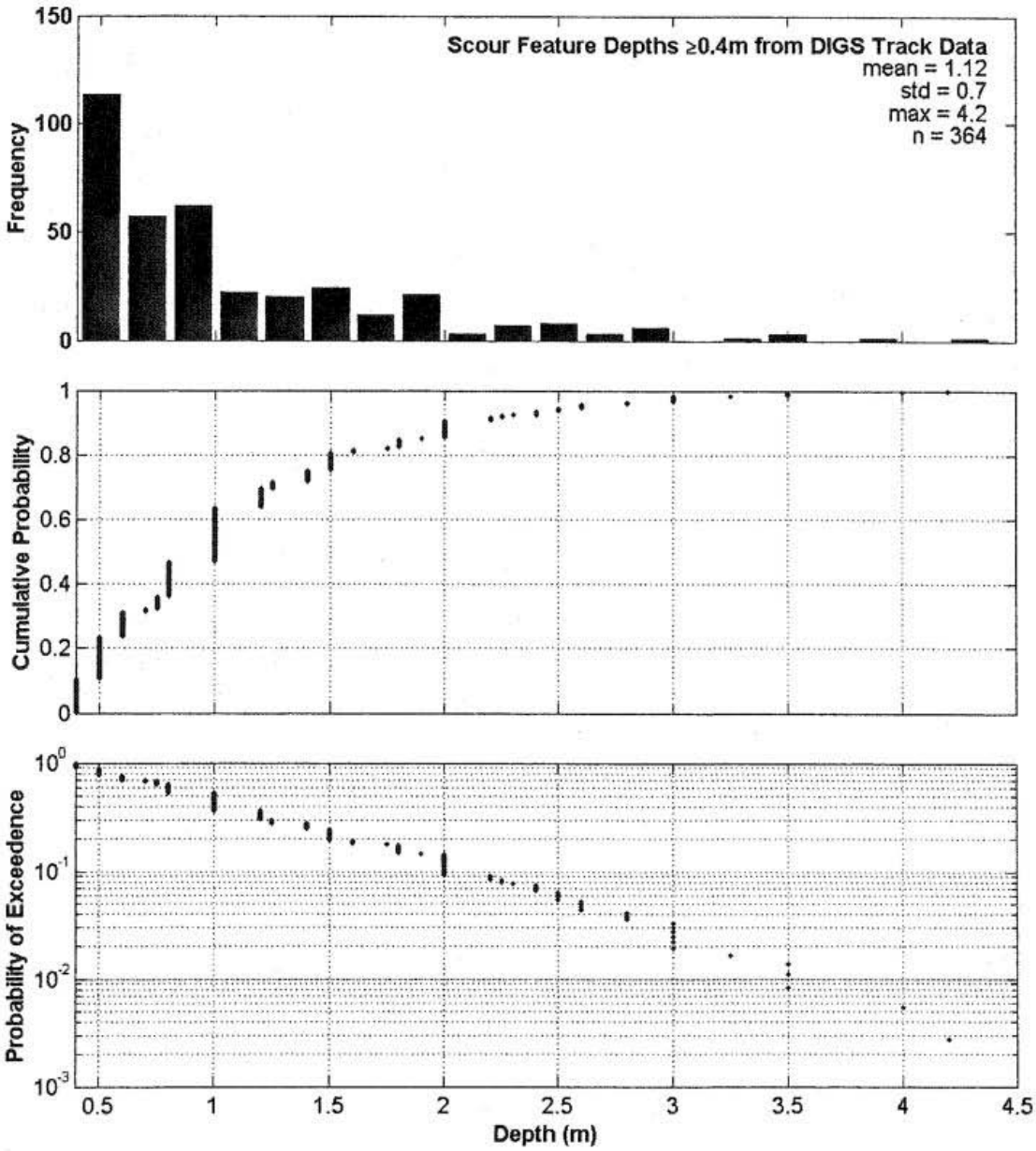

Figure 73 Distribution of scour feature depths ≥0.4 m measured during DIGS project

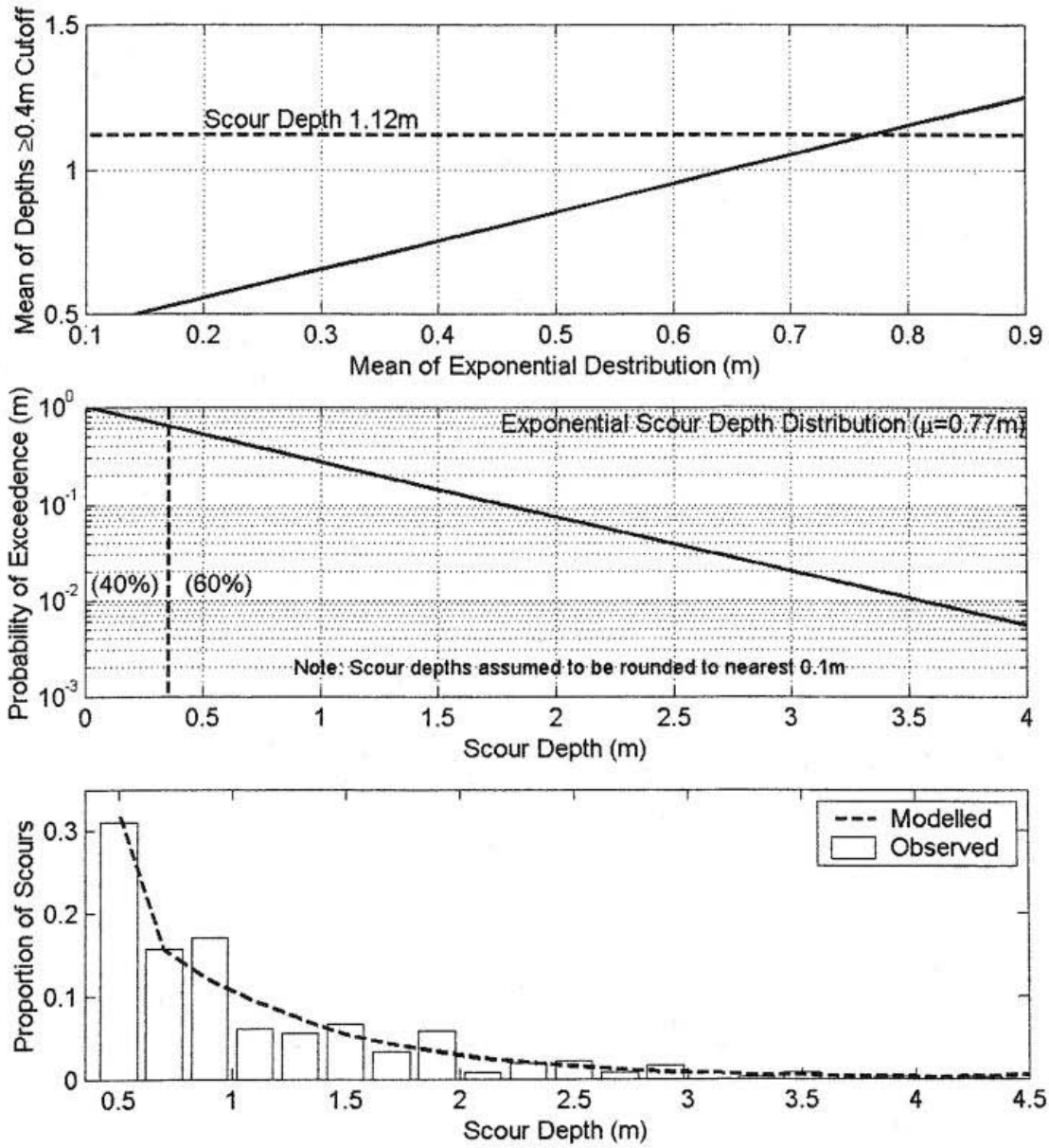

Figure 74 Methodology for correcting for sub-resolution DIGS scours: (top) calculating mean scour depth, (middle) determining proportion of sub-resolution scours, and (bottom) a comparison of measured and modeled scour depths

An alternate approach for determining the influence of sub-resolution scours was conducted using the side-scan mosaics directly. The scour mosaics were analyzed to determine the number of scours that crossed the ship's tracks. It was also possible to determine the corresponding water depth and soil type corresponding to each scour feature. Table 23 shows the number of scour features that were counted for each mosaic, along with the number of scour features tabulated in the DIGS report, and the associated mean depth. The resolution of the Huntec profiling system is 0.25 to 0.30 m, so the depth of excess scours (scours in excess of the tabulated number of scours) was conservatively estimated to be 0.30 m. This allowed an "adjusted" mean to be calculated. The adjusted mean scour depth (μ_a) was calculated as follows:

$$\mu_a = (\mu_m N_m + 0.3(N_{obs} - N_m))/ N_{obs} \qquad (6.1)$$

where N_m is the number of scour feature depths measured during the surveys, μ_m is the mean of the measured depths, and N_{obs} is the number of scour features observed in mosaics to cross the ship's tracks. This is essentially a weighted mean.

Table 23 Adjusted Scour Depths from DIGS Survey Based on Manually Tabulated Track Crossings

Mosaic	Track Crossings	Tabulated Scour Features (DIGS)	Mean Depth (m)	"Adjusted" Mean (m)
Repetitive Mapping	255	102	1.16	0.64
Bertha	88	52	0.83	0.61
Anastasia	116	38	1.11	0.57
Gladys	427	209	1.01	0.65
All	886	401	1.04	0.64

The analysis of the DIGS mosaics involved a careful visual examination of both paper copies of the mosaics and scanned images upon which the ship's tracks were superimposed. The mosaics were scanned on a large black and white scanner at a resolution of 200 dpi (the best available for scanning large charts), and thus were not ideal for identifying scours crossing the ship's tracks. However, using a digitizing routine, the images were useful for determining the boundaries of the mosaics, the extent of the various sediment types and the locations of the various bathymetric contours. Likewise, the locations where scour features were seen to cross the ship's tracks were recorded using a variation of the digitizing routine. Features that were counted were those that were clearly visible and intersected the ship's track. Other less distinct features were not tabulated. The quality of the copies of the mosaic were not high, and better quality prints might have allowed greater numbers of crossings to tabulated. Figure 75 to Figure 78 show where scour crossings of ship's tracks were identified.

It must be pointed out that the scour depths tabulated in the DIGS study were derived from the echo sounder records, not the mosaics. The limiting factors for the number of scour depths identified from the depth sounder were the actual number of scours, their depth distribution and the resolution of the instrument. Track crossings reported here were derived from the mosaics. The limiting factors for the number of track records recorded from the mosaic were the actual number of scours, the quality of the side-scan record and the quality of the reproduction of the mosaic.

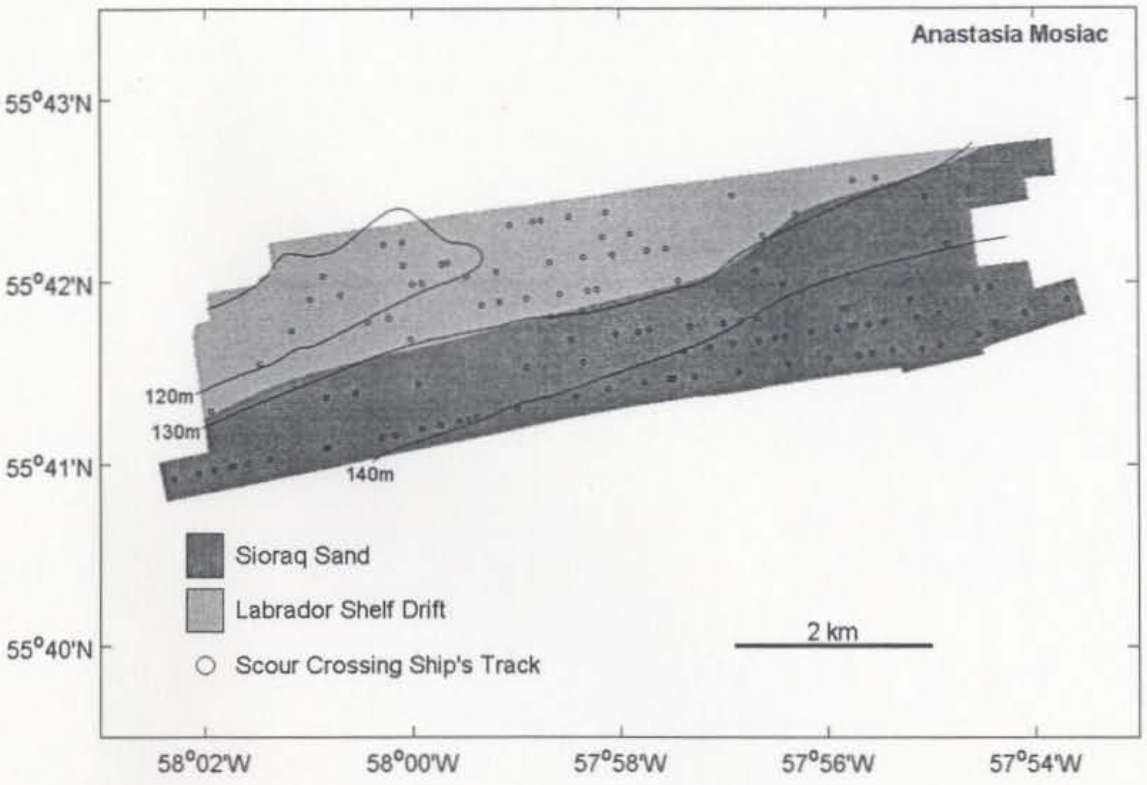

Figure 75 Anastasia mosaic obtained during DIGS study showing bathymetry, sediment types and locations of scour crossings of ship's track

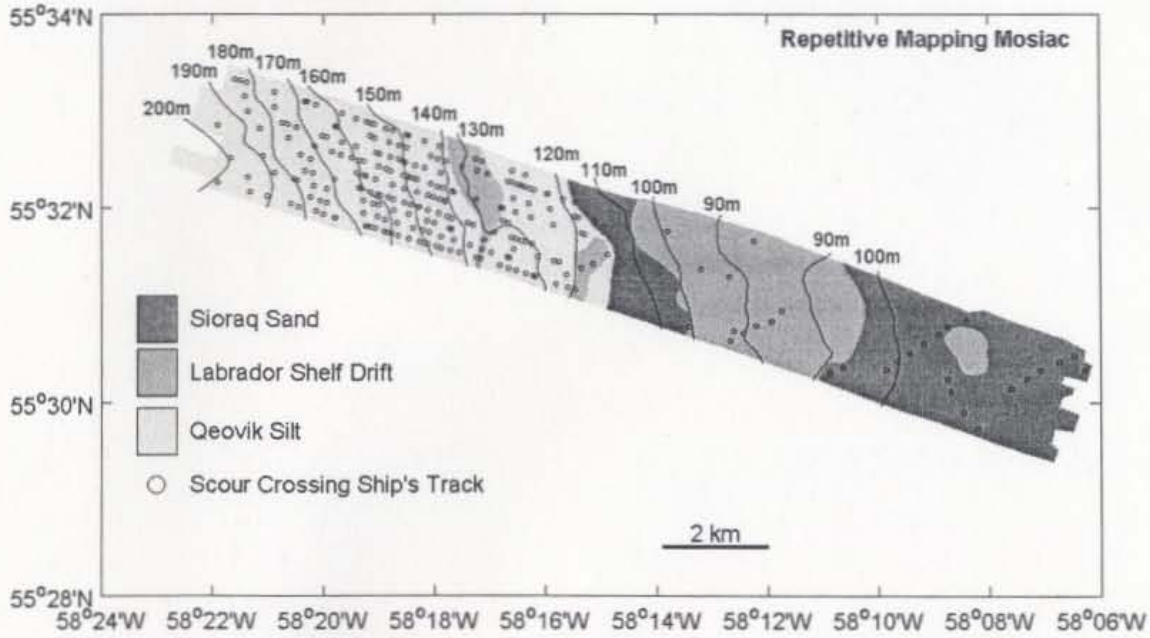

Figure 76 Repetitive Mapping mosaic obtained during DIGS study showing bathymetry, sediment types and locations of scour crossings of ship's track

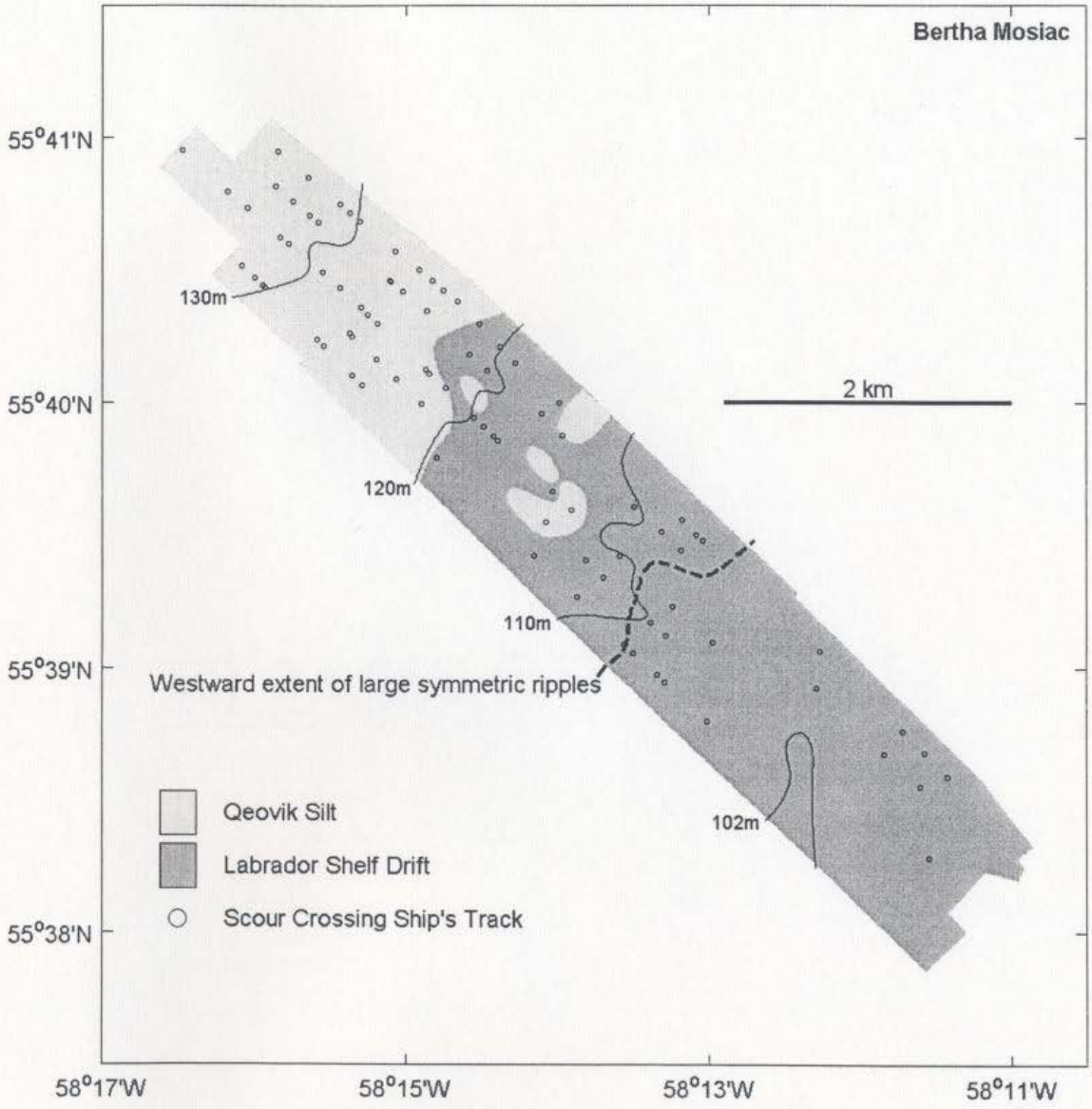

Figure 77 Bertha mosaic obtained during DIGS study showing bathymetry, sediment types and locations of scour crossings of ship's track

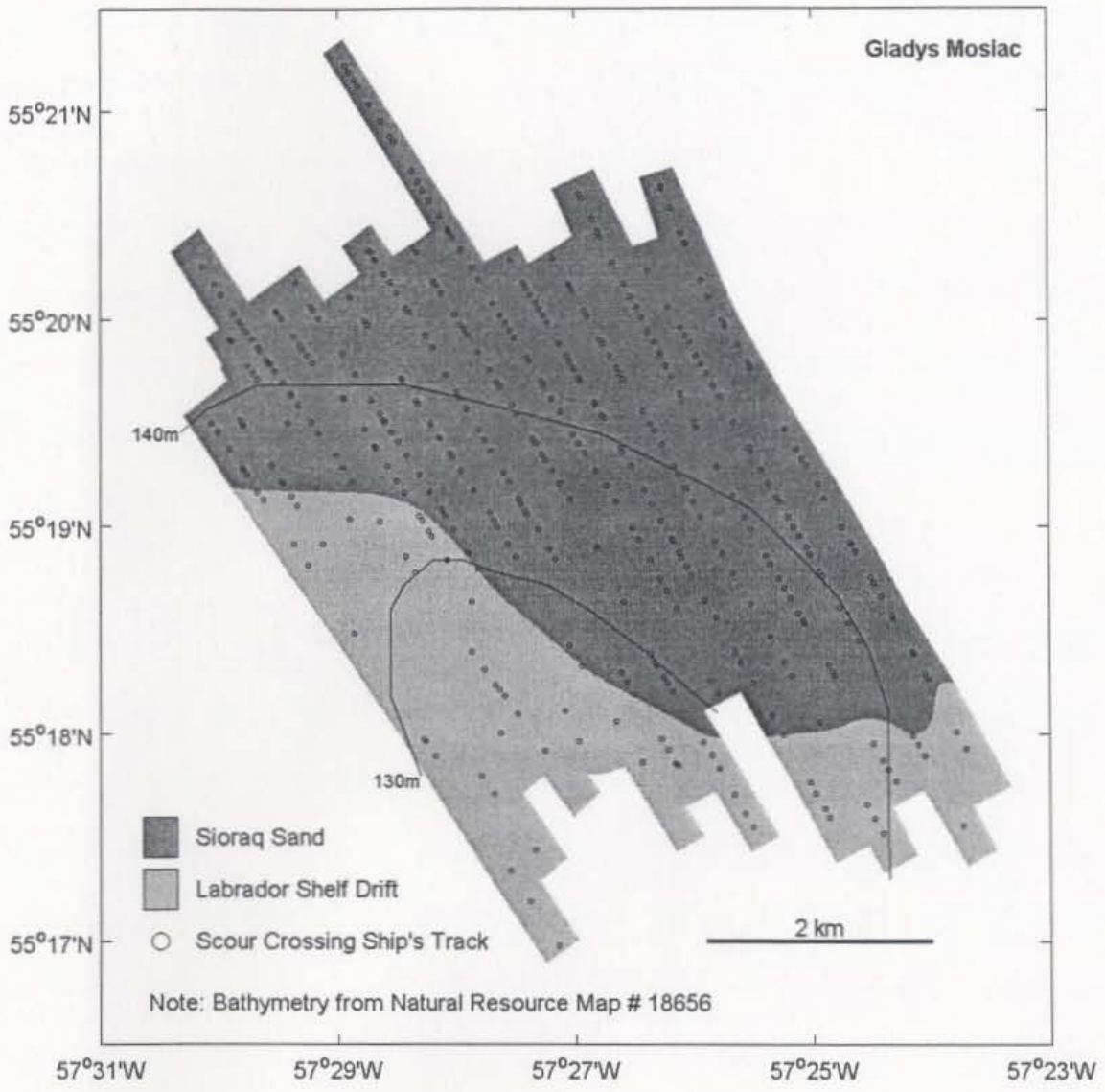

Figure 78 Gladys mosaic obtained during DIGS study showing bathymetry, sediment types and locations of scour crossings of ship's track

Table 24 shows the combined depth data for all mosaics analyzed according to soil type. Table 25 shows the combined depth data for all mosaics analyzed according to water depth. Table 26 shows the mean scour depth for the surveys, broken down by sediment type and water depth. The mean uncorrected scours depths in the Labrador Shelf Drift are shallower than those seen in the other two sediment types, however the corrected depth is greater because fewer crossings were identified in the mosaics. In almost all cases, the clarity of the side-scan mosaic on the Labrador Shelf Drift is worse than for adjacent sediment types on the same mosaic. This was particularly evident in the Gladys mosaic, where the number of track crossings counted from the mosaic was less than the number of depth measurements documented in the DIGS report (although this mosaic was dark, further compounding the problem).

There appears to be a positive correlation between corrected scour depth and water depth. However, shallow scours in water depths less than 110 m could be due to infilling of scours due to sediment transport. The contrast in the density of scour/ship track crossings in shallow water versus deeper water in the Bertha and Repetitive Mapping mosaics would seem to support this. Deeper scours observed in water depths beyond 170 m could be due to a couple of reasons. Scours in deeper water could be relict scours, and therefore not be representative of modern scours. Alternatively, there may have been sensor resolution issues associated with deeper water depths. The Repetitive Mapping mosaic (the only mosaic covering these water depths) was indistinct in water depths greater than 170 m, limiting the number of track crossings that could be identified.

A mean corrected scour depth of 0.62 m was seen in the 110 to 170 m water depth range. For all water depths, a mean corrected scour depth of 0.64 m was seen. The average corrected scour depth for the different soil types was 0.66 m. A mean scour depth of 0.64 m was selected as the result of this analysis.

Table 24 Scour Depth from DIGS Profiler Data and Examination of Mosaics, according to Soil Type

Soil Type	Scour Depths Measured (DIGS)	Mean Depth (m)	Standard Deviation (m)	Track Crossings Visible	Revised Mean Depth (m)
Labrador Shelf Drift	125	0.94	0.74	177	0.75
Soiraq Sand	108	1.18	0.73	255	0.67
Qeovik Silt	168	1.01	0.67	454	0.56

Table 25 Scour Depth from DIGS Profiler Data and Examination of Mosaics, according to Water Depth

Water Depth Range (m)	Scour Depths Measured (DIGS)	Mean Depth (m)	Standard Deviation (m)	Track Crossings Visible	Revised Mean Depth (m)
80-90	2	0.60	0.28	5	0.42
90-100	6	0.70	0.30	10	0.54
100-110	29	0.64	0.47	37	0.56
110-120	19	1.06	0.59	39	0.66
120-130	70	1.01	0.69	140	0.66
130-140	140	0.97	0.68	254	0.67
140-150	76	1.11	0.77	291	0.51
150-160	19	1.24	0.86	40	0.75
160-170	21	1.10	0.55	30	0.86
170-180	9	1.70	0.67	21	0.90
180-190	7	1.81	1.04	10	1.36
190-200	2	0.65	0.21	6	0.41
200-210	1	3.50	N/A	0	N/A

Table 26 Scour Depth from DIGS Profiler Data and Examination of Mosaics, According to Water Depth and Soil Type

	Soil Type	Water Depth (m)	Scour Depths Measured	Mean Depth (m)	Track Crossings Visible	Revised Mean (m)	Comments
Anastasia	Labrador Shelf Drift	110-120	8	0.99	12	0.76	Scours in Soiraq Sand very distinct but lack clarity in Labrador Shelf Drift.
		120-130	13	1.29	30	0.73	
	Soiraq Sand	120-130	0	0.00	1	N/A	
		130-140	12	0.98	41	0.50	
		140-150	5	1.18	32	0.44	
Bertha	Labrador Shelf Drift	100-110	21	0.62	24	0.58	Entire mosaic very dark. Scours in areas not covered by sand ripples reasonably distinct.
		110-120	8	1.23	14	0.83	
		120-130	1	1.00	4	0.48	
	Qeovik Silt	110-120	0	0.00	2	N/A	
		120-130	12	0.93	29	0.56	
		130-140	10	0.79	15	0.63	
Gladys	Labrador Shelf Drift	120-130	36	0.93	33	N/A	Entire mosaic very dark. Scours on Labrador Shelf Drift extremely difficult to distinguish.
		130-140	28	0.97	28	N/A	
		140-150	1	3.00	7	0.69	
	Soiraq Sand	120-130	7	1.11	10	0.87	
		130-140	82	0.95	144	0.68	
		140-150	55	1.12	205	0.52	
Repetitive Mapping	Labrador Shelf Drift	80-90	2	0.60	5	0.42	Scours on Labrador Shelf Drift are difficult to distinguish. Soiraq Sand scours lack clarity, areas seem "washed out" Scours in 120-170m range in Qeovik Silt are distinct, however they indistinct below 170m, worsening with depth.
		90-100	6	0.70	6	0.70	
		100-110	1	0.40	1	N/A	
		110-120	0	0.00	3	N/A	
		120-130	0	0.00	7	N/A	
		130-140	0	0.00	3	N/A	
	Soiraq Sand	90-100	0	0.00	4	N/A	
		100-110	7	0.71	12	0.54	
		110-120	0	0.00	2	N/A	
	Qeovik Silt	110-120	3	0.80	6	0.55	
		120-130	1	0.80	26	0.32	
		130-140	8	1.36	23	0.67	
		140-150	15	0.94	47	0.51	
		150-160	19	1.25	40	0.75	
		160-170	21	1.10	30	0.86	
		170-180	9	1.70	21	0.90	
		180-190	7	1.81	10	1.36	
		190-200	2	0.65	6	0.42	
		200-210	1	3.50	0	N/A	

6.4.3 Grand Banks Scour Depths

Grand Banks scour depths, specifically those documented in the White Rose study (C-CORE, 2001b) are worth considering since they represent the most recent and accurate measurements of scour depth and are a legitimate basis of comparison for scours on the Makkovik Bank in similar water depth ranges and soil types. The water depth range in the White Rose study region is 110-140 m and the seabed is comprised primarily of sand with gravel patches.

Scour depth records were extracted from the Grand Banks Scour Catalog (GBSC) for an area representative of White Rose (see Figure 61). If only measured scour depths were considered, the mean of the 132 measured scour depths in the White Rose study region was 0.5m. However, approximately 2/3 of the scours for which depth measurements were attempted were below the system resolutions (either 0.5, 0.3 or 0.1m, depending on the source). These scours were randomly assigned scour depths between zero and the system resolution. The resulting distribution, with a mean of 0.34m, is shown in Figure 79.

A total of 65 pit depths were also recorded in the White Rose study area. The mean pit depth was 1.1m, with a maximum measured of 5.2m. The distribution of pit depths also followed an exponential distribution.

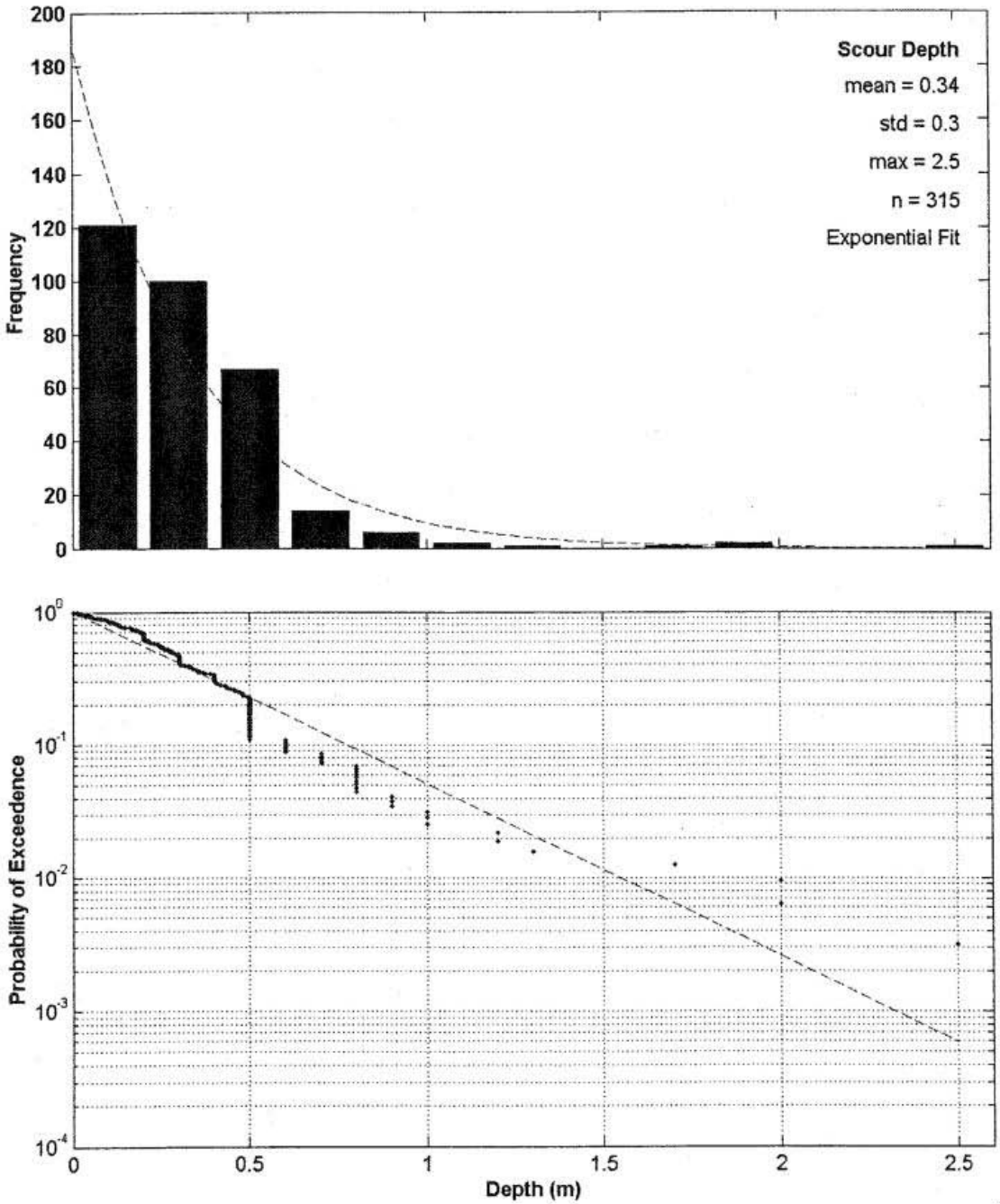

Figure 79 Scour depth distribution from White Rose study region (from C-CORE, 2001b)

6.4.4 Scour Depths from Regional Ice Scour Database

The Regional Ice Scour Database (Geonautics, 1989) gives a mean scour depth of 1.35 m for the Labrador Shelf and 1.6 m for the Makkovik and Harrison Banks. For comparison, a mean scour depth of 0.9 m was given for the Grand Banks in water depths less than 90 m and 1.4 m in water depths greater than 90 m. The obvious discrepancy between Grand Banks scour depths from the GBSC and the Regional Ice Scour Database clearly indicates that scour depth values from the Regional Ice Scour Database are biased. This example illustrates the danger of using iceberg scour depth data without accounting for the effect of sensor resolution.

6.4.5 Scour Depth Distribution for Risk Analysis

Fitting an exponential distribution to the scour depth data from the Bjarni and DIGS surveys yielded mean scour depths of 0.60 m and 0.77 m, respectively. Inspection of the DIGS mosaics indicated a mean scour depth of 0.64 m. The average of these values is 0.67 m. This value should be increased to account for the effect of sediment infill. Gaskill (1985) suggested a correction factor of 1.07 for the Grand Banks, based on simulations of infill for scour with exponential depth distributions. Given that sediment infill rates may be faster on the Makkovik Bank (although not likely to be substantially higher in the water depths considered) a corrected mean scour depth of 0.75 will be adopted. Therefore, an exponential depth distribution with a mean of 0.75 m will be used for the pipeline risk analysis.

6.5 Scour Riseup

The scour riseup is the difference in water depth at the beginning and end of a scour. A decrease in water depth is implied, however scours have been noted to scour both up and down slopes. Scour riseup is not a factor in the grounding model or the pipeline risk analysis, however it was used in the Petro-Canada (1983) study to determine the proportion of iceberg keels that would scour over a pipeline, and thus will be given some consideration.

Woodworth-Lynas et al. (1986) analyzed a number of sidescan mosaics and scour maps, as well as iceberg track data, to assess scour riseup. A maximum scour riseup of 15 m was determined from seabed records, while a maximum scour riseup of 45 m was inferred from iceberg track data. As shown in Table 27, the majority of scours did not have a measurable riseup, within the limitations of the available bathymetric data. This would imply a mean riseup less than 1 m. Although scour truncation by the edge of the mosaic would play a role, it would not be expected to significantly increase the mean riseup. An analysis of iceberg tracks on the Makkovik Bank indicated 25 scouring icebergs, of which 20 had riseups greater than 2 m, with a maximum riseup of 45 m. The shortest interpreted scour was 2.5 km, while the longest was 96.25 km. An analysis of iceberg tracks on the Saglek Bank indicated 21 scouring bergs, all of which had riseups in excess of 1 m, with a maximum of 35 m. The minimum interpreted scour track was 2.5 km, while the longest was 220 km. The obvious discrepancy between riseups interpreted from seabed surveys versus iceberg tracks suggests that, at least with respect to mean

riseups, a higher degree of confidence would be associated with riseups interpreted from seabed surveys.

Table 27 Scour Riseup Interpreted from Seabed Surveys (Woodworth-Lynas et al., 1986)

Site	Latitude	Total Scours	Measurable Riseup	Maximum Riseup
Hekja	62°20′ N	775	48 ≥ 1 m	4.5 m
Rut	59°10′ N	327	48 ≥ 0.5 m	3.25 m
Saglek East	61°45′ N	532	101 ≥ 1 m	13.5 m
Saglek West	62°15′ N	265	71 ≥ 1 m	7.5 m
Iceberg Caroline	59°21′ N	305	50 ≥ 0.5 m	4.0 m
Nain Bank	57°37′ N	22	18 ≥ 0.5 m	4.5 m
Bjarni	55°30′ N	300	88 ≥ 1 m	15 m
North Bjarni	55°35′ N	219	22 ≥ 1 m	3 m
Snorri	57°20′ N	697	285 ≥ 0.5 m	12.5 m
DB Wellsite	54°45′ N	43	24 ≥ 1 m	---
East Harrison	55°16′ N	108	23 ≥ 1 m	7 m
Hibernia East	46°44′ N	10	2 ≥ 1 m	---

Based on an analysis of the DIGS mosaics, Hodgson et al. (1988) reported a mean riseup of 1.8 m, with a maximum in excess of 25 m (239 scours). Again, it is acknowledged that scour truncation by the edge of the mosaics could result in a higher mean riseup.

A review of the White Rose scour data indicates a mean scour riseup of 0.46 m (664 records, 448 ≤ 1 m riseup). The maximum riseup recorded in the White Rose area is 11 m. The mean riseup for scours with lengths of a least 1 km is 1.7 m (81 records, 72 ≥ 1 m riseup). This agrees with the other mean riseup values determined from seabed records, suggesting that the mean riseup for the Makkovik Bank is less than 2 m.

6.6 Comparison With Petro-Canada (1983) Scour Parameters

The scour depth distribution used for the Petro-Canada (1983) iceberg scour risk analysis was assumed to be exponential with a mean of 1.45 m. The scour distribution that will be used for the estimation of iceberg scour risk is exponential, with a mean of 0.75 m. Figure 80 shows a comparison of the probability of exceeding specified scour depths, based on these two mean values. As can be seen in Figure 80, the probability of exceeding a 2.5 m scour depth is reduced by a factor of 5 for a 0.75 m mean scour depth, versus a 1.45 m mean scour depth.

The Petro-Canada (1983) risk analysis used scour riseup to determine the proportion of the iceberg population that would scour over a pipeline segment. Based on maximum observed riseups (10 m), it was assumed that the proportion of icebergs that could scour over a pipeline segment was equal to the proportion of icebergs with drafts greater than the water depth and less than the water depth plus 10 m. However, a reasonable number to use, rather than the maximum riseup (which exceeds 10 m) would be the mean riseup. If the mean riseup had been used, the crossing rate would have been reduced by a factor of 5 to 10.

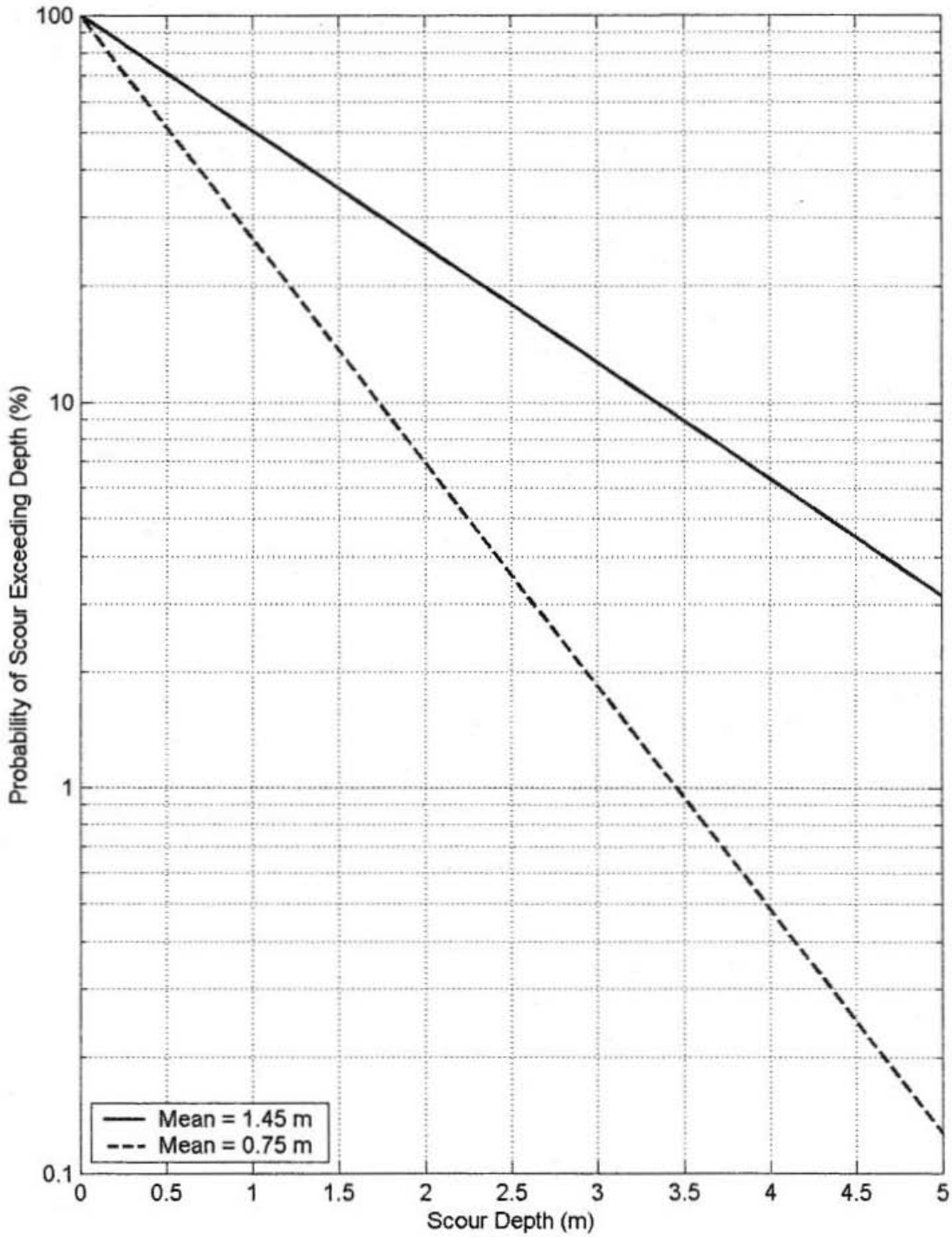

Figure 80 Comparison of exponential scour depth distributions (present study: mean = 0.75 m, Petro-Canada (1983) study: mean = 1.45 m)

7 RISK ANALYSIS

7.1 Introduction

The pipeline risk analysis can be broken down into three steps: (1) calculation of the rate at which scours are formed per unit area of seabed, (2) evaluation of the resulting number of scours that cross over the pipeline, and (3) determining the proportion of scours crossing the pipeline that cause damage. For the risk analysis, the pipelines were broken down into 0.5 km segments and the risk was evaluated for each segment, with the total risk being the sum of the risks for the segments.

7.2 Analysis Procedure for Scour Rate

For each pipeline segment, the grounding rate was calculated from the areal density of icebergs, the mean iceberg drift speed, the distribution of iceberg drift directions, the magnitude and direction of the seabed slope, and the proportion of the iceberg keels in a 1 m increment above the seabed (which was a function of the water depth and the iceberg draft distribution). Where insufficient iceberg drift track information existed to determine the distribution of drift direction, a uniform distribution was assumed. The calculated grounding rate was assumed to be equal to the scour rate, which has been shown to be a reasonable assumption using Grand Banks data.

7.3 Analysis Procedure for Pipeline Crossing Frequency

The frequency of scours passing over each pipeline segment was determined from the scour rate calculated for each segment, the length of the pipeline segment, and the mean

scour length. Since scour orientation was unknown for a large proportion of the pipeline routes, pipeline failure rates were based on a uniform distribution of scour orientation.

7.4 Pipeline Failure Criteria

Once the frequency at which iceberg scours occur over the various pipeline segments was been established, the pipeline failure rate per segment was determined by multiplying the scour crossing frequency by the proportion of scours that penetrate deep enough into the seabed to cause damage to the pipeline. The scour depth required for pipeline damage has previously been assessed using pipeline/iceberg contact or an analysis of the effect sub-scour soil deformations.

7.4.1 Iceberg Keel/Pipeline Contact

The contact criterion for pipeline damage requires that the scouring iceberg keel directly contacts the pipeline. This was the same criterion used during the original Petro-Canada (1983) analysis and was typical of many of the earlier studies addressing pipeline burial depths (Marcellus and Morrison, 1986). The probability of this event is determined directly from the scour depth distribution. For the base case presented here, the probability an exponential distribution with a mean of 0.75 m (mean scour depth) exceeding 2.5 m (pipeline cover) is 3.6%. This value is very sensitive to the mean scour depth. For example, mean scour depths of 1.45 m and 0.5 m give probabilities of 17.8% and 0.7%, respectively of exceeding 2.5 m.

7.4.2 Scour Depth Plus Sub-Scour Allowance

PRISE (Pressure Ridge Ice Scour Experiment) was used to establish soil reaction forces and soil deformations beneath scours (Clark et al., 1998; Woodworth-Lynas et al., 1996). This work was used to develop and calibrate a finite element model to determine the response of a pipeline below a scouring iceberg or ice ridge keel (Kenny et al., 2000). This model has been used to determine appropriate sub-scour pipeline clearances for risk analyses of pipelines on the Grand Banks. For the White Rose pipeline risk analysis (C-CORE, 2001a), it was possible to meet the target safety levels by considering scour depths only up 0.5 m depth. For scours up to this depth it was determined that an iceberg keel/pipeline crown clearance of 0.25 m was sufficient to protect the pipe from damage due to sub-scour deformations. For longer gas export pipelines (C-CORE, 2000), where the total cumulative risk is longer and deeper scours must be considered to govern pipeline burial depths, a more conservative iceberg keel/pipeline crown clearance equal to the scour depth was used. The White Rose analysis was based on a series of finite element analyses using specific pipeline and soil parameters, while the export pipeline analysis considered a more general case. Given the lack of a detailed finite element analyses for the Bjarni pipelines, the more conservative 1 gouge depth clearance was adopted as an approximation. Table 28 compares the failure criteria used with that originally used by Petro-Canada (1983).

Table 28 Pipeline Failure Criteria used for Bjarni Pipeline Risk Studies

Study	Pipeline Failure Criteria
Petro-Canada (1983)	Direct contact between iceberg keel and pipeline
This Study	Clearance between scouring iceberg keel and pipeline crown less than one scour depth

7.5 Results

7.5.1 Preliminary Results

Initially, it was assumed that the pipelines would be trenched along the entire route in sediment to achieve a uniform cover depth of 2.5 m. This was the burial depth assumed in the initial Bjarni study (Petro-Canada, 1983). Figure 81 shows the water depth profile for the Bjarni pipeline and the annual scour crossing rate calculated per kilometer of pipeline. The total annual number of pipeline crossings is 5.3, which equates to 1 pipeline failure per year, assuming a 1 scour depth pipeline/iceberg keel clearance, or 1 every 5 years using the direct iceberg keel/pipeline contact criterion. As shown in Figure 81, a substantial portion of the iceberg scour risk for the pipelines is accrued during the shore approach portion of the pipeline route just before entering the canyon where pipelines are protected from iceberg scour. This portion of the route, approximately 3 km long, is on a steep slope (≈7%) in relatively shallow water (50-120 m). The combination of steep slope and the higher proportion of iceberg keels in this water depth range accounts for the high failure rates along this portion of pipeline. However, as shown in Figure 82, this section of the route is rock, with no soil cover (Petro-Canada, 1983). This was not considered in the Petro-Canada (1983) iceberg risk analysis, where a 2.5 m cover depth was also assumed for this section of pipeline. Since rock is much stronger than ice, iceberg keels contacting the seabed will not penetrate the surface. If the pipeline can be placed below the surface of the rock, the threat of iceberg scour is eliminated. This could be accomplished using blasting or specialized trenching equipment. Subsea power conduits have been trenched 7.5 m into granite (http://www.rocksaw.net/subsea.html).

Any further iceberg scour risk analysis assumes that this 3 km portion of the route is trenched into rock.

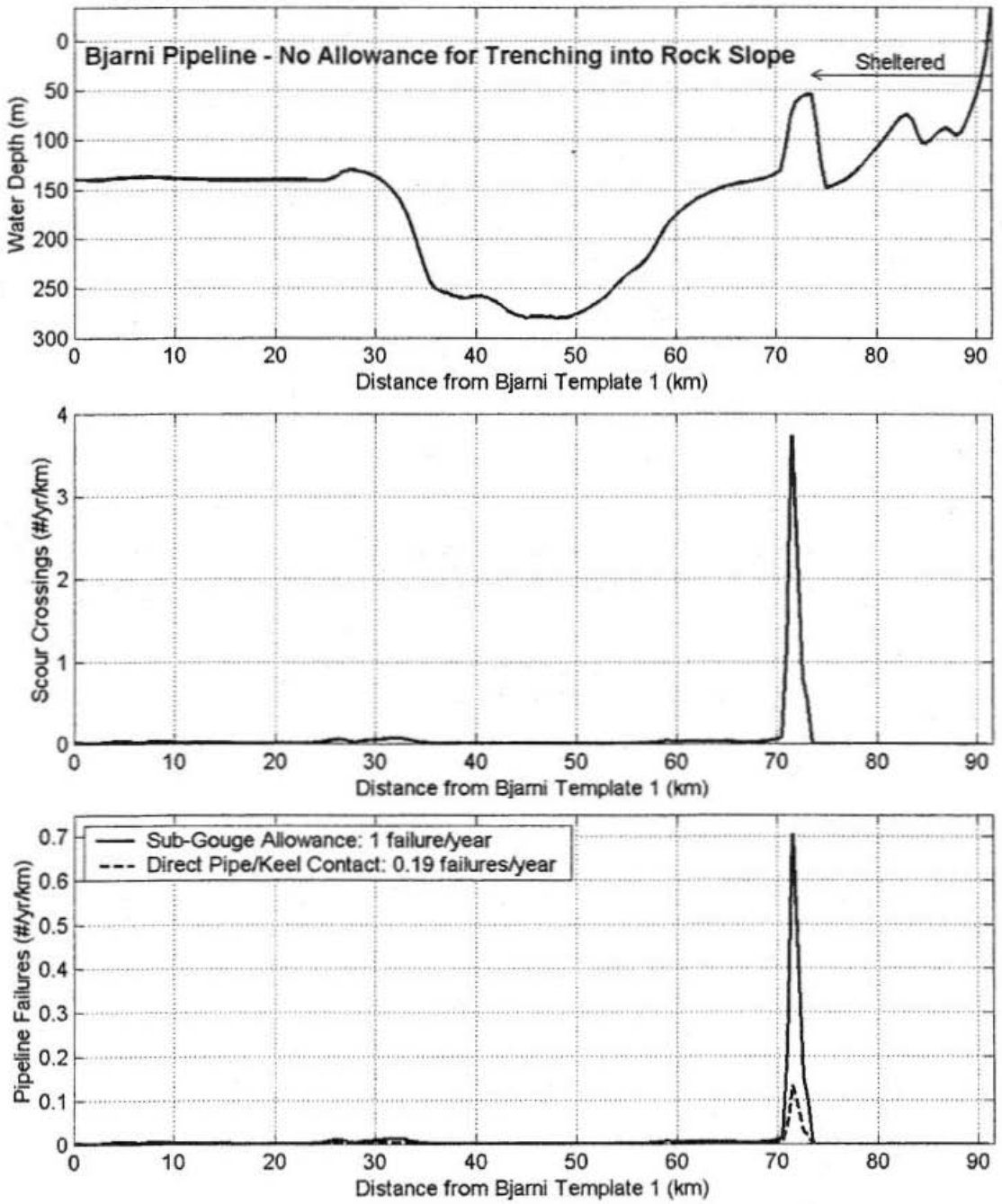

Figure 81 Preliminary risk analysis for Bjarni pipeline

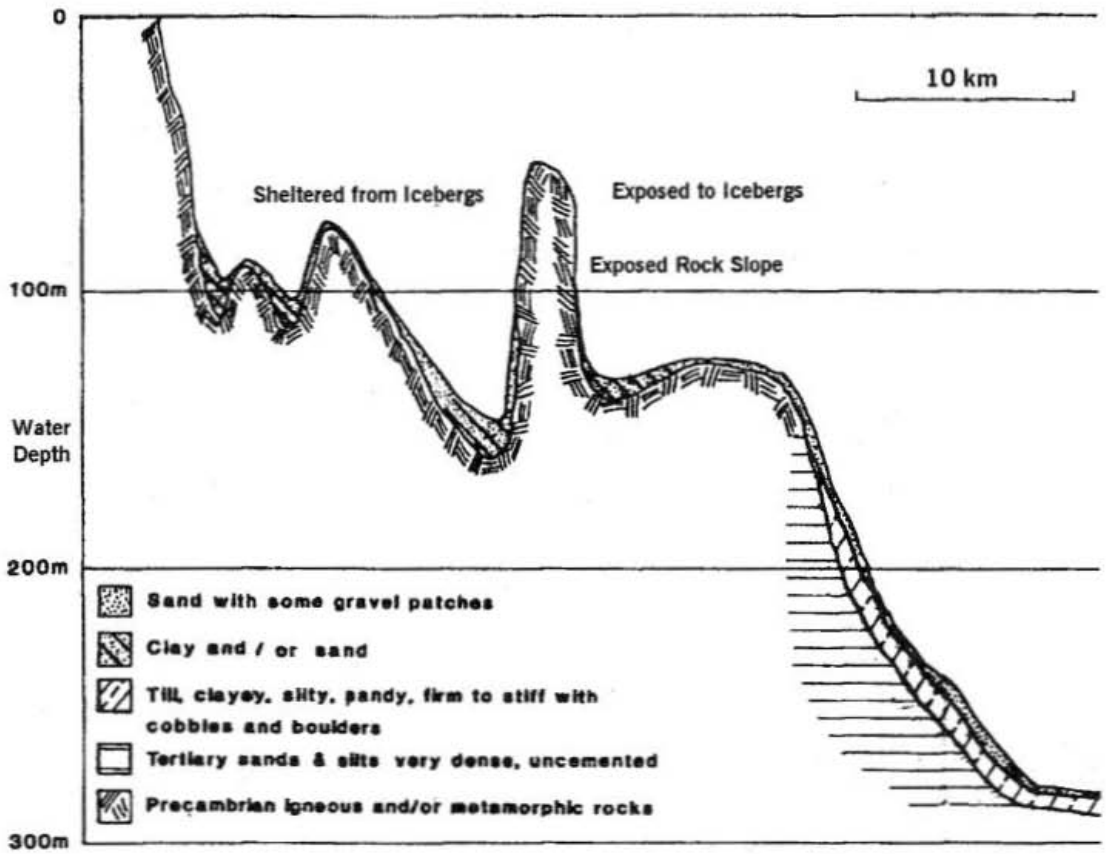

Figure 82 Geological cross-section of shore approach showing exposed rock slope requiring trenching into rock (after Petro-Canada, 1983)

7.5.2 Results

Figure 83 to Figure 85 show the results for the three pipelines. Each figure indicates the water depth along the pipeline route, the iceberg scour crossing rate per kilometer of pipe and the pipeline failure rate.

Table 29 compares the total annual number of iceberg scours crossing each of the pipelines with rates determined from the Petro-Canada (1983) risk analysis. The results from this analysis are approximately 20 times lower than the original analysis. The total pipeline crossings for the Pigging and North Bjarni pipelines are higher than for the Bjarni pipeline due to steeper seabed slopes. The original risk analysis (Petro-Canada, 1983) did not consider seabed slope and the difference in crossings rates between the various routes was essentially a function of total route length and water depth.

Table 29 Total Pipeline Crossings Compared to Results from Petro-Canada (1983) Study

Pipeline Route	Annual Pipeline Scour Crossings	
	This Analysis	Petro-Canada (1983)
Bjarni	1.00	25.78
Pigging	1.55	26.24
North Bjarni	1.20	20.54

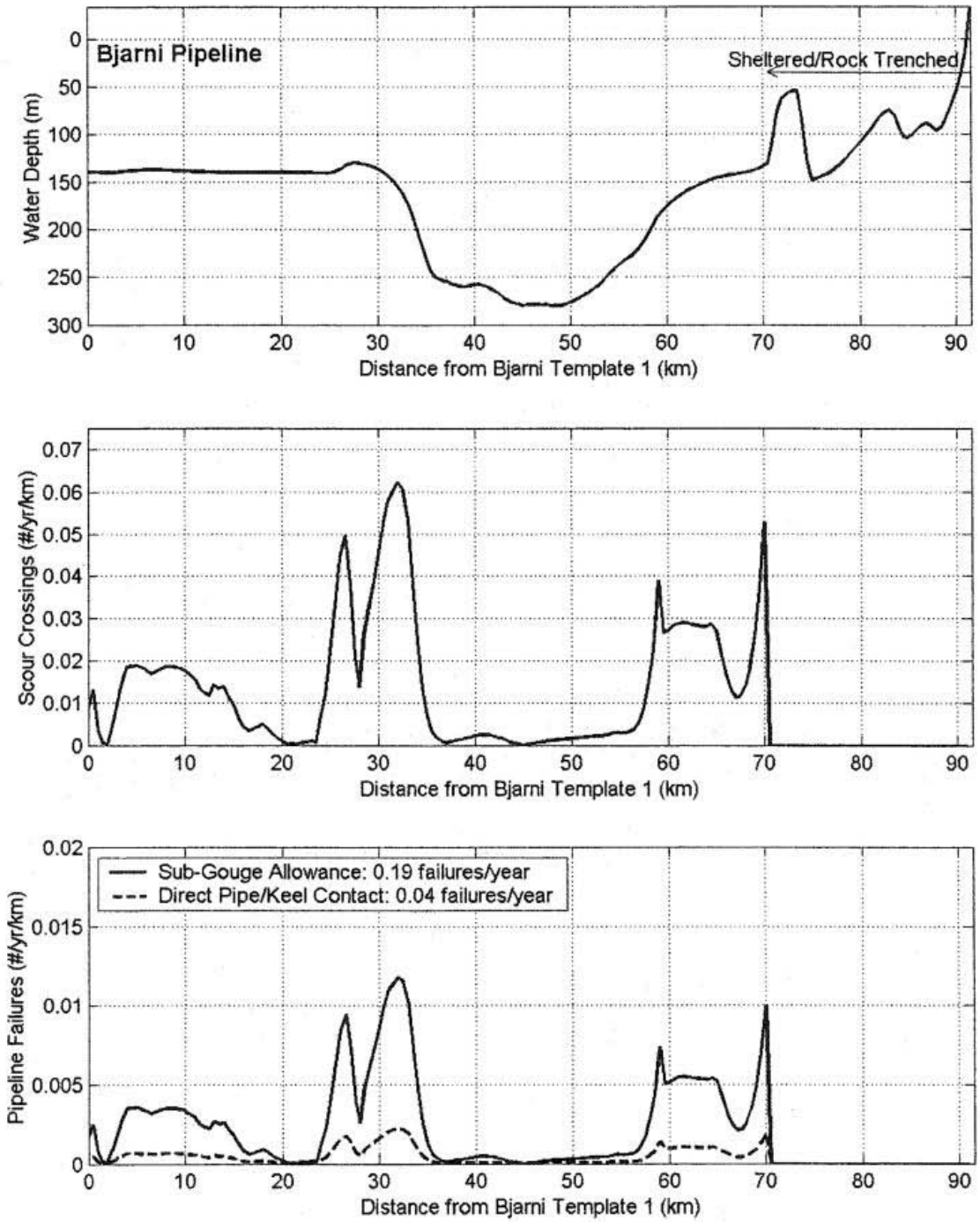

Figure 83 Risk analysis results for Bjarni Pipeline (2.5 m cover depth, 0.75 m mean scour depth)

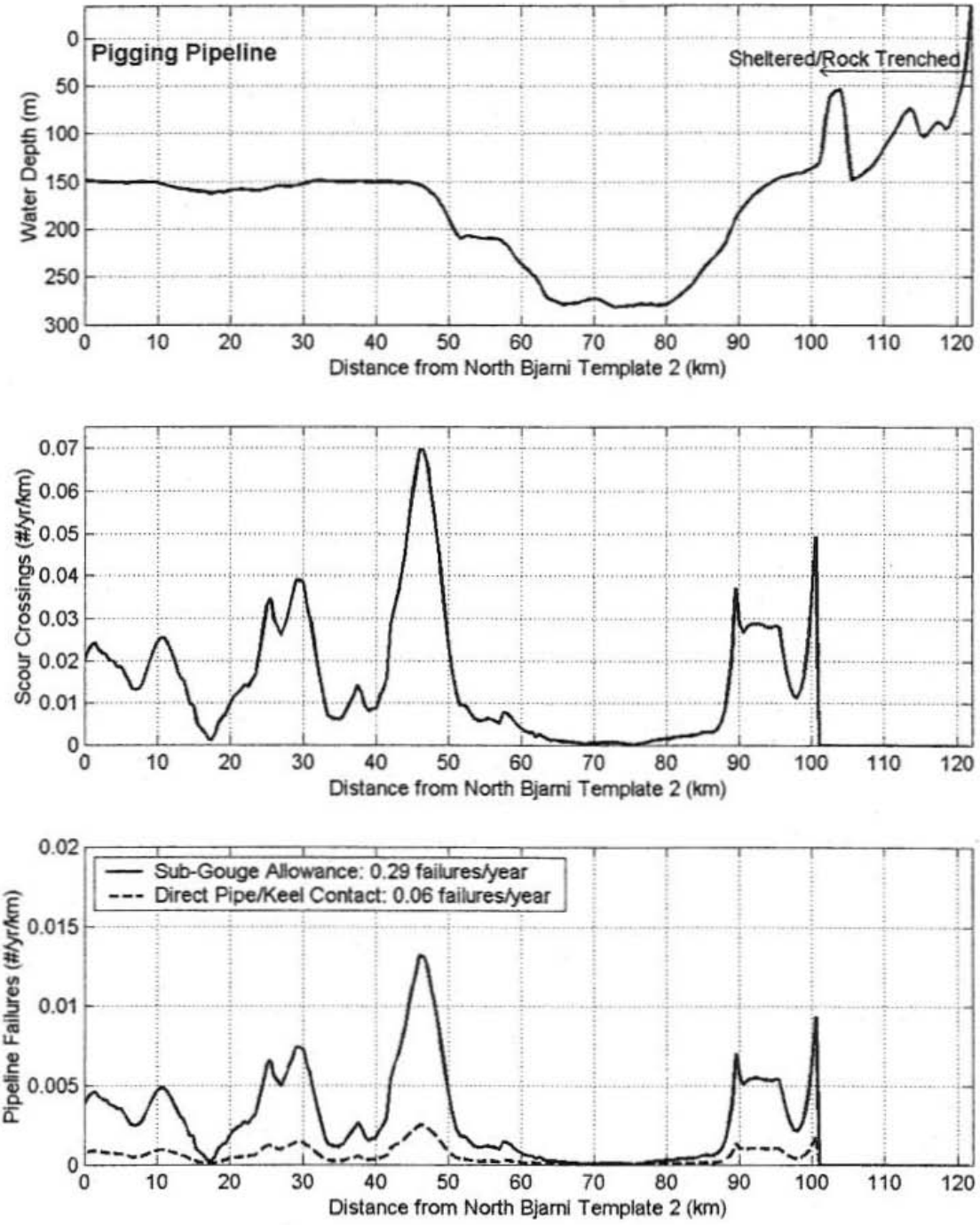

Figure 84 Risk analysis results for Pigging Pipeline (2.5 m cover depth, 0.75 m mean scour depth)

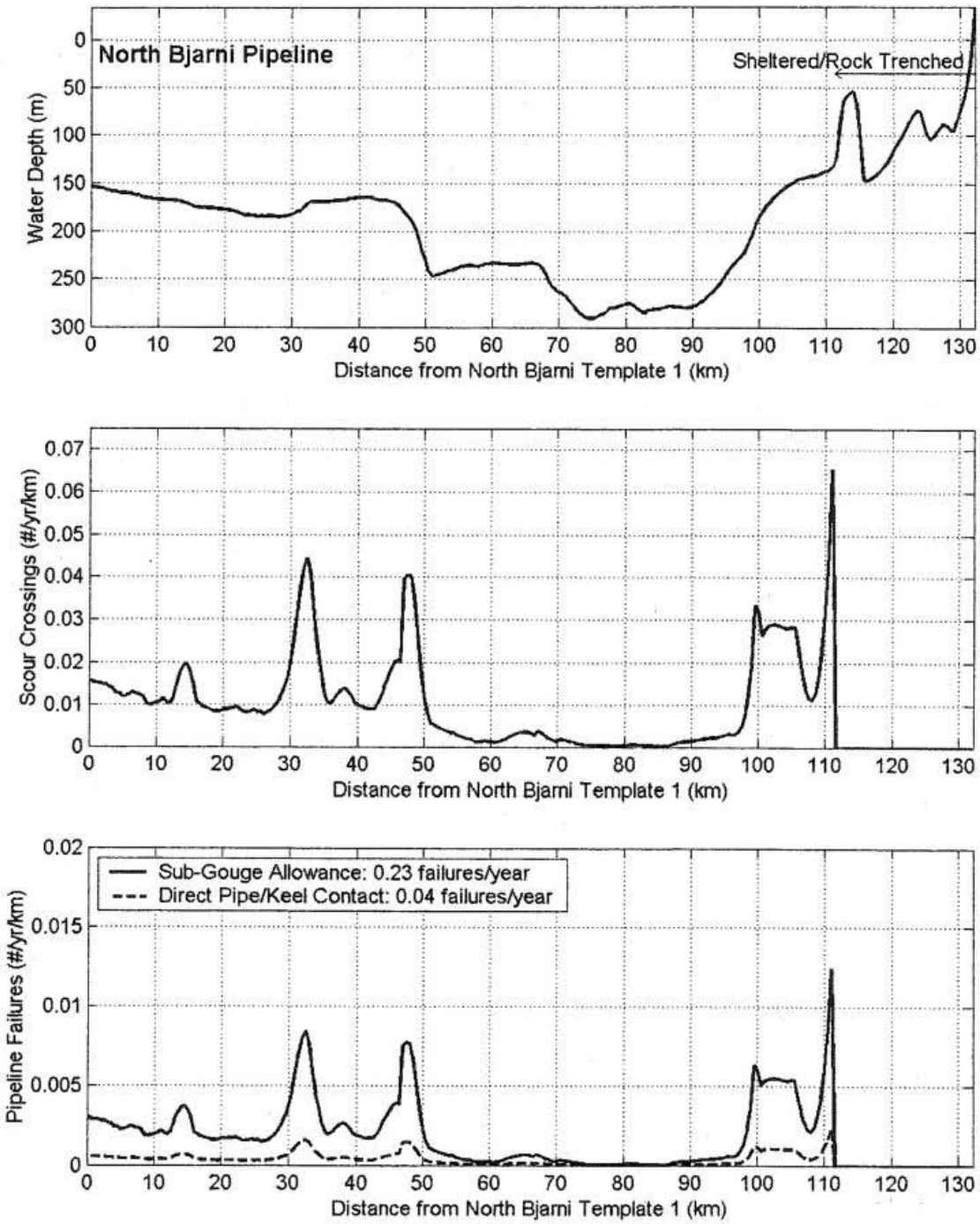

Figure 85 Risk analysis results for North Bjarni Pipeline (2.5 m cover depth, 0.75 m mean scour depth)

Table 30 compares the annual failure rates from the present analysis with those from the Petro-Canada (1983) analysis for the various pipeline routes. The failure rates predicted from this analysis are 20 to 100 times lower to those from the Petro-Canada (1983) analysis, depending on the criterion used for failure. The contact criterion has been presented primarily for comparison with the original analysis. While the 1 scour depth iceberg keel/pipeline crown clearance criteria is conservative, the use of a direct iceberg keel/pipeline contact criteria for pipeline failure would not now be considered an acceptable basis for determining pipeline burial depths. If a detailed finite analysis of pipeline response were performed and combined with a gouge geometry distribution, the failure rates would likely be lower than those predicted using the 1 gouge depth clearance criterion.

Table 30 Annual Pipeline Failure Rates Compared to Results from Petro-Canada (1983) Study (2.5m cover above crown of pipe)

Pipeline Route	This Analysis		Petro-Canada (1983) (Direct Contact)
	Sub-gouge Clearance Allowance Criterion	Direct Pipeline Contact Criterion	
Bjarni	0.19	0.04	4.59
Pigging	0.29	0.06	4.68
North Bjarni	0.23	0.04	3.66

It can be seen in Figure 83 to Figure 85 that the majority of risk is associated with steeper slopes in the shallower portions of the route. Detailed bathymetry could be used to optimize the pipeline route by avoiding steep slopes (except when necessary to get into deeper water).

Figure 86 shows the sensitivity of the results to the mean scour depth. Failure rates for each of the pipelines decrease significantly with a decrease in mean scour depth. It is likely that a high-quality seabed survey would result in decreased mean scour depths. A constant cover depth of 2.5 m and the 1 gouge depth clearance requirement was used to generate these curves. Using a mean scour depth of 0.5 m (a value that could be used for conservative risk calculations for the Grand Banks) more than doubles the mean time between pipeline failures compared to those obtained using a mean scour depth of 0.75 m. The upper range of the mean scour depth considered corresponds to the value used by Petro-Canada (1983).

Figure 87 shows the effect of varying cover depth. The results shown are for the Bjarni pipeline and used the 1 scour depth clearance failure criterion. Varying the mean cover depth has a more pronounced effect as the mean gouge depth is decreased. The maximum cover depth considered (4m) corresponds to the upper limit of mechanical trenching systems (i.e. Rocksaw). Selectively trenching certain portions of the pipeline deeper (if technically feasible) where the risk is higher could be used to reduce overall risk. The additional cost associated with trenching certain portions of the pipeline deeper could be recovered by reducing cover depths where the risk is low (i.e. in the deeper portions of the marginal trough). This could also be treated as an optimization exercise.

It should be noted that pits were not addressed as part of the risk analysis. There are insufficient data, particularly depth data, to perform any reasonable assessment. The uncertainty associated with the classification of pit features is also an issue with regard to

the Labrador seabed records. For the White Rose pipeline risk study (C-CORE, 2001a) pits accounted for approximately 10% of total risk. It is assumed that a similar relationship would hold here.

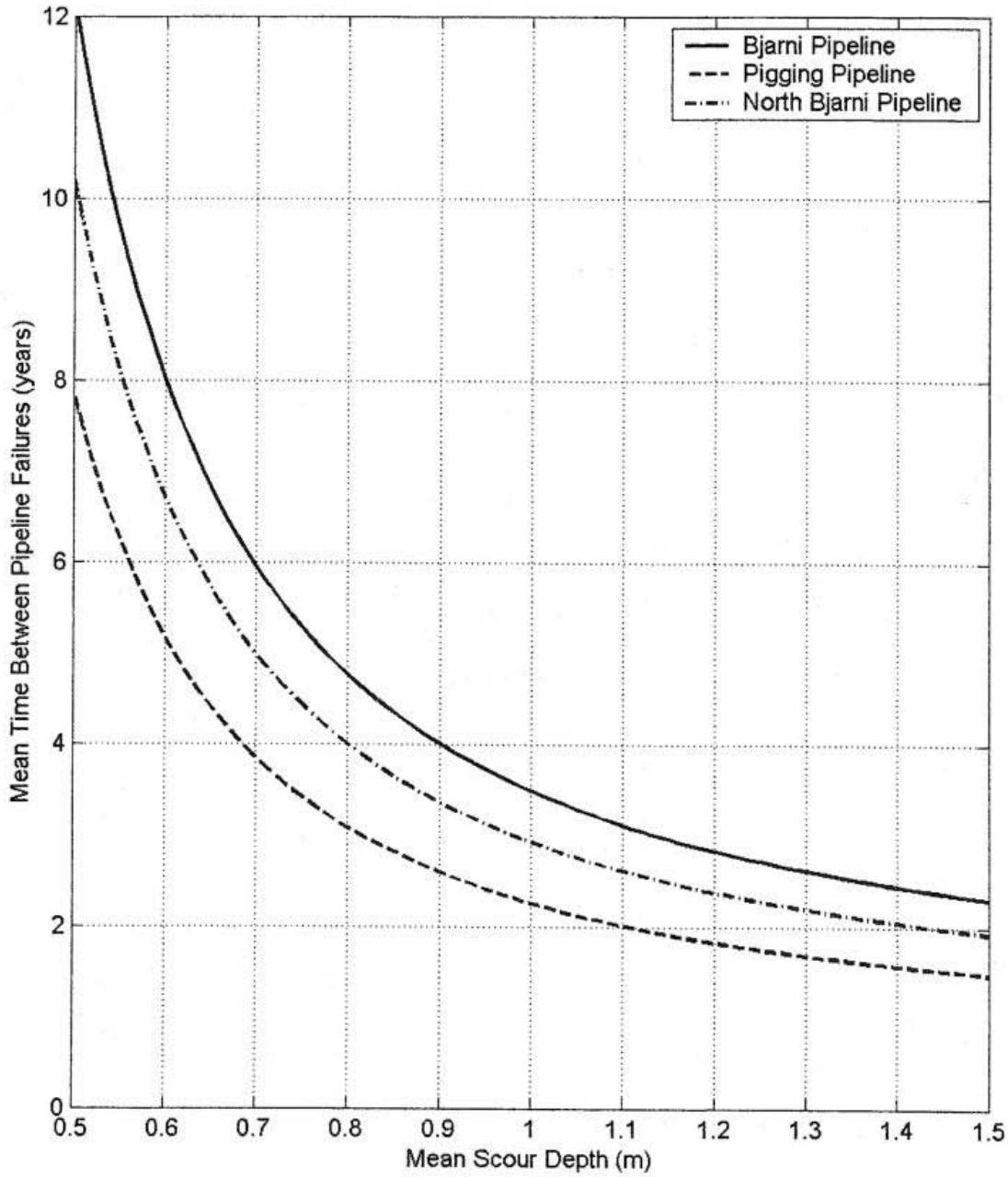

Figure 86 Mean time between pipeline failures as a function of mean scour depth (exponential distribution) using 2.5 m cover depth and 1 scour depth clearance allowance

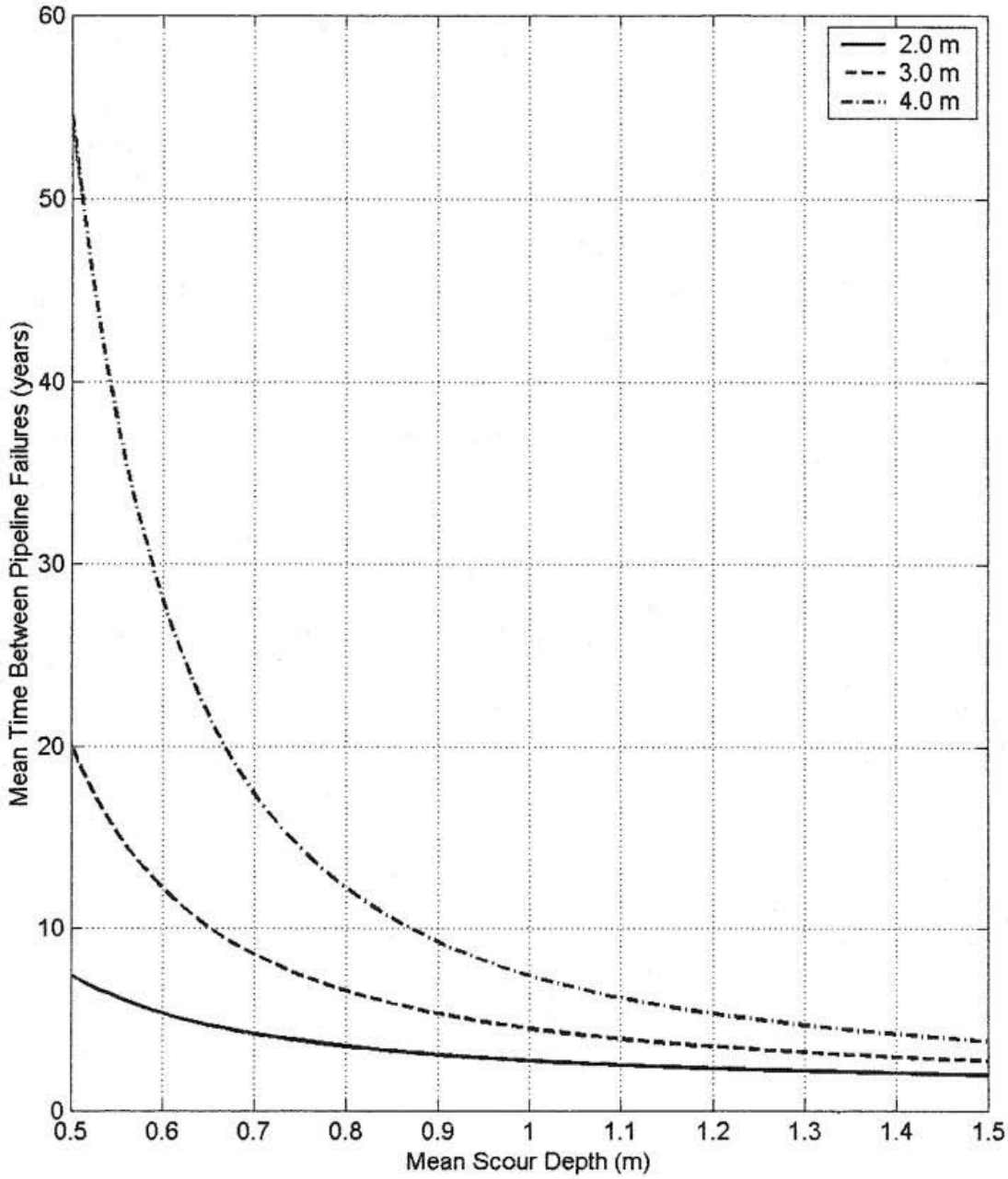

Figure 87 Mean time between failures for Bjarni pipeline a function of mean scour depth (exponential distribution) using a range of cover depths and 1 scour depth clearance allowance

8 SUMMARY, CONCLUSIONS AND RECOMMENDATIONS

8.1 Summary

The analysis presented in this thesis was conducted to assess the risk of iceberg scour damage for gas pipelines on the Labrador Shelf. A pipeline network proposed for transporting gas from known reserves on the Makkovik Bank to Cape Harrison (Petro-Canada, 1983) was assumed for the analysis. The approach used for the original iceberg risk analysis was reviewed and the results were presented. A model was developed to estimate iceberg grounding rates on the seabed. The model was tested and verified using data from the Grand Banks, where iceberg parameters are well-established and iceberg scour rates have been determined for a number of sites. The relationship between iceberg grounding rates and pipeline scour crossing and failure rates was presented. Data sources for risk analysis parameters for the Makkovik Bank region were reviewed and analyzed and appropriate input parameters for the risk analysis were established. Pipeline failure rates were determined and compared to those obtained from the original analysis (Petro-Canada, 1983). Pipeline failure rates were determined using a direct pipeline/iceberg keel contact criterion, as in the original analysis, as well as a more stringent 1-scour depth clearance requirement between the iceberg keel and the pipeline crown. The effects of burial depth and mean scour depth on failure rates were considered.

8.2 Conclusions

8.2.1 Grounding Model

The grounding model was found to produce reasonable estimates of iceberg scour rates when applied to sites on the Grand Banks where scour rates have been established from seabed records. Grounding rates were calculated for the Hibernia and White Rose sites using iceberg density, drift speed and drift direction distribution, iceberg draft distribution, and seabed slope and orientation. The model predicted grounding rates of 8×10^{-4} groundings/km^2/year for Hibernia and 7×10^{-4} groundings/km^2/year for White Rose, compared with scour rates of 4×10^{-4} scours/km^2/year and 1×10^{-3} scours/km^2/year determined from seabed surveys for Hibernia and White Rose, respectively. Due to the uncertainties associated with deriving scour rates from seabed records, a conservative approach was taken and the grounding rate predicted by the grounding model was assumed equal to the scour rate.

8.2.2 Iceberg Drift Velocity

Iceberg drift speeds and orientations were calculated for the Makkovik Bank region from iceberg trajectory data collected during drilling operations. The mean drift speed from these data was 0.24 m/s, which was lower than the 0.34 m/s value typical of the White Rose/Hibernia area.

8.2.3 Iceberg Size and Draft Distribution

Iceberg waterline length observations from a variety of sources in the vicinity of, or on, the Makkovik Bank were compared and considerable variation was observed between the

various data sets. It was determined that the iceberg waterline length distribution used for the Grand Banks (exponential with a mean of 59 m) matched the distribution observed during International Ice Patrol aerial surveys, exceeded two other data sets obtained during detailed aerial surveys but was less than that observed during iceberg towing operations on the Makkovik Bank (although the latter is justifiably considered to be biased towards larger icebergs). Therefore, the iceberg waterline length distribution used on the Grand Banks was used to generate the iceberg keel draft distribution for the risk analysis.

8.2.4 Iceberg Frequency

Iceberg frequency data for the Makkovik Bank region were reviewed. A number of International Ice Patrol aerial surveys conducted during the 1960's provided the best coverage for the region. However, since the 1960's had relatively low iceberg frequencies it was considered appropriate to apply a correction factor to reflect recent iceberg numbers. Limited data for the region from the Canadian Ice Service were consistent with those derived by the IIP. Given the uncertainty associated with iceberg density values in the region, a conservative average annual density of 0.01 icebergs/km^2 was adopted for use in the risk analysis.

8.2.5 Iceberg Scour Plan Dimensions

Iceberg scour plan dimensions (length and width) were analyzed from mosaics derived from seabed surveys conducted on the Makkovik Bank and comparisons were made to data from the Grand Banks. The mean scour width on the Makkovik Bank was observed

to be 20 m, compared to a mean scour width of 25 m for the Grand Banks. Establishing the mean scour length was complicated by the truncation of scour by the edges of the mosaics. However, an analysis of scour records from a large mosaic from the Bjarni wellsite indicates a mean scour length of 600 m, which agrees very well with estimates of mean scour length on the Grand Banks.

8.2.6 Iceberg Scour Depth Distribution

Determining the scour depth distribution for the risk analysis required the assessment of the effect of the resolution of the data from the original surveys. The survey used as the basis for the original pipeline risk analysis, for example, reported almost no scour depths less than 1 m due to limitations in the resolution in the depth sounder data. Corrected scour depth distributions were determined from the available data by fitting exponential distribution to the truncated data. An alternate approach was also used that compared the number of reported scour depth measurements in the track line data with the number of scours observed to cross the ship's tracks in the mosaics. The corrected scour depths were determined using the various data sets and approaches were averaged, and an additional factor to account for sediment infilling was applied. A mean scour depth of 0.75 m was obtained and used for the risk analysis. This is substantially lower than the 1.45 m mean scour depth used in the original Petro-Canada (1983) study. The 0.75 m value is still is still significantly higher than the various estimates of mean scour depth that have been reported for the Grand Banks (0.34 m to 0.5 m). Detailed seabed surveys on the Makkovik Bank would very likely indicate shallower scour depths those used in this analysis.

8.2.7 Bathymetric Considerations

Bathymetric data for the study region were analyzed, and seabed slope and orientation were determined. In general, seabed slopes are steeper on the Makkovik Bank than on the Grand Banks, and some steep slopes (>2%) are encountered along the pipeline routes. A short section of the route on the shore approach is exposed rock and requires trenching or blasting into the rock to shield the pipelines from iceberg keels.

8.2.8 Pipeline Failure Rates

The failure rates for the various pipelines determined from the risk analysis range depend on the criteria used to define pipeline failure. A constant cover depth of 2.5 m above the crown of the pipeline was used for the analysis. If it is assumed that pipeline failure occurs when an iceberg scours deeper than half the cover depth, failure rates vary from 1 every 3.5 years to 5.3 years for the three pipelines. If it is assumed that pipeline failure occurs when an iceberg scour exceeds the cover depth and direct contact occurs between the iceberg and the pipeline, failure rates vary from 18 to 28 years. A risk analysis based on detailed finite element modeling of soil/pipeline interaction below the scouring icebergs would yield some intermediate value. Deeper cover depths and lower mean scour depths would increase the mean time between pipeline failures. The failure rates predicted from this risk analysis are much lower than those from the original study that predicted more than three failures per year for each of the pipelines at a cover depth of 2.5 m using the direct iceberg/pipeline contact failure criterion.

8.3 Recommendations

The recommendations have been broken down according to issues that can be addressed by additional research and analysis, by the collection of additional data, and by the consideration of alternate development and operation alternatives for the proposed pipeline network.

8.3.1 Research and Analysis and Modelling

A finite element analysis using specific pipeline and soil properties would allow the strains developed in the pipe during scour events to be more accurately defined. The results of the finite element analysis could be combined with a scour width/depth distribution and pipeline scour crossing frequencies to obtain pipeline failure probabilities.

A re-analysis of the original DIGS data, archived at the Bedford Institute of Oceanography, would be very useful. This would allow the frequency of sub-resolution scours to be assessed, allowing a better assessment of scour depth. The scour data could be compiled into a database, similar to the Grand Banks Scour Catalog, which would form the basis for a new scour database for the Labrador Shelf. If any repeat surveys were to be performed for any of these sites, this would be a valuable resource.

The grounding model does not account for the effects of bathymetric shielding. A detailed iceberg drift model using environmental data specific to the Makkovik bank

region could be combined with bathymetric data and iceberg characteristics to model iceberg grounding events.

Additional physical modelling of iceberg scour processes and pipeline response would allow the finite element model used to predict pipeline response to be further refined. Centrifuge modeling of iceberg scour has been used to define soil deformations below the scour, but additional test data would be useful. Additional centrifuge scour modeling incorporating an instrumented model pipeline would be very useful; it would seem reasonable the presence of the pipeline would be an additional factor influencing soil deformations. Ideally, full scale modeling of a scour event over an instrumented pipeline could be performed.

8.3.2 Data Collection

A better definition of iceberg scour depth distribution would have a significant impact on the risk of pipeline failure. The collection of high-quality seabed survey data in the study region is strongly recommended. These data also could be compared with previous surveys to determine scour rates if the same areas were surveyed. The shore approach region should also be surveyed to determine scour parameter distributions and as a check on the effectiveness of the canyon on the shore approach for shielding the pipelines from the effects of iceberg scouring.

Ongoing monitoring of icebergs in the study area is recommended. Iceberg frequency is poorly defined for the study area. Present data are limited and there is currently very

limited monitoring during the peak of the iceberg season. Data could be collected using aerial surveys, satellites or shore-based radar. Shore-based radar would also be useful for documenting iceberg drift velocities and potential grounding events. Detailed aerial surveys would also provide a better assessment of the iceberg size distribution.

8.3.3 Operational and Development Alternatives

The elimination of the pigging pipeline would result in significant capital cost savings. The possibility of alternate technologies regarding multi-phase flow enhancement could potentially eliminate the necessity of pigging. Alternatively, instead of using a pigging pipeline, an AUV (Autonomous Underwater Vehicle) could be used to ferry pigging spheres out to the site. The AUV could also be used to perform regular surveys of the pipeline route to assess the formation of new scours or to perform reconnaissance of icebergs to determine if an iceberg has a draft deep enough to pose a risk to subsea installations.

The use of alternate landfalls could be assessed. The flow of iceberg broadens below Cape Harrison, causing a reduction in iceberg density. If the concurrent development of the Gudrid site were to be considered, a more southerly landfall could be used. Deep water in the marginal trough would reduce or eliminate trenching requirements and a subsea canyon at approximately 54°N latitude could be used for the final shore approach. This canyon is oriented to the south-east, further enhancing its ability to shield pipelines from iceberg scouring.

9 REFERENCES

Abdelnour, R., Lapp, D., Haider, S., Shinde, S.B., and Wright, B. (1981). Model tests of sea bottom scouring. The Sixth International Conference on Port and Ocean Engineering under Arctic Conditions, Quebec, July 27-31, Vol 2, pp. 688-705.

Amos, C.L. and Barrie, J.V. (1982). The frequency of ice scouring on the Northeastern Grand Banks of Newfoundland using the interrelationship of scours and bedform migration. Proceedings, NRC Workshop on Ice Scouring, Montebello, Quebec, February, 3 p.

Anderson, C. (1971). The Flow of Icebergs Along the Canadian East Coast. Proceedings of the Canadian Seminar on Icebergs, Halifax, N.S., Dec. 6-7, 1971, pp. 52-61.

Astafyev, V.N., Surkov, G.A., and Truskov, P.A. (1997). Methods for determining optimal subsea pipelines burial cross section. Translation of Chapter 8 of: Ridges and Stamukhas of the Okhotsk Sea. V.V. Panov (ed.). Progress-Pagoda, St. Petersburg.

d'Apollonia, S.J. and Lewis, C.F.M. (1986). Numerical model for calculating spatial distribution and mean frequency of iceberg grounding events. *In* Ice Scour and Seabed Engineering. Lewis, C.F.M., Parrott, D.R., Simpkin, P.G., and Buckley, J.T. (eds). Environmental Studies Revolving Funds Report No. 049. Ottawa, pp. 287-292.

Allan, D. (1986). Risk assessment for iceberg-scour damage: Labrador Sea and Grand Banks. *In* Ice Scour and Seabed Engineering. Lewis, C.F.M., Parrott, D.R., Simpkin, P.G., and Buckley, J.T. (eds). Environmental Studies Revolving Funds Report No. 049. Ottawa, pp. 240-248.

Banke, E. (1989a). Case Histories of the Groundings of Icebergs 001 and 004 During March, 1989 on the Grand Banks. Submitted to the Atlantic Geoscience Centre, Bedford Institute of Oceanography, Dartmouth, Nova Scotia, 62 pp.

Banke, E. (1989b). Recent Iceberg Groundings on the Grand Banks of Newfoundland. Geological Survey of Canada, Open File 2528.

Ball, P., Gaskill, H.S., and Lopez, R.J. (1981). Iceberg Motion: An Analysis of Two Data Sets Collected at Drill Sites in the Labrador Sea. C-CORE Report No. 81-2, April, 121 pp.

Barrie, J.V. (1980). Iceberg-seabed interaction (northern Labrador Sea). Annals of Glaciology. (1), pp 71-76.

Barrie, J.V., Lynas, C.M.T., and Gidney, G. (1981). Iceberg Grounding Review from Well-Site Observations. Geological Survey of Canada, Open File 880, 38 p.

Barrie, J.V., Collins, W.T., Clark, J.I., Lewis, C.F.M., and Parrot, D.R. (1986). Submersible observations and origin of an iceberg pit on the Grand Banks of Newfoundland. Current Research, Part A, Geological Survey of Canada, Paper 86-1A, pp. 251-258.

Been, K., Palmer, A., and Comfort, G. (1990). Analysis of Subscour Stresses and Probability of Ice Scour-Induced Damage for Buried Submarine Pipelines: Volume 2, Deterministic Model of Ice-Soil-Pipe Interaction. Prepared for: Panel for Energy Research and Development (PERD); Canada Oil and Gas Lands Administration; Energy, Mines and Resources; Indian and Northern Affairs, 204p.

Canadian Seabed Research (2000). The 1999 Update of the Grand Banks Scour Catalog. Contract Report for the Geological Survey of Canada, Atlantic.

C-CORE (1998). Analysis of Pack Ice and Iceberg data from the 1997 CCGS *Henry Larson* Probe to Voisey's Bay. Contract Report prepared for Canadian Coast Guard, Fisheries and Oceans Canada, June, C-CORE Publication 98-C7.

C-CORE (1999). Pipeline Route Selection. C-CORE News, Vol. 24, No. 3, p. 7.

C-CORE (2000). Iceberg Risk and Routing Considerations for Grand Banks and Export Pipelines. Contract report for Pan-Maritime Energy Services Inc. on Behalf of the Department of Mines and Energy, Government of Newfoundland and Labrador, Report No.: 05-2008-00-P-3-005, C-CORE Report Number 00-C23, December.

C-CORE (2001a). Iceberg Risk to Pipelines at White Rose. Contract Report Prepared for Husky Oil Operations Ltd., C-CORE Report Number 00-C45.

C-CORE (2001b). Iceberg Scour Characteristics at White Rose. Contract Report Prepared for Husky Oil Operations Ltd., C-CORE Report Number 00-C44.

C-CORE (2001c). Integrated Ice Management R&D Initiative – Year 2000, Final Report. Contract Report for Chevron Canada Resources, Husky Oil Operations Limited, Mobil Oil Canada Properties, Norske Hydro Canada Oil & Gas Inc., Petro-Canada and Panel on Energy Research and Development. C-CORE Publication Number 00-C36, May, 2001.

C-CORE (2001d). Documentation of Iceberg Grounding Events from the 2000 Iceberg Season. Report Prepared for Geological Survey of Canada – Atlantic, C-CORE Contract Report 01-C10, June.

Chari, T.R. (1975). Some Geotechnical Aspects of Iceberg Grounding. Ph.D. Thesis, Memorial University of Newfoundland, St. John's, Newfoundland.

Clark J.I., Phillips R and Paulin M (1998) Ice scour research for the safe design of pipelines: 1975-1997. Proceedings of Ice Scour & Arctic Marine Pipelines

Workshop. 13th International Symposium on Okhotsk Sea & Sea Ice, Mombetsu, Japan.

CNOPB (2001). The Canada-Newfoundland Offshore Petroleum Board Annual Report 2000-2001. 36 pp.

CNSOPB (1997). Sable Offshore Energy Project: Development Plan Decision Report. prepared by the Canada-Nova Scotia Offshore Petroleum Board. 92 pp.

Crocker, G., English,G. and McKenna, R. (2000). Evaluation of Berg Bit Populations on the Grand Banks. Contract report submitted to the Institute for Marine Dynamics, National Research Council Canada, C-CORE Publication Number 00-C3.

Davidson, S.H., and Simms, A. (1997). Characterisation of Iceberg Pits on the Grand Banks of Newfoundland. Environmental Studies Research Funds Report No. 133, Calgary, 162 p.

Dunwoody, A.B. (1983). The design ice island for impact against an offshore structure. 1983 Offshore Technology Conference, Houston, paper 4550, vol. 2, pp. 325-330.

Dunwoody, A.B., Losch, J.A., and Been, K. (1984). Ice/berm interactions. Proceedings of the 16th Annual Offshore Technology Conference, Houston, Texas, May 7-9, pp 223-228

Ebbesmeyer, C.C., Okubo, A., and Helseth, J.M. (1980). Description of iceberg probability between Baffin Bay and the Grand Banks using a stochastic model. Deep-Sea Research, Vol. 27A, pp. 975-986.

El-Tahan, M., El-Tahan, H., Courage, D., and Mitten, P. (1985). Documentation of Iceberg Groundings. Environmental Studies Revolving Funds Report No. 007. Ottawa, 162 p.

FENCO (1975). An Analytical Study of Ice Scour on the Sea Bottom. Report for Arctic Petroleum Operators Association, APOA Project No. 69, 241 p.

Fillon, H.F., and Harmes, R.A. (1982). Northern Labrador Shelf glacial chronology and depositional environments. Canadian Journal of Earth Sciences, Vol. 19, No. 1 pp. 162-192

Fuglem, M., Jordaan, I. And Crocker, G. (1996). Iceberg-structure interaction probabilities for design. Canadian Journal of Civil Engineering, (23), pp. 231-241.

Gaskill, H., Nicks, L., and Ross, D. (1985). A non-deterministic model of populations of iceberg-scour depths. Cold Regions Science and Technology, 11:107-122.

Gaskill, H, and Lewis, C.F.M. (1988). On the spatial frequency of linear ice scours on the seabed. Cold Regions Science and Technology, (15), pp 107-130.

Geomarine Associates Ltd. (1976). Bjarni Wellsite Bathymetry and Iceberg Scours. Prepared for Eastcan Exploration Ltd. 137 p.

Geomarine Associates Ltd. (1980). Wellsite Survey Report, North Bjarni F-06, Makkovik Bank, Labrador, August 20 - August 25, 1980, Contract report prepared for the Labrador Group.

Geonautics Ltd. (1987). Design of an Iceberg Scour Repetitive Mapping Network for the Canadian East Coast. Environmental Studies Research Funds, Report No. 043, 45 pp.

Geonautics Ltd. (1989). Regional Ice Scour Data Base Studies. Environmental Studies Research Funds, Report No. 105, 168 pp.

Grass, J. (1986). Ice scour and ice-ridging studies in Lake Erie. *In* Ice Scour and Seabed Engineering. Lewis, C.F.M., Parrott, D.R., Simpkin, P.G., and Buckley, J.T. (eds). Environmental Studies Revolving Funds Report No. 049. Ottawa, pp. 29-30.

Green, H.P. (1984). Geotechnical Modelling of Iceberg-Seabed Interaction. M.Eng. Thesis. Memorial University of Newfoundland, 165 p.

Gustajtis, K.A. (1979). Iceberg Scouring on the Labrador Shelf, Saglek Bank. C-CORE Publication 79-13. 89 pp.

Gustajtis, K.A. (1979). Iceberg Population Distribution Study in the Labrador Sea. C-CORE Publication 79-8.

Hodgson, G.J. (1986). Design of a repetitive-mapping network for ice scour: east coast. *In* Ice Scour and Seabed Engineering. Lewis, C.F.M., Parrott, D.R., Simpkin, P.G., and Buckley, J.T. (eds). Environmental Studies Revolving Funds Report No. 049. Ottawa, pp. 287-292.

Hodgson, G.J., Lever, J.H., Woodworth-Lynas, C.M.T., and Lewis C.F.M. (editors). (1988). The Dynamics of Iceberg Grounding and Scouring (DIGS) Experiment and Repetitive Mapping of the Eastern Canadian Continental Shelf. Environmental Studies Research Funds Report No. 049. 315 p.

Hotzel, S.I., Miller, J.D. (1983). Icebergs: their physical dimensions and the presentation and application of measured data. Annals of Glaciology 4, pp 116-123.

Hynes, F. (1996). Centrifuge Modelling of Ice Scour in Sand. Masters Thesis, Memorial University of Newfoundland, St. John's, Newfoundland.

IIP (2001). How Many Icebergs Last Long Enough to Reach the Atlantic Shipping Lanes (South of 48 N)? http://www.uscg.mil/lantarea/iip/FAQ/faq7.html

Jordaan, I.J. (1983). Risk analysis with application to fixed structures in ice. Seminar/Workshop on Sea Ice Management, Memorial University of Newfoundland, November, paper #14.

Jordaan, I.J., Fuglem, M., Crocker, G., and Olsen, C. (1995). Canadian Offshore Design for Ice Environments, Volume 1, Environment and Routes, Prepared for Department of Industry, Trade and Technology, Canada-Newfoundland Offshore Development Fund, Government of Newfoundland and Labrador, September, 1995.

Jordaan, I., Press, D., and Milord, P. (1999). Iceberg Databases and Verification. Prepared for National Research Council Canada, Canadian Hydraulics Centre, March 1999.

Kenny, S., Phillips, R., McKenna, R.F., and Clark, J.I. (2000). Response of buried arctic marine pipelines to ice gouge events. International Conference on Offshore Mechanics & Arctic Engineering, New Orleans, February 2000, paper 00-5001.

King, L.H. (1976). Relict iceberg furrows on the Laurentian Channel and western Grand Banks. Can. J. Earth Sci., 13, pp. 1082-1092.

King, E.L., and Gillespie, R.T. (1986). Regional iceberg scour distribution and variability on the eastern Canadian continential shelf. *In* Ice Scour and Seabed Engineering. Lewis, C.F.M., Parrott, D.R., Simpkin, P.G., and Buckley, J.T. (eds). Environmental Studies Revolving Funds Report No. 049. Ottawa, pp. 172-181.

Kioka, S., Yasunaga, Y., Matuo, Y., Watanabe, Y., and Saeki, H. (2001). Medium-scale model tests on ice gouge. Proceedings of the 16th International Conference on Port and Ocean Engineering under Arctic Conditions (POAC'01), August 12-17, Ottawa, Ontario, pp. 1029-1038.

Kollmeyer, R.C. (1977). West Greenland glaciers: iceberg sources. Iceberg Utilization: Proceedings of the First International Conference. A.A. Husseiny (ed.), October 2-6, Ames, Iowa, pp. 25-28.

Lach, P.R. (1996). Centrifuge Modelling of Large Soil Deformation Due to Ice Scour. Ph.D. Thesis, Memorial University of Newfoundland, St. John's, Newfoundland.

Lewis, C.F.M. (1977). The frequency and magnitude of drift-ice groundings from ice-scour tracks in the Canadian Beaufort Sea. POAC 1977, pp. 568-579.

Lewis, C.F.M. and Parrott, D.R. (1987). Iceberg scour rate studies, Grand Banks of Newfoundland. *In* Current Research, Part A. Geological Survey of Canada, Paper 87-1A, pp. 825-833.

Lewis, C.F.M. and Blasco, S.M. (1990). Character and distribution of sea-ice and iceberg scours, *in* Proceedings of the Workshop on Ice Scouring and Design of Offshore Pipelines, Calgary, Alberta. Pp. 56-101.

MacLaren Marex Inc. (1980). Environmental Observations Offshore Labrador Summer 1979. February.

MacLaren Plansearch (1981). Ice and Environmental Surveillance, 1980. March.

MacLaren Plansearch (1982). Environmental Observations Labrador Shelf (June-October, 1981). February.

Marcellus R.W. and Morrison, T.B. (1986). Some recent studies relating to the determination of pipeline depths. *In* Ice Scour and Seabed Engineering. Lewis, C.F.M., Parrott, D.R., Simpkin, P.G., and Buckley, J.T. (eds). Environmental Studies Revolving Funds Report No. 049. Ottawa, pp. 295-303.

Marine Environmental Services Ltd. (1977). Wellsite Environmental Observations Offshore Labrador 1976, D.V. Pelican, Petrel and Zapata Ugland.

MEDS (1997). Canadian Offshore Oil and Gas Environmental Data. Marine Environmental Data Service, National Energy Board, March, 1997 (CD-ROM).

Miller, J.D. (1981). Extreme Iceberg Flux Estimates for the Labrador Coast. (L.E.E.A. – 1981-2). PEX Internal Memorandum.

Mudie P.J. (1986). Palynology as a method for dating iceberg scours. *In* Ice Scour and Seabed Engineering. Lewis, C.F.M., Parrott, D.R., Simpkin, P.G., and Buckley, J.T. (eds). Environmental Studies Revolving Funds Report No. 049. Ottawa, pp. 233-239.

Murphy, D.L., and Wright, G.F. (1989). Iceberg Movement Determined by Satellite Tracked Platforms. Annual Report of the International Ice Patrol Service in the North Atlantic, pp. 87-97.

Murphy, D.L., Viekman, B., and Channel, C. (1996). New gridded currents for the International Ice Patrol operations area. Proceedings: Oceans 96 MTS/IEEE, Fort Lauderdale, Florida, 23-26 September, pp. 613-618,

Murray, J.E. (1969). The drift, deterioration and distribution of icebergs in the North Atlantic Ocean. CIM Special Vol. 10, The Ice Seminar, pp. 3-18.

Myers, R., Sonnichsen, G.V. and Campbell, P. (1996). Terra Nova Development Studies 1995: Seafloor Repetitive Mapping Analysis. Prepared for Petro-Canada, 44p.

Nessim, M.A. (1986). Pilot Study to Examine Ice Scour Statistics for the Canadian Beaufort Continental Shelf. Contractor report submitted by Det Norske Veritas (Canada) Ltd. to the Geological Survey of Canada.

Noble, P.G. and Comfort, G. (1980). Damage to an underwater pipeline by ice ridges. Proceedings of a Workshop on Sea Ice Ridging and Pileup, 22-24 October , Calgary Alberta, pp. 248-284.

PAL (2000). 2000 Ice Season Database. Provincial Airlines.

Palmer, A. (1990). Design of marine pipelines in seabed vulnerable to ice scour. Workshop on Ice Scouring and Design of Offshore Pipelines, Calgary, Alberta, April 18-19, pp. 167-178.

Paulin, M.J. (1992). Physical Model Analysis of Iceberg Scour in Dry and Submerged Sand. M.Eng. Thesis, Memorial University of Newfoundland, St. John's, Newfoundland, 183 p.

PanCanadian Energy Corporation (2002). Deep Panuke Offshore Gas Development – Volume 1 (Project Summary). March.

PERD (1999). Compilation of Iceberg Shape and Geometry Data for the Grand Banks Region. Prepared by Canatec, ICL Isometrics, Coretec & Westmar for the National Research Council of Canada. PERD/CHC Report 9-80.

PERD (2000). Study of Iceberg Scour & Risk in the Grand Banks Region. Prepared by K.R. Croasdale & Associates, C-CORE, Canadian Seabed Research , Ballicater Consulting and Ian Jordaan and Associates for the National Research Council of Canada. PERD/CHC Report 31-26.

PERD (2001). Update and Quality Assurance of the PERD Grand Banks Iceberg Database. Prepared by Fleet Technology Limited for the National Research Council of Canada. PERD/CHC Report 20-59.

PERD (2002). Laboratory Experiments of Ice Scour Process. Prepared by Anne Barker and Garry Timco, Technical Report CHC-TR-004, PERD/CHC Report 31-28, March, 36p.

Petro-Canada (1983). Bjarni/North Bjarni Production Perspectives Study. Prepared by Petro-Canada Resources – Frontier Development Group for The Labrador Group of Companies. 10 volumes.

Pilkington, G.R. and Marcellus, R.W. (1981). Methods of determining pipeline trench depths in the Canadian Beaufort Sea. POAC 1981, pp. 674-687.

Pilkington, R. (1986). Estimating ice-scour frequency and the risk to buried pipelines. *In* Ice Scour and Seabed Engineering. Lewis, C.F.M., Parrott, D.R., Simpkin, P.G., and Buckley, J.T. (eds). Environmental Studies Revolving Funds Report No. 049. Ottawa, pp. 213-220.

Poorooshasb, F., Clark, J.I., and Woodworth-Lynas, C.M.T. (1989). Small scale modelling of iceberg scouring of the seabed. Proceedings of the 10th International Conference on Port and Ocean Engineering under Arctic Conditions, Lulea, Sweden, Vol. 1, pp. 133-145.

Sanderson, T.J.O. (1988). Ice Mechanics: Risks to Offshore Structures. Graham and Trotman Inc., Norwell, Massachusetts, 253p.

Schofield, A.N. (1980). Cambridge geotechnical centrifuge operations. Geotechnique, 30, No. 3, pp. 227-268.

Sheps, S., Gorman, J. and Hawkins, D. (1992). Offshore Labrador gas: a challenge for the future. NOIA Conference '92 Proceedings, pp. 185-205.

Simms, A. (1986). Multivariate Analysis of Iceberg Data Collected for the Labrador Shelf from 1973-1980. Masters Thesis, University of Calgary.

Surkov, G.A. (1995). Method for Determining the Optimum Burial Depth Profile for Subsea Pipeline Facilities in Freezing Seas. Dissertation for a degree of candidate of technical services, Sakhalin Research and Design Institute.

Walter, D.J. and Phillips, R. (1988). PRISE – Force Models for Drained and Undrained Steady State Scouring. Contract Report, C-CORE Publication 98-C33.

Todd, B.J., Lewis, C.F.M., and Rydall, P.J.C. (1988). Comparison of trends of iceberg scour marks with iceberg trajectories and evidence of paleocurrent trends on Saglek Bank, northern Labrador Shelf. Canadian Journal of Earth Sciences, 25(9), pp. 1374-1383.

Weaver, J.S., Johnson, B.M., and Thibeaux, J.F. (1988). A large scale model facility to study ice gouge-soil-pipeline interactions. Proceedings of the Seventh International Conference on Offshore Mechanics and Arctic Engineering, Houston, Texas, pp. 317-326.

Weeks, W.F., Barnes, P.W., Rearic, D.M. and Reimnitz, E. (1983). Statistical Aspects of Ice Gouging on the Alaskan Shelf of the Beaufort Sea. CRREL Report 83-21, 34 p.

Woodworth-Lynas, C.M.T. (1983). The Relative Age of Ice Scours Using Cross-Cutting Relationships. C-CORE Publication No. 83-3, 54p.

Woodworth-Lynas, C.M.T., Simms, A. and Rendell, C.M. (1985). Iceberg grounding and scouring on the Labrador Continental Shelf. Cold Regions Science and Technology, 10, pp 163-186.

Woodworth-Lynas, C.M.T., Bass, D.W., and Bobbitt, J. (1986). Inventory of Upslope and Downslope Iceberg Scouring. Environmental studies Revolving Funds Report No. 039, 103p.

Woodworth-Lynas, C.M.T. (1990). Observed deformation structures beneath relict iceberg scours. Ice Scouring and the Design of Offshore Pipelines. Calgary, April 18-19, pp.103-125

Woodworth-Lynas, C.M.T. (1992). The Geology of Ice Scour. PhD. Thesis, University of Wales, 269p.

Woodworth-Lynas, C.M.T., Nixon, J.F., Phillips, R. and Palmer, A. (1996). Subgouge deformations and the security of arctic marine pipelines. Proceedings of Offshore Technology Conference, Houston, May 1996, Vol 4, pp 657-664.

Woodworth-Lynas, C.M.T., Phillips, R., Clarke, J.I., Hynes, F., Xiao, X. (1998). Verification of centrifuge model results against field data: results from the Pressure Ridge Ice Scour Experiment (PRISE). Proceedings of the 13th International Symposium on Okhotsk Sea and Sea Ice, Mombet, Japan, Feb. 1-4, pp. 123-138.

Yang, Q.S., Poorooshasb, H.B., and Lach, P.R. (1996). Centrifuge modeling and numerical simulation of ice scour. Soils and Foundations, Vol. 36, No. 1, March, pp 85-96.